8-1989

Air Stripping of Volatile Organic Compounds from Groundwater: An Evaluation of a Centrifugal Vapor-Liquid Contactor

Surinder Paul Singh
University of Tennessee - Knoxville

To the Graduate Council:

I am submitting herewith a dissertation written by Surinder Paul Singh entitled "Air Stripping of Volatile Organic Compounds from Groundwater: An Evaluation of a Centrifugal Vapor-Liquid Contactor." I have examined the final electronic copy of this dissertation for form and content and recommend that it be accepted in partial fulfillment of the requirements for the degree of Doctor of Philosophy, with a major in Civil Engineering.

Gregory D. Reed, Major Professor

We have read this dissertation and recommend its acceptance:

R. M. Counce, W. T. Davis, R. B. Robinson

Accepted for the Council:

Carolyn R. Hodges

Vice Provost and Dean of the Graduate School

(Original signatures are on file with official student records.)

To the Graduate Council:

I am submitting herewith a dissertation written by Surinder Paul Singh entitled "Air Stripping of Volatile Organic Compounds from Groundwater: An Evaluation of a Centrifugal Vapor-Liquid Contactor." I have examined the final copy of this dissertation for form and content and recommend that it be accepted in partial fulfillment of the requirement for the degree of Doctor of Philosophy, with a major in Civil Engineering.

Gregory D. Reed, Major Professor

We have read this dissertation
and recommend its acceptance:

Accepted for the Council:

Vice Provost
and Dean of The Graduate School

AIR STRIPPING OF VOLATILE ORGANIC COMPOUNDS FROM GROUNDWATER: AN EVALUATION OF A CENTRIFUGAL VAPOR-LIQUID CONTACTOR

A Dissertation

Presented for the

Doctor of Philosophy

Degree

The University of Tennessee, Knoxville

Surinder Paul Singh

August 1989

ACKNOWLEDGMENTS

This work was performed in the Chemical Technology Division of the Oak Ridge National Laboratory* and was funded by the Air Force Engineering and Services Center (AFESC) at Tyndall Air Force Base, Florida. I am grateful for the comments and guidance of Captain Richard Ashworth.

I would like to acknowledge the advice and encouragement of my thesis advisor, Dr. G. D. Reed and other members of the Committee: Dr. R. M. Counce, Dr. W. T. Davis, and Dr. R. B. Robinson. Additionally, I would like to acknowledge the advice and suggestions of Dr. J. H. Wilson, Dr. J. F. Villiers-Fisher, H. L. Jennings, T. L. Hebble of Oak Ridge National Laboratory, and A. J. Lucero of University of Tennessee. I wish to thank J. D. Allgood who typed this dissertation.

Finally, I wish to thank my parents for their support and encouragement throughout my entire educational endeavors.

*Operated by Martin Marietta Energy Systems, Inc., for the U.S. Department of Energy.

ABSTRACT

The performance of a centrifugal vapor-liquid contactor equipped with high specific surface area packing (>2000 m^2/m^3) was evaluated for air stripping of jet fuel components from groundwater. Hydraulic test data indicated that the Sherwood flooding correlation which has been proposed for use in designing centrifugal vapor-liquid contactors overestimates the rotational speeds at which flooding occurs. For the mass transfer performance, a concept of area of a transfer unit (ATU) was introduced to account for the change in fluid loading with radius of the packing torus. The ATU was found to be a strong function of the specific surface area of the packing and to a lesser extent a function of rotor speed and liquid flow rate. A correlation based on the specific surface area of the packing is proposed for predicting the ATU. A simple empirical model is also proposed for determining the power consumed in turning the packing torus at various operating conditions. Previous claims in the literature that centrifugal vapor-liquid contactor is resistant to fouling because of high shear force were found not to be valid for groundwater with high iron content.

TABLE OF CONTENTS

SECTION		PAGE
1.	INTRODUCTION	1
2.	GROUNDWATER TREATMENT TECHNOLOGIES	3
	2.1 Air Stripping with Emissions Control	6
	2.2 Liquid Phase Activated Carbon Adsorption	11
	2.3 Membrane Separation	12
	2.4 Biological Treatment	13
	2.5 Chemical Oxidation	15
3.	REVIEW OF PREVIOUS WORK WITH THE CENTRIFUGAL VAPOR-LIQUID CONTACTOR	18
	3.1 Description of Centrifugal Vapor-Liquid Contactor	19
	3.2 Results of Previous Studies	25
4.	DESIGN OF AIR STRIPPERS	58
	4.1 Thermodynamic Considerations	58
	4.2 Mass Transfer Theory	62
	4.3 Design Equations	67
5.	EXPERIMENTAL	78
	5.1 Air Stripping System	78
	5.2 Centrifugal Vapor-Liquid Contactor	80
	5.3 Procedure for Hydraulic Tests	86
	5.4 Procedure for Mass Transfer Tests	86
	5.5 Sample Analysis	91
	5.5.1 Equipment	91
	5.5.2 Procedure	92
6.	RESULTS AND DISCUSSION	95
	6.1 Hydraulic Performance	95
	6.1.1 General Characteristics	95
	6.1.2 Hydraulic Capacity Correlation	100
	6.1.3 Pressure Drop Correlation	103

SECTION PAGE

6.2 Mass Transfer Performance.....113
6.2.1 General Characteristics.....113
6.2.2 Experimental Design Analysis.....125
6.2.3 Comparison with Existing Correlations.....128
6.2.4 New Correlation Based on Specific Surface Area of Packing.....130

6.3 Power Consumption.....135
6.3.1 General Characteristics.....135
6.3.2 Development of an Empirical Correlation.....136

6.4 Fouling of the Packing.....141

7. CONCLUSIONS AND RECOMMENDATIONS.....147

REFERENCES.....151

APPENDIXES.....159

APPENDIX A. HENRY'S LAW CONSTANT DETERMINATION.....160
APPENDIX B. EXPERIMENTAL DATA.....163

VITA..... 286

LIST OF TABLES

TABLE		PAGE
2-1.	Full scale air strippers	8
3-1.	Mass transfer coefficients for the centrifugal vapor-liquid contactor using oxygen and water	30
3-2.	Mass transfer coefficients for the centrifugal vapor-liquid contactor using ammonia and water	32
4-1.	Coefficients for the temperature dependence of Henry's Law Constant expression for the temperature range from 0 to 30 °C (1 atm)	74
4-2.	Henry's Law Constant as a function of temperature for the temperature range from 10 to 35 °C	75
4-3.	Component parameters for the temperature regression equation	76
5-1.	Hydraulic test conditions	87
6-1.	Comparison of experimental Henry's Law constants with the literature values	116
6-2.	Results of central composite experiment design analysis	127
6-3.	Elemental analysis of the precipitate	145

LIST OF FIGURES

FIGURE		PAGE
2-1.	Subsurface behavior of spilled hydrocarbons	4
3-1.	The Sherwood flooding correlation	20
3-2.	A schematic of centrifugal vapor-liquid contactor	21
3-3.	Packing of the centrifugal vapor-liquid contactor	23
3-4.	Effect of acceleration on the height of a transfer unit	27
3-5.	Liquid film mass transfer coefficients for 1 mm glass beads	36
3-6.	Liquid film mass transfer coefficients for 12 filament copper gauge packing	37
3-7.	Empirical correlation of flooding and loading data with the Sherwood correlation	39
3-8.	Gas-liquid interfacial area for 3 mm glass beads as a function of rotor speed	40
3-9.	Effects of liquid flow rate on gas-liquid interfacial area	41
3-10.	Comparison of experimental and predicted mass transfer coefficients for 3 mm glass beads	42
3-11.	Power consumption as a function of rotor speed at various operating conditions	46
3-12.	Effect of liquid flow rate and rotor speed on residence time of the liquid phase	47
3-13.	Centrifugal vapor-liquid contactor air stripping system	49
3-14.	Pressure drop across the rotor for varying rotor speed (liq. flow = 5.0-5.7 L/s; temp.=12°C)	50
3-15.	Benzene removal as a function of gas/liquid ratio (liq. flow = 5.0-5.7 L/s; temp.=12°C)	52

FIGURE PAGE

3-16. Mass transfer coefficient for benzene 53

3-17. Power consumption as a function of rotor speed and gas/liquid ratio (liq. flow = 5.0-5.7 L/s) .. 56

4-1. The stagnant film model 64

4-2. Sherwood flooding correlation 69

4-3. Differential volume element for the packing torus 70

5-1. A schematic of air stripping with emissions control system 79

5-2. Centrifugal vapor-liquid contactor system 81

5-3. Liquid sample tube 85

5-4. Central composite design 89

5-5. Mass transfer test conditions for each rotor..... 90

6-1. Theoretical operating envelope for the centrifugal vapor-liquid contactor 96

6-2. Pressure drop as a function of rotor speed without liquid flow (76.20-cm-diam. rotor) 97

6-3. Pressure drop with both liquid and gas phases flowing (liq. flow = 0.63 L/s; 76.20-cm-diam. rotor) 98

6-4. Effect of packing depth on pressure drop (liq. flow = o L/s; rotor speed = 700 rpm) 101

6-5. Comparison of limit of operability data with that predicted by the Sherwood flooding correlation ..104

6-6. Effect of gas flow rate on pressure drop (liq. flow = 0.63 L/s) 107

6-7. Effect of liquid flow rate on pressure drop (gas flow = 47.2 L/s) 108

6-8. Effect of packing depth on pressure drop at several gas flow rates (liq. flow = 0; rotor speed = 700 rpm) 110

FIGURE PAGE

6-9. Comparison of the calculated and experimental pressure drop 112

6-10. Variation in the feed for the mass transfer tests with the 45.72-cm-diam rotor 114

6-11. Plot of mass transfer data to determine end effects (o-xylene data) 118

6-12. Plot of mass transfer data from centerpoint runs (o-xylene data) 119

6-13. Effect of acceleration on the area of a transfer unit (o-xylene data) 121

6-14. Comparison of area of transfer unit for the different rotors 122

6-15. Effect of liquid flow on the area of transfer unit 123

6-16. Effect of gas/liquid ratio on area of transfer unit 124

6-17. Comparison of the experimental ATU with that predicted by correlation proposed by Vivian et al. 129

6-18. Comparison of the experimental and predicted ATU for the wire gauze packing 131

6-19. Comparison of the experimental and predicted ATU for the Sumitomo packing 132

6-20. Comparison of the experimental and calculated ATU using correlation based on the specific surface area of packing 134

6-21. Effect of gas flow rate on power consumption 137

6-22. Effect of outer rotor radius on power consumption 138

6-23. Effect of rotor speed on power consumption 139

6-24. Effect of liquid flow rate on power consumption .140

6-25. Comparison of the experimental and calculated power consumption 142

FIGURE PAGE

6-26. Rise in pressure drop as a result of fouling for the 45.72-cm-diam rotor 144

7-1. Comparison of limit of operability data with that predicted by the Sherwood flooding correlation 148

1. INTRODUCTION

Groundwater has been an important source of freshwater in the past and will continue to be one in the future. Groundwater contains close to 95% of the usable freshwater of the world and approximately 50% of the United States population uses it as a source of drinking water (Barbash and Roberts, 1986). However, groundwater which is contaminated with industrially produced organic compounds is being encountered with greater and greater frequency. Contamination of groundwater with organic compounds is not limited to vicinities near industrial operations because many of these compounds are present in household consumer products. Some of these compounds show evidence of carcinogenicity, mutagenicity, and teratogenicity and have a very long life span due to low biological and chemical reactivity. The major sources of contaminants are accidental spills, underground storage tanks, waste lagoons, landfills, and septic tanks (Althoff et al., 1981). It has been common practice to cap a well when the water from that well was discovered to contain synthetic organic compounds and to have a new well drilled. However, this can no longer be done in many places because a major portion of the groundwater is contaminated. Because groundwater movement is very slow, it may take decades or even centuries for natural processes to eliminate the organic compounds from groundwater. Therefore, when groundwater is the primary source of water for a community, artificial means of removing the organic compounds from water are required. The purpose of this project is to evaluate the performance of a centrifugal vapor-liquid contactor for

air stripping of volatile organic compounds from contaminated groundwater and to develop a design concept for wider application of this technology.

2. GROUNDWATER TREATMENT TECHNOLOGIES

In order to effectively treat groundwater contaminated with volatile organic compounds (VOCs), it is important to understand the behavior of these compounds in the subsurface environment. Figure 2-1 shows the movement of the VOCs once a leak has occurred. As the VOCs move downward due to gravity, some of the compounds become adsorbed onto the soil and the spill also begins to spread horizontally to a small extent due to capillary action. The amount of material adsorbed on the soil depends upon the nature of the soil. The soils that have high organic contents will tend to adsorb more VOCs (Lee et al., 1987). With continued downward movement, the spill eventually reaches the top of the water table. When the spill first reaches the top of the water table, the water is initially pushed downward until the hydrostatic pressure stops the downward movement of the spill. At this point, the VOCs that are more dense than water continue moving down through the water and the lighter VOCs begin to spread horizontally over the water. A small quantity of the VOCs also dissolves in the water. The horizontal movement of the VOCs on the top of the water table results in reduced weight on the water and the water level rises again back to the original level. As this happens, the VOCs that adsorbed onto the soil when the water level was lower remain behind and slowly dissolve as the groundwater moves due to hydraulic gradients. Thus, in treating groundwater contaminated with VOCs, it is important to consider the quantity of VOCs dissolved in the water, adsorbed on the soil, and present in the free layers on top and bottom of the water table.

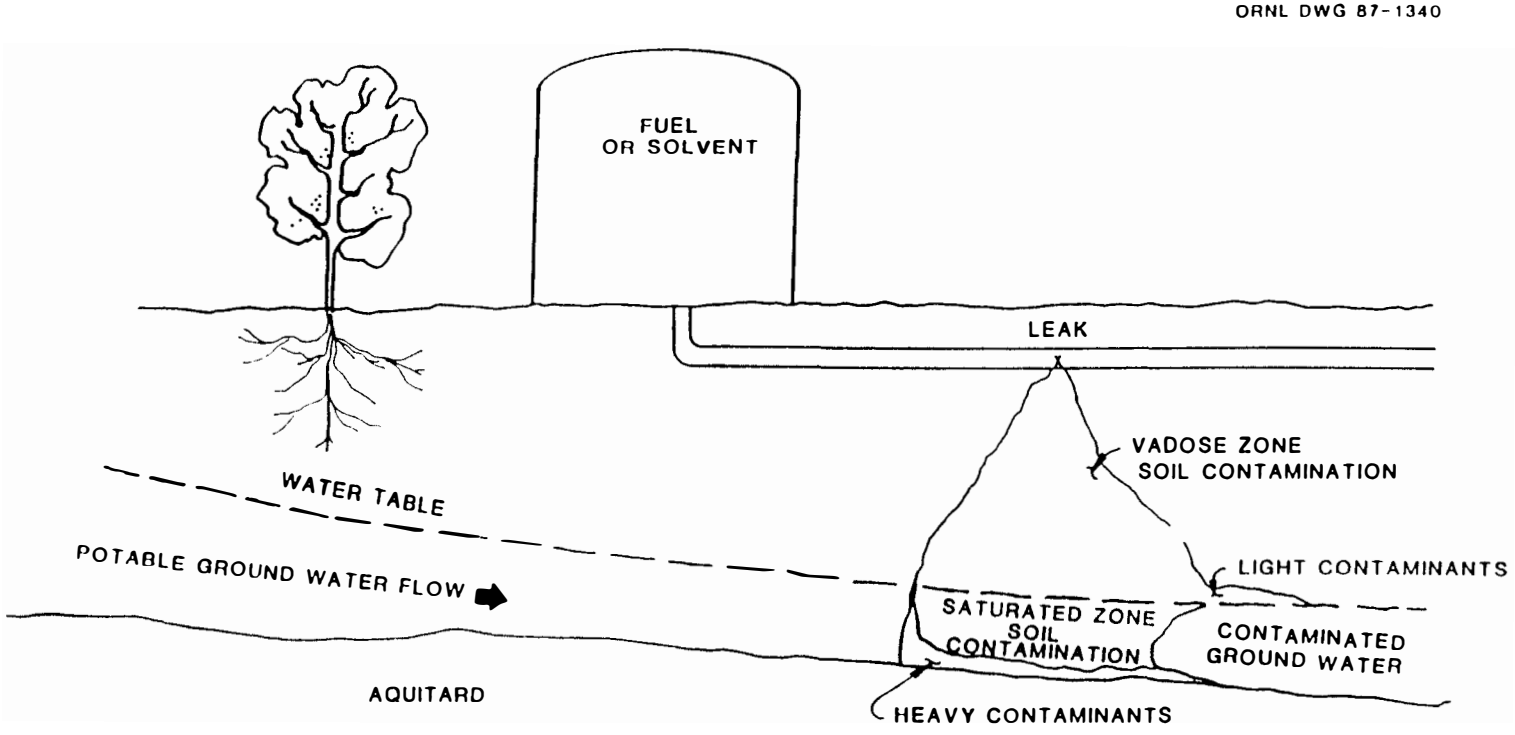

Fig. 2-1. Subsurface behavior of spilled hydrocarbons.

The treatment of groundwater contaminated with VOCs is different from other type of waste water treatment due to the following reasons: nonconventional contaminants, low concentration of contaminants, fluctuations in flow, variability in influent concentration, and uncertainty of system life (Berger et al., 1987). The groundwater treatment technologies can be divided into two broad categories: above ground and in situ. In the above ground treatment method, the water is pumped to the surface and the volatile organic compounds removed using some conventional treatment. The in situ method also requires some withdrawal of the water, but the major removal of the compounds occurs in the subsurface environment. In some cases both above ground and in situ treatments may be employed to make the process more cost effective.

Technologies which have been employed to treat water contaminated with VOCs include air stripping, biological treatment, carbon adsorption, chemical oxidation, and membrane separation. The type of technology employed in the removal of VOCs from groundwater depends to large extent on the ultimate use of the treated water. If the water is to be used as a source of drinking water or in certain industries such as food and pharmaceutical then almost complete removal (greater than 99%) will be required (O'Brien, 1985). Some of the technologies may not be able to meet this requirement when used alone and thus have to be combined with other technologies to achieve the final product requirements. The choice of technology may be influenced by generation of secondary pollutants which may require further treatment or proper disposal. The capital and operating costs of a technology are also a

major factor because the clean up of groundwater is expected to be a long-term project. Thus, these variables along with site specific requirements, should be used to select the technology which best suits the needs.

2.1 Air Stripping with Emissions Control

Air stripping is a process by which water contaminated with slightly soluble VOCs may be purified by transferring the contaminants from the water to air. Air stripping was used for aesthetic reasons in the nineteenth century to remove VOCs which imparted taste and odor to the drinking water (McCarty, 1983). Since air stripping involves the transfer of the contaminants from the liquid phase to the gaseous phase, intimate contact between the two phases is required. The contact between the two phases may be accomplished by mechanical surface aeration, diffused aeration, spray or tray towers, open-channel cascades, spray fountains, and countercurrent packed towers. Mechanical surface aeration systems are simplest to design since only an aerator and a holding tank are required. The efficiency of the surface aeration system depends upon power-to-volume ratio, type of aerator, temperature, and detention time (Kang et al., 1985). In the diffused air system, compressed air is bubbled through the holding tank. The efficiency of this system may range from 50% to 85% because of small interfacial area and short contact time between the two phases (Gross, 1985). The best liquid-gas contact is usually achieved in a packed column. In a packed column, water is broken into a number of slow-moving films which form over the packing. This creates large

amount of interfacial area which is constantly being renewed and thus results in very efficient mass transfer.

A recent survey for the United States Environmental Protection Agency (EPA) identified one hundred and seventy seven air stripping systems in the United States (EPA-450\3-87-017). The report did not indicate what fraction of the total air stripping systems were still operating. Table 2-1 gives data on some of the full scale air stripping systems. From Table 2-1, it can be seen that aromatic and chlorinated (both aliphatic and aromatic) can be removed by air stripping.

Although air stripping is an effective technology for removing VOCs from groundwater, it simply transfers the contaminant from water to air. Because the quantity of air used in air stripping is large, the concentration of the VOCs in air is usually low. However, future regulations could limit the emission of VOCs from air strippers. If air emissions become a problem, emissions control technologies which have been employed in industrial applications could be used in air stripping operations. The three most commonly used techniques for controlling VOCs from air streams are: (1) adsorption onto activated carbon, (2) catalytic destruction, and (3) thermal destruction.

The use of emission control devices alters the method of operation of the air stripper itself. For example, when emissions-control devices are not needed, high gas-to-liquid ratios are employed to reduce the concentration of the VOCs in the exit air stream. With emission controls, however, a lower gas-to-liquid ratio will need to be used to reduce the cost of the emission control. Of the 177 air

Table 2-1. Full scale air strippers.

Source	Liquid flow (gal/min)	Type of contactor	Compound
Malot and Wood	1500	Spray tower	Vinyl chloride 1,1,1-trichloroethane cis-1,2-dichloroethane 1,1-dichloroethane
Reijnen et al.	160	Packed tower	Tetrachloroethene Trichlorethane
McIntyre et al.	150	Packed tower	Benzene Chlorobenzene 1,1-dichloroethane Trans-1,2-dichloro-propane Ethylbenzene Methylene chloride Toluene Trichlorofluoromethane m-xylene o-xylene
Bishop et al.	9000	Packed tower	Chloroform Dichlorobromomethane Bromoform
Byers and Morton	3500	Packed tower	1,1,2,2-tetrachloro-ethane Trans-1,2-dichloro-ethylene Trichloroethylene Tetrachloroethylene
McKinnon and Dyksen	1400	Packed tower	Methyl tertiary-butyl ether Diisopropyl ether Trichloroethylene
Gross and TerMaath	300-600	Packed tower	Trichloroethylene
Dietrich et al.	100	Rotary air stripper	Benzene Toluene Xylenes Trichloroethylene 1,2-dichlorethane Tetrachloroethylene

strippers identified in the EPA report, only 17 were equipped with emission control devices. These 17 include 12 activated carbon units, one catalytic incinerator, 2 open flares and 2 thermal incinerators.

Activated carbon has been used since the 1930s to remove VOCs from air streams, and the technology is well established (Metcalfe and Wilkins, 1984). The adsorption of the VOCs onto the activated carbon is mainly due to Van der Waal forces and no chemical reaction takes place. Organic compounds of molecular weights of over 45 and boiling points greater than 0°C are readily adsorbed onto the carbon from a gas stream (Cheremisinoff, 1987). The adsorption of the VOCs from the gas stream onto the activated carbon depends upon the type of carbon, relative humidity, temperature, concentration and type of volatile organic compound, and the regeneration step used (Foster, 1985). Of these variables, the relative humidity is probably of most concern in the operation of an air stripper system.

In using activated carbon for emission control, a decision has to be made on whether to throw away or regenerate the used carbon. In most cases the amount of activated carbon used for vapor phase removal of VOCs is small enough that throwing away the spent carbon is a viable economic option. If large quantities of activated carbon will be required, then on site regeneration may be the most viable option. Several methods of regenerating the carbon are available and these include: steam-regeneration (Foster, 1985), inert gas regeneration (Howard, 1984 and Mattia, 1970), and supercritical fluid regeneration (Kander, 1983).

In the catalytic destruction process for emission control, a catalyst is used to promote the oxidation of the organic compounds at lower temperature than required for thermal destruction. The catalyst increases the rate of the reaction by bringing the reactants together or by lowering the activation energy of the reaction. The performance of a catalytic destruction device depends upon temperature, type and concentration of VOCs, space velocity (residence time), and the type of catalyst. Spivey et al. (1987) conducted a literature review on heterogeneous catalytic destruction of potential environmentally hazardous compounds. They present an excellent review of the mechanism of catalytic oxidation reactions and a comparison of metal oxide and precious metal catalysts. Listed below are some findings reported in their survey report:

- Oxides of copper, manganese, cobalt, chromium and nickel are most active single metal oxide catalyst.
- Mixed metal oxide catalyst generally have higher activity than single metal oxide catalyst.
- Metal oxide catalyst are less active than precious metal catalyst, but metal oxide catalyst are more resistant to certain poisons such as halogens, arsenic, lead, and phosphorus.

Approximately 500 to 2000 catalytic incinerators are currently used to control the emission of VOCs in various industries (Jennings et al., 1984). Although catalytic destruction is widely used in industry to control emissions of VOCs, this technology cannot be directly extended to air stripping operations because of low concentration of VOCs in the air stream, high humidity of the air stream, wide range of contaminants, and the possible presence of mineral aerosols and poisons (Kosusko et al., 1987).

Thermal incineration for emission control avoids the use of catalyst and relies on heat energy to overcome the activation energy barrier of the oxidation reactions. Thermal incineration gives very high destruction efficiency and can be used when substances which poison a catalyst are present. The drawback of thermal incineration is the large amount of fuel needed to achieve the necessary temperatures (1000 to 2500°F). Also, thermal incineration is usually better suited for streams which contain high concentration of VOCs.

Jennings et al. (1984) compared vapor phase carbon adsorption, catalytic destruction, and thermal incineration with respect to general applicability, environmental and energy considerations, and operation and maintenance requirements. The reader is referred to this source for more details on the emission control methods.

2.2 Liquid Phase Activated Carbon Adsorption

Removal of organic compounds from water using activated carbon is a well developed process. Activated carbon treatment has been preferred for drinking water because large number of compounds can be removed. In 1982, about 20 utilities were using activated carbon to remove VOCs from contaminated groundwater (Love and Miltner, 1982). Activated carbon is most effective in removing nonpolar compounds which contain 4 to 20 carbon atoms (Berger et al., 1987). Also, unsaturated organic compounds such as ethylenes are removed more effectively than saturated compounds (Dyksen, 1982). To design an activated carbon system, experimental data are usually required to determine the capacity of the carbon for a particular compound. The Calgon Carbon

Corporation has developed an accelerated carbon test which can be used to evaluate the feasibility of using activated carbon in much less time than conventional tests (Stenzel and Gupta, 1985).

The life of the carbon bed can be affected by bacteria, iron, manganese, and nonvolatile compounds that may be present in the groundwater (Hall and Mumford, 1987). The presence of natural humics in groundwater can also decrease the adsorption capacity of the carbon because these compounds adsorb strongly onto the carbon and may not be removed in the regeneration step (Baldauf, 1985). Pretreatment steps such as aeration and coagulation can be used to extend carbon bed life when iron, manganese, and humics are present.

Because the cost of replacing the carbon can be high, on site regeneration may be required for long term projects. The regeneration technologies have been previously discussed in the section on air stripping with emission controls. IT Corporation performed cost analyses of liquid phase carbon adsorption with on-site steam regeneration of the loaded carbon (Parmele et al., 1986). Their cost analysis indicated that when the water flow is greater than 100 gpm and treatment is required for several years, liquid phase carbon adsorption with on-site steam regeneration is a cost effective alternative to air stripping when greater than 99% removal of VOCs is required.

2.3 Membrane Separation

Separation of VOCs from groundwater using membranes may be one of the most promising technologies for the future. Membrane separation will not be a stand-alone process, but could be used in conjunction

with other treatment processes to make the overall process more cost effective. A hybrid membrane separation and air stripping without emission control process could be economically competitive (Weber and Bowman, 1986). In this process, a membrane system is first used to reduce the volatile organic concentration in the water by 85% to 90%. The clean water stream from the membrane system is then put through an air stripper which further reduces the VOCs in the water. Using the air stripper after the membrane system avoids the need for expensive emission control devices because the contaminant concentrations are greatly reduced in the influent water to the air stripper.

2.4 Biological Treatment

There are two approaches in using biological treatment for removal of VOCs from groundwater. The first approach is to pump the water to the surface and use conventional biological treatment methods. In the second approach, treatment is accomplished in situ by promoting indigenous microbial growth or by addition of acclimated microorganisms. Of the two approaches, in situ biological treatment has received the greatest attention in recent years. An advantage of in situ treatment over the above ground method is that the treatment moves with the plume and thus can reach VOCs trapped in the soil.

Contrary to previously held belief that groundwater is sterile, microorganisms of densities up to 10^6 organisms per gram of soil have been found in some aquifers (EPA/625/6-87/016). Laboratory studies using microorganisms from contaminated aquifers indicate that contaminants such as n-alkanes and chlorobenzenes are degraded under

aerobic conditions and that chlorinated aliphatics are probably degraded under anaerobic conditions. The chlorinated aliphatics such as tetrachloroethylene may not be completely converted to carbon dioxide and water, but may be converted into intermediate products such as trichloroethylene, dichloroethylene and vinyl chloride (Lee et al., 1987). In some cases, the partial degradation products are more toxic than the original parent compound. The important factors in the microbial degradation of the VOCs in the subsurface environment include: dissolved oxygen, pH, temperature, oxidation-reduction potential, availability of mineral nutrients, salinity, soil moisture, the concentration of the specific VOCs, and the nutritional quality of the VOCs.

Several field studies have been conducted in which oxygen and nutrients have been added to groundwater contaminated with petroleum hydrocarbons to stimulate biodegradation of the VOCs (Ohneck and Gardner, 1982; Yaniga, 1982; Yaniga and Smith, 1985; Downey et al., 1987; Wetzel et al., 1987).

Ohneck and Gardner inoculated the effluent from the liquid-phase carbon adsorption treatment process with hydrocarbon-degrading bacteria and nutrients prior to re-injection. The dissolved oxygen content of the water was also increased prior to re-injection. The main purpose of this treatment was to establish biological growth around the soil particles in the vadose (unsaturated soil) zone to degrade chemicals entrapped in the soil. Ohneck and Gardner report "with the addition of the biological treatment, cleanup effectiveness was increased while the cost of the operation and maintenance were decreased."

Yaniga and Smith used air stripping and in-situ biological treatment to remove benzene, toluene, and xylenes from groundwater. They report the use of hydrogen peroxide as a source of oxygen to enhance biological growth. The hydrogen peroxide was added to the effluent from the air stripper prior to re-injection and was also introduced into the groundwater through a well. An advantage of using hydrogen peroxide is that dissolved oxygen concentration is not limited by the mass transfer equipment. The disadvantages of using hydrogen peroxide include the high cost of hydrogen peroxide, toxicity to microbes at levels above 50 to 100 mg/L, and precipitation of minerals caused by reaction with hydrogen peroxide which result in decreased permeability of the soil.

One of the limitations of in situ biological treatment has been the ability to transfer the technology from the laboratory to the field. Problems associated with the delivery of chemicals required to enhance biological growth in the subsurface environment have not been resolved.

2.5 Chemical Oxidation

Chemical oxidation has been used in water and waste water treatment to convert undesirable chemicals into compounds which are less objectionable. Like biological treatment, chemical oxidation for groundwater cleanup can be carried out above ground or in-situ. The above ground method has been used most often due to side reactions of the oxidants that occur in the subsurface environment.

The oxidizing agents which have been used in water and wastewater treatment include: oxygen or air, ozone, hydrogen peroxide, potassium permanganate, chlorine or hypochlorites, and chlorine dioxide (Weber, 1972). For treating water contaminated with VOCs, laboratory studies have shown that ozone is effective in destroying aromatics and alkenes but not alkanes (Mayo et al., 1986). In Germany, groundwater containing petroleum hydrocarbons has been treated successfully using ozone (Berger et al., 1987).

In recent years, ultraviolet light has been used in combination with oxidizing agents to make the chemical oxidation process more effective. The U.S. Army has investigated ozone oxidation with ultraviolet light to treat the wastewater from mobile field hospitals call MUST [Medical Unit, Self-contained, Transportable] (McCarthy, 1977). This study was conducted with synthetic laboratory waste which contained the following compounds: diethyl ether, methanol, urea, glycerol, ethanol, 10% formaldehyde, o-phenylphenol, o-benzyl-p-chlorophenol, xylenol, isopropanol, and acetone. The rate of chemical destruction was unexpectedly low in all experiments. It was postulated that the low destruction was caused by an insufficient concentration of ozone in the water (0.1 to 0.4 mg/L). The destruction of methanol was most affected by the dissolved concentration of the ozone and the destruction of acetone was affected by the absence or presence of ultraviolet light. In another study, McShea et al. (1987) report the use of ozone and ultraviolet light to treat water containing trichloroethylene and tetrachloroethylene.

The U.S. Navy has investigated the use of ultraviolet light and hydrogen peroxide to treat trinitrotoluene contaminated wastewater (Andrew, 1980). The treatment process was found to be effective in treating the contaminated wastewater and was found to be more economical than ultraviolet-ozone treatment or carbon adsorption.

Summary

In summation, several technologies are available for the removal of VOCs from groundwater and these include air stripping, biological treatment, carbon adsorption, chemical oxidation, and membrane separation. Of these technologies, air stripping and carbon adsorption have been used in large scale operations. One of the problems with using air stripping is the emission of VOCs in the air stream. However, this problem can be overcome by using vapor phase carbon adsorption, catalytic destruction, or thermal destruction to clean the air stream. Although in situ biological treatment has not been demonstrated on large scale, it has the advantage that the VOCs trapped in the soil can also be destroyed. In some case, technologies such as air stripping and biological treatment have been combined to make the overall process more efficient.

3. REVIEW OF PREVIOUS WORK WITH THE CENTRIFUGAL VAPOR-LIQUID CONTACTOR

The development of the centrifugal vapor-liquid contactor was related to several events that occurred in the 1970s. The first event was the escalating cost of chemical plant equipment which made new plants and expansion of existing plants very unattractive. Chemical companies were searching for mass transfer equipment which would be more efficient than the existing equipment and which would also be smaller and less costly to fabricate. The second event was a request by the United States National Aeronautics and Space Administration for experiments which could be conducted in the zero gravity environment of outer space. Both of these events led Colin Ramshaw of Imperial Chemical Company, Ltd. (Great Britain) to the idea of a centrifugal vapor-liquid contactor. After initial tests with laboratory units, Imperial Chemical Company built a full scale unit and demonstrated the concept of the centrifugal vapor-liquid contactor for a distillation process. Because Imperial Chemical Company was not a manufacturer of mass transfer equipment, it sold the world wide marketing rights for the centrifugal vapor-liquid contactor to Glitsch, Inc., of Dallas, Texas. Glitsch is currently marketing the centrifugal vapor-liquid contactor under the generic name HIGEE (high 'g'). The following two sections describe the centrifugal vapor-liquid contactor and present the results of previous studies.

3.1 Description of Centrifugal Vapor-Liquid Contactor

In the design of a conventional packed tower, the hydraulic capacity is determined using the Sherwood flooding correlation which is shown in Fig. 3-1. The abscissa of the Sherwood flooding correlation is a function of the flow rate and density of the two fluids. The ordinate also contains the fluid properties as well as the superficial gas velocity, packing specific surface area and voidage, and the acceleration term. For conventional packed towers, the acceleration term is a constant, and thus, the packing densities and gas velocities which can be used have a limited range. In the centrifugal vapor-liquid contactor, the acceleration term is no longer constant and can be increased well beyond the earths gravitational acceleration of 9.8 m/s^2. An increase in the acceleration term means that the packing density and the superficial gas velocity can be increased while retaining a constant value of the ordinate in the Sherwood flooding correlation. The higher superficial gas velocity and packing density result in improved hydraulic capacity and mass transfer in the centrifugal vapor-liquid contactor.

A schematic of the centrifugal vapor-liquid contactor is shown in Fig. 3-2. The centrifugal vapor-liquid contactor is composed of two major components: the rotating packing and the stationary housing. The liquid phase is fed into the center of the rotating packing and flows outward due to the centrifugal force. After exiting the packing, the liquid phase impacts the housing wall and flows by gravity out of the unit. The vapor phase is introduced into the annular space between the packing and the housing and flows inward due to the pressure driving

ORNL DWG 88-1079R

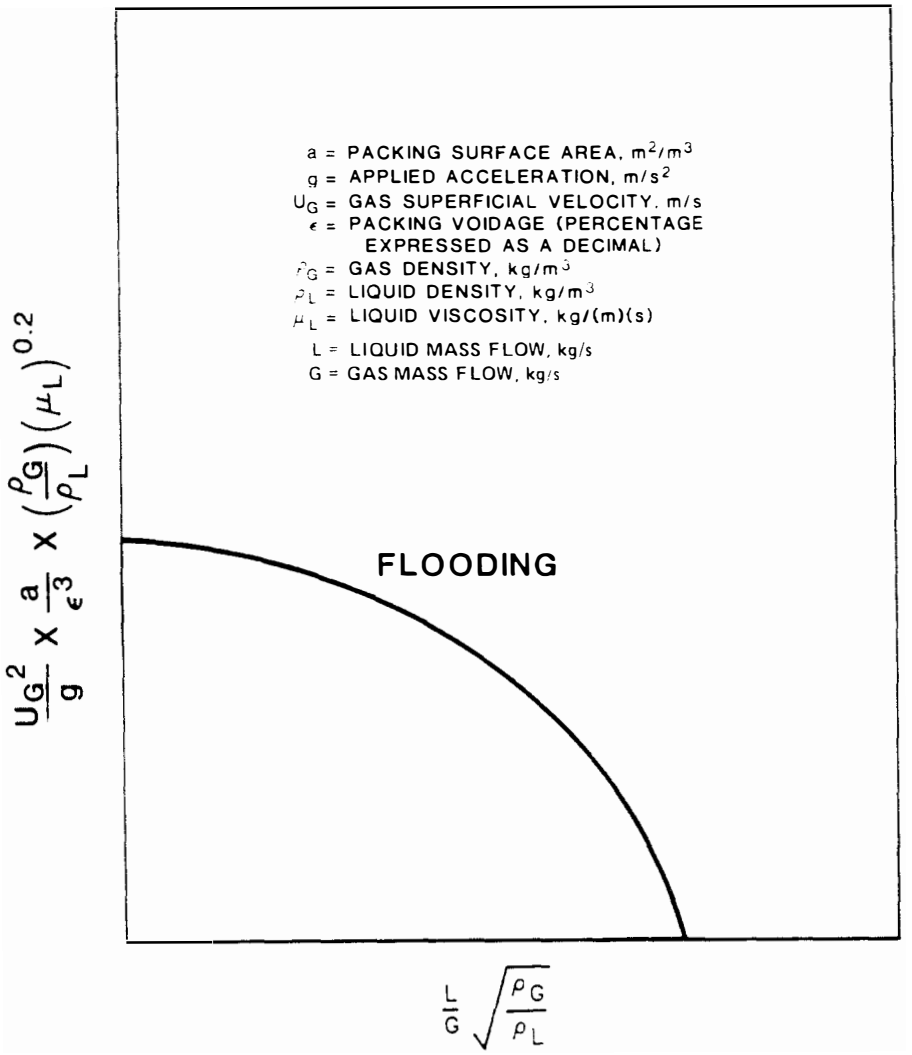

Fig. 3-1. The Sherwood flooding correlation.

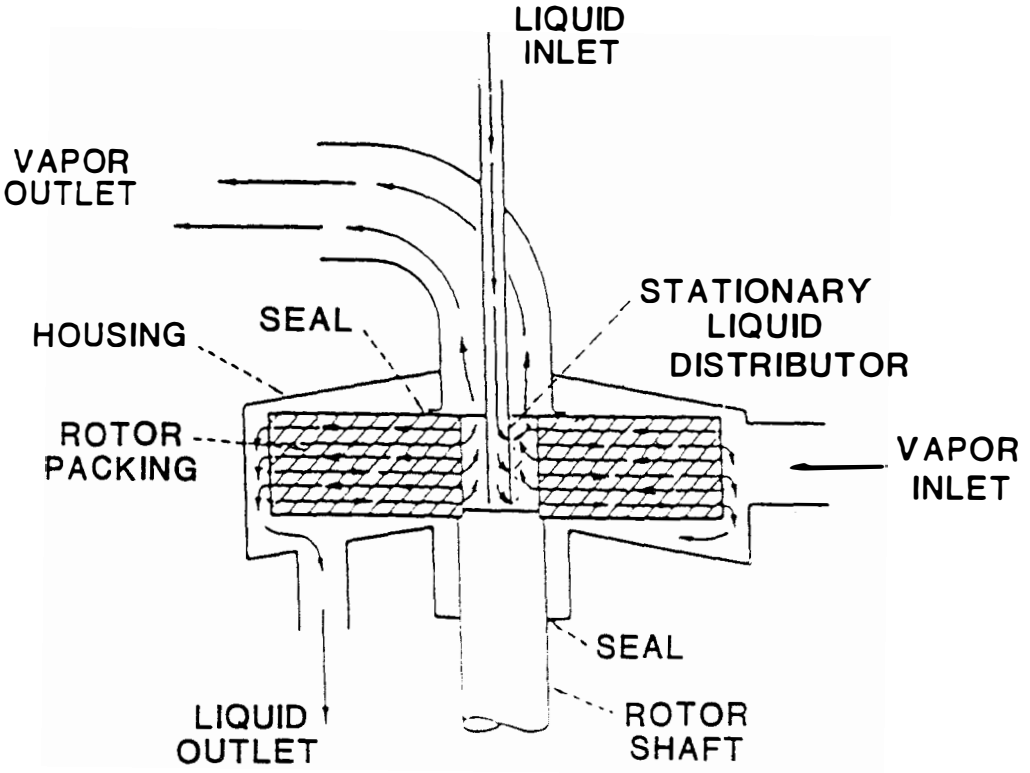

Fig. 3-2. A schematic of centrifugal vapor-liquid contactor.

force. Seals are provided between the rotating packing and the housing to prevent the vapor phase from bypassing the packing. The high shear forces experienced by the liquid phase cause the formation of very thin films and rapid renewal of the interfacial surfaces. The rotation of the packing also cause considerable turbulence in the vapor phase. Both of these factors contribute to efficient mass transfer.

The rotating packing of the centrifugal vapor-liquid contactor is shaped like a torus as shown in Fig. 3-3. The hydraulic capacity of a centrifugal vapor-liquid contactor is determined by the inner surface area of the packing because the highest fluid velocities are encountered at this location. The outer radius of the packing is limited by the structural strength of the packing material and the support basket used to contain the packing. The overall packing dimensions (outer radius and axial length) are constrained by mechanical considerations such as bearing loads and vibration moments. The packing of the early laboratory units consisted of glass beads or wire mesh contained in a rotating basket. The specific surface area of these packing materials ranged from 2000 to 5000 m^2/m^3 and the voidage ranged from 90 to 95% (Ramshaw, 1983). The packing of the full scale units is usually made from reticulated metal with specific surface are of 2500 m^2/m^3 and voidage of 90% (Mohr and Khan, 1987). The reticulated metal is made by first molding polyurethane foam and applying a conductive coating on the foam. The metal is electroplated on the coated foam in the next step. Finally, the material is heat treated to burn out the polyurethane. The resulting metal is in form

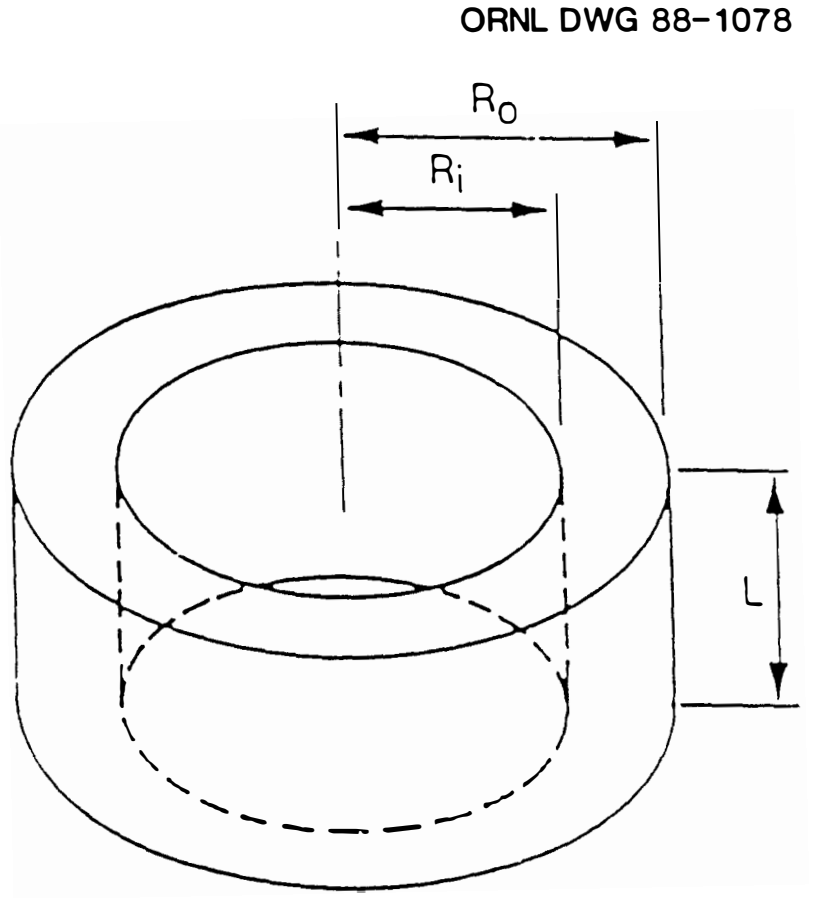

Fig. 3-3. Packing of the centrifugal vapor-liquid contactor.

of a sheet 2 to 10 mm thick. The metal sheet is then wound around from the outside to inside to form the packing torus. The density of the reticulated metal determines the tensile and compressive strength of the packing (Bucklin and Johnston, 1987).

Although the centrifugal vapor-liquid contactor is claimed to be a more efficient device than conventional packed tower, it is also a more complex rotating machine. Thus, the centrifugal vapor-liquid contactor must offer other advantages if it is to replace more conventional equipment. The other advantages of the centrifugal vapor-liquid contactor are small size, short residence time of the process fluids in the packed section, insensitivity to motion, and the rapid achievement of steady state. The small size is particularly beneficial in situations such as at Air Force bases where removal of volatile organic compounds from groundwater using air stripping with conventional packed towers may not be possible because the height of structures is limited. In cold climates where conventional packed towers may become non-operational due to freezing, the centrifugal vapor-liquid contactor can be easily housed in a small building. The centrifugal vapor-liquid contactor can also be mounted on a skid for easy transportation to different sites. The short residence time and the rapid achievement of steady state can be important advantages in the chemical industry where hazardous chemicals are to be processed and low inventory of these chemicals is desirable for safety reasons. The insensitivity to motion in a centrifugal vapor-liquid contactor may make vapor-liquid mass transfer operations possible on ships and off shore platforms.

The disadvantages of a centrifugal vapor-liquid contactor over conventional packed towers include: (1) centrifugal vapor-liquid contactor is a rotating machine and thus prone to bearing and seals failure, and (2) additional power is required to rotate the packing. Because the rotational speeds used in the centrifugal vapor-liquid contactor are not excessive, conventional bearings and seals are used to reduce replacement costs. The power consumption of the centrifugal vapor-liquid contactor depends upon the frictional losses in the system, the energy required to accelerate the liquid to rotor speed, and the power recovered in the movement of vapor phase from the outer diameter of the rotor to the inside (Fowler and Khan, 1987). In most processes, the power required to accelerate the liquid is most dominant and thus power costs can be optimized by changing process conditions.

3.2 Results of Previous Studies

From 1930 to 1960, several models were proposed to predict the mass transfer in packed columns. Some of these models were based on theoretical considerations, but most were derived using dimensional analysis and then regression fit to the available data. In few of the dimensionless correlations, the liquid film mass transfer coefficient was dependent on gravitational acceleration. The exponent on the acceleration term varied from 1/6 to 1/3 depending upon the model. Because the acceleration term was a constant in all experiments performed, it was difficult to determine whether this term was a real variable or merely a term needed to make the correlation dimensionless.

In the early 1960s, Vivian et al. (1965) proposed to determine the effect of acceleration on the liquid film mass transfer coefficient. The experiment consisted of mounting a small column on a large centrifuge and varying the acceleration experienced by the liquid phase by changing the rotational speed of the centrifuge. The column was mounted in such a manner that it was free to swing at an angle from the vertical position. The column was 15.24 cm (6 in.) in diameter (inside diameter) and was packed with 1.91 cm (3/4 in.) stoneware Raschig rings made by U.S. Stoneware Corporation to give packing depth of 30.5 cm (1 ft). The liquid film mass transfer coefficient was determined by desorbing carbon dioxide from water into air. Several data points were taken with the column in the vertical position both prior to and after the runs at higher acceleration to ascertain any change that might have occurred in the packing. The data from the column in vertical position indicated that the packing had remained unchanged throughout the test and thus any changes observed in the liquid film mass transfer coefficient were indeed due to the acceleration term. The results of these experiments are presented in Fig. 3-4. The experiments shown in Fig. 3-4 were conducted at liquid loading of 7.06 kg/s-m^2 (5,200 lb/h-ft^2) and 5.03 kg/s-m^2 (3,700 lb/h-ft^2), and air loading of 0.31 kg/s-m^2 (230 lb/h-ft^2). Because samples were not obtained from inside the packing, the H_L shown in Fig. 3-4 was calculated using the inlet and outlet concentration and thus include the end effect. The data from these experiments indicate that the liquid film mass transfer coefficient varies with acceleration with an exponent of 0.41 to 0.48 and that the exponent is dependent upon the liquid loading rate.

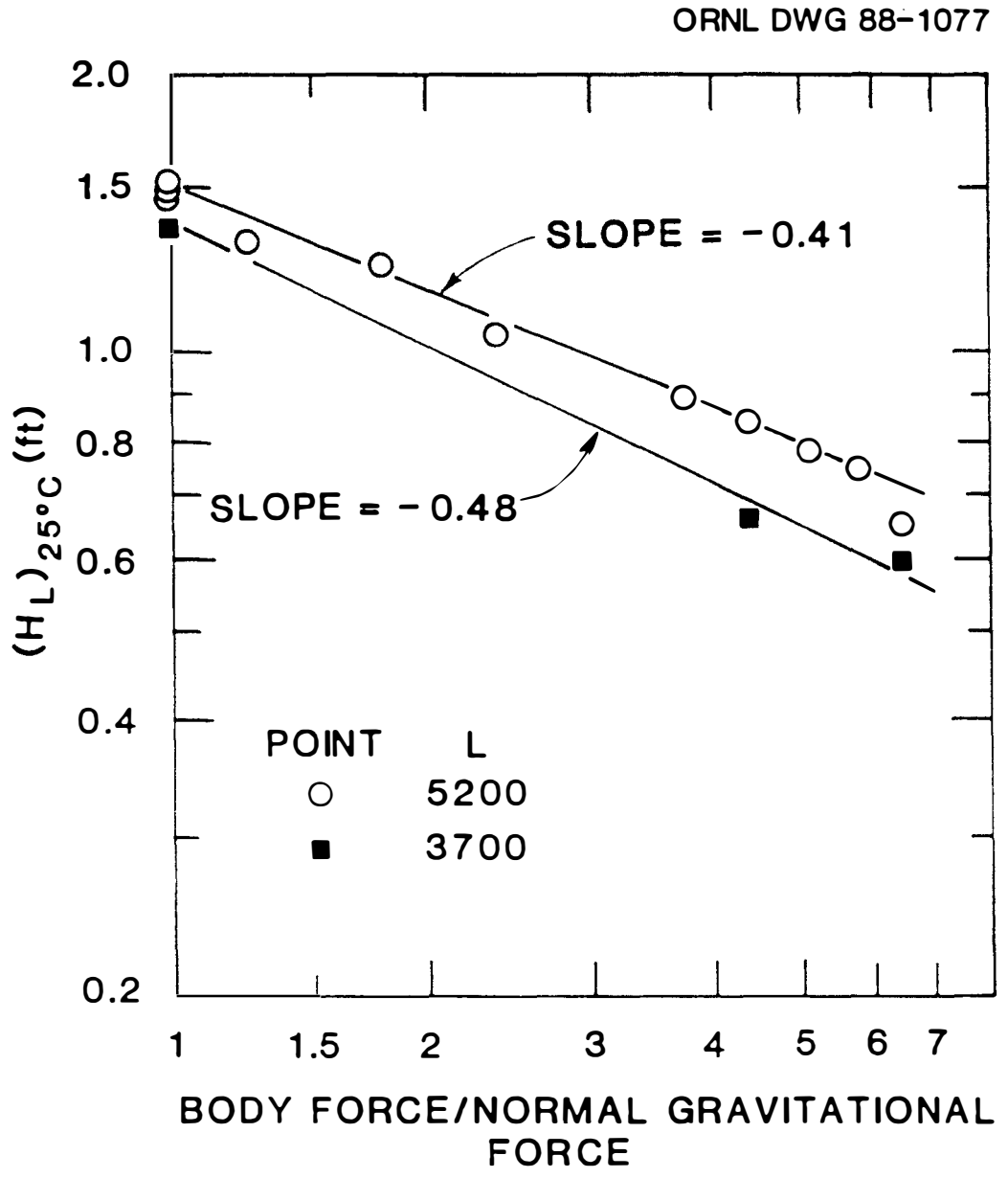

Fig. 3-4. Effect of acceleration on the height of a transfer unit.

The next reported study on the mass transfer with the centrifugal vapor-liquid contactor is the work done by the Imperial Chemical Industries, Ltd. (Ramshaw and Mallinson, 1981). In these studies, both the liquid and gas film mass transfer coefficients were determined using small laboratory development units.

The liquid film mass transfer coefficients were determined by absorbing oxygen into water. The packing element had inner radius of 4 cm and outer radius of 9 cm. [Note: no information is given on the axial length of the packing element in the patent document]. Packing materials were 1 mm glass beads with specific surface area of 3300 m^2/m^3 and 12 filament copper gauge with specific surface area of 1650 m^2/m^3. The deoxygenated water was fed into the center of the packing and the oxygen concentrations measured in the inlet and outlet water streams. The liquid film mass transfer coefficient was calculated using the following equation:

$$k_l = \frac{Q}{V\ a_t} \ln \left[\frac{[C_{el} - C_1]}{[C_{el} - C_2]} \right] \qquad (3\text{-}1)$$

where k_l = liquid film mass transfer coefficient (m/s)

Q = liquid flow rate (m^3/s)

V = volume of the packing (m^3)

C_1 = dissolved oxygen concentration of the inlet water

C_2 = dissolved oxygen concentration of the outlet water

C_{el} = equilibrium dissolved oxygen concentration at the operating conditions

a_t = specific surface area of the packing (m^2/m^3)

In using this equation, it is assumed that the interfacial area for mass transfer is equal to the specific surface area of the packing material. The results of these experiments are shown in Table 3-1. From the results, it can be seen that the liquid side mass transfer coefficient increases with the rotational speed of the packing and the liquid flow rate. Because the data presented in the patent application is incomplete, it is difficult to draw any other conclusions.

The gas side mass transfer coefficients were determined by absorption of ammonia into water. The vapor phase in these experiments was a 5% (vol) mixture of ammonia and air. The packing dimensions are not given in the report although it appears that the unit used in determining the liquid film mass transfer coefficient was used in these experiments. The packing materials were 1.5 mm glass beads with specific surface area of 2400 m^2/m^3 and stainless steel gauge with specific surface area of 1650 m^2/m^3. The gas film mass transfer coefficients were calculated using the equation:

$$k_g = \frac{M_w\, Q\, (C_2 - C_1)}{V\, a_t\, P_t} \left[\frac{\ln\left[\frac{(Y_1 - Y_{e1})}{(Y_1 - Y_{e1})}\right]}{[(Y_1 - Y_{e1}) - (Y_2 - Y_{e2})]} \right] \qquad (3\text{-}2)$$

where k_g = gas film mass transfer coefficient (s/m)

M_w = molecular weight of ammonia (kg)

Q = liquid flow rate (L/s)

C_1 = ammonia concentration in the inlet liquid (mol/L)

Table 3-1. Mass transfer coefficients for the centrifugal vapor-liquid contactor using oxygen and water.

Water flowrate ($m^3/s \times 10^5$)	Type of packing[a]	Rotational speed (rpm)	Mean acceleration (m/s^2)	Mass transfer coeff. ($m/s \times 10^5$)
3	1	1250	1197	21.2
3	1	1500	1727	24.9
4	2	1500	1727	19.4
4	2	1750	2354	20.6
5	1	1500	1727	20.3
5	1	1750	2354	21.7
6	2	1500	1727	26.7
6	2	1750	2354	31.5

[a]1= glass beads
2= knitmesh copper gauge

Source: Ramshaw, C. and R. H. Mallinson, 1981.

C_2 = ammonia concentration in the outlet liquid (mol/L)

V = volume of the packing (m^3)

a_t = specific surface area of the packing (m^2/m^3)

P_t = total pressure of system (N/m^2)

Y_1 = mole fraction of ammonia in the inlet gas stream

Y_{e1}= mole fraction of ammonia in the gas phase in in equilibrium with an ammonia/water solution of concentration C_1

Y_2 = mole fraction of ammonia in the outlet gas gas stream

Y_{e2}= mole fraction of ammonia in the gas phase in in equilibrium with an ammonia/water solution of concentration C_2

The calculated gas film mass transfer coefficients are given in Table 3-2. Again, like the liquid film mass transfer coefficient, the gas film mass transfer coefficient increases with increasing rotational speed. The stainless steel gauge packing material which has smaller specific surface area than the glass bead gives higher gas film coefficients. This could possibly be a result of dead air space which may occur between the beads of the glass packing. Dead air spaces are less likely in the stainless steel packing due to the wiry nature of the packing material and thus higher gas film mass transfer coefficient are obtained.

In addition to these tests, the Imperial Chemical Industries, Ltd. operated a small centrifugal vapor-liquid contactor to demonstrate its use in a distillation process. The packing torus used for this demonstration had inner and outer radii of 6 cm and 9 cm, respectively. The torus was packed with 12 filament stainless steel gauge with

Table 3-2. Mass transfer coefficients for the centrifugal vapor-liquid contactor using ammonia and water.

Water flowrate ($m^3/s \times 10^5$)	Type of packing[a]	Rotational speed (rpm)	Mean acceleration (m/s^2)	Mass transfer coeff. ($s/m \times 10^8$)
1.7	1	1000	760	3.94
1.7	1	1750	2354	4.83
1.7	2	1000	760	10.8
1.7	2	1750	2354	12.69

[a] 1= glass beads
2= stainless steel gauge

Source: Ramshaw, C. and R. H. Mallinson, 1981.

specific surface area of 1650 m^2/m^3. The distillation process was performed using methanol/ethanol mixture because equilibrium data were readily available. The system was operated at total reflux with a feed mixture consisting of 70 mole percent methanol and 30 mole percent ethanol going to the boiler. At steady state, the liquid in the condenser had composition of 9 mole percent ethanol and 91 mole percent methanol. The McCabe-Thiele method was used to calculate the number of transfer unit from which height of a transfer unit and the mass transfer coefficient (K_G) determined. At rotor speed of 845 rpm, a mass transfer coefficient of 4.4×10^{-4} mol/m^2s was obtained. For comparative purposes, the same distillation process using 1/2 in. Intalox saddles in a conventional tower gave mass transfer coefficient of 5.4×10^{-5} mol/m^2s. Again, the data reported is incomplete and difficult to analyze.

Tung and Mah (1985) attempted to analyze the liquid film mass transfer data presented by Ramshaw and Mallinson using the penetration theory of mass transfer and the Onda correlation used in the design of conventional packed towers. The equation based on the penetration theory used by Tung and Mah is:

$$\frac{k_l\, d}{D} = 0.96\ Sc^{1/2}\ Re^{1/3} \left[\frac{a_t}{a_e}\right]^{1/3} \left[\frac{d^3\, \rho^2\ g}{\mu^2}\right]^{1/6} \qquad (3\text{-}3)$$

where a_e = effective area for mass transfer per unit volume of packing (m^2/m^3)

a_t = specific surface area of packing (m^2/m^3)

D = diffusivity (m^2/s)

d = diameter of packing material = $6(1-\epsilon)/a_t$, (m)

g = acceleration (m/s^2)

k_l = liquid film mass transfer coefficient (m/s)

L = liquid mass flow rate (kg/m^2s)

Re = Reynolds number = $L/(a_t \mu)$

Sc = Schmidt number = $\mu/(\rho D)$

ϵ = voidage of packing

μ = viscosity (kg/m-s)

ρ = density (kg/m^3)

In the derivation of Eq. (3-3), complete mixing of the liquid at the junction on the packing was assumed and effects of Coriolis acceleration and packing material geometry were neglected. The acceleration term in the above equation is based on studies performed with mass transfer from falling films.

The expression for the liquid film mass transfer coefficient given by the Onda correlation (Onda et al., 1968) can be written as:

$$k_l \left[\frac{\rho}{\mu g}\right]^{1/3} = 0.0051\ Re^{2/3} \left[\frac{a_t}{a_e}\right]^{2/3} Sc^{-0.5}\ (a_t\ d)^{0.4} \qquad (3\text{-}4)$$

Tung and Mah used two expressions to evaluate the (a_t/a_e) term in Eqs. (3-3) and (3-4). Both expression gave similar results and thus only the expression given by Onda is presented here. The expression for (a_t/a_e) given by Onda is:

$$(a_t/a_e) = 1 - \exp[-1.45\ (\sigma_c/\sigma)^{0.75}\ Re^{0.1}\ Fr^{-0.05}\ We^{0.2}] \qquad (3\text{-}5)$$

where Fr = Froude number = $L^2 a_t / \rho^2 g$

We = Weber number = $L^2 / \sigma a_t$

σ_c = critical surface tension of packing material (N/m)

σ = surface tension of liquid (N/m)

To evaluate these data, Tung and Mah made the following assumptions since the information given by Ramshaw and Mallinson is incomplete: (1) experiments performed at 25°C and 1 atm pressure, (2) voidage of filament copper gauge is 0.6, (3) axial length of packing torus is equal to inner radius (4 cm), and (4) average value of variables evaluated at inner and outer radii can be used. The results of the analysis performed by Tung and Mah are given in Figs. 3-5 and 3-6. The reported values given in Figs. 3-5 and 3-6 are those given by Ramshaw and Mallinson which are based on the assumption that interfacial area is equal to specific surface area of the packing material. The estimated values are calculated using the reported values and the interfacial area predicted by Eq. (3-5). From Figs. 3-5 and 3-6, it can be seen that mass transfer coefficients predicted by Eq. (3-3) are close to those estimated. However, the 1/6 power on the acceleration term is in disagreement with the results reported by Vivian et al. (1965) in Fig. 3-4. Because the data used by Tung and Mah is incomplete, their analysis is open to question.

Munjal (1986) built a centrifugal vapor-liquid contactor similar to the unit used by ICI in an effort to elucidate the hydraulic and mass transfer performance. For the hydraulic tests, the packing material was either 1.0 to 1.18 mm diam spherical glass beads or 3 mm diam glass beads. The flooding in the unit was indicated by

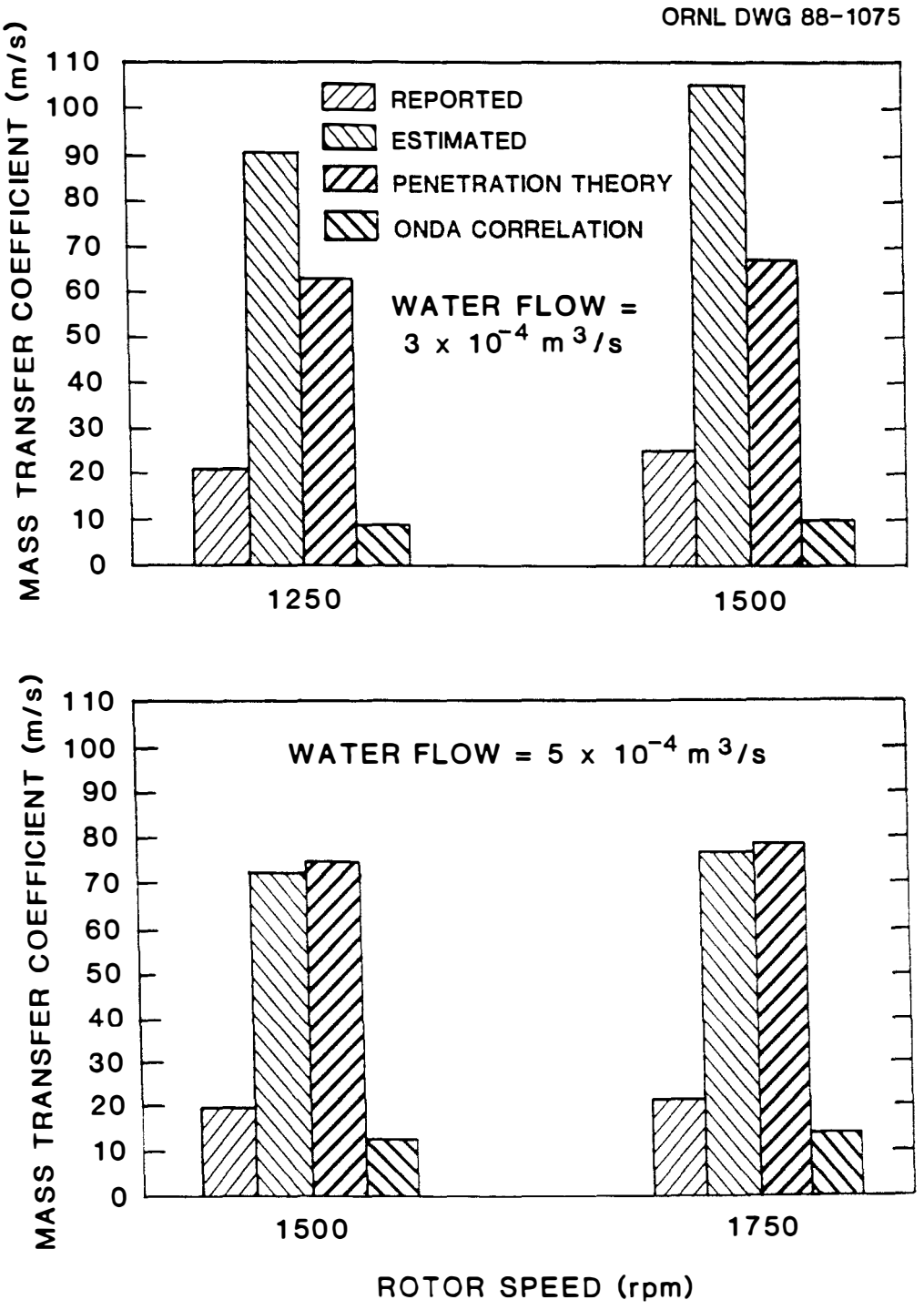

Fig. 3-5. Liquid film mass transfer coefficients for 1 mm glass beads.

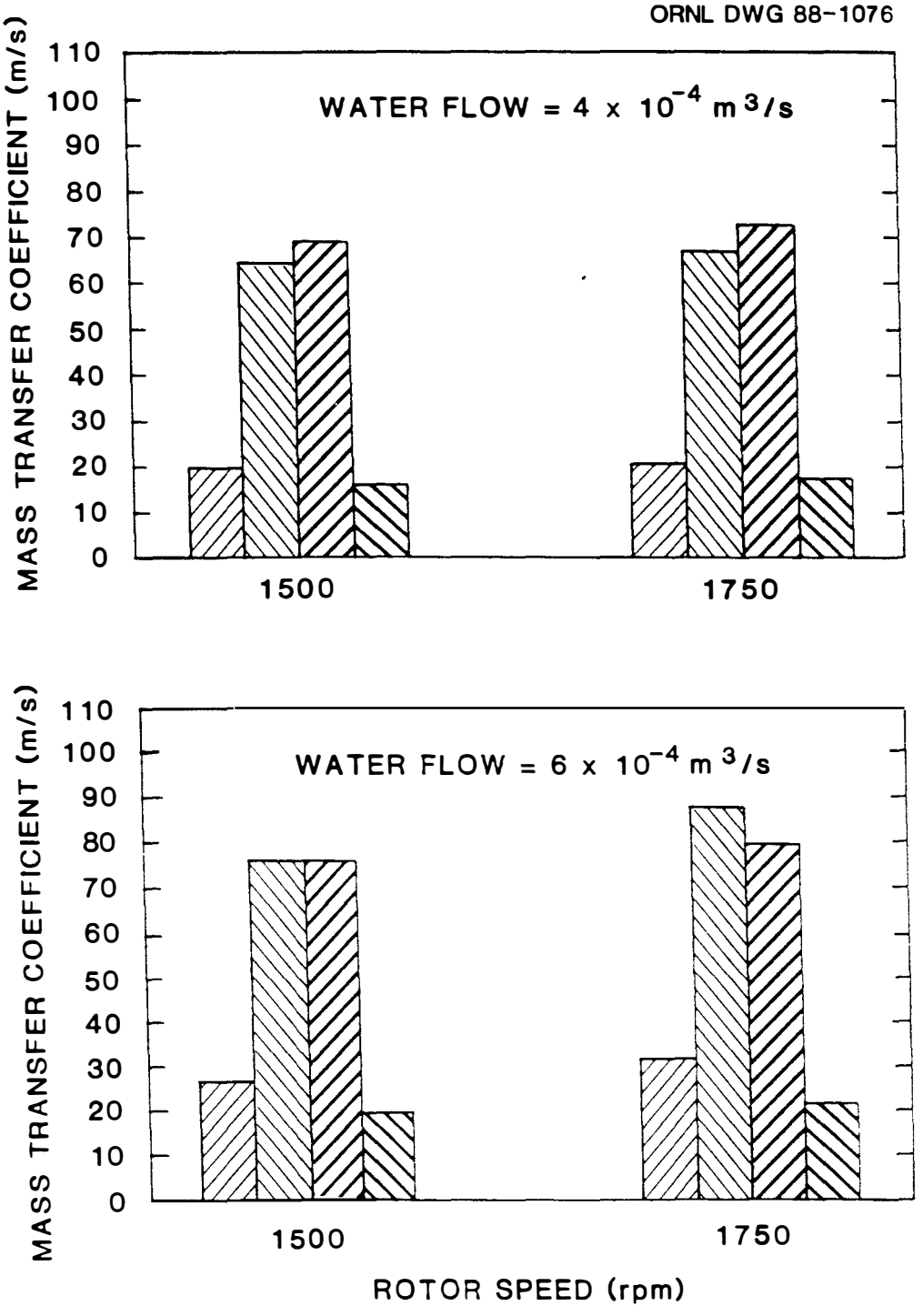

Fig. 3-6. Liquid film mass transfer coefficients for 12 filament copper gauge packing.

"(1) appearance of an opaque mist in the center of the rotor, (2) heavy water spray in the gas exit pipe, and (3) wide fluctuations in the pressure drop and flow meter readings." The results of the flooding test are shown in Fig. 3-7 along with the Sherwood flooding correlation for conventional packed tower. As can be seen from Fig. 3-7, the Sherwood correlation for dumped packings underestimates the flooding superficial gas velocity. Thus, if the Sherwood flooding correlation is used to design a centrifugal vapor liquid contactor, it should provide a conservative estimate of the hydraulic capacity.

The effect of various operating variables on the gas-liquid interfacial area and the liquid side mass transfer coefficient in Munjal's work was determined by the absorption and reaction of carbon dioxide into a sodium hydroxide solution. The packing in these tests was 3 mm diam glass beads. The effects of packing torus rotational speed and bed volume on the gas-liquid interfacial area are shown in Fig. 3-8, and the effect of liquid flow rate is shown in Fig. 3-9. The gas-liquid interfacial area increases with an increase in both the rotational speed of the packing and the liquid flow rate. The increase in the gas-liquid interfacial area with an increase in the bed volume would be expected as long as the liquid flow rate is sufficient to wet the packing. The variation of the liquid side mass transfer coefficient with rotational speed of the packing is shown in Fig. 3-10. Also shown are the mass transfer coefficients calculated from an equation derived by Davidson (1959) for conventional packed towers by assuming that the packing in a column consists of small vertical flat plates. The form of this equation used by Munjal is:

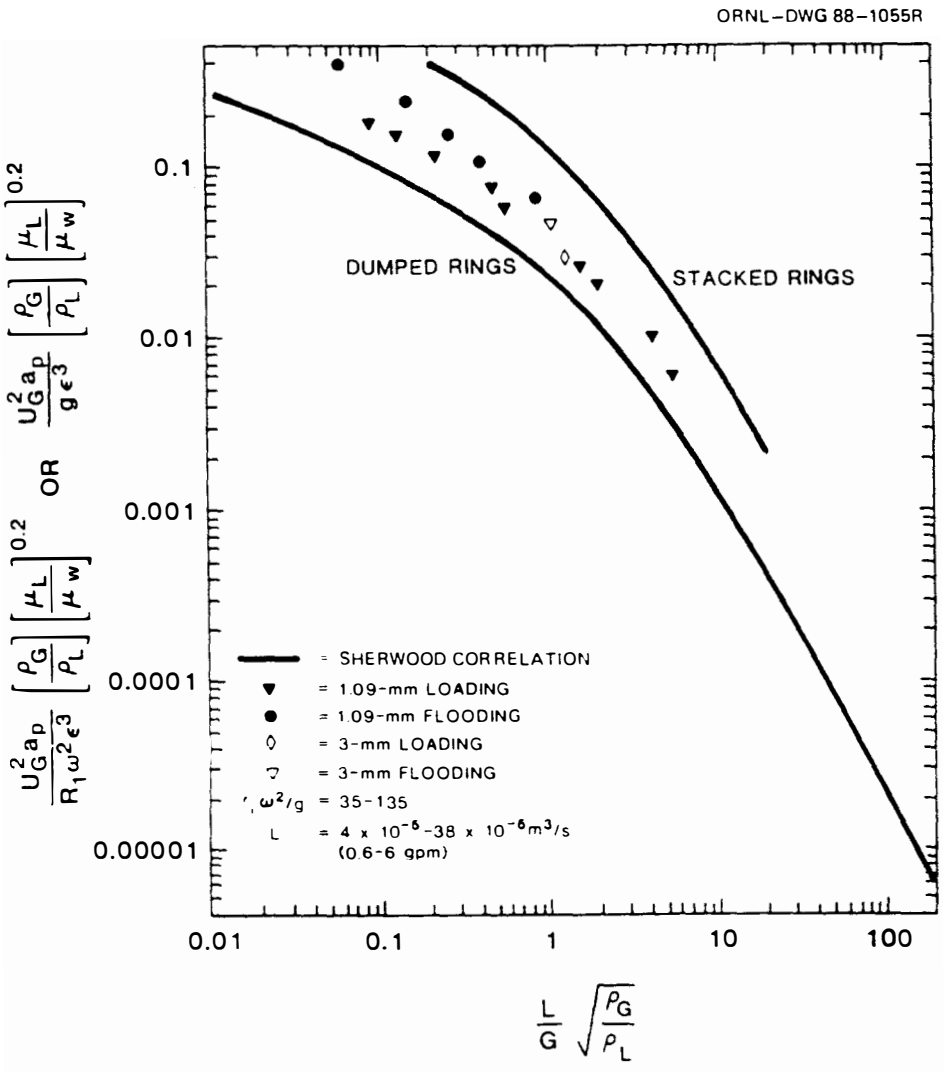

Fig. 3-7. Empirical correlation of flooding and loading data with the Sherwood correlation.

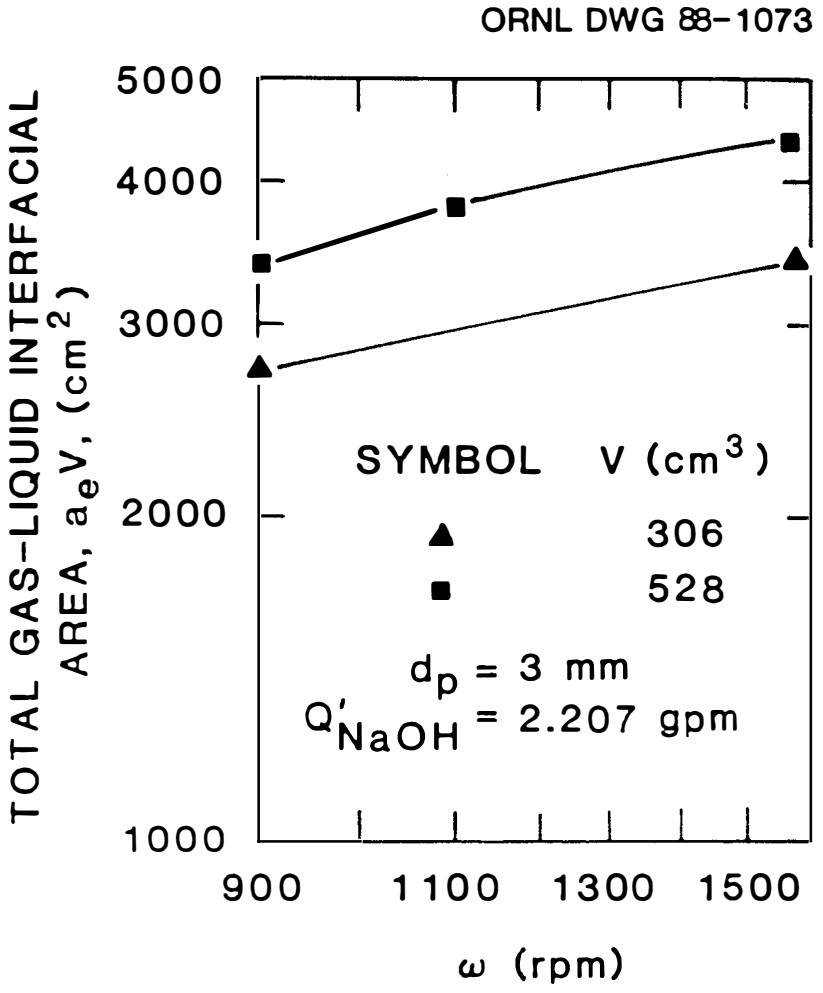

Fig. 3-8. Gas-liquid interfacial area for 3 mm glass beads as a function of rotor speed.

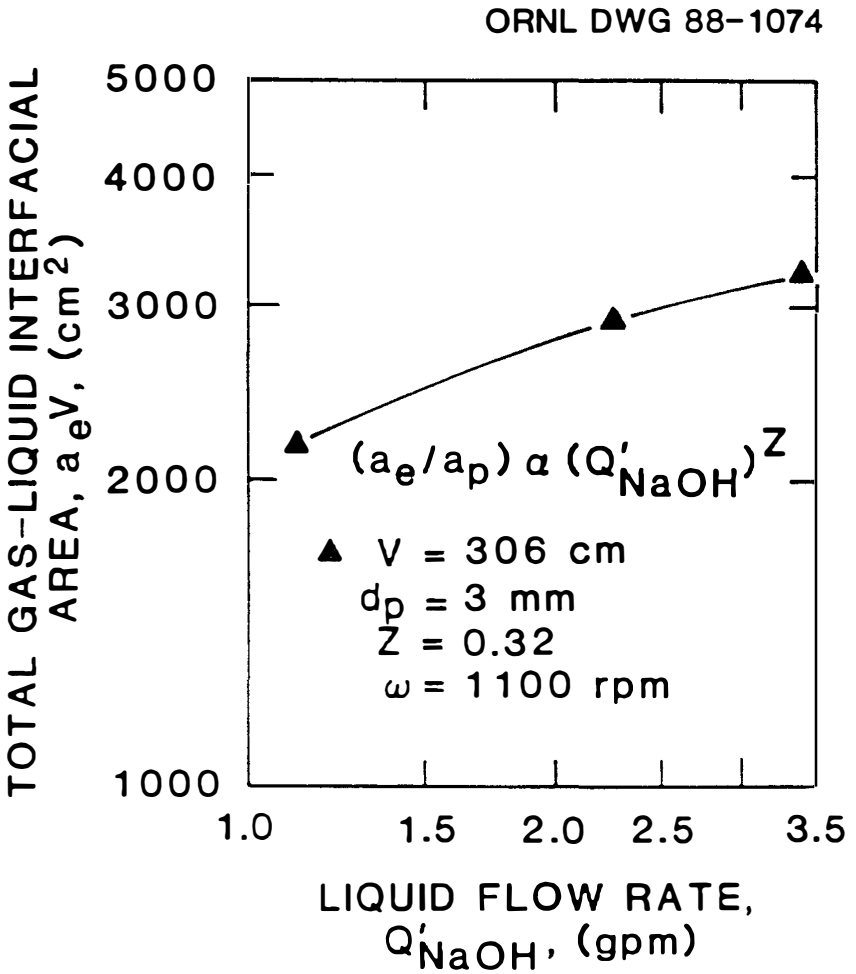

Fig. 3-9. Effects of liquid flow rate on gas-liquid interfacial area.

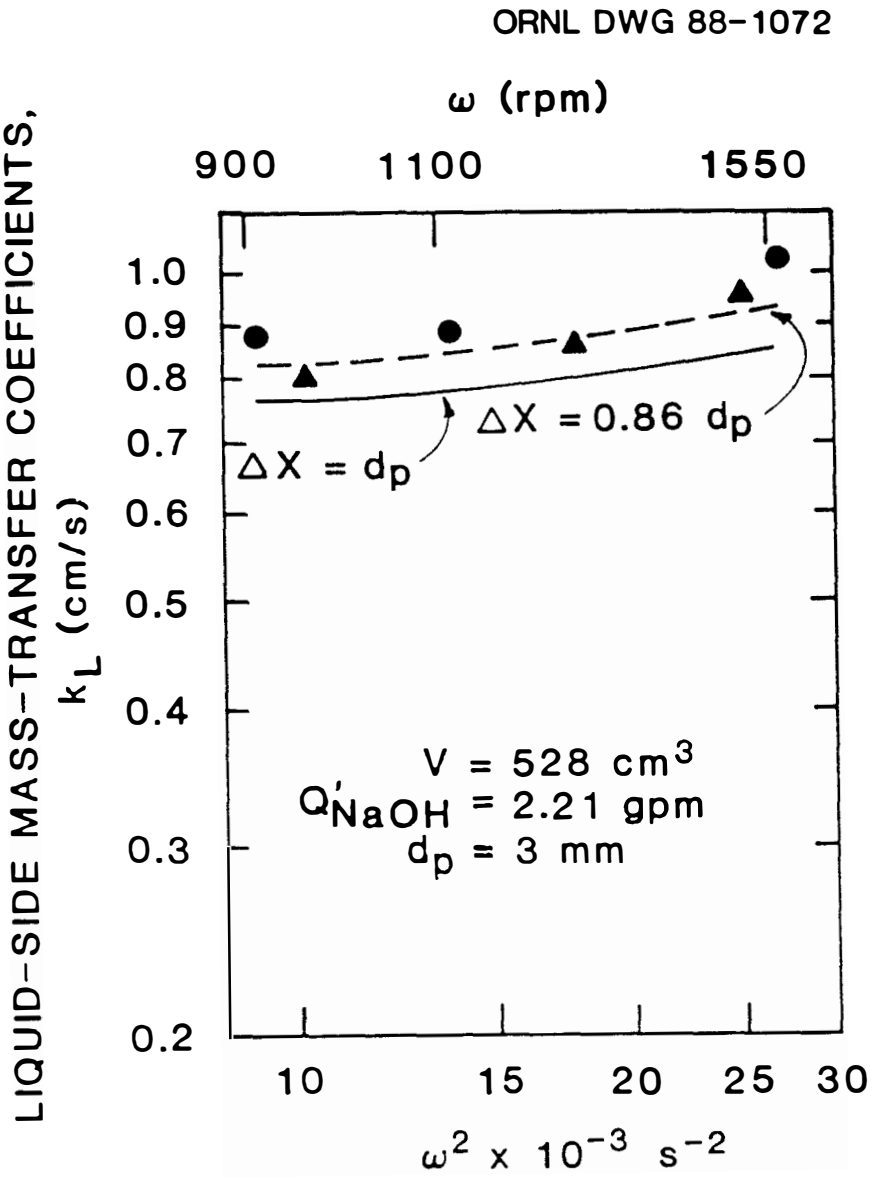

Fig. 3-10. Comparison of experimental and predicted mass transfer coefficients for 3 mm glass beads.

$$k_L = 2.6 \frac{Q_w}{(\Delta X)} Sc^{-1/2} Re^{-2/3} Gr^{1/6} \quad (3\text{-}6)$$

where Q_w = liquid flow rate per unit width in a packed bed

$= (\pi L/2 a_e \rho_L)$, m^2/s

ΔX = distance traveled by the liquid film, m

Re = Reynolds number
$= (2 \pi L/a_e \mu_L)$

Gr = Grashof number
$= (R_{avg} \omega^2 \Delta X^3)/(\mu_L/\rho_L)^2$

$R_{avg} = (R_1 + R_2)/2$, m

L = superficial liquid flow rate based on the average radius, $(kg^3/s\text{-}m^2)$

ω = angular velocity, rad/s

ρ_L = liquid density (kg/m^3)

μ_L = liquid viscosity (kg/m-s)

R_1, R_2 = inner and outer radius of packing (m)

Davidson used two models for the distance traveled by the liquid film. The first model assumed that the packed bed consists of randomly inclined flat surfaces of equal lengths (length equal to packing diameter, d_p) and the second model is similar to the first except the length of the flat surface varies randomly between zero and d_p. For the first model ΔX is equal to d_p in Eq. (3-6) and in the second model ΔX is equal to $d_p/2$. From Fig. 3-10, it appears that the Davidson equation does a reasonable job of predicting the liquid side mass transfer although ΔX equal to $0.86d_p$ describes the experimental data more accurately.

Keyvani and Gardner (1988) studied the operating characteristics of centrifugal vapor-liquid contactors using packing torus made from a

single piece of porous aluminum. Three different packing tori with specific surface areas of 656, 1476, and 2952 m^2/m^3 and void fraction of 0.92 were used in the evaluation. All three packing tori had inner diameter of 25.4 cm, outer diameter of 45.7 cm, and an axial length of 4.4 cm.

Keyvani and Gardner attempted to model the pressure drop characteristics by assuming that the total pressure drop is a sum of the pressure drop inside the rotor, and the pressure drop between the stationary housing and the spinning torus. Momentum balances were written for each component of the total pressure drop and the resulting equations were solved numerically. Although this approach described the data with some degree of accuracy, the assumptions made in deriving the equations are difficult to verify, and the values of the constants needed in the equations are difficult to estimate. In addition, Keyvani and Gardner observed an anomaly in their data which the model could not account for. The pressure drop in their experiments with both liquid and gas flowing was lower than with just the gas flowing. They propose that one possible explanation for the lower pressure drop with both phases flowing may be that the liquid acts as a lubricant thus reducing the drag forces between the gas and the packing material. However, since the area open for flow is constant in a given packing, the velocity of the gas through the packing should be higher with both phases flowing and this should result in higher pressure drop.

Keyvani and Gardner in their mass transfer studies with CO_2-water system found that the results were in general agreement with those

reported by Vivian et al. (1965) and Munjal (1986). They also report that Eqs. (3-3) and (3-5) gave a reasonable prediction of the height of a transfer unit for their system except for the packing with specific surface area of 656 m^2/m^3 in which case the calculated height of a transfer unit was twice as large as the experimental value.

The results of the experiments performed by Keyvani and Gardner to determine the power consumption and residence time are shown in Fig. 3-11 and 3-12. The total power consumption was assumed to be the sum of power consumed in accelerating the liquid, overcoming bearing friction, and windage effects. Of these three, the power to accelerate the liquid is the most dominant term. A small quantity of energy is also recovered from the vapor phase. The liquid residence time was found to vary with rotational speed and the liquid flow rate as would be expected. The mean residence time varied from 0.4 to 1.8 s depending on the operating conditions.

To date there has been only one study done in which the centrifugal vapor-liquid contactor was used to remove volatile organic compounds from groundwater. This study was more of a demonstration of technology rather than a research project. The evaluation was performed at the United States Coast Guard Air Station in Traverse City, Michigan (Dietrich et al., 1987). The groundwater at this site was contaminated with fuel oil components.

The design criteria for the centrifugal vapor-liquid contactor in this demonstration was:

Liquid flow rate	6.3 L/s (100 gal/min)
Gas flow rate	943.3 L/s (2000 scfm)
Percent toluene removal	99.5%

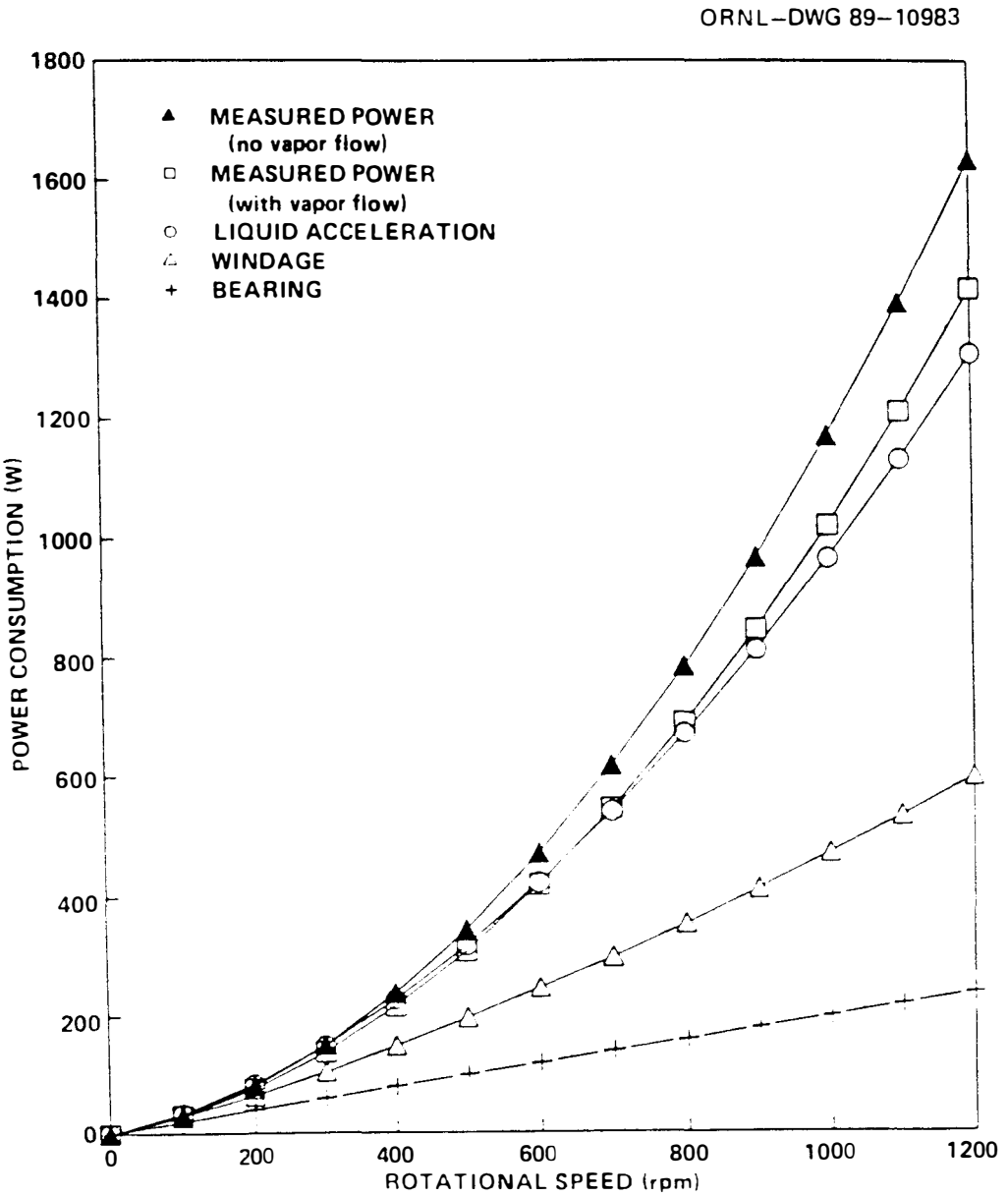

Fig. 3-11. Power consumption as a function of rotor speed at various operating conditions.

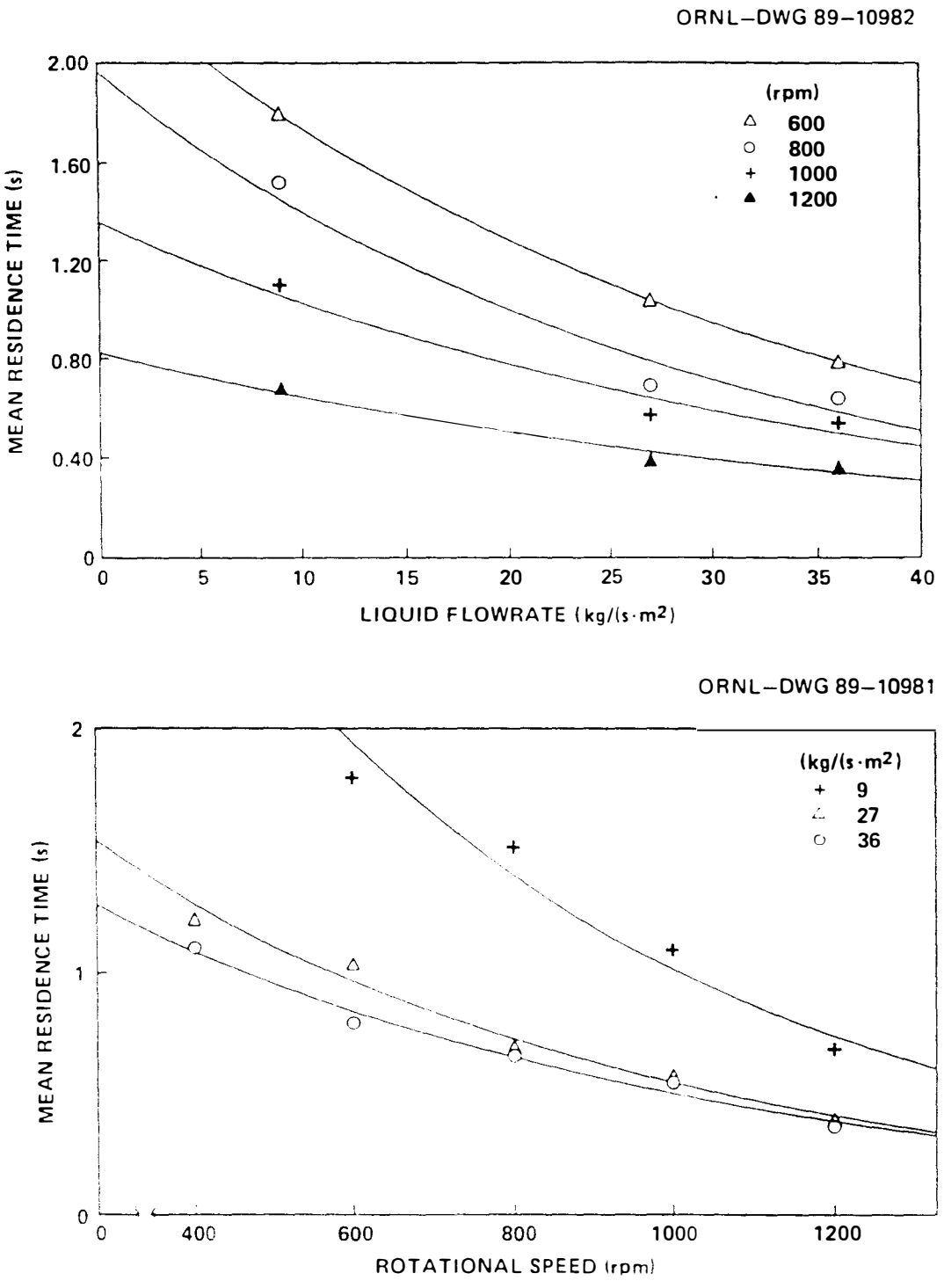

Fig. 3-12. Effect of liquid flow rate and rotor speed on residence time of the liquid phase.

To meet this criteria, a contactor with the following packing torus dimensions was built:

Outer radius	0.4 m
Inner radius	0.14 m
Axial length	0.16 m
Packing voidage	0.9-0.95 %
Packing specific surface area	2500 m^2/m^3

A schematic of the treatment system is shown in Fig. 3-13. The groundwater was pumped from the wells into a 18,750 L (5000 gal.) surge tank. The water was then put through filters (AMF Cuno Model 12DC cartridge filter) and fed to the centrifugal vapor-liquid contactor. The effluent air stream from the contactor was routed to a catalytic destruction unit and discharged to the atmosphere. The catalytic destruction unit was equipped with a heat exchanger which could be used to increase the temperature of the influent water to the centrifugal vapor-liquid contactor.

To determine the hydraulic performance of the centrifugal vapor-liquid contactor, the pressure drop across the packing torus was measured as a function of gas to liquid ratio and torus rotational speed at given liquid flow rates. The results of these experiments are shown in Fig. 3-14. For gas to liquid ratios of 34 and 57 in Fig. 3-14, there is a minimum in the pressure drop curve. The curve at gas to liquid ratio of 20 probably also has a minimum, but it is not seen because data below torus speed of 350 rpm was not taken. To the left of the minimum pressure drop value, the centrifugal force is insufficient to drive the liquid phase through the packing which leads to high pressure drop. The increase in the pressure drop to the right of the minimum value is the result of the packing torus acting as a

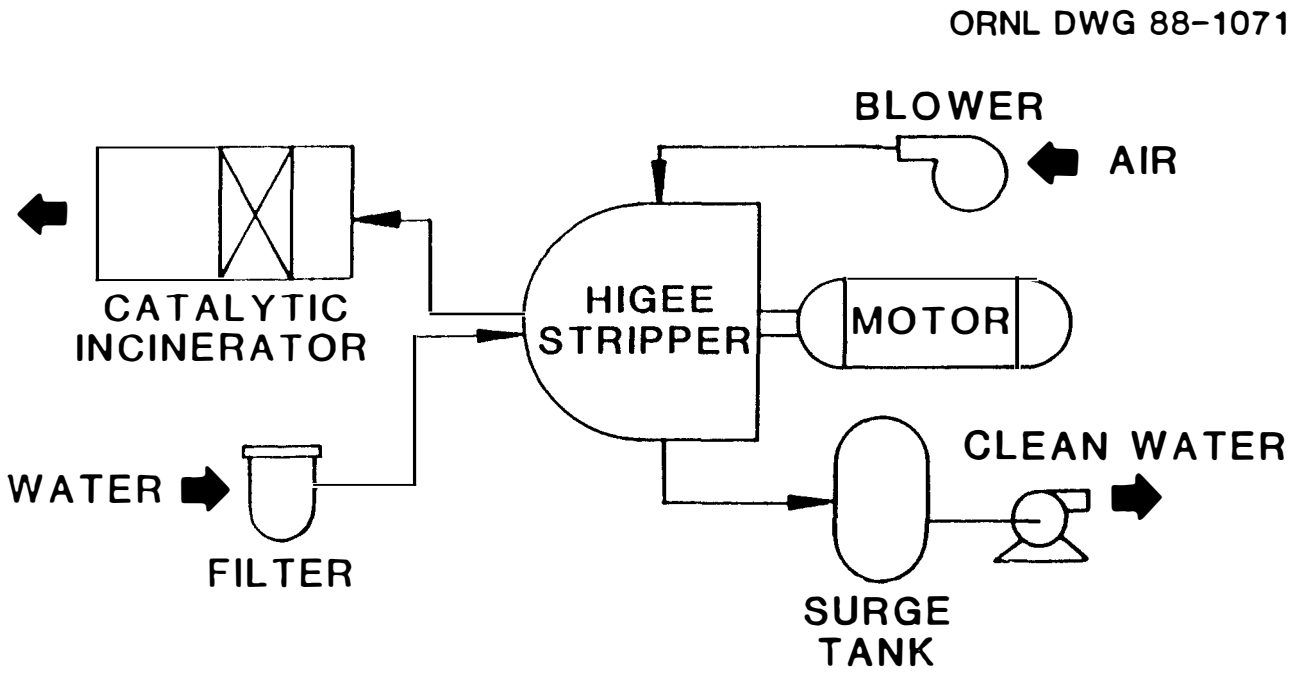

Fig. 3-13. Centrifugal vapor-liquid contactor air stripping system.

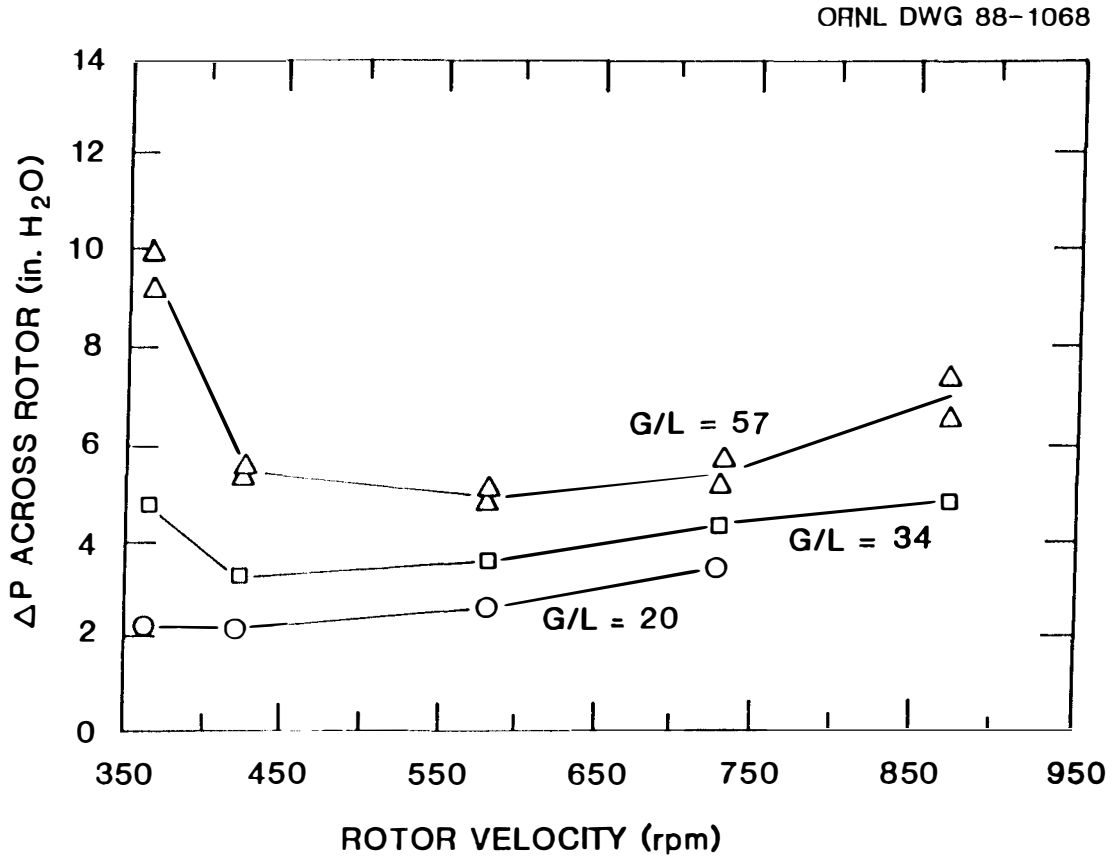

Fig. 3-14. Pressure drop across the rotor for varying rotor speed (liq. flow = 5.0-5.7 L/s; temp. = 12°C).

centrifugal pump which interferes with the inward movement of the vapor phase. In actual operation, the unit will most likely be operated at torus speed higher than that which corresponds to the minimum pressure drop since the mass transfer efficiency also increases with rotor speed.

The percent benzene removal as a function of torus speed and gas to liquid ratio is shown in Fig. 3-15. From Fig. 3-15, it can be seen that the amount of benzene removed increases with an increase in the gas to liquid ratio up to a value of about 30 after which little increase in the removal efficiency is realized with further increase in the gas flow rate. A similar phenomena is observed with the influence of rotor speed on the removal efficiency. Increasing the torus speed above approximately 600 rpm produces very small change in the removal efficiency.

Using the inlet and outlet liquid stream benzene concentrations, Dietrich et al., calculated the liquid film mass transfer coefficient. The results of these calculations are shown in Fig. 3-16. An increase in the mass transfer coefficient with increasing torus speed is observed. The effect of gas to liquid ratio and of liquid flow rate are not as obvious. It should be pointed out that calculating mass transfer coefficients using the inlet-outlet concentrations can be inaccurate since end effects are not taken into account, and only the origin and one additional data point are used to calculate the slope of the line (mass transfer coefficient).

In addition to tests with groundwater, experiments were conducted using synthetic liquid feed containing 1,2-dichloroethane,

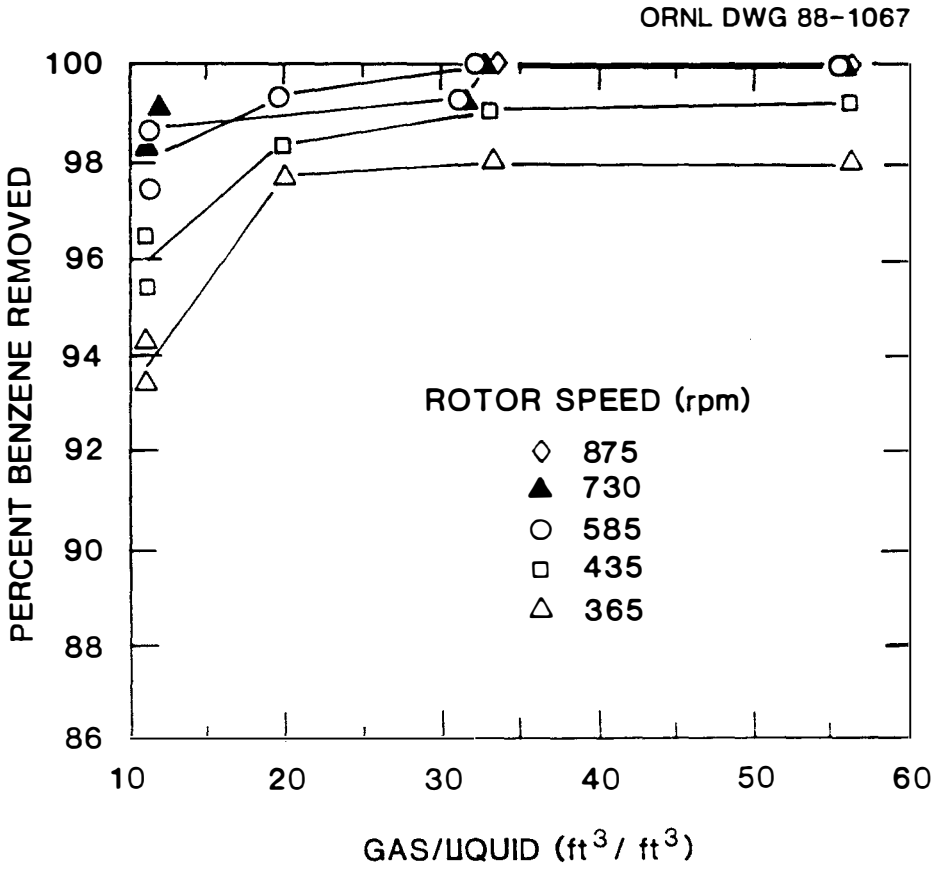

Fig. 3-15. Benzene removal as a function of gas/liquid ratio (liq. flow = 5.0-5.7 L/s; temp = 12°C).

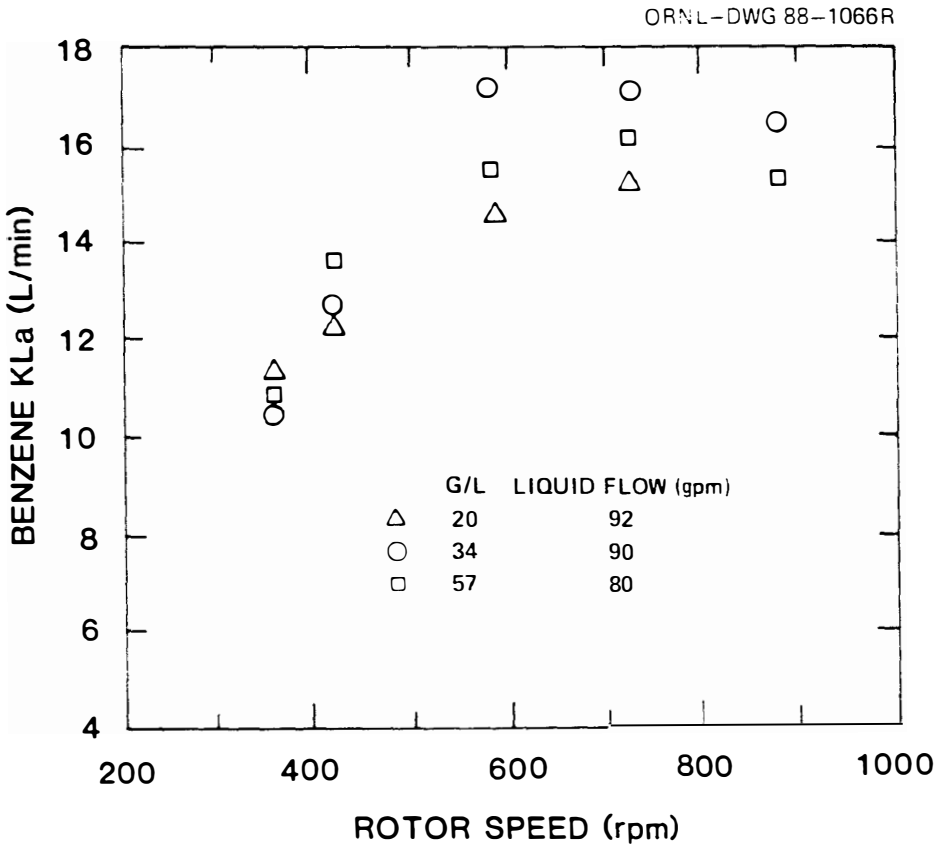

Fig. 3-16. Mass transfer coefficient for benzene.

trichloroethylene, and tetrachloroethylene. Greater than 99% removal of trichloroethylene and tetrachloroethylene was achieved at gas to liquid ratio of 20 and packing torus speed of 435 rpm. Relatively low (<95%) removal of 1,2-dichloroethane was observed even at gas to liquid ratio of 60 and torus speed of 800 rpm. This low removal efficiency is to be expected since the Henry's Law constant for 1,2-dichloroethane is an order of magnitude smaller than the other two compounds. Removal efficiency of greater than 99% was achieved for 1,2-dichloroethane at gas to liquid ratio of 155 and torus speed of 802 rpm.

The low removal efficiency of 1,2-dichloroethane allows analysis of performance of the centrifugal vapor-liquid contactor since the error is the analytical procedure is reduced. The data can be analyzed using the General Linear Modeling (GLM) routine of Statistical Analysis System (SAS). The dependent variable in the model is removal efficiency and the independent variables include liquid flow rate, gas to liquid ratio, acceleration at the inner radius of the packing torus, and the concentration of 1,2-dichloroethane in the influent liquid stream. The analysis reveals that liquid flow rate and gas to liquid ratio had statistically significant effect on the removal efficiency. The independence of removal efficiency from changes in the influent concentration is to be expected since the data were taken in the region in where Henry's Law is valid. The statistically insignificant effect of acceleration on removal efficiency may indicate that as long as there is sufficient centrifugal force present to drive the liquid phase through the packing little improvement in the mass

transfer efficiency is realized with any further increase in the torus rotational speed. If the independence of mass transfer efficiency from acceleration can be proved with further tests, then electrical power costs can be reduced by operating the contactor at lower torus speeds.

The electrical power consumption (torus drive motor, air blower and effluent liquid discharge pump) as a function of gas to liquid ratio and torus speed is shown in Fig. 3-17. The area above the solid line represents conditions at which greater than 99% removal of benzene is attained. At low gas to liquid ratios, higher torus speeds are required to achieve the removal. The higher torus speed probably provides increased contact between the two phases and thus better mass transfer. The increase in power consumption to the right of gas to liquid ratio of 30 is caused by the air blower. From Fig. 3-17, it is apparent that the operating conditions need to be optimized to reduce the electrical power costs.

Although the demonstration of the centrifugal vapor-liquid contactor was successful in the Traverse City study, there were two problems encountered. The first problem was concerned with the biological precipitation of iron which resulted in the plugging of the filters. The effect of solid precipitation on the packing of the centrifugal vapor-liquid contactor is not known at the present since the unit was not operated without the filters. The second problem was the excessive entrainment of liquid in the effluent air stream from the contactor. The excessive moisture was of concern because it could

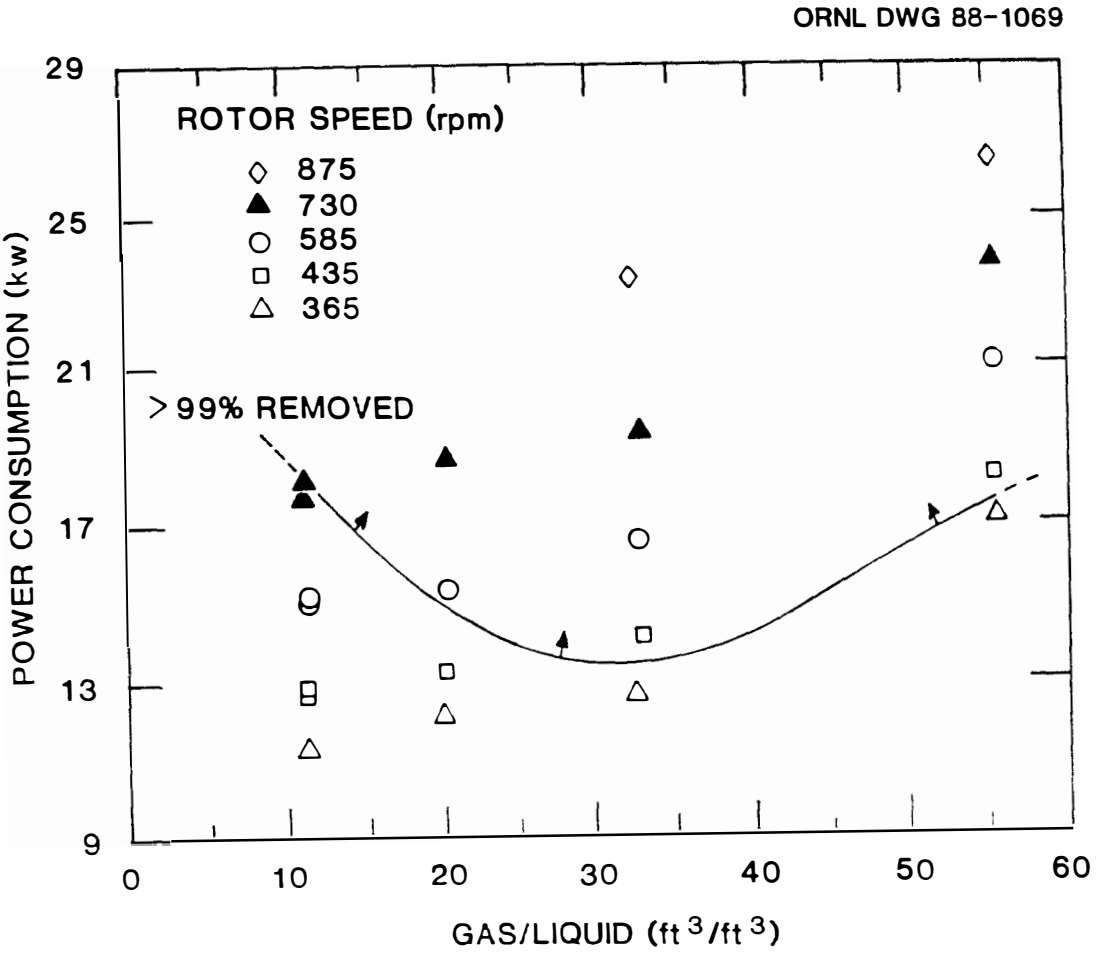

Fig. 3-17. Power consumption as a function of rotor speed and gas/liquid ratio (liq. flow = 5.0-5.7 L/s).

lead to spalling of the catalyst. This problem can be remedied by installing a demister between the centrifugal contactor and the catalyst.

4. DESIGN OF AIR STRIPPERS

4.1 Thermodynamic Considerations

When groundwater containing VOCs is brought into contact with air, the dissolved VOCs will distribute between the two phases so as to establish an equilibrium. At constant pressure and temperature, an equilibrium for a given solute is reached when the fugacity of that compound is equal in the two phases. Fugacity can be thought of as the escaping tendency of a solute from a phase and is reported in units of pressure. Thus, at equilibrium, the following equation can be written for solute i:

$$f_i^L = f_i^V \tag{4-1}$$

where the superscripts L and V refer to the liquid and vapor phases, respectively. The fugacity of the vapor phase is given by:

$$f_i^V = y_i \phi_i P_t \tag{4-2}$$

where y_i = mole fraction of specie i in the vapor phase

ϕ_i = fugacity coefficient for specie i

P_t = total pressure of the system, Pa (atm).

In environmental applications, the vapor phase is assumed to behave ideally (fugacity coefficient equal to unity) and thus the fugacity becomes equal to the partial pressure of the solute.

The liquid phase fugacity is given by:

$$f_i^L = x_i \delta_i f_r \tag{4-3}$$

where x_i = mole fraction of specie i in the liquid phase

δ_i = activity coefficient for specie i

f_r = reference fugacity - fugacity of the pure solute at the system temperature, Pa (atm).

At atmospheric pressure, the reference fugacity is equal to the vapor pressure of the pure solute. The activity coefficient can be described according to two conventions. In the first convention, the activity coefficient goes to one as the mole fraction (x) goes to one, and in the second convention the activity coefficient goes to one at infinite dilution which occurs as the mole fraction of solute goes to zero (Balzhiser et al., 1972). The activity coefficient is often determined by measuring the solubility of the solute in water. For a pure solute in equilibrium with water, the fugacity expression can be written as:

$$x_L \delta_L f_r = x_w \delta_w f_r \qquad (4\text{-}4)$$

where the subscripts L and w refer to the liquid solute and water phases, respectively. The reference fugacity for both phases is the vapor pressure of pure solute. If it is assumed that the solubility of water in the liquid solute phase is negligible, then x_L and δ_L both have a value of unity and the aqueous phase activity coefficient (δ_w) is simply the reciprocal of solubility of the solute in water (x_w). Substituting for the activity coefficient (δ_i) in Eq. (4-3) and then equating Eqs. (4-2) and (4-3) gives:

$$y_i P_t = \frac{x_i \, P^{vap}}{x_w} \qquad (4\text{-}5)$$

dividing both sides by P_t and x_i yields:

$$\frac{y_i}{x_i} = \frac{p^{vap}}{x_w P_t} \qquad (4\text{-}6)$$

The right hand side of Eq. (4-6) is a constant at a given temperature, pressure, and water composition, and is referred to as the Henry's Law constant. This constant is thus used to describe the distribution of a particular VOCs between the liquid and vapor phases. Since the Henry's Law constant is theoretically a function of temperature, pressure and water composition, considerable work has been conducted to discern this relationship.

The temperature dependence of Henry's Law constant is usually described using the Arrhenius type of equation. In using this approach, the enthalpy of volatilization of the solute from the solution is assumed to be constant over the temperature range (Ashworth et al.). The change in Henry's Law constant with pressure is small and can be neglected if the change in pressure is less than one atmosphere (Munz and Roberts, 1987). The effect of water composition on the Henry's Law constant has been studied by several investigators. In their studies with VOCs, Munz and Roberts observed the following: the Henry's Law constant was independent of solute concentration for solute mole fractions up to 10^{-3}, cosolvent concentration in excess of 10 g/L was required to reduce the Henry's Law constant, and presence of other compounds in low concentrations had no effect on Henry's Law constant. Gossett (1987) reports that there was no mutual effect on Henry's Law constant in a mixture of five chlorinated compounds up to

total concentration of 375 mg/L, and that ionic strength of greater than 0.2 M (KCl) was required to decrease the Henry's Law constant by more than 10%. Yurteri et al. (1987) determined Henry's Law constants for trichloroethylene and toluene in distilled/deionized water, natural water, and synthetically prepared water containing known quantities of various salts, surfactants, and humic material. They report that ionic strength combined with surfactants and other dissolved organic matter can have a significant effect on Henry's Law constant at ion strength of 0.06 to 0.12 M, and that Henry's Law constant for toluene in natural water differed by as much as 24% when compared with values in distilled water.

When Henry's Law constant for a particular compound is not available in literature, it can be estimated or determined experimentally. An estimate of Henry's Law constant for a particular compound can be obtained using Eq. (4-6) if the vapor pressure and solubility data are available. Often solubility data is not available and is estimated using activity coefficients calculated from the UNIFAC (UNIQUAC [UNIversal QUAsiChemical] Functional-group Activity Coefficients) group contribution method (Fredenslund et al., 1977). Leighton and Calo (1981) found that for VOCs the UNIFAC consistently over predicts the temperature dependence of the activity coefficient, and Ashworth et al. report that Henry's Law constants estimated using UNIFAC can vary as much as 400% from the experimental values for some compounds. Thus, caution must be exercised when using these estimated Henry's Law constants.

Nirmalakhandan and Speece (1988) present another approach for estimating Henry's Law constant called Quantitative structure-activity relationship (QSAR). The proposed method employs an empirical model based on theoretical considerations and uses "easy-to-calculate structural descriptors." The coefficients for the empirical model were determined using an experimental data set containing 180 compounds.

Several experimental methods have been used to determine Henry's Law constant and these include: batch air stripping method (Mackay et al., 1981), Equilibrium Partitioning in Closed Systems [EPICS] (Gossett, 1987), Multiple Equilibration [ME] (Munz and Roberts, 1981), and direct ratio (Leighton and Calo, 1981). Depending on the type of compounds and desired accuracy, all four methods are capable of providing reproducible values of Henry's Law constants.

Although the Henry's law constant gives the equilibrium distribution of a particular VOCs between the liquid and vapor phases, it does not state how fast or slow the VOCs move between the two phases when non-equilibrium conditions are present. The rate of movement between the two phases in air stripping operations is usually described with one or more of the interfacial mass transfer models.

4.2 Mass Transfer Theory

A rigorous theoretical description of mass transfer between two phases is usually not possible, and thus, conceptually simple models which may not be realistic are used. In these models, it is assumed that most of the resistance to mass transfer exists in thin regions next to the interface in both phases. The resistance (R) to mass

transfer is defined as the ratio of the concentration driving force to the transport rate (N) normal to the interface per unit area and can be written as:

$$R_A = \frac{(C_{Ai} - C_A)}{N_A} \tag{4-7}$$

where C_{Ai} and C_A refer to the concentration of specie A at the interface and in the bulk fluid phase, respectively. Rearrangement of Eq. (4-7) gives:

$$N_A = \frac{1}{R_A} (C_{Ai} - C_A) \tag{4-8}$$

The quantity of $1/R_A$ is referred to as the mass transfer coefficient and is denoted using the letter K. With this substitution, Eq. (4-8) becomes:

$$N_A = K_A (C_{Ai} - C_A) \tag{4-9}$$

Since the mass transfer coefficient in Eq. (4-9) is simply a proportionality constant, several models have been formulated to relate this constant to physical phenomena that may be occurring at the interface between the two phases. The three most commonly used models are stagnant-film model, penetration model, and surface renewal model.

The stagnant film model is about 80 years old and is the simplest to visualize. This model assumes that there is a stagnant film on both sides of the interface as shown in Fig. 4-1, and that the mass transfer through both films is by molecular diffusion. This model also

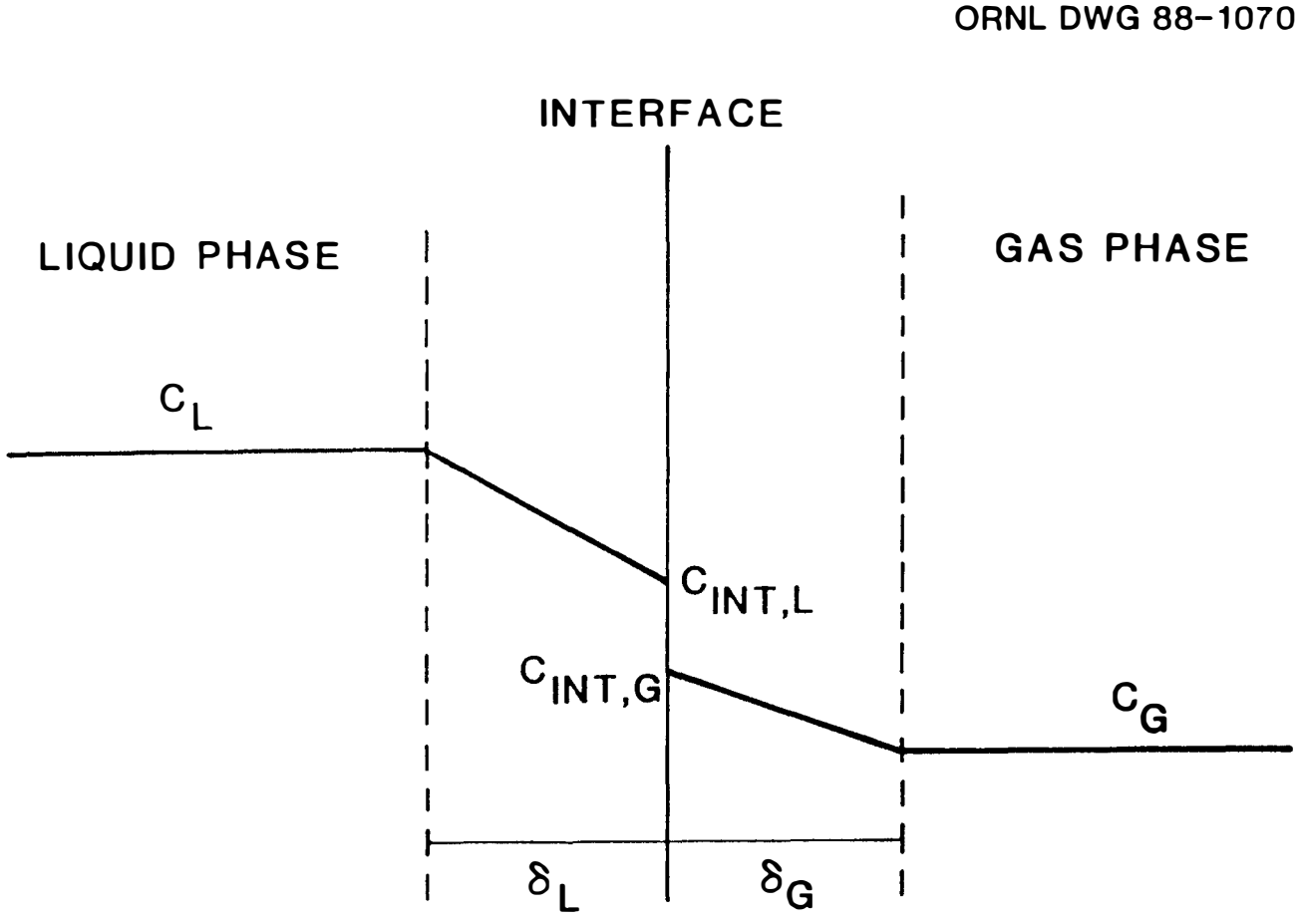

Fig. 4-1. The stagnant film model.

assumes that the total resistance to mass transfer is the sum of the resistance in stagnant film of each phase and that there is no resistance to mass transfer at the boundary between the two phases. The boundary is defined as the "distance corresponding to molecular mean free paths in the two phases on either side of the phase boundary" (Sherwood et al., 1975). According to this model, the rate of transfer of a solute specie A from the interface to the bulk fluid or vice versa is:

$$N_A = \frac{D_A}{\delta} (C_{Ai} - C_A) \qquad (4\text{-}10)$$

where D_A = diffusion coefficient in the respective phase (m^2/s)

δ = film thickness (m).

The hydrodynamic and physical properties of a system are incorporated into the thickness of the film in this model. Comparing Eq. (4-9) and (4-10), it can be seen that the stagnant film model predicts a first order dependence of the mass transfer coefficient on the molecular diffusivity. Some experimental data indicate that this dependence may not be correct.

Although the stagnant-film model is adequate for some applications, it does not totally represent what actually occurs in a packed column. In a packed column, a particular liquid element is briefly exposed to the vapor phase as the liquid flows over the small packing pieces and then the liquid is mixed. The penetration model attempts to describe the mass transfer in a packed column by assuming

that small fluid elements from the bulk fluid are brought to the interface for a short time period. After brief exposure at the interface, the element is transported back into the bulk fluid. It is assumed that the fluid element is stagnant during the stay at the interface. The mass transfer rate for this model is given by:

$$N_A = (4D_A/\pi t)^{1/2} (C_{Ai} - C_A) \qquad (4\text{-}11)$$

where t is the exposure time. The exposure time takes into account the hydrodynamic and physical properties of a system. Comparison of Eq. (4-11) with Eq. (4-9), shows that the penetration model predicts that the mass transfer coefficient varies with the square root of molecular diffusivity. Vivian and King (1964) found that the removal rate of slightly soluble gases from water in a packed tower varied with the square root of molecular diffusivity thus providing some validity to the penetration model.

The surface-renewal model is an extension of the penetration model. Unlike the penetration model which assumes that all the fluid elements are exposed for a constant time period, the surface-renewal model uses varying exposure time period which can range from zero to infinity. In this model, a surface age distribution function $\phi(t)$ is introduced and is defined as:

$$\phi(t) = S\, e^{-t} \qquad (4\text{-}12)$$

where S is the fraction rate of surface renewal of the area exposed to penetration and is assumed to be a constant. The mass transfer rate according to the surface-renewal model is:

$$N_A = (D_A S)^{1/2} (C_{Ai} - C_A) \qquad (4\text{-}13)$$

Like the penetration model, the surface-renewal model predicts a square root dependence of the mass transfer coefficient on the diffusivity.

Although all three models given above are mathematically simple, each contains a parameter (δ,t,S) which is difficult to measure experimentally. In addition, the dependence of the mass transfer rate on molecular diffusivity is difficult to verify experimentally because diffusivities cannot be accurately measured at the present (Charpentier, 1981). Even with these shortcomings, these models have been successfully used as starting points for developing empirical correlations needed to design packed vapor-liquid contactors.

4.3 Design Equations

The concepts used to design conventional packed towers can be modified for the design of the centrifugal vapor-liquid contactors. In designing a conventional packed tower, the diameter of the tower and the depth of packing are the two variables which need to be determined. Similarly for the centrifugal vapor liquid contactor, the cross-sectional at the inner radius and a value of the outer radius are the two variables that need to be determined. An additional complexity arises in the design of the centrifugal vapor-liquid contactor because the cross-sectional area at the inner radius can be varied by changing either the radius or the axial length. This results in an iterative design process in which the inner radius, outer radius, and axial length are varied to arrive at an optimum design solution.

The cross-sectional area required at the inner radius is dependent upon the hydraulic capacity required. Munjal (1986) has presented data that indicates the Sherwood flooding correlation shown in Fig. 4-2 may be used to determine the cross-sectional area at the inner radius. The data presented is, however, for a single type of packing, and thus, hydraulic tests with other packing are desirable to further validate the application of the Sherwood flooding correlation.

The equation needed to calculate the outer radius of the packing torus can be derived using the transfer unit concept from conventional packed tower design. Using the schematic of the packing torus shown in Fig. 4-3, a material balance can be written for a differential volume of the packing. At steady state, the material balance for the liquid phase is:

$$LX_1 - LX_2 - K_La(X - X^*)\,\Delta V = 0 \qquad (4\text{-}14)$$

where L = liquid flow (kg/s)

X_1, X_2 = mole fraction of solute in the inlet and outlet liquid streams to and from the differential volume, respectively

$X - X^*$ = driving force for mass transfer in the differential volume

ΔV = differential volume (m^3)

Rearranging Eq. (4-14) gives:

$$-\frac{L(X_2 - X_1)}{\Delta V} = K_La(X - X^*) \qquad (4\text{-}15)$$

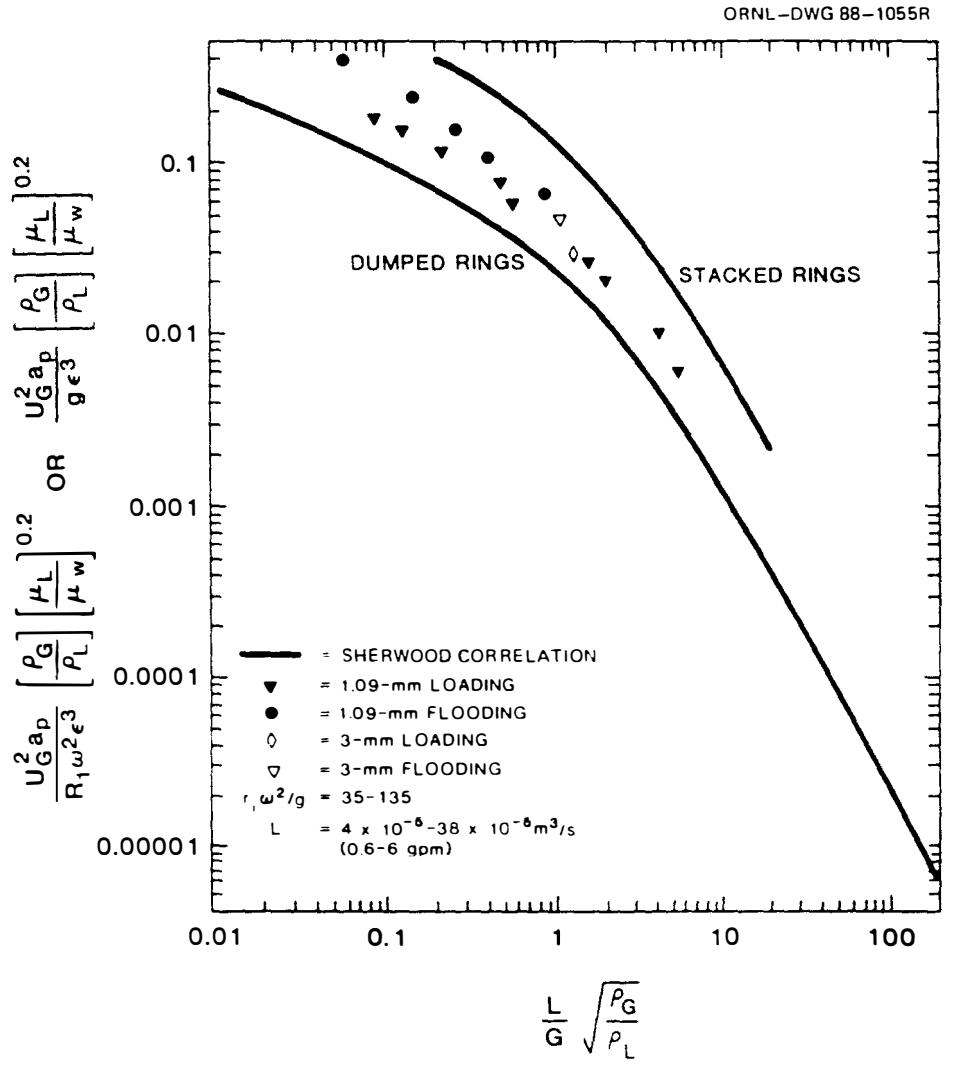

Fig. 4-2. Sherwood flooding correlation.

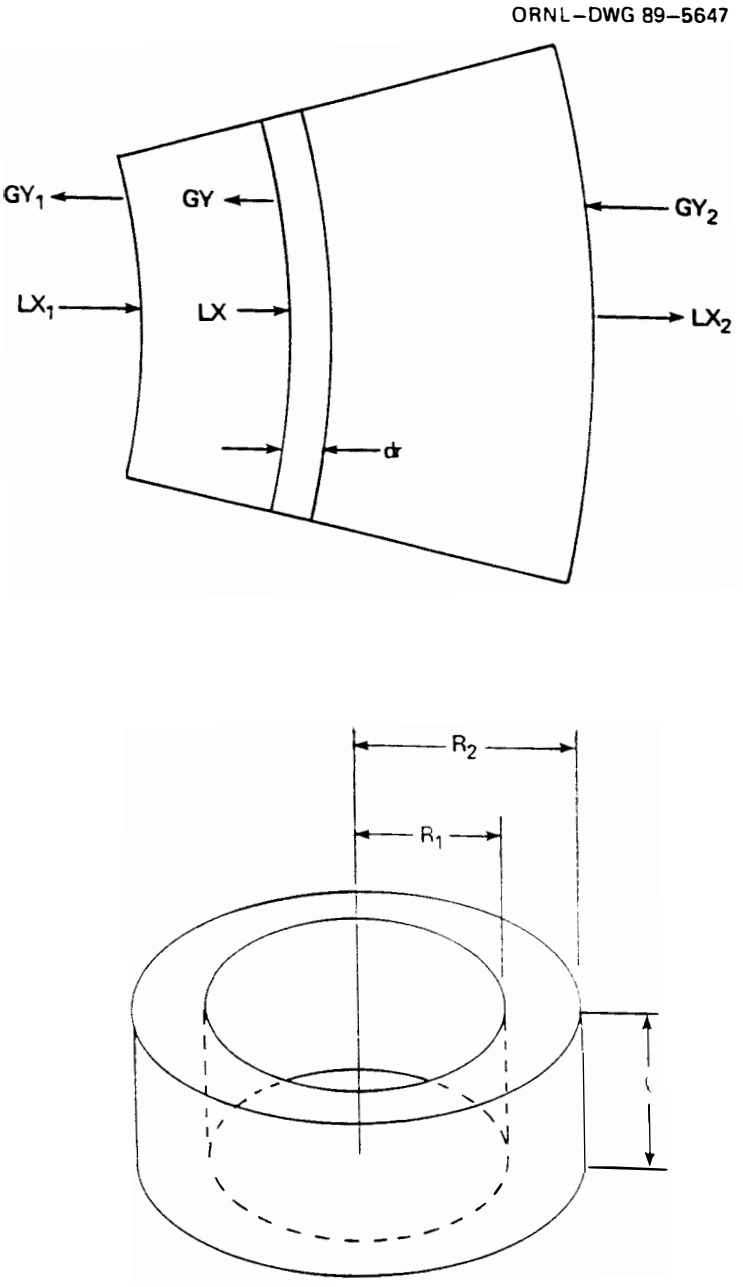

Fig. 4-3. Differential volume element for the packing torus.

The differential form of Eq. (4-15) can be written as:

$$- \frac{L\, dX}{dV} = K_L a(X - X^*) \tag{4-16}$$

The volume differential can be written in terms of the radius as:

$$dV = 2\pi l r dr \tag{4-17}$$

where l is the axial length of the packing. Substitution of Eq. (4-17) into Eq. (4-16) and subsequent rearrangement gives:

$$- \frac{L}{lK_L a} \int_{X_1}^{X_2} \frac{dx}{(X - X^*)} = 2\pi \int_{r_1}^{r_2} r dr \tag{4-18}$$

incorporating the negative sign into the integral on the left hand side yields:

$$\frac{L}{lK_L a} \int_{X_2}^{X_1} \frac{dx}{(X - X^*)} = 2\pi \int_{r_1}^{r_2} r dr \tag{4-19}$$

The equation is now in a form similar to that used for conventional packed towers. Since the height of a transfer unit (HTU) term used in design of conventional towers does not seem to be appropriate in polar coordinates, an area of transfer unit (ATU) expression can be used and written as:

$$ATU = \frac{L}{lK_L a} \tag{4-20}$$

The number of transfer unit (NTU) characterizes the difficulty of removing the VOCs from the groundwater and is independent of the coordinate system. The NTU can be expressed as:

$$NTU = \int_{X_2}^{X_1} \frac{dx}{(X - X^*)} \tag{4-20}$$

Equation (4-21) can be integrated to give (Colburn, 1941):

$$NTU = \frac{\ln\left[\left[\frac{X_1 - Y_2/H}{X_2 - Y_2/H}\right](1 - 1/S) + (1/S)\right]}{(1 - 1/S)} \tag{4-22}$$

where H is the Henry's Law constant and S is the stripping factor which is defined as:

$$S = \frac{HG}{L} \tag{4-23}$$

where G is the air flow rate. Combining Eq. (4-22) with Eq. (4-19) gives:

$$\frac{L}{lK_La} \frac{\ln\left[\left[\frac{X_1 - Y_2/H}{X_2 - Y_2/H}\right](1 - 1/S)+(1/S)\right]}{(1 - 1/S)} = \pi(r_2^2 - r_1^2) \tag{4-24}$$

In order to use Eq. (4-24), it is necessary to know the values of the Henry's Law constant and the mass transfer coefficient. Experimentally determined Henry's Law constants for some of the environmentally harmful VOCs are available in the literature and these are given in

Tables 4-1 through 4-3. If the Henry's Law constant for a particular compound is not available, it can be estimated using the procedure outlined in Section 4.1.

Experimental values of mass transfer coefficients for the centrifugal vapor-liquid contactor are almost nonexistent. Even the small quantity of data that is available is difficult to interpret due to incompleteness or scatter.

Two empirical correlations which might be used to estimate the mass transfer coefficient have been proposed in the literature. Both of these empirical correlations are based on the penetration model. The first correlation is that proposed by Tung and Mah (1985)(Eq. 3-3):

$$\frac{k_l\, d}{D} = 0.96\ Sc^{1/2}\ Re^{1/3} \left[\frac{a_t}{a_e}\right]^{1/3} \left[\frac{d^3\ \rho^2\ g}{\mu^2}\right]^{1/6}$$

and the second one is that used by Vivian et al. (1965):

$$\frac{(k_L a)d}{D} = 0.023\ Sc^{1/2}\ Gr^{0.38} \left(\frac{dL}{\mu}\right)^{1/2} \left\{1\text{-}1.02\ \exp\left[-\ (0.15) \left(\frac{dL}{\mu}\right)^{0.4}\right]\right\} \qquad (4\text{-}25)$$

where d = characteristic dimension of packing (m),

D = liquid-phase diffusion coefficient (m^2/s),

L = liquid mass loading ($kg/s\text{-}m^2$),

and other variables are the same as those defined in Eq. 3-3. Notice that this equation unlike that used by Tung and Mah does not require knowledge of the interfacial area.

Table 4.1. Coefficients[a] for the temperature dependence of Henry's Law Constant expression for the temperature range from 0 to 30°C (1 atm).

Compound	A	B
1,1,1-trichloroethane (1,1,1-$C_2H_3Cl_3$)	21.68	4375
1,1-dichloroethylene (1,1-$C_2H_2Cl_2$)	23.12	4618
trichloroethylene (C_2HCl_3)	21.89	4647
tetrachloroethylene (C_2Cl_4)	22.68	4735
methylene chloride (CH_2Cl_2)	17.42	3645
chloroform ($CHCl_3$)	18.97	4046
carbon tetrachloride (CCl_4)	22.22	4438
ethylene dichloride (1,2-$C_2H_4Cl_2$)	16.05	3539
1,1,2-trichloroethane (1,1,2-$C_2H_3Cl_3$)	16.20	3690
s-tetrachloroethane (s-$C_2H_2Cl_4$)	14.91	3547
1,2-dichloropropane (1,2-$C_3H_6Cl_2$)	19.60	4333
1,3-dichloropropane (1,3-$C_3H_6Cl_2$)	17.13	3917
1,2,3-trichloropropane (1,2,3-$C_3H_5Cl_3$)	14.61	3477
1-chlorobutane (1-C_4H_9Cl)	18.51	3482
2-chlorobutane (2-C_4H_9Cl)	22.29	4499
1,4-dichlorobutane (1,4-$C_4H_8Cl_2$)	13.79	3128
1-chloropentane (1-$C_5H_{11}Cl$)	23.04	4727
1,5-dichloropentane (1,5-$C_5H_{10}Cl_2$)	8.79	1597
1-chlorohexane (1-$C_6H_{13}Cl$)	22.16	4459
benzene (C_6H_6)	19.02	3964
chlorobenzene (C_6H_5Cl)	16.83	3466
toluene ($C_6H_5CH_3$)	18.46	3751
o-chlorotoluene (o-$C_6H_4(CH_3)Cl$)	17.18	3545

[a] $m = y/x = \exp [A - B/T]$ where T is in K.

Source: Leighton, D. T. and J. H. Calo, 1981.

Table 4-2. Henry's Law Constant as a function of temperature for the temperature range from 10 to 35°C.

Compound	Temperature dependence[a] regression equation (T, K) H = exp(A − B/T)	
	A	B
tetrachloroethylene	12.45	4918
trichloroethylene	11.37	4780
1,1-dichloroethylene	8.845	3729
cis-1,2-dichloroethylene	8.479	4192
trans-1,2-dichloroethylene	9.341	4182
vinyl chloride	7.385	3286
1,1,1-trichloroethane	9.777	4133
1,1-dichloroethane	8.637	4128
chloroethane	5.974	3120
carbon tetrachloride	11.29	4411
chloroform	9.843	4612
dichloromethane	6.653	3817
chloromethane	9.358	4215

[a]The units for the Henry's Law Constant are m^3-atm/mol.

Source: Gossett, J. M., 1987.

Table 4-3. Component parameters for the temperature regression equation.

Component	A	B	r^2
nonane	- 0.1847	202.1	0.013
n-hexane	25.25	7530	0.917
2-methylpentane	2.959	957.2	0.497
cyclohexane	9.141	3238	0.982
chlorobenzene	3.469	2689	0.965
1,2-dichlorobenzene	-1.518	1422	0.464
1,3-dichlorobenzene	2.882	2564	0.850
1,4-dichlorobenzene	3.373	2720	0.941
o-xylene	5.541	3220	0.966
p-xylene	6.931	3520	0.989
m-xylene	6.280	3337	0.998
propylbenzene	7.835	3681	0.997
ethylbenzene	11.92	4994	0.999
toluene	5.133	3024	0.982
benzene	5.534	3194	0.968
methyl ethylbenzene	5.557	3179	0.968
1,1-dichloroethane	5.484	3137	0.993
1,2-dichloroethane	-1.371	1522	0.878
1,1,1-trichloroethane	7.351	3399	0.998
1,1,2-trichloroethane	9.320	4843	0.968
cis-1,2-dichloroethylene	5.164	3143	0.974
trans-1,2-dichloroethylene	5.333	2964	0.985
tetrachloroethylene	10.65	4368	0.987
trichloroethylene	7.845	3702	0.998
tetralin	11.83	5392	0.996
decalin	11.85	4125	0.919
vinyl chloride	6.138	2931	0.970
chloroethane	4.265	2580	0.984
hexachloroethane	3.744	2550	0.768
carbon tetrachloride	9.739	3951	0.997
1,3,5-trimethylbenzene	7.241	3628	0.962
ethylene dibromide	5.703	3876	0.928
1,1-dichloroethylene	6.123	2907	0.974
methylene chloride	8.483	4268	0.988
chloroform	11.41	5030	0.997
1,1,2,2-tetrachloroethane	1.726	2810	0.194
1,2-dichloroproprane	9.843	4708	0.820
dibromochloromethane	14.62	6373	0.914
1,2,4-trichlorobenzene	7.361	4028	0.819
2,4-dimethylphenol	-16.34	-3307	0.555
1,1,2-trichlorotrifluoroethane	9.649	3243	0.932

Temp. regression equation: $H = \exp(A - B/T)$, H in atm-m^3/mol T in K.

Source: Ashworth, et al.

The accuracy of these correlations for the design of a centrifugal vapor-liquid contactor is still in question because the data needed to establish their validity is lacking.

Summary

The principles used in the design of conventional packed towers for air stripping operations can be easily modified for the design of the centrifugal vapor-liquid contactor. Equilibrium data for the VOCs and a value of the mass transfer coefficient are required for the design of both types of contactors. The equilibrium data for many VOCs are available in the literature while data on the mass transfer coefficients in the centrifugal vapor-liquid contactor are lacking.

5. EXPERIMENTAL

The centrifugal vapor-liquid contactor employed in this study was a part of a larger system which was used to demonstrate innovative air stripping techniques and materials in concert with emissions control technologies. The project was sponsored by the Air Force Engineering & Services Center (AFESC) at Tyndall Air Force Base, Florida, and the tests were conducted at Eglin Air Force Base in Florida. The groundwater at Eglin Air Force Base is contaminated with JP-4 jet fuel. A brief description of the overall system is given below as a background material for the reader.

5.1 Air Stripping System

A schematic of the air stripping system is shown in Fig. 5-1. The contaminated groundwater from the wells was passed through a 50 μm filter (Cole and Parmer) and routed to a 7,560 L (2000 gal.) surge tank. The surge tank could be filled either from the bottom or the top. The surge tank contained 1.5-in. polypropylene balls which minimized the loss of the VOCs. From the surge tank, the groundwater was routed either to the conventional packed tower or the centrifugal vapor-liquid contactor. The groundwater flow rate to the strippers was measured using a ComPak 8500 flow transmitter (Signet Industrial, El Monte, California) with range of 0 to 5 L/s (0 to 80 gal/min). A rotameter was also installed in series with the paddle-wheel sensor for comparison purposes. The VOC depleted water from the strippers was discharged to an existing aeration basin or sprayed on the original spill site using sprinklers.

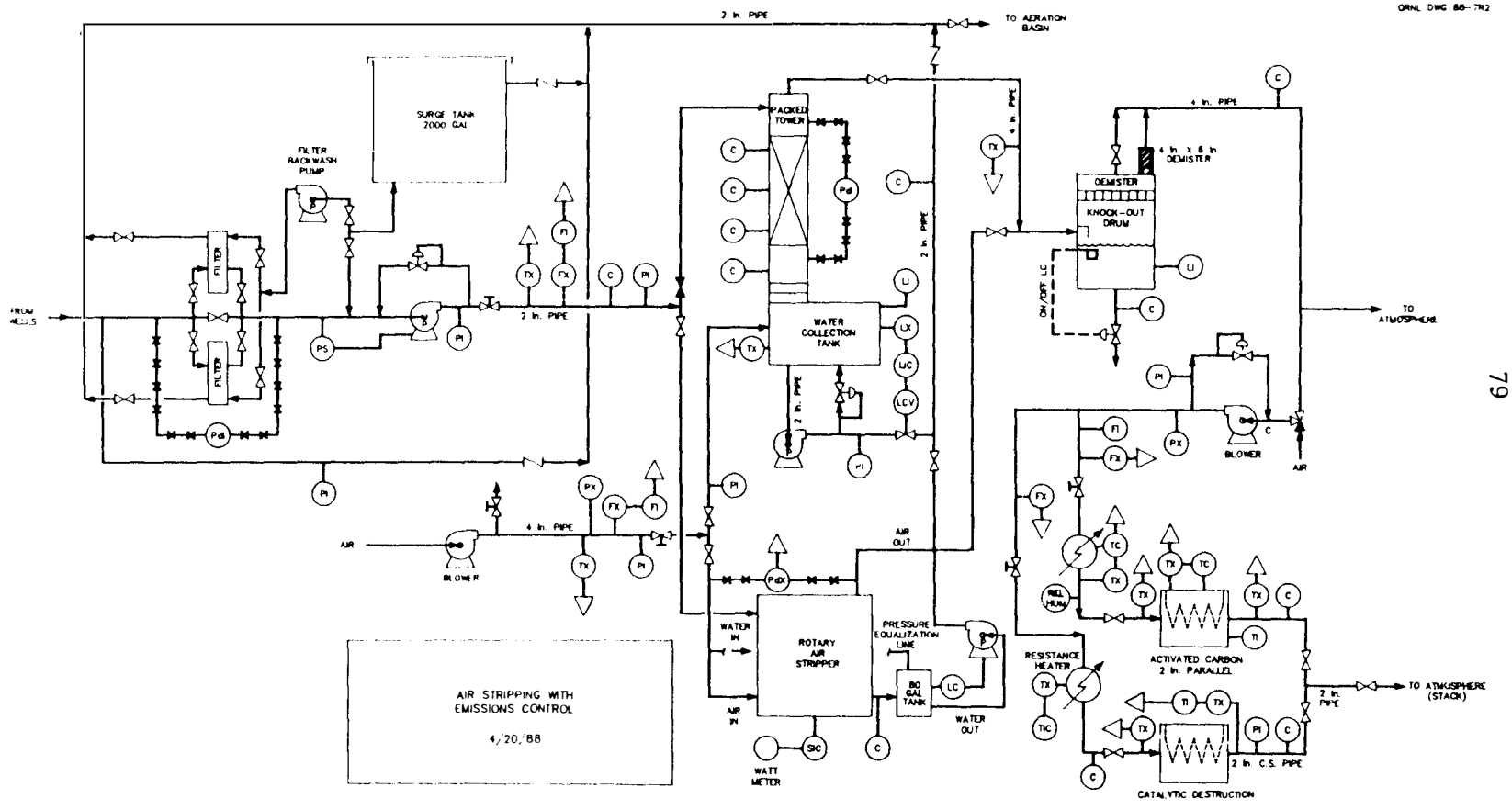

Fig. 5-1. A schematic of air stripping with emissions control system.

The air to both strippers was supplied by 60.96 cm (24-in.) blower (New York Blower) which could deliver 330 L/s (700 cfm) of air at 11.2 kPa (45-in. of H_2O) static pressure and 21.1°C (70°F). The air flow rate to the strippers was measured using an orifice meter. The exit air stream from either the conventional packed tower or the centrifugal vapor-liquid contactor was passed through a knockout drum to remove the excessive quantities of mist. The major portion of the air from the knockout drum was discharged to the atmosphere while a small side stream was routed to an activated carbon bed or a catalytic destruction unit. The air from the carbon bed and the catalytic unit was discharged to the atmosphere.

All the instruments shown with triangles in Fig. 5-1 were tied to a personal computer based data acquisition and control system. Labtech Notebook (Omega Engineering, Inc., Stamford, Connecticut) software package was used for data storage and retrieval.

5.2 Centrifugal Vapor-Liquid Contactor

A schematic of the centrifugal vapor-liquid contactor system is shown in Fig. 5-2. The unit was skid mounted for ease of transportation and installation. The housing that contains the rotating packing was made from a 850 L (225 gal.) fiberglass tank (Warner Fiberglass Products, Belding, Michigan). A fiberglass housing is lighter than a comparable sized metal housing and also provides superior corrosion resistance.

The structural support for the rotating packing was made from aluminum. The bottom plate of the rotor was machined from 7.5 cm

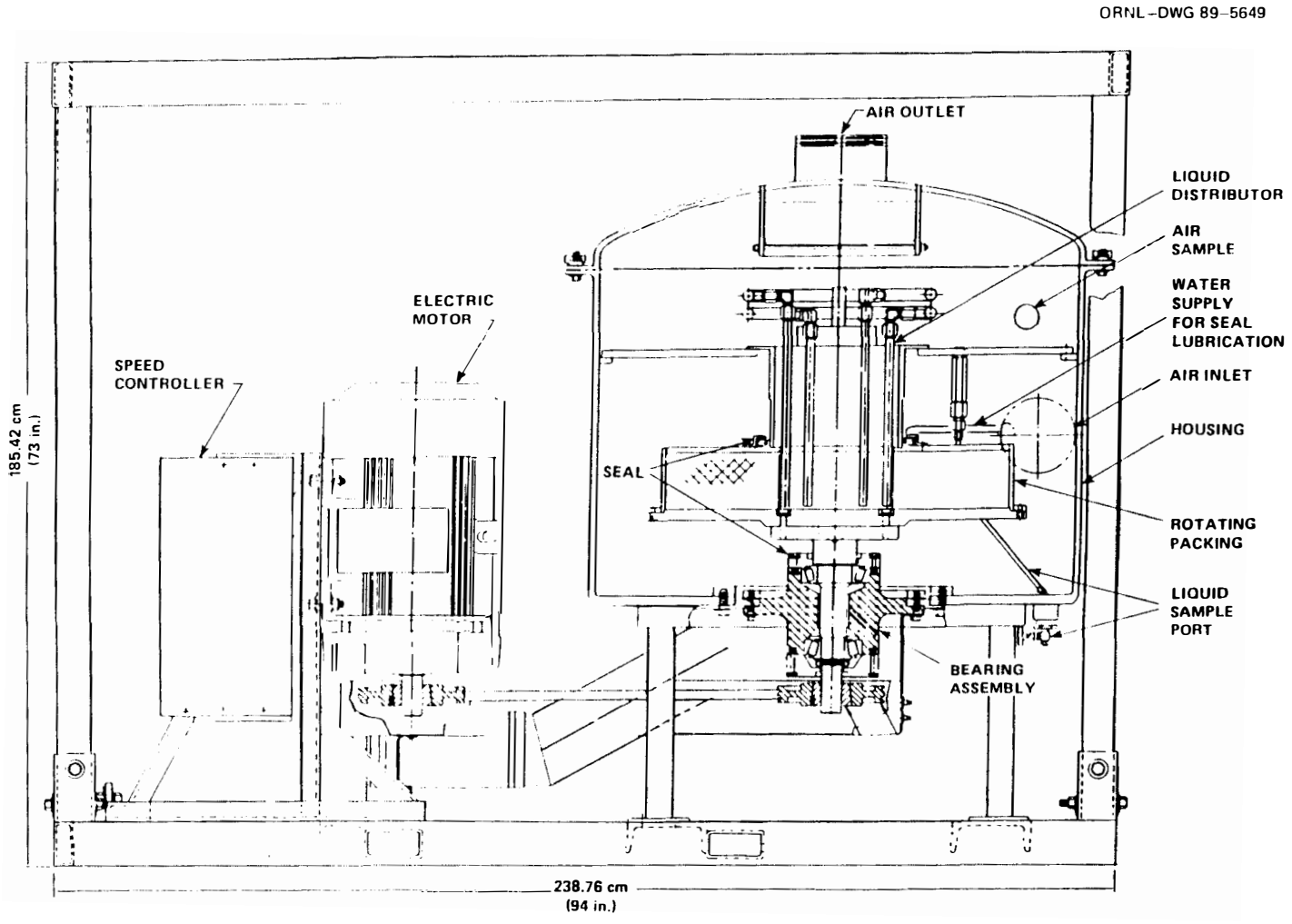

Fig. 5-2. Centrifugal vapor-liquid contactor system.

(2-15/16 in.) stock material and the top plate was 1.27 cm (1/2 in.) thick. The support plate on the outside radius of the rotor was made from 0.95 cm (3/8 in.) thick plate into which 1.59 cm (5/8 in.) holes with 2.06 cm (13/16 in.) spacing between center lines were drilled to provide 53% open area.

The packing for the rotors was a metal sponge like material made of 85% nickel and 15% chromium (Sumitomo Electric Industries, Ltd. 1-1-1, Kooa-kita, Itami, Hyogo, 644 Japan). The material is manufactured in sheets which are 450 mm x 500 mm. The packing material was cut into desired dimensions using Hydrojet cutting to minimize distortion.

The rotors were packed by starting at the outer radius and laying the packing material into place one sheet at a time until the desired inside radius is reached. Two thickness of the packing material was used. All the packing material except the last sheet at the inner radius was 2 mm thick. This material had specific surface area of 2500 m^2/m^3 and voidage of 0.95. The packing material at the inner radius was 10 mm thick and had specific surface area of 1700 m^2/m^3. The use of the less porous and extra thick packing at the inside radius served two purposes. First, it provided the rigidity necessary to keep the rest of the packing from becoming loose at the inner radius and second the less porous material allows the liquid phase to enter the rotating packing with minimal splash back. After packing, the rotor assembly is balanced to 5 gr-in. at 900 rpm.

A second type of packing made from wire gauge was also tested. This packing material had specific surface area of 2067 m^2/m^3 and

voidage of 0.934. According to Ray Fowler of Glitsch, Inc., this type of packing material is less expensive and more readily available.

The rotating packing was driven by a 220 volt, three-phase 20 horsepower motor (Baldor Electric Co., Ft. Smith, Arkansas). The speed of the motor was controlled by a variable frequency drive (General Electric AF-250E). The power consumed by the motor was measured using a three phase power meter (General Electric, Cat. No. 700X22G2).

Since it is extremely difficult to withdraw liquid samples from the inside of the rotating packing, three different rotors were used in this study. Each rotor had an inner radius and axial length of 12.7 cm (5 in.). The outer radii of the three rotors excluding the support plate were 22.9 cm (9 in.), 30.5 cm (12 in.), and 38.1 cm (15 in.) giving packing depths of 10.2 cm (4 in.), 17.8 cm (7 in.), and 25.4 cm (10 in.), respectively.

Two mechanical seals were used to prevent leakage between the rotating and stationary surfaces. The first seal was part of the bearing assembly and was grease lubricated. The second seal which was above the rotating packing was lubricated using an external water supply.

The liquid distributor at the inner radius of the packing was made in two sections. Each section consisted of three 1.91 cm (3/4 in.) aluminum tubes spaced 120° apart connected to a common circular supply header. This split arrangement permitted operation over a wide range of liquid flow rates while maintaining adequate discharge velocity by simply closing off one section. The liquid from each tube exited through a series of 0.24 cm (0.093 in.) holes which were drilled using

electron discharge machining. This type of machining provides holes with smooth finish and thus eliminates irregular spray patterns. The holes are offset from one tube to another to provide complete coverage of the packing material. The liquid spray from each tube is angled in the direction of the rotating packing in an attempt to match the liquid velocity with that of the packing. The liquid exiting the packing flowed into an opening at the bottom of the housing. The liquid exit line contained a 152 cm (60 in.) hydraulic jackleg which served as a seal and a sample port.

The air was introduced into the housing through a 15.2 cm (6 in.) opening that is tangential to the rotating packing. The air exists through a 20.3 cm (8 in.) opening at the top of the housing. The unit was equipped with a demister element for the exiting air stream, however, this was not used in any of the experiments.

A liquid sample tube was installed inside the housing next to the outer radius of the packing torus as shown in Fig. 5-3. The radial location of the sample tube was varied to match the outer radius of the rotating packing. The purpose of this type of sampling system was to minimize the variability between the end effects which may be caused by the rotors of different outer diameters. Also, some measure of the removal of VOCs that may occur after the water leaves the rotor can be obtained from the concentration difference between a sample from the tube and the water exit stream from the centrifugal vapor-liquid contactor.

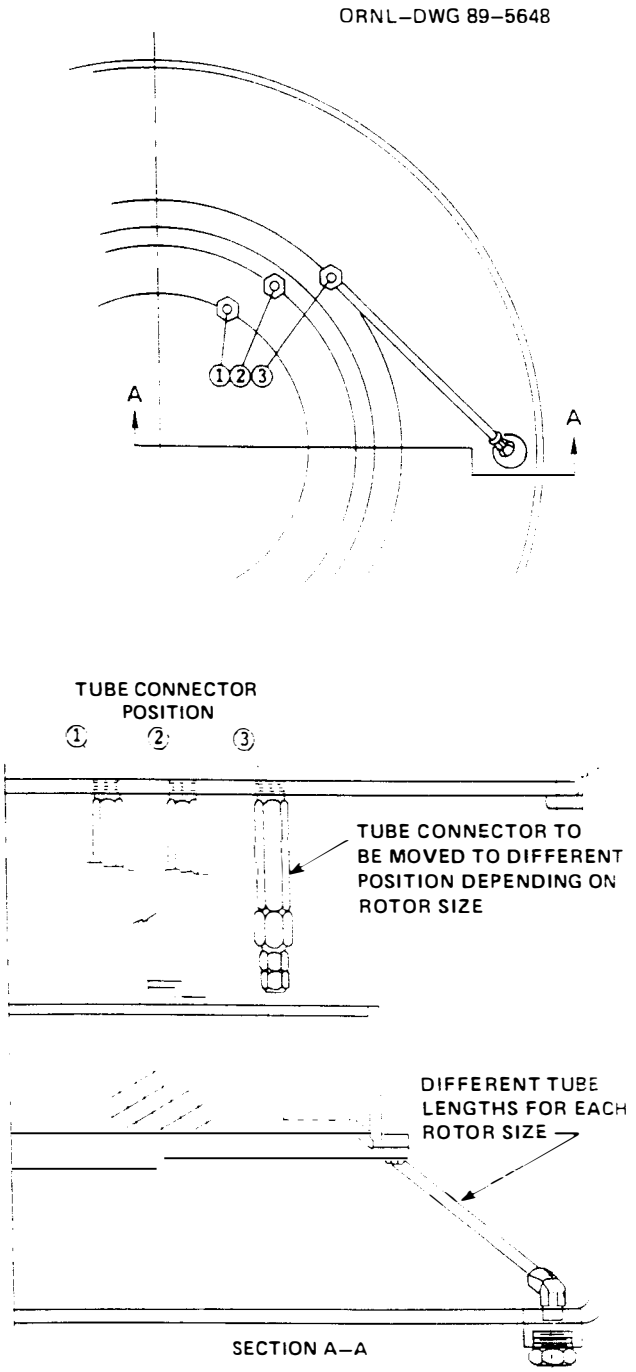

Fig. 5-3. Liquid sample tube.

5.3 Procedure for Hydraulic Tests

The main dependent variables in the hydraulic tests were pressure drop and power consumption, and the independent variables included: water flow rate, gas flow rate, rotational speed and depth of packing. The hydraulic tests were performed using clean water which was recirculated back to the surge tank.

A hydraulic run was started by setting the rotor speed at 1000 rpm and then establishing the liquid and gas flows at the desired values. After three minutes, the pressure drop across the packing and power consumption were measured. The rotor speed was then decreased by 100 rpm and the two dependent variables remeasured. This procedure was repeated until either the desired air flow rate could not be maintained because of high pressure drop or the inside eye of the rotor filled with water. The liquid and gas flows used in the hydraulic tests are given in Table 5-1 along with the criteria for accepting a particular run.

5.4 Procedure for Mass Transfer Tests

In order to reduce the number of runs required to characterize the mass transfer performance of the centrifugal vapor-liquid contactor, a central composite design was chosen for the experiments (Hebble, 1988). A description of this design presented by Anderson and McLeon (1974) is given below:

> "A composite design (Box and Wilson, 1951; Myers, 1971; and Davies, 1971) has three parts: a basic two-leveled factorial or fractional factorial, an extra point at the center of the entire design and 2k (where k = number of factors) extra points, one at either extreme of each factor and at the center of all other

Table 5.1. Hydraulic test conditions.

Liquid rate (L/s)		Gas rate (L/s)	
0	(0 gal/min)	0	(0 scfm)
0	(0)	47.2	(100)
0	(0)	141.6	(300)
0	(0)	236.0	(500)
0	(0)	330.4	(700)
0.63	(10)	47.2	(100)
0.63	(10)	141.6	(300)
0.63	(10)	236.0	(500)
0.63	(10)	330.4	(700)
1.26	(20)	47.2	(100)
1.26	(20)	141.6	(300)
1.26	(20)	236.0	(500)
1.26	(20)	330.4	(700)
1.89	(30)	47.2	(100)
1.89	(30)	141.6	(300)
1.89	(30)	236.0	(500)
1.89	(30)	330.4	(700)
2.52	(40)	47.2	(100)
2.52	(40)	141.6	(300)
2.52	(40)	236.0	(500)
2.52	(40)	330.4	(700)
3.15	(50)	9.4	(20)
3.15	(50)	26.0	(55)
3.15	(50)	47.2	(100)
3.15	(50)	141.6	(300)
3.15	(50)	236.0	(500)
3.15	(50)	330.4	(700)

Criteria for accepting a run:

Variable	Acceptable Variance
rotor speed	±5 rpm
liquid flow	±5% of set point
gas flow	±10% of set point

> points [Fig. 5-4]. Hence, in a composite design with a complete factorial experiment in it there are $2^k + 2k + 1$ treatment combinations. Correspondingly, if there was a fractional factorial instead of a complete factorial experiment in the design, the 2^k would be reduced as required. The particular type of composite design depends on the location of the extreme points. If the extreme points are located at the same standardized distance from the center point as the factorial points, the design is called a rotatable composite design (sometimes the word "central" is included in the title of these designs to indicate that there is a center point)....
>
> The advantage of a composite design over the fractional or complete three-leveled factorial is in the reduction of the number of treatment combinations required to estimate the squared terms in a second-order model [for a three factor design, the number of treatment combinations can be reduced to 15 from 27].... Two disadvantages in using the composite design instead of the three leveled factorial are (1) estimating effects with unequal variances..., and (2) having fewer degrees of freedom for error....
>
> In general for optimum designs, the five degrees of freedom in the composite design for the error estimate is adequate and the composite design is preferred over the three-leveled factorial."

In addition because it is difficult to change rotors, the experimental design is a block design rather than a completely randomized design.

A summary of the operating conditions used in the mass transfer tests is given in Fig. 5-5. It should be pointed out that the center point run shown in Fig. 5-4 (855 m/s^2, 2.21 L/s, and G/L ratio of 10.1) was the first run performed and was repeated after every two runs. This was done to achieve the necessary degrees of freedom required for error estimate and to detect any changes that may be occurring in the packing.

Before starting a set of mass transfer experiments, the feed tank was filled from the bottom and allowed to overflow overnight. This was done to assure the homogeneity of the feed. Just prior to beginning a

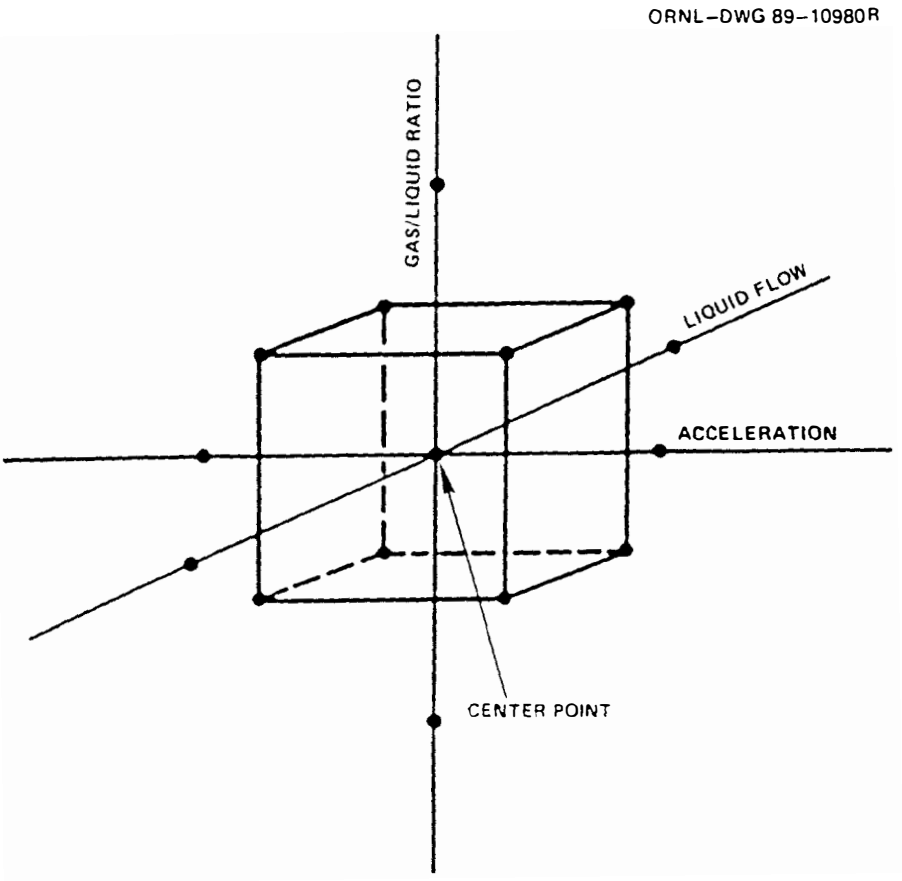

Fig. 5-4. Central composite design.

Fig. 5-5. Mass transfer test conditions for each rotor.

Acceleration at inner radius:

1. 340 m/s^2 (500 rpm)
2. 549 m/s^2 (633 rpm)
3. 855 m/s^2 (790 rpm)
4. 1161 m/s^2 (921 rpm)
5. 1370 m/s^2 (1000 rpm)

Liquid flow rate:

1. 1.26 L/s (20 gal/min)
2. 1.64 L/s (26.1 gal/min)
3. 2.21 L/s (35 gal/min)
4. 2.77 L/s (43.9 gal/min)
5. 3.15 L/s (50 gal/min)

Gas/liquid ratios (vol/vol):

1. 5.7 (R = 1.2 for Toluene)
2. 7.5
3. 10.1 (R = 2.1 for Toluene)
4. 12.7
5. 14.4 (R = 3.0 for Toluene)

Variables monitored: Rotor speed, air flow rate, liquid flow rate, inlet-outlet gas and liquid temperature, and pressure drop.

Samples to be taken: Inlet, outlet, and exit liquid. All liquid samples taken in duplicates.

Compounds analyzed for:

1. Benzene
2. 1-2-4 methylbenzene
3. Methyl cyclohexane
4. Pentane
5. Toluene
6. m-xylene
7. o-xylene
8. Naphthalene

Criteria for accepting a run:

Variable	Acceptable variance
rotor speed	±5 rpm
liquid flow	±5% of set point
gas flow	±10% of set point for 1 hour
temperature	±2°C

run, the filling of the tank was changed to the top and the water to the stripper was pumped from the bottom of the tank. This prevented any free jet fuel that may have accumulated in the tank from going to the stripper.

A mass transfer run was begun by setting the desired rotor speed, liquid flow and gas flow. The exit air stream from the stripper was then continuously monitored using a total hydrocarbon analyzer (Model 400A Hydrocarbon Analyzer, Beckman Industrial Corp., La Habra, California) to assure attainment of steady state prior to taking samples. When the total hydrocarbon analyzer reading did not change for thirty minutes, liquid samples were collected into prelabeled 40 mL glass bottle which contained 0.5 mL of 50% sodium hydroxide. All sample taps were left running continuously at a rate of approximately 250 mL/min in order to collect representative samples. In collecting the samples, the bottles were allowed to fill until overflowing and then sealed with a cap equipped with a teflon septum. The bottles were then checked for absence of air bubbles, shaken for 30 s, and placed in a refrigerator until analysis. The samples bottles were used only once and then discarded.

5.5 Sample Analysis

5.5.1 Equipment

The liquid samples were analyzed using a Tracor 540 gas chromatograph (Tracor Instruments Austin, Inc., Austin, Texas) equipped with a Megabore column (3-micron film thickness (DB-624), 30-m-long, 0.544 mm I.D., Cat. No. 1251334, J&W Scientific, Folsom, California),

flame ionization detector, and a Spectra-Physics SP4270 Integrator (Spectra-Physics, San Jose, California). The hydrogen fuel to the GC was supplied using Elhygen Mark V hydrogen generator (LDC/Milton Roy Chromatography Systems). In addition, the analytical system also contained a Tekmar LSC 2000 purge and trap apparatus and Model ALS automatic laboratory sampler (Tekmar Company, Cincinnati, Ohio). The ALS is a 10 station sampler equipped with Supelco needle sparge samplers (Cat. no. 2-2724, Supelco, Inc., Bellefonte, Pennsylvania). The LSC purge trap system contains Tenax trap for the capture and concentration of the volatile organic compounds.

5.5.2 Procedure

Because the analysis procedure for volatile organic compounds is relatively sensitive to the technique used in handling the samples and numerous problem can be encountered in the field laboratory, the Air Force requested in the statement of work that a chemist familiar with the purge and trap method be hired for the project. Brett Lemon of Maecorp Inc. (Caledonia, Michigan) was hired to perform all sample analysis.

Prior to shipment of the analytical equipment to Eglin Air Force Base, the entire analytical system was set up and checked out by the Quality and Technical Services Division at the Oak Ridge Gaseous Diffusion Plant. During this period, the Environmental Protection Agency Method 602 for purgeable aromatics was fined tuned for the compounds which were present in the groundwater at Eglin Air Force Base. The oven of the GC was programmed for the following

temperatures: start at 40°C and hold for 6 min, increase at rate of 3°C/min to 135°C, hold for 3.4 min, increase at the rate of 25°C/min to 180°C and hold for 2 min (At Eglin Air Force Base, hold times were changed to 0.01 min and 4 min, respectively. This was done to decrease run time and to completely elute late peaks before the next run). During checkout at Oak Ridge, it was noticed that the recovery of some of the compounds in low concentration standards from the latter samples on the ALS sampler was consistently lower than from the first few samples run. After eliminating several possibilities that could cause the loss of volatile compounds (leaks, biological activity, photodegradation), it was suggested by J. F. Villiers-Fisher of Oak Ridge National Laboratory that the organic compounds may be adsorbing on the glass tubes of the automatic sampler and that these adsorption sites could be tied up by making the samples basic using sodium hydroxide. After changing the standards to basic solution, no further loss was observed.

At Eglin Air Force Base, the gas chromatograph was calibrated using standards containing 1, 50, 100, 500 ppb of each compound given in Fig. 5-5. The standards were prepared by diluting a methanol solution which contained 1,000 ppb of each compound. The water used for diluting the samples and standards was prepared by passing tap water through an activated carbon filter.

Prior to loading the samples on the automatic sampler, the sample bottles were removed from the refrigerator and allowed to come to room temperature. When the samples had reached room temperature, a 5 mL aliquot was placed into sampler tubes and the tubes immediately

attached to the ALS sampler. The liquid from each sample bottle was analyzed in triplicates to ensure greater reliability of the final results.

A quality control program consisting of the following measures was also implemented. A blank sample, which was prepared by passing tap water through an activated carbon bed, was analyzed with each set of three samples from a particular run. The separation and identification of the peak on the chromatogram was ensured by spiking certain samples with standard solution. The proper functioning of the equipment was also checked by running standard samples. When the relative error from the standard and spiked samples was greater than 10%, steps were taken to isolate and correct the problem.

6. RESULTS AND DISCUSSION

6.1 Hydraulic Performance

The hydraulic operating envelope of a centrifugal vapor-liquid contactor has two boundaries as shown in Fig. 6-1. The upper boundary arises from the design and is purely mechanical. This boundary is the maximum operating speed of the particular machine. Once the machine is designed and fabricated, this boundary is difficult to change without significant modifications to the unit. The lower boundary on the other hand depends upon the operating conditions. It is this boundary which was investigated in the hydraulic tests.

6.1.1 General Characteristics

The effect of gas flow rate and rotor speed on pressure drop without any aqueous flow is shown in Fig. 6-2. As would be expected, the pressure drop increases with an increase in both the air flow rate and rotor speed. Notice that even with no gas flowing through the packing there is some pressure drop across the packing. This pressure drop is due to the packing torus acting as a centrifugal pump. The leveling out of the curves at rotational speeds less than 200 rpm for the higher gas flows results from inleakage of the water used to lubricate the seal into the center of the packing torus.

A typical family of pressure drop curves with both the liquid and gas phases flowing is shown in Fig. 6-3. Like the pressure drop behavior with no liquid flow, the pressure drop initially decreases with a decrease in rotational speed. After some critical rotor speed

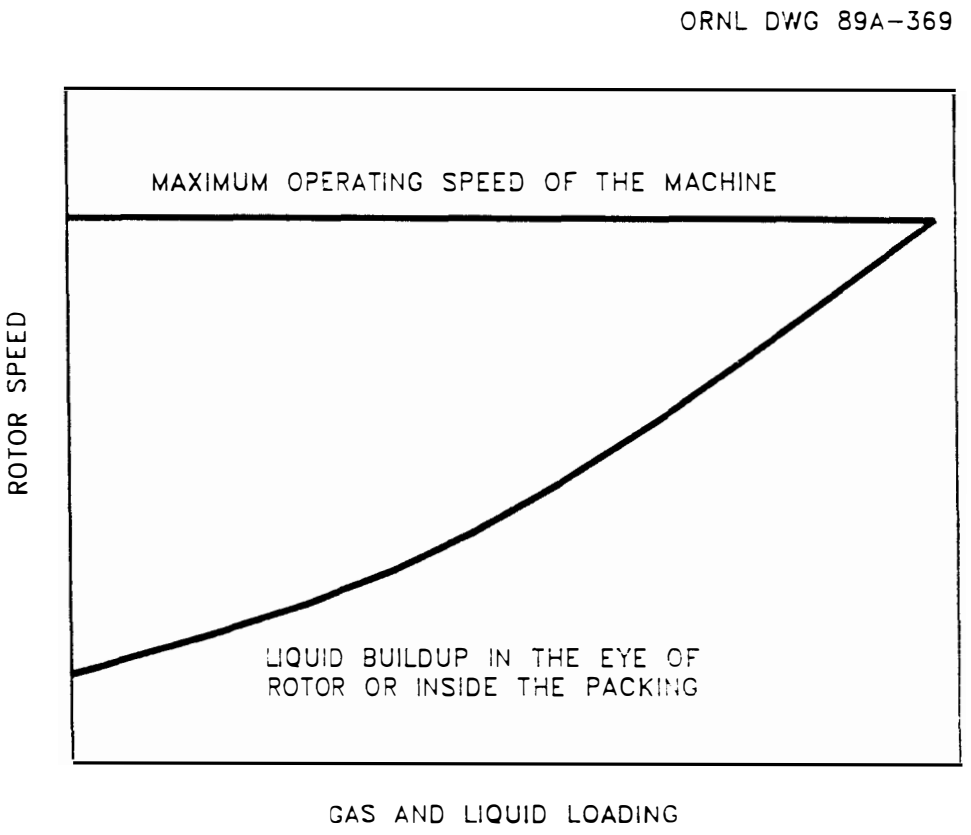

Fig. 6-1. Theoretical operating envelope for the centrifugal vapor-liquid contactor.

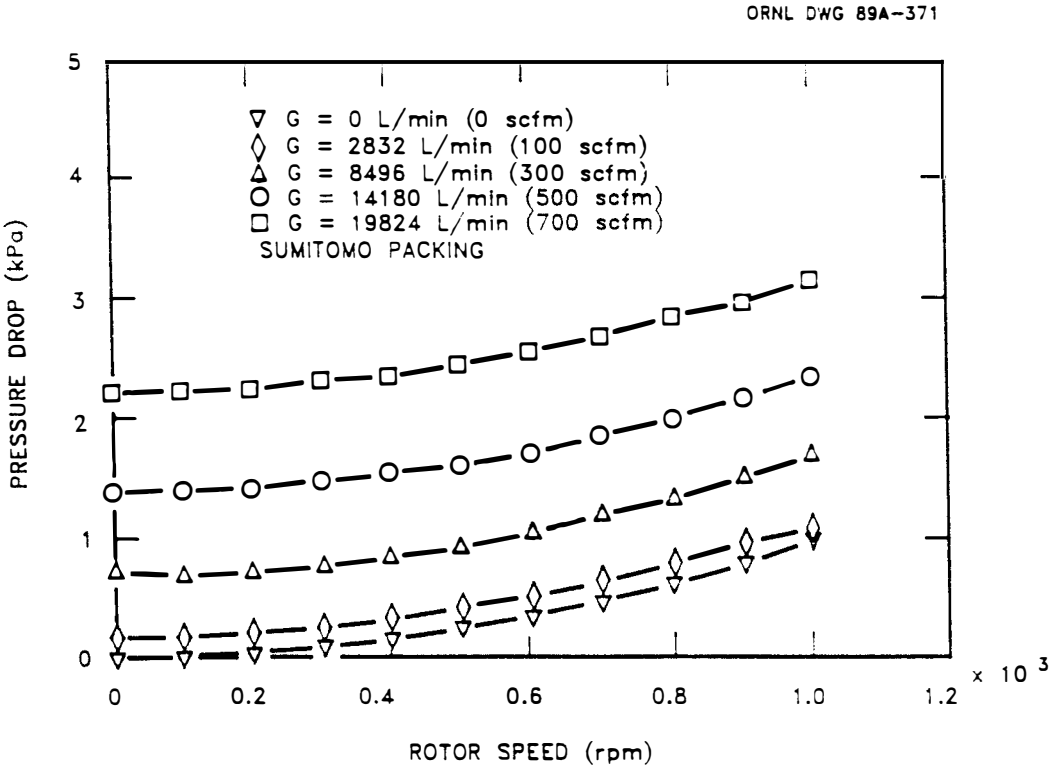

Fig. 6-2. Pressure drop as a function of rotor speed without liquid flow (76.20-cm-diam. rotor).

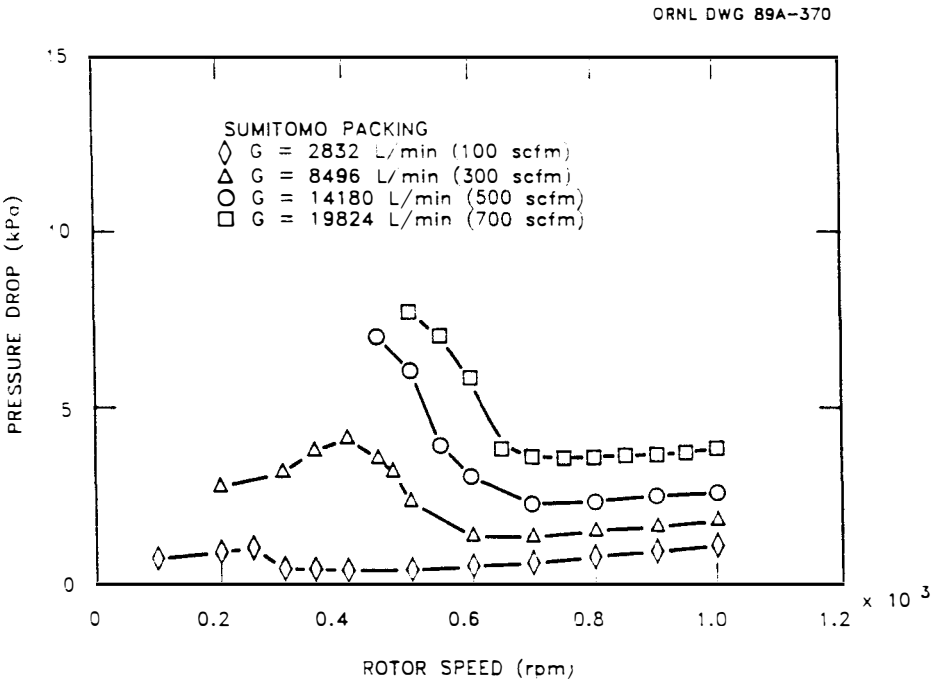

Fig. 6-3. Pressure drop with both liquid and gas phases flowing (liq. flow = 0.63 L/s; 76.20-cm-diam. rotor).

is reached, the pressure drop begins to increase very rapidly. The rotor speed at which the pressure drop begins to increase thus is a point on the lower boundary in Fig. 6-1. This demarcation is very sharp with changes in rotation speeds of less than 25 rpm resulting in large pressure changes. The rise in pressure drop can be caused by either the failure of the water to enter the packing or the lack of sufficient centrifugal force to drive the water through the packing once it enters the packing. Because the hydraulic tests were performed with the top of the unit removed, visual inspection of the inner eye of the packing torus indicated that initial increase in pressure drop as rotor speed is decreased results from lack of sufficient centrifugal force. Although some mist was noticed in the exit air stream when the pressure drop first started to increase, the eye of the packing torus did not begin to fill up until the rotor speed was further reduced by almost by 200 rpm. Another observation which tends to support the insufficient centrifugal force hypothesis was the slow increase in pressure drop reading with time at a constant rotation speed in the critical region indicating buildup of liquid in the packing.

The second decrease in pressure drop at low gas flows in Fig. 6-3 results from phenomena where the liquid phase flows through the lower section of the packing and the gas phase flows through the top section. This type of flow pattern results because the water leaving the distributor simply hits the packing and runs downward rather than being accelerated into the packing. This phenomena is not noticed at the higher gas flows because the gas velocity through the packing is too high to permit the countercurrent flow of the aqueous phase.

The effect of packing depth (outer radius minus inner radius) on pressure drop is shown in Fig. 6-4. An anomaly is seen in this data. The data from the 60.96-cm-diam rotor (17.8 cm packing depth) shows considerably higher pressure drop than would be expected from examining the data from the two other rotors. Since a logical explanation for this behavior was not readily apparent, the fabrication and assembly process of the three rotors were examined. Ray Fowler of Glitsch, Inc., indicated that Sumitomo packing used in the 76.20-cm-diam rotor (25.4 cm packing depth) was brand new while the packing used for the other two rotors had been previously used in a unit to selectively remove H_2S from natural gas. He also believed that since the H_2S removal is a clean process the packing should not have been plugged with anything, but he stated that pressure drop for the 60.96-cm-diam rotor was higher than what would be expected from their data with other units. Due to lack of sufficient time and funds for the project, the rotors could not be disassembled and a detailed examination of the packing performed. Thus, the data from the 60.96-cm-diam rotor was only used for analysis of end effects in the mass transfer tests and for determining power consumption requirements.

6.1.2 Hydraulic Capacity Correlation

The onset of flooding in conventional packed towers is usually defined as a region of operating conditions where countercurrent flow of the two phases is disturbed and pressure drop across the column begins to oscillate. Although not totally applicable to the centrifugal vapor-liquid contactor, this definition can be useful in

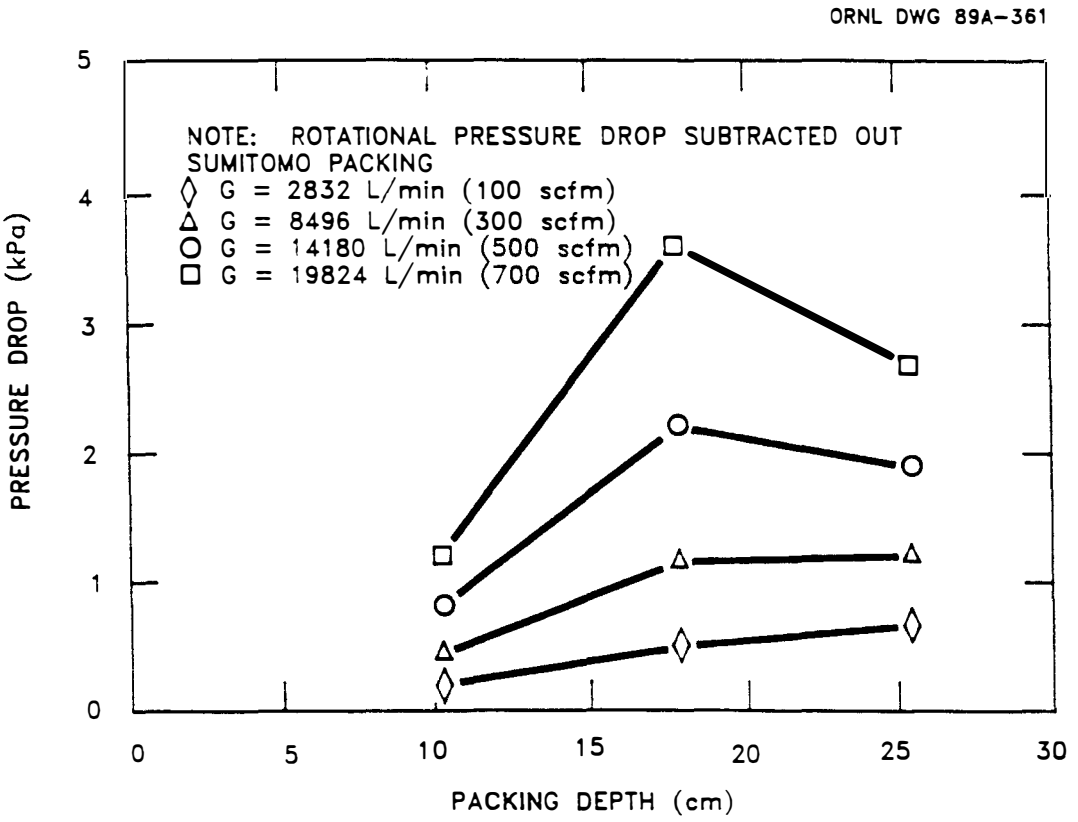

Fig. 6-4. Effect of packing depth on pressure drop (liq. flow = 0 L/s; rotor speed = 700 rpm).

characterizing hydraulic performance. Unlike conventional packed towers in which flooding is achieved by increasing gas and liquid flows, flooding in a centrifugal vapor-liquid contactor can be initiated at constant fluid flows by decreasing the rotational speed of the packing torus. This approach was utilized in developing a hydraulic capacity correlation.

The Sherwood flooding correlation for conventional packed towers has been recommended by several authors (Munjal, 1986; Fowler and Kahn, 1987) for designing centrifugal vapor-liquid contactor. Thus, it would be beneficial to compare data from this study with the Sherwood flooding correlation. To perform this comparison, a quantitative definition of what constitutes limit of operability was established. Examination of the hydraulic data from all the runs indicated that as rotational speed was decreased initially the pressure drop decreased at a rate of approximately 24.9 Pa/100 rpm (0.1 in. of H_2O/100 rpm). After some critical operating speed was reached, the pressure drop would start to increase at a rate of 498 Pa/100 rpm (2 in. of H_2O/100 rpm) or higher. This is a significant rise in pressure drop indicating something in operating characteristics has changed. The limit of operability rotational speed was thus defined as a speed below which the pressure drop increased at a rate greater than or equal to 498 Pa/100 rpm. For example, if at certain operating conditions a decrease in speed from 500 to 400 rpm resulted in pressure drop increase of 498 Pa/100 rpm, then 500 rpm was taken as the limit of operability rotational speed. Although the choice of 498 Pa/100 rpm is somewhat arbitrary, it provides a quantitative definition which is easy

to use. Tests with the 76.20-cm-diam rotor at 9.4 L/s (20 scfm) did not exhibit a sharp increase in pressure drop and the limit of operability speed was assumed to be the speed below which no further decrease in pressure drop occurred.

The results of hydraulic capacity tests are shown in Fig. 6-5 along with the Sherwood correlation. These results indicate that the Sherwood correlation underestimates the limit of operability rotational speed for the Sumitomo packing while there is good agreement for the wire gauze packing. A second order polynomial curve fit for the experimental data is also shown in Fig. 6-5. The equation of this curve is:

$$\log y = -2.274484 - 1.1367\log(x) - 0.168118\,[\log(x)]^2 \qquad (6\text{-}1)$$

with coefficient of determination (r^2) of 0.80. From Fig. 6-5, it is interesting to note that although the 60.96-cm-diam rotor exhibited unusually high pressure drop the limit of operability rotational speeds are identical to those of the other two rotors.

6.1.3 Pressure Drop Correlation

The pressure drop across the rotating packing torus of a centrifugal vapor-liquid contactor is difficult to model theoretically. Thus, a semi-theoretical approach based on experimental observation must be used. The pressure drop across the packing can be divided into two terms. The first term accounts for the pressure drop due to rotation of the packing and the second term accounts for pressure drop resulting from the flow of fluids through a porous media.

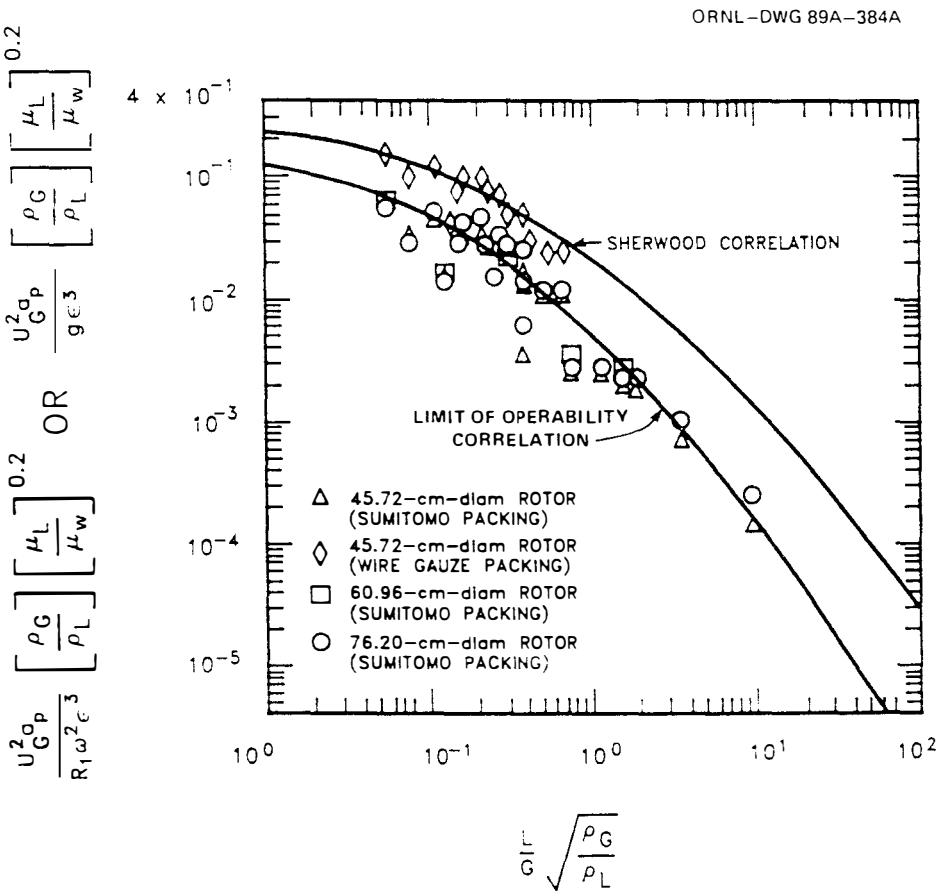

Fig. 6-5. Comparison of limit of operability data with that predicted by the Sherwood flooding correlation.

The rotational pressure drop term can be modeled theoretically. In a packing torus rotating at a constant speed, the centrifugal force acting on a fluid element of volume dV and density ρ at a radius r from the axis of rotation has a value of $\rho r\omega^2 dV$ (Leonard, 1980). The resulting pressure can be calculated by dividing the centrifugal force by the area perpendicular to the radius on which it acts. In differential form the pressure drop across the packing torus can be written as:

$$dp = \rho\omega^2 \, r \, dr \tag{6-2}$$

integrating this equation between the outer (r_2) and inner (r_1) radii gives:

$$Prot = \frac{\rho_{air} \, \omega^2}{2} (r_2^2 - r_1^2) \tag{6-3}$$

Since it is difficult to measure pressure drop very close to the inner and outer radii, a constant (A) can be added to account for end effects and Eq. (6-3) becomes:

$$Prot = A \frac{\rho_{air} \, \omega^2}{2} (r_2^2 - r_1^2) \tag{6-4}$$

The pressure drop caused by flow of fluid through a porous media is conventionally modeled as consisting of a viscous term and an inertial term (Perry, 1973). In mathematical terms this equation can be written as:

$$\frac{\Delta P_{flow}}{L} = \alpha\mu \, V + \beta\rho \, V^2 \tag{6-5}$$

where α = viscous resistance coefficient

β = inertial resistance coefficient

μ = viscosity of fluid

ρ = density of fluid

L = thickness of porous medium

V = superficial fluid velocity

Several complications arise in trying to apply Eq. (6-5) to the centrifugal vapor-liquid contactor. First, Eq. (6-5) assumes that the superficial velocity remains constant through the entire depth of the porous medium. This is not the case for the packing torus because the cross sectional area changes with the radius. Second, Eq. (6-5) assumes pressure drop varies linearly with depth of packing and this may not be true for the packing torus. These assumptions can be addressed by use of an average superficial velocity through the packing torus and if the difference between the inner and outer radii is small then linear dependence of pressure drop with packing torus may not be an unreasonable assumption.

The effects of superficial gas and liquid velocities on pressure drop in the region where rotational speed is greater than limit of operability speed are shown in Fig. 6-6 and 6-7, respectively. The gas and liquid velocities shown are average values which were calculated using:

$$\underset{[a,b]}{\text{AVG } f} = \frac{1}{b-a} \int_a^b f \qquad (6\text{-}6)$$

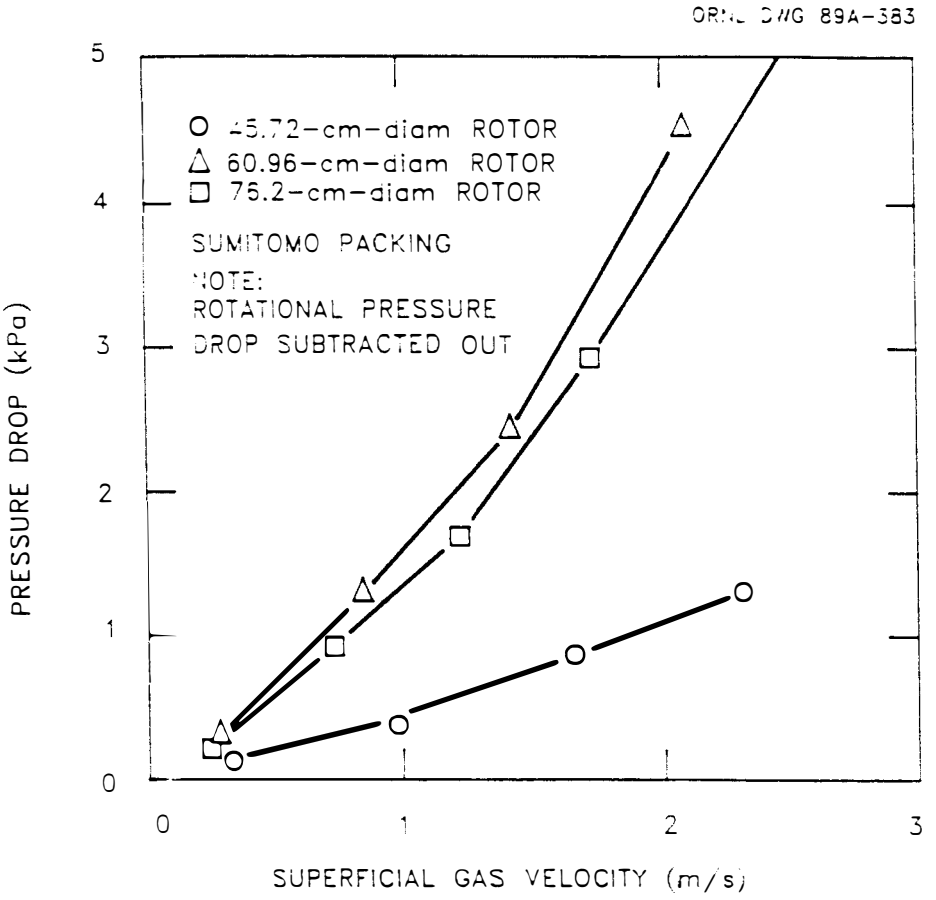

Fig. 6-6. Effect of gas flow rate on pressure drop (liq. flow = 0.63 L/s).

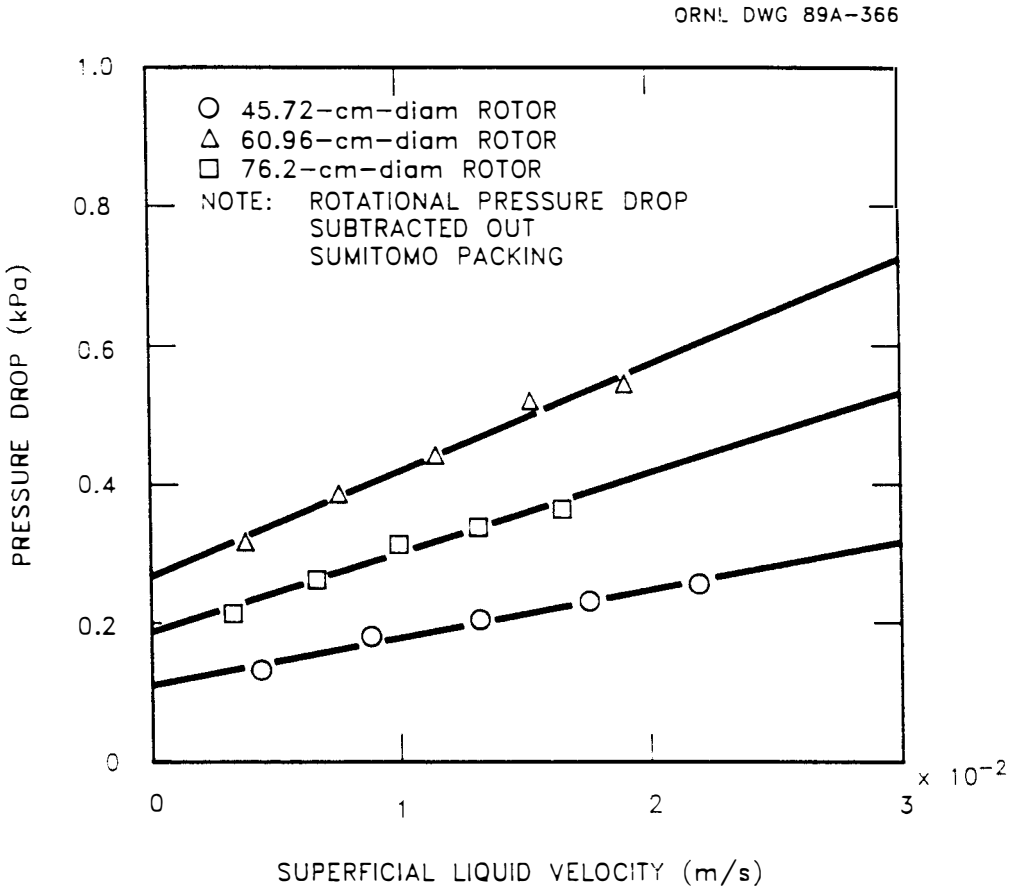

Fig. 6-7. Effect of liquid flow rate on pressure drop (gas flow = 47.2 L/s).

where f is a function. For gas velocity, this equation becomes:

$$\text{AVG V} = \frac{1}{r_2 - r_1} \int_{r_1}^{r_2} \frac{Q}{2 \pi \, rl} \, dr \qquad (6\text{-}7)$$

where Q is the volumetric gas flow rate and l is the axial length of the packing.

As can be seen from Fig. 6-7, the effect of liquid flow rate on pressure drop is relatively minor and can be neglected. The nonlinearity of data in Fig. 6-6 shows that the inertial term (second term) in Eq. (6-5) is the dominant term for the experimental conditions. So as a further simplification, the first term in Eq. (6-5) can be neglected.

The effect of packing depth on pressure drop for the 45.72 and 76.20-cm-diam rotors is shown in Fig. 6-8. This figure shows that for the experimental conditions the assumption that pressure drop varies linearly with packing depth is valid. Thus, the pressure drop due to flow of gas through the packing can be written as:

$$\Delta P_{flow} = \beta \rho_{air} (r_2 - r_1) V^2_{avg} \qquad (6\text{-}8)$$

The value of β can be estimated using the Ergun equation (Bird et al., 1960). The Ergun equation however uses the concept of mean particle diameter to define β. The particle diameter is difficult to estimate for the type of packings used in the centrifugal vapor-liquid contactors. It would be more convenient to express β in terms of the

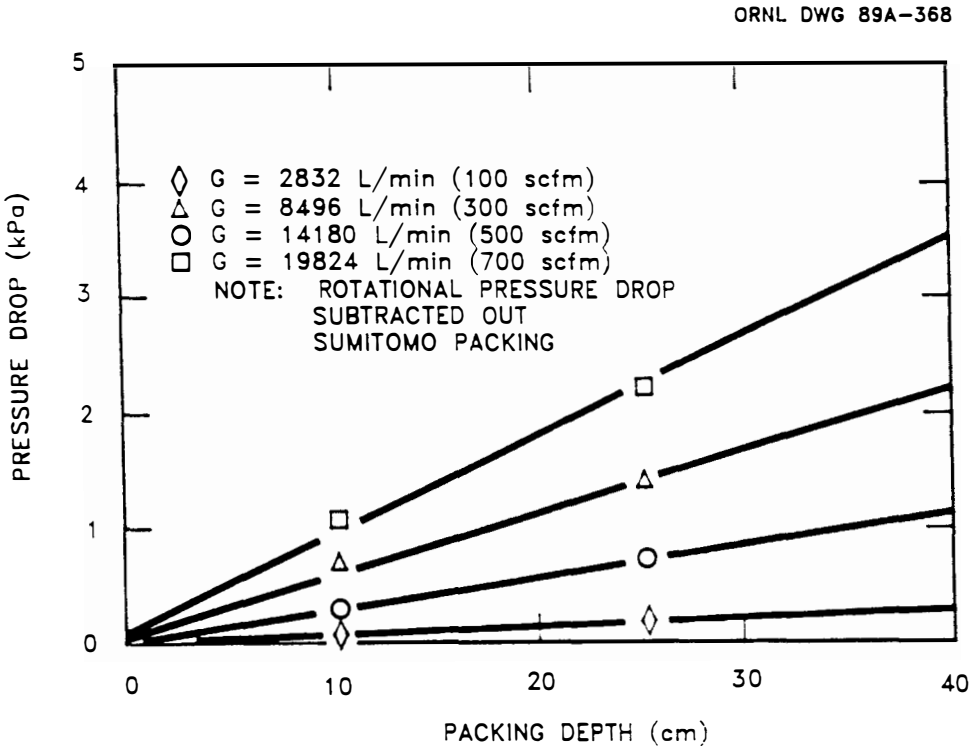

Fig. 6-8. Effect of packing depth on pressure drop at several gas flow rates (liq. flow = 0; rotor speed = 700 rpm).

specific surface area of the packing. Since β is simply an empirical constant, Eq. (6-8) can be modified to give:

$$\Delta P_{flow} = \beta \, 1\frac{a_p}{\epsilon} \, \rho_{air}(r_2-r_1)V^2_{avg} \tag{6-9}$$

where a_p is the specific surface area of packing and ϵ is the voidage of the packing material. Combining Eqs. (6-4) and (6-9) for calculation of total pressure drop gives:

$$P_{tot} = A \frac{\rho_{air} \, \omega^2}{2} (r_2^2-r_1^2)+\beta_1 \frac{a_p}{\epsilon} \rho_{air}(r_2-r_1)V^2_{avg} \tag{6-10}$$

The constants A and β_1 can be evaluated from the experimental data using regression analysis. The pressure drop data from the 45.92-cm-diam and 76.20-cm-diam rotors for rotational speeds greater than the limit of operability speed give the following equation:

$$P_{tot} = 0.923 \, \rho_{air} \, \omega^2(r_2^2-r_1^2) + 0.992\frac{a_p}{\epsilon} \rho_{air}(r_2-r_1)V^2_{avg} \tag{6-11}$$

where the dimensions on the variables are: P=pascals, ρ_{air}=kg/m^3, r=m, a_p=m^2/m^3, ω=rad/s, and V=m/s. The coefficient of determination (r^2) for the regression fit is 0.94. The calculated and experimental pressure drop values are compared in Fig. 6-9. Although the approach outlined above is a rather simple representation of a complicated system, it does a reasonable job in describing the experimental data and is easy to use.

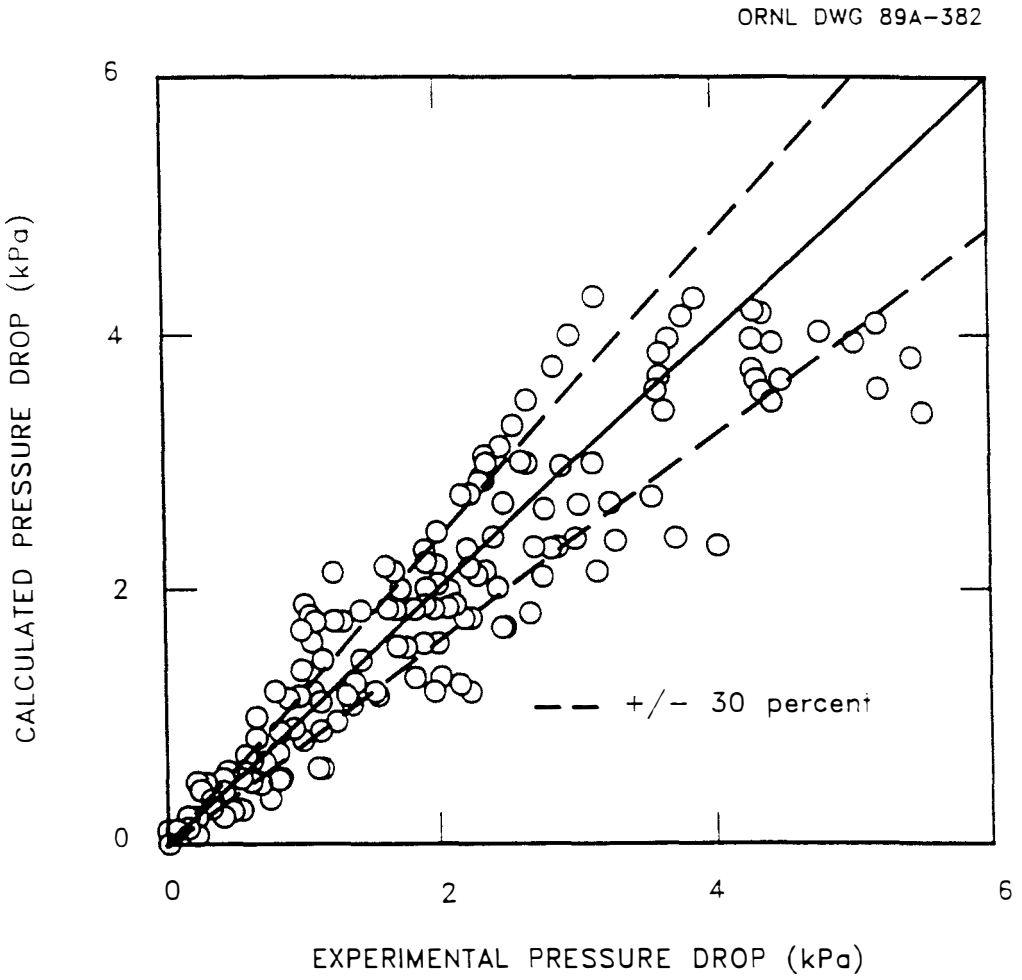

Fig. 6-9. Comparison of the calculated and experimental pressure drop.

6.2 Mass Transfer Performance

Since very little data on the mass transfer performance of a centrifugal vapor-liquid was available during the design phase of this project, it was decided that three rotors containing Sumitomo packing with varying outer radii would be used to determine the concentration profiles. The inner radius and the axial length of all three rotors would be identical. The operating conditions were chosen over as wide a range as possible with respect to limitations of the ancillary equipment.

6.2.1 General Characteristics

The accuracy of the mass transfer data can be affected by large variations in the composition of the feed material. The groundwater at Eglin AFB had been pumped for several years and the concentration of VOCs in the water was expected to be relatively constant. The well pumps were left running during this entire project to promote steady state movement of the groundwater in the vicinity of the spill area. Composition of the feed water during the mass transfer tests with the 45.92-cm-diam rotor is shown in Fig. 6-10. The data in Fig. 6-10 represent a time span of approximately two weeks and shows that the variations in the feed water composition are relatively minor.

Variations in Henry's Law constant can also affect the mass transfer results. Since there were some studies in the literature which hinted that Henry's Law constants for VOCs in groundwater may not be the same as in pure water, the EPICS method was modified to measure Henry's Law constants for the compounds that were to be followed in the

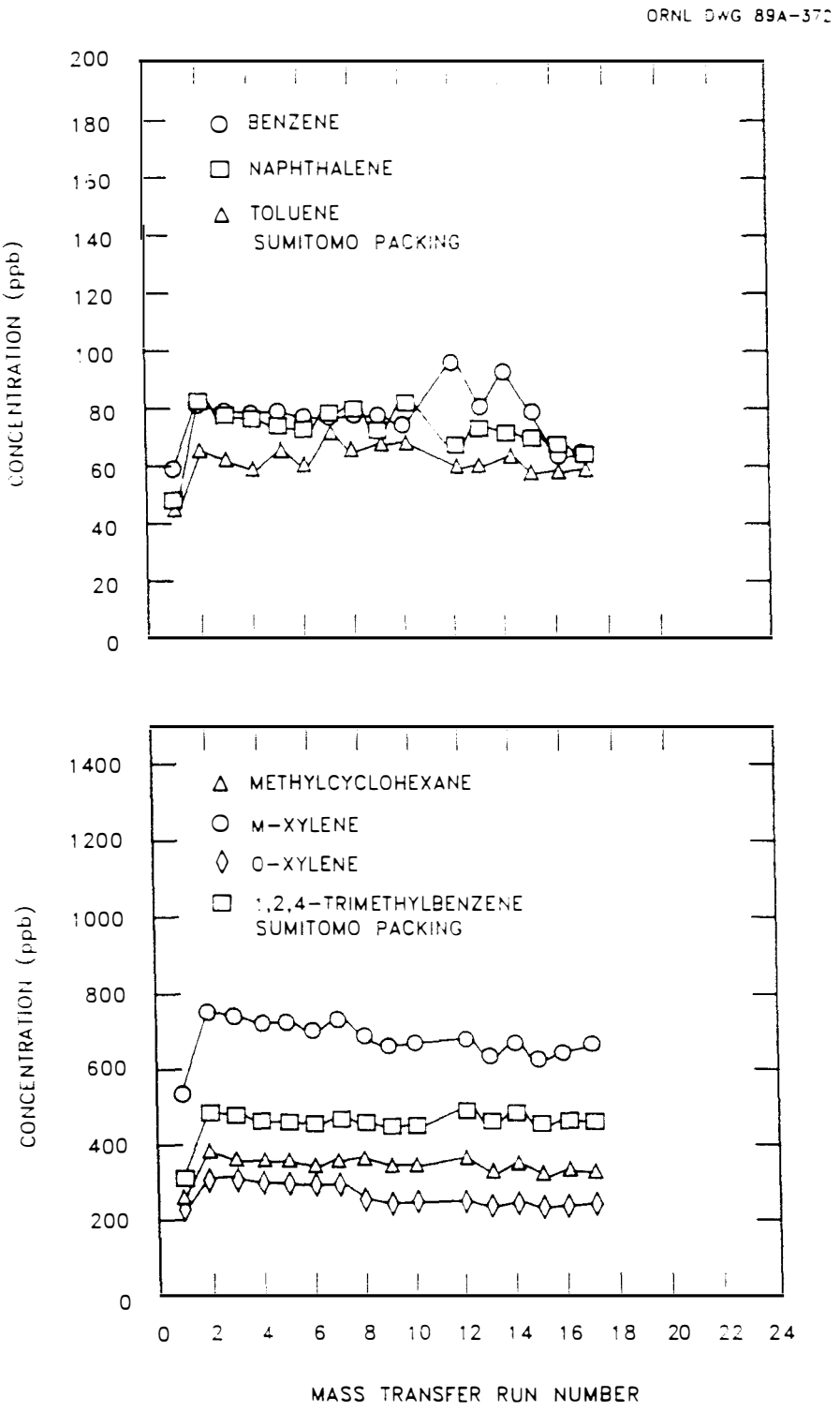

Fig. 6-10. Variation in the feed for the mass transfer tests with the 45.72-cm-diam rotor.

mass transfer tests. The modification of the EPICS is given in Appendix A. The measured Henry's Law constants are compared with literature values in Table 6-1. Because experimental Henry's Law constant for 1,2,4-trimethylbenzene was not available in the literature, the value determined from this study is compared with the Henry's Law constant for 1,3,5-trimethylbenzene. Table 6-1 shows that the measured Henry's Law constants do not differ appreciably from the literature values. Because the Henry's Law constants in this study were measured at only one temperature and did not differ significantly from literature values, temperature correlations for Henry's Law constants given in literature were used to analyze the mass transfer data.

One of the problems in characterizing the mass transfer performance of a packing torus is separating the mass transfer that occurs inside the packing from that which occurs outside the packing (end effects). The use of three rotors and a special sampling system were proposed as possible solutions to the problem. As it turned out, the number of transfer units in the 76.20-cm-diam rotor was so large at the majority of the operating conditions that very high removals were achieved. Measuring very low concentrations (<1 ppb) in the exit water stream introduced a large degree of uncertainty in the final results. In addition, the anomalous pressure drop behavior from the 60.96-cm-diam rotor made the mass transfer results from this rotor questionable. With these observations, it was decided that a good estimate of end effects could only be obtained from those operating conditions where the exit water stream concentrations for the

Table 6-1. Comparison of experimental Henry's Law constants with the literature values.

Compound	Henry's Law Constant (atm-m^3/mol) at 20°C		
	Experimental	Literature	Source
Date: 1-4-1989			
Benzene	0.00307	0.00467	Ashworth et al.
Toluene	0.00588	0.00588	"
o-xylene	0.00438	0.00430	"
m-xylene	0.00586	0.00604	"
1,2,4-trimethylbenzene	0.00469	0.00564*	"
Methylcyclohexane	0.227	0.428	Nirmalakhandan
Napthalene	0.00078	0.00041	"
Date: 1-19-1989			
Benzene	0.00393	0.00467	Ashworth et al.
Toluene	0.00609	0.00588	"
o-xylene	0.00414	0.00430	"
m-xylene	0.00596	0.00604	"
1,2,4-trimethylbenzene	0.00429	0.00564*	"
Methylcyclohexane	0.519	0.428	Nirmalakhandan
Napthalene	0.00079	0.00041	"

* This value is for 1,3,5-trimethylbenzene

76.20-cm-diam rotor were high enough (10ppb) to be measured accurately. There were only 4 runs out of 15 where such high concentrations were observed and the results from two of these runs are plotted using Eq. (4-24) in Fig. 6-11. Statistical analysis of four runs indicated that the intercept which is a measure of the end effects was not significantly different from zero. It was thus concluded that the sampling system had effectively eliminated the end effects. It is interesting to note that the pattern of data for both set of conditions in Fig. 6-11 is almost identical and only the slope changes. The data from all the centerpoint runs (855 m/s^2, 2.21 L/s, and G/L ratio of 10.1) are shown in Fig. 6-12. Although this plot shows that there are some end effects, this is probably due to the uncertainty in the number of transfer units from the 76.20-cm-diam rotor where concentrations were all below 1 ppb. This figure shows that even with the uncertainties associated with analytical analysis, the large number of transfer units measured in the 76.20-cm-diam rotor seem reasonable.

The conclusion that the sampling system was successful in eliminating the end effects allows the data from each rotor to be analyzed independently. Since the concentration in the exit water stream from all the tests with the 45.92-cm-diam rotor were well above the detection limit of the analytical equipment, these data were analyzed in greatest detail. Figure 6-12 shows the reproducibility for the centerpoint runs with the 45.92-cm-diam rotor. The coefficient of variation for the number of transfer units (o-xylene data) was 8% for the Sumitomo packing and 6.4% for the wire gauge packing.

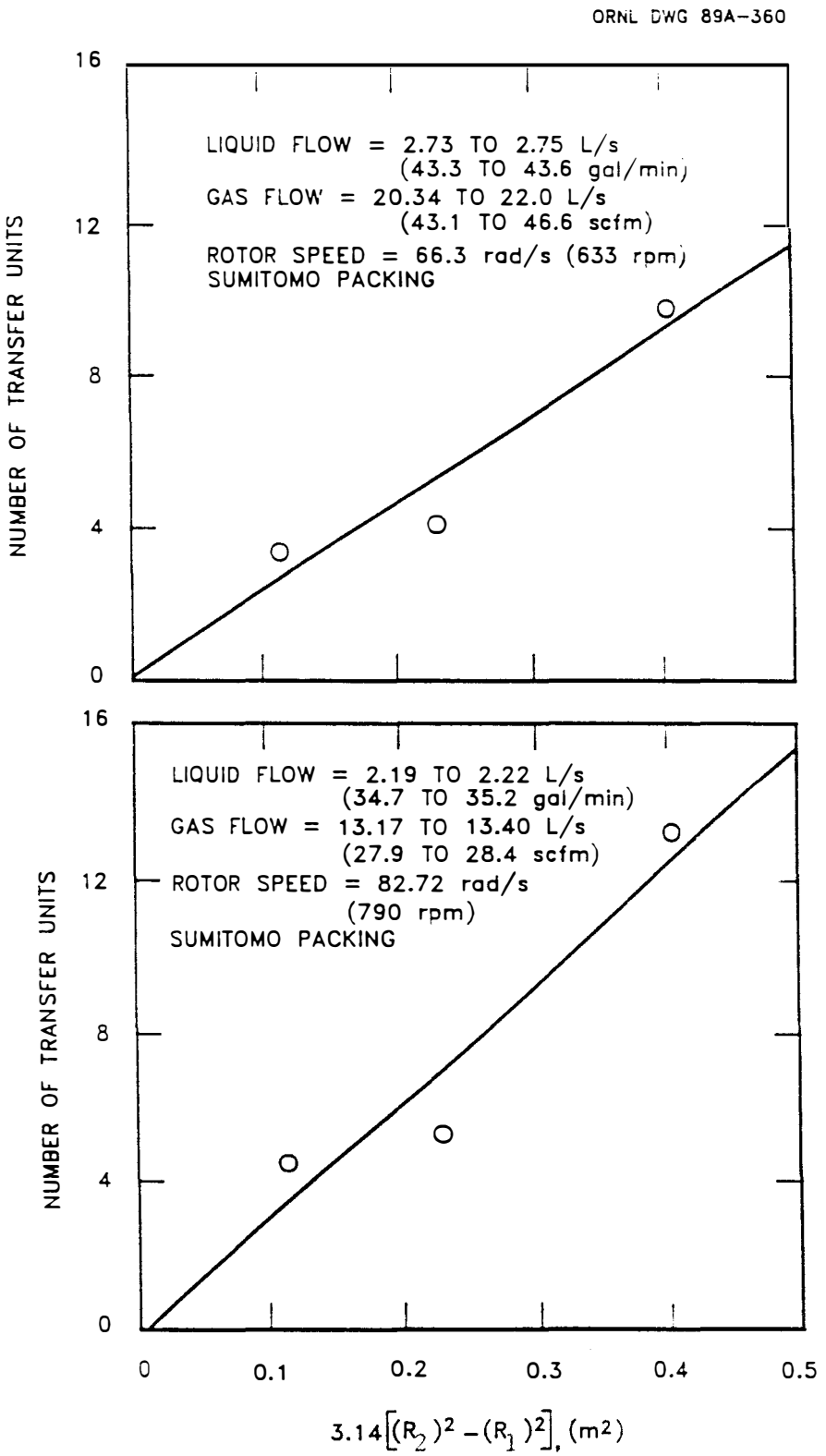

Fig. 6-11. Plot of mass transfer data to determine end effects (o-xylene data).

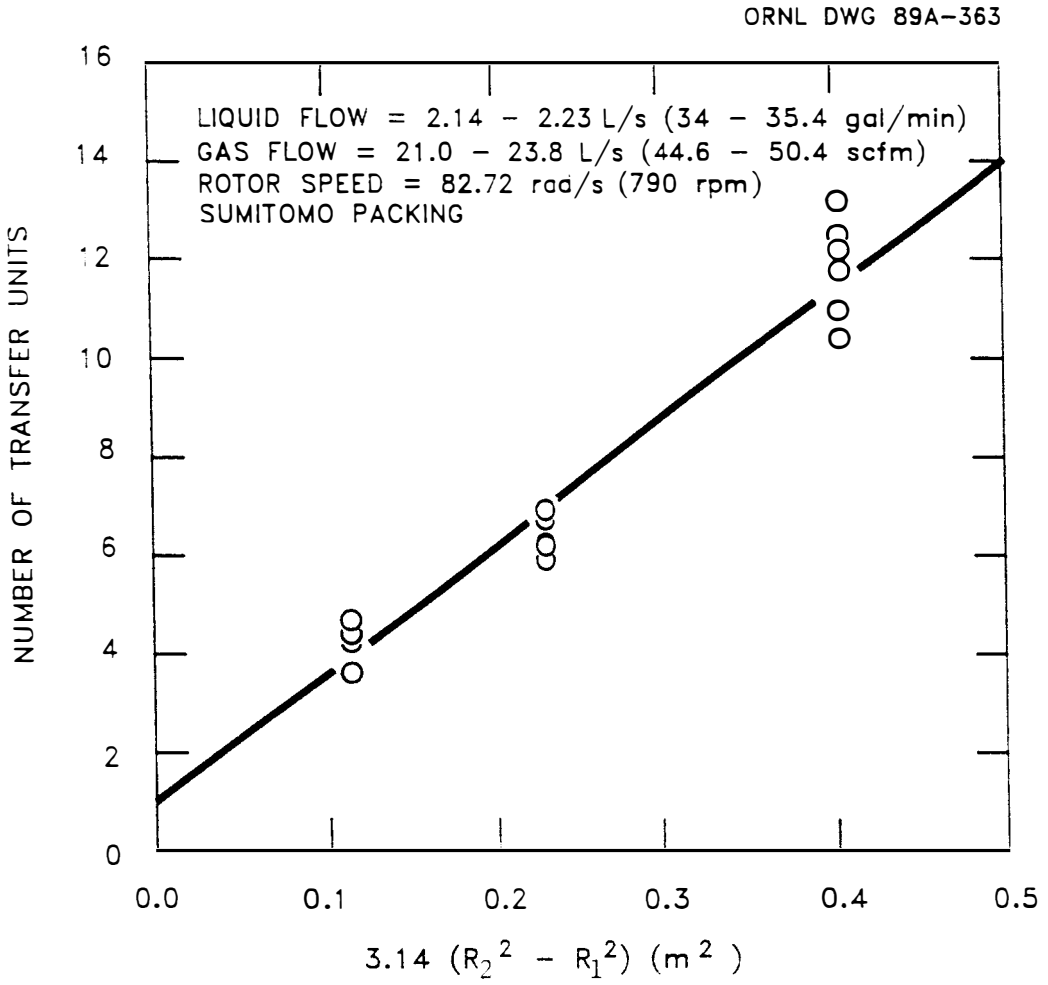

Fig. 6-12. Plot of mass transfer data from centerpoint runs (o-xylene data).

The effect of acceleration on the area of a transfer unit (ATU) for the 45.72-cm-diam rotor is shown in Fig. 6-13. The ATU decreases with an increase in acceleration for both types of packings. The decrease in ATU appears to level out at accelerations greater than 1000 m/s^2. Also shown in Fig. 6-13 is a data point from the 76.20-cm-diam rotor. Notice that this rotor gives considerably higher ATU at the same operating conditions as the 45.92-cm-diam rotor. This rise in ATU with outer rotor radius may be indicative of incomplete wetting of the packing at the outer edge. This phenomenon was investigated further by comparing data at other conditions. Since only four runs were available for the 76.92-cm-diam rotor, the comparison was rather limited. Figure 6-14 shows ATU values for two run conditions. From this figure, it can be seen that at low rotational speed (500 rpm) there is significant difference in the ATU values for the two rotors while at 790 rpm the difference is relatively minor. Thus, it can be concluded that to achieve the same value of an ATU the large diameter rotor would have to be operated at higher speeds which leads to higher operating costs. It would be more cost effective from operations viewpoint to build rotors that increase the quantity of packing by increasing axial length.

The effect of liquid flow rate and gas/liquid ratio on the ATU is shown in Figs. 6-15 and 6-16, respectively. Both types of packing exhibit an analogous behavior. The ATU increases with liquid flow rate. This would be expected since the mass transfer rate of the three compounds is liquid film controlled and the thickness of the liquid film increases with an increase in the liquid flow rate. The effect of

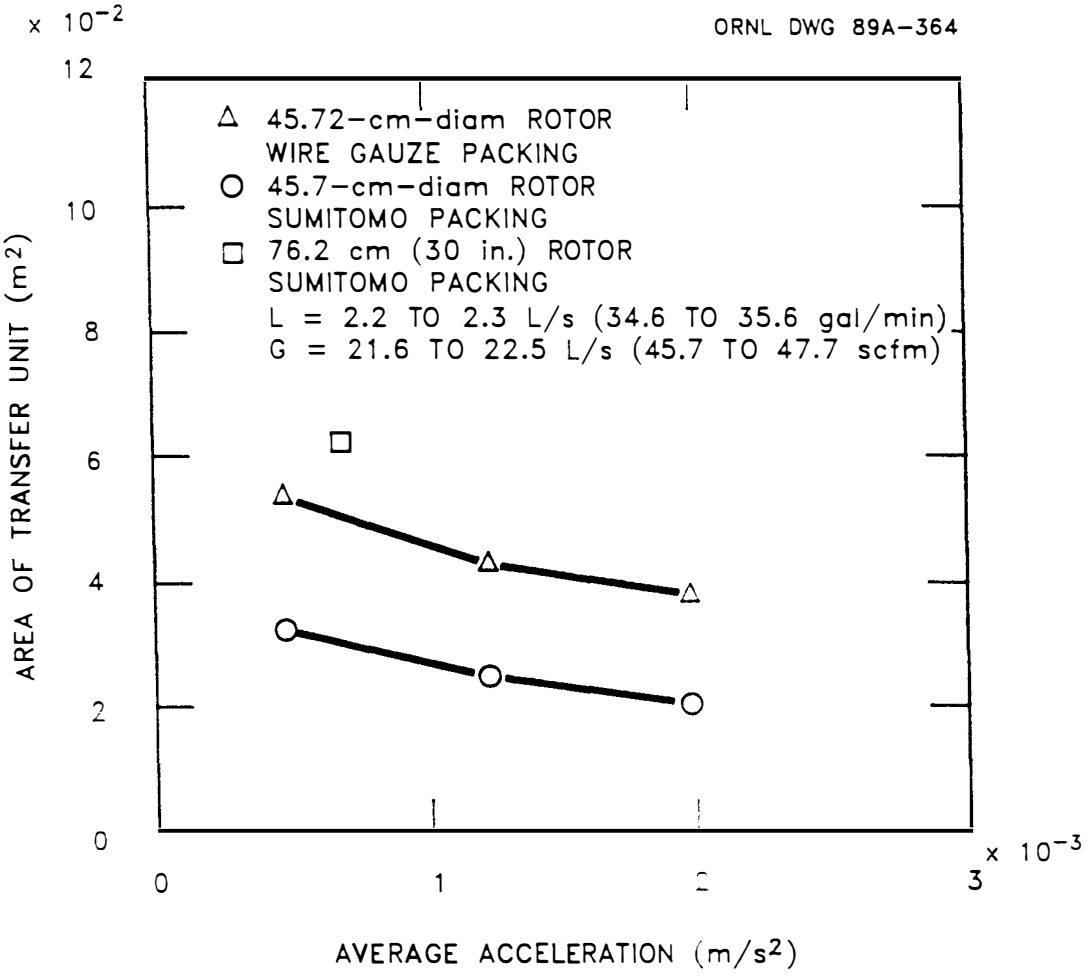

Fig. 6-13. Effect of acceleration on the area of a transfer unit (o-xylene data).

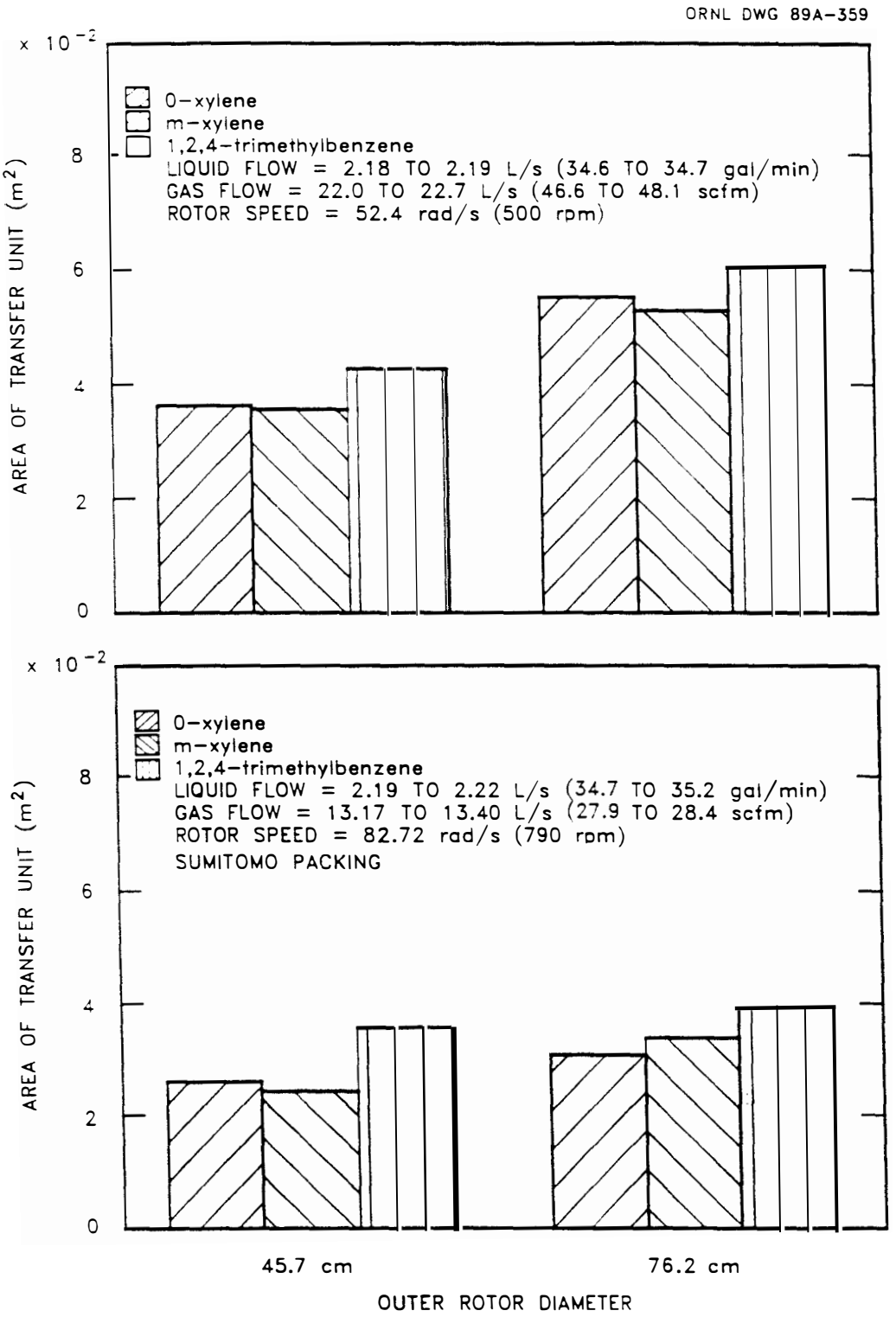

Fig. 6-14. Comparison of area of transfer unit for the different rotors.

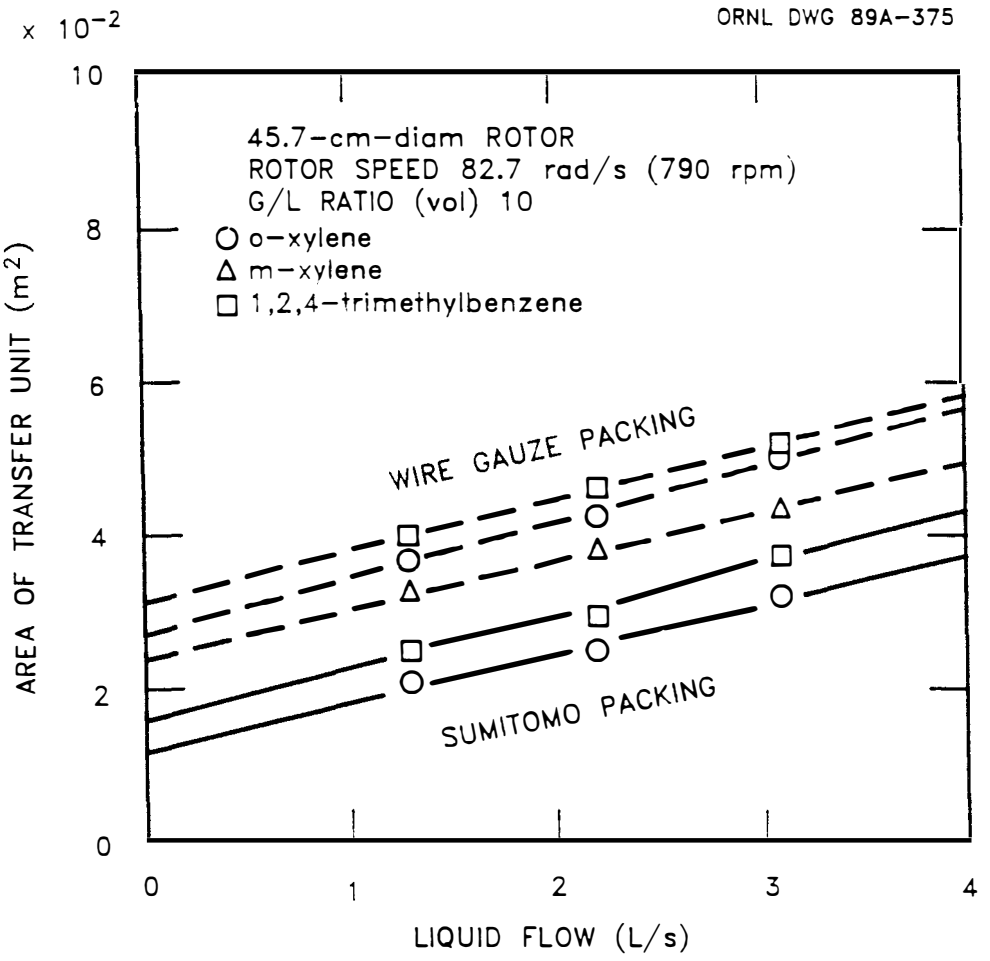

Fig. 6-15. Effect of liquid flow on the area of transfer unit.

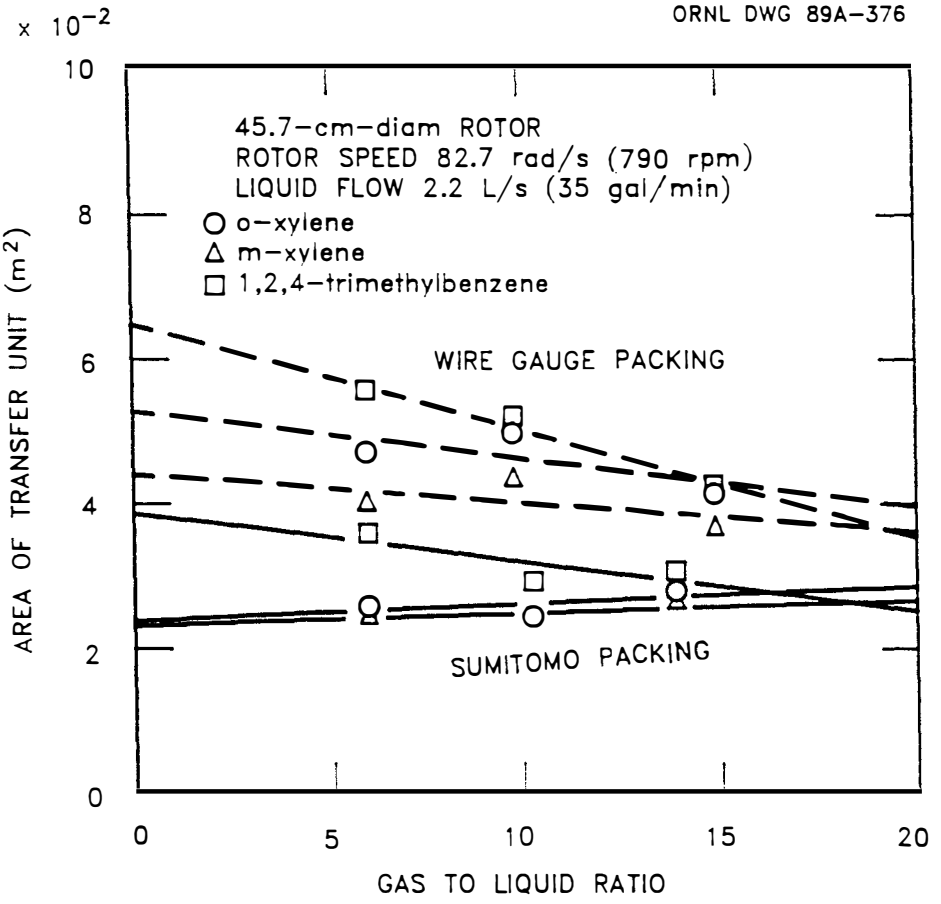

Fig. 6-16. Effect of gas/liquid ratio on area of transfer unit.

the gas/liquid ratio on ATU appears to be negligible for o-xylene and m-xylene with the Sumitomo packing. While results from the wire gauze packing shows greater scatter for these two compounds, the change in ATU is still rather small. The ATU for 1,2,4-trimethylbenzene increases at low gas/liquid ratio for both packings. This rise in ATU probably results from the use of an estimated Henry's Law constant. Experimental Henry's Law correlation for variance with temperature was not available and the correlation for 1,3,5-trimethylbenzene was used instead. If Henry's Law constants are not the same for both compounds, it is possible that equilibrium conditions existed for 1,2,4-trimethylbenzene since at low gas/liquid ratio the stripping factor is very close to value of unity. Existence of equilibrium conditions would give an erroneous measurement of an ATU since no further removal could be achieved no matter how large the packing torus.

6.2.2 Experimental Design Analysis

The central composite design was analyzed to determine which independent variables had a significant effect on the area of transfer unit. The following general linear model was used in the analysis:

$$ATU = Z_o + Z_1L + Z_2a + Z_3(G/L) + Z_4L^2 + Z_5a^2 + Z_6(G/L)^2 + Z_7La + Z_8L(G/L) + Z_9a(G/L) \quad (6\text{-}12)$$

where $Z_o \ldots Z_9$ = regression coefficients

L = liquid flow (L/s)

a = average acceleration (m/s^2)

G/L = gas to liquid ratio (vol.)

Table 6-2 shows the terms in Eq. (6-12) which were significant at the 0.05 level for o-xylene. 0-xylene data were used in this analysis because the o-xylene peak on the chromatogram was very distinct and had no side peaks which could give erroneous measurements. For both packings the variance of the repeated center point runs was less than that observed for the whole model. This implies that the change in ATU with operating conditions was real and not just due to the scatter in the observed data.

In order to reduce the number of terms in the above model a SAS regression procedure was used. In this analysis, independent variables are added to the model one by one if the corresponding F statistic for a variable is significant at a prescribed level. Each time a variable is added all variables already in the model are examined and those that do not produce significant F statistic are eliminated. The entrance and elimination levels used are somewhat arbitrary. For this work, the default entrance and elimination levels of 0.15 given in SAS were used. The final model for the Sumitomo packing given by this technique is:

$$ATU = 0.031 - 8.6\times10^{-6}a + 4.7\times10^{-9}a^2 + 1.3\times10^{-3}\,L^2 - 3.8\times10^{-6}aL - 5.4\times10^{-7}a(G/L) + 4.0\times10^{-4}L(G/L) \qquad (6\text{-}13)$$

and model given for the wire gauze packing is:

$$ATU = 0.037 + 8.1\times10^{-3}L - 8.3\times10^{-7}a(G/L) \qquad (6\text{-}14)$$

The coefficients of determination (r^2) for the two models were 0.96 and 0.75, respectively. Although these models can be used to design a centrifugal vapor-liquid contactor for conditions similar to those in

Table 6-2. Results of central composite experiment design analysis.

Packing	Terms with Significant Effect
Sumitomo	a^2
	aL
Wire Gauze	a
	L
	aL
	L(G/L)

this study, it would be more beneficial to develop general correlation similar to those used for conventional packed towers.

6.2.3 Comparison with Existing Correlations

As stated earlier, there are two correlations which have been proposed for possible use in modeling the mass transfer performance of a centrifugal vapor-liquid contactor. The first one is given in Eq. (4-25)

$$\frac{(K_L a)d}{D} = 0.023\ Sc^{1/2}\ Gr^{0.38}\ (dL/\mu)^{1/2} * (1 - 1.02\exp[-0.15(dL/\mu)^{0.4}])$$

and the second one is given in Eq. (3-3)

$$\frac{k_l\ d}{D} = 0.96\ Sc^{1/2}\ Re^{1/3}\ (a_t/a_e)^{1/3}\ Gr^{1/6}$$

Both of these equations require a characteristic dimension for the packing. In evaluating the predictive capability of the correlations, the characteristic dimension for the Sumitomo packing was taken as the thickness (0.002 m) of one sheet of packing. For the wire gauze packing the total thickness of the packing (0.1 m) was used since no other dimension was available. In addition, average values for acceleration and liquid loading calculated using Eq. (6-6) were used. The diffusion coefficient for o-xylene in water was calculated using the Wilke-Chang equation (Wilke and Chang, 1955).

The ATU calculated using Eq. (4-25) is compared with the experimental values in Fig. 6-17. This correlation over predicts the value of the ATU by a factor of 3 to 5. The results of similar

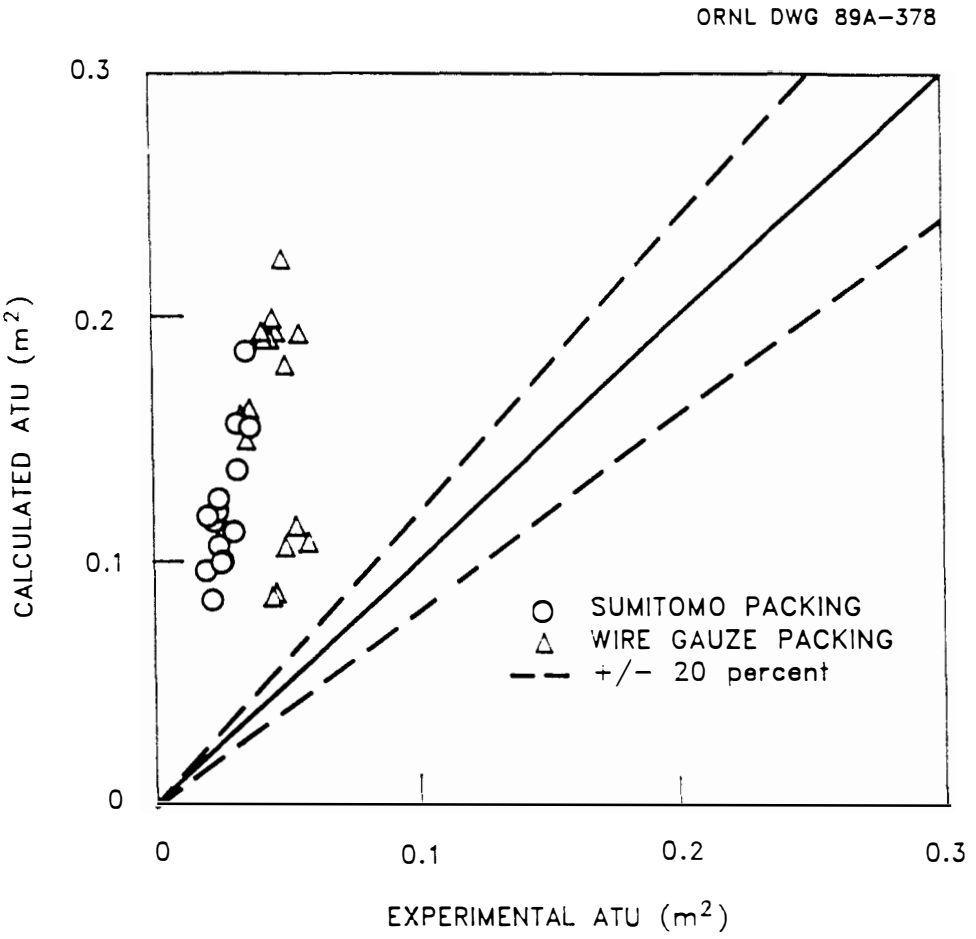

Fig. 6-17. Comparison of the experimental ATU with that predicted by correlation proposed by Vivian et al.

comparison for Eq. (3-3) are given in Figs. 6-18 and 6-19. Two values of the interfacial area were used. First, it was assumed that the interfacial area was equal to the total specific surface area of the packing. For the second set of calculations, the interfacial area given by Eq. (3-5) was used. This correlation seems to do a reasonable job in predicting the ATU for the Sumitomo packing while it overestimates the values for the wire gauze packing. This suggests that choice of characteristic length is very important. It also suggests that the reasonable prediction for the Sumitomo packing is just a coincidence since a packing with similar characteristics could be fabricated out of different thickness material. Thus, it was concluded that these two correlation are not appropriate for use with the type of packings used in this study.

6.2.4 New Correlation Based on Specific Surface Area of Packing

Because existing correlations were unable to predict the ATU of the centrifugal vapor-liquid contactor, a new correlation which uses the specific surface area of packing instead of characteristic length was developed. The correlation was developed assuming that the ATU is a function of the following variables: liquid flow (L_f), liquid viscosity (μ_L), liquid density (ρ_L), specific surface area of packing (a_p), and acceleration (a_c). This function can be written as:

$$ATU = f(L_f, \mu_L, \rho_L, a_p, a_c) \qquad (6\text{-}15)$$

Using Buckingham's Pi Theorem, these variables can be combined into dimensionless groups. This method is based on the premise that

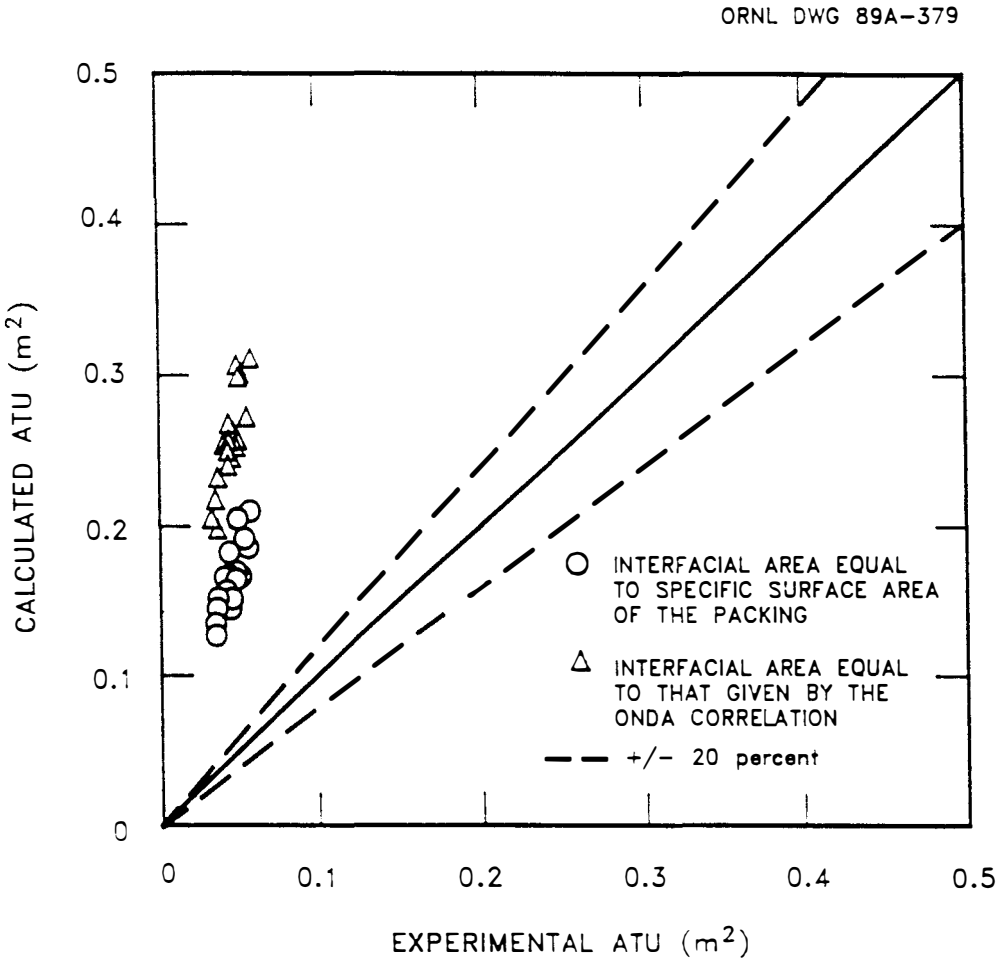

Fig. 6-18. Comparison of the experimental and predicted ATU for the wire gauze packing.

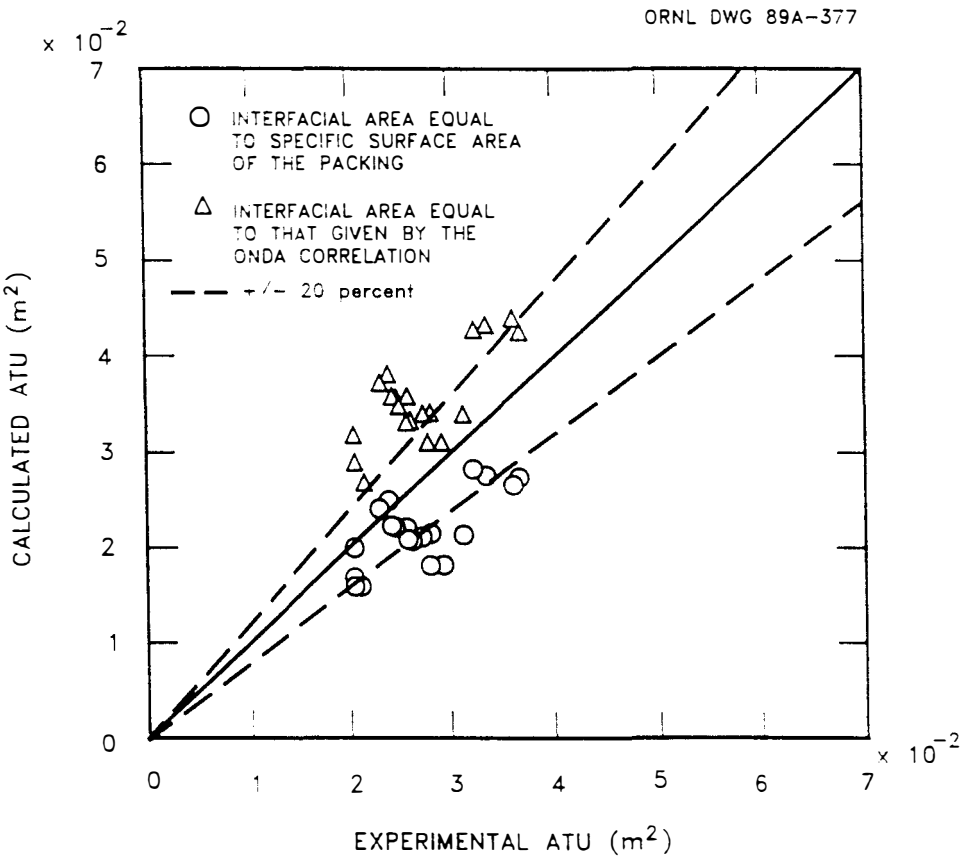

Fig. 6-19. Comparison of the experimental and predicted ATU for the Sumitomo packing.

the equation describing the system must be dimensionally homogeneous. Upon carrying out the necessary mathematics, the equation becomes:

$$ATU = (1/a_p^2)(L_f/\mu_L\ a_p)^X\ (\rho_L^2\ a_c/\mu_L^2\ a_p^3)^Y \qquad (6\text{-}16)$$

where X and Y are constants determined from the experimental data. Notice that the dimensionless groups are simply Reynolds number and Grashof number based on the specific surface area of the packing. The data for both Sumitomo and wire gauze packings with the 45.72-cm-diam rotor were used to determine the values of X and Y. Again average values of L_f and a_c calculated using Eq. (6-6) were used. The equation given by this data is:

$$ATU = \frac{337{,}143.86}{a_p^2}\ (L_f/\mu_L\ a_p)^{0.6}\ (\rho_L^2\ a_c/\mu_L^2\ a_p^3)^{-0.15} \qquad (6\text{-}17)$$

where dimensions on the variables are: ATU = m^2, L_f = kg/m^2-s, ρ_L = kg/m^3, μ_L = kg/m-s, a_p = m^2/m^3, a_c = m/s^2. The coefficients on both the Reynolds number and Grashof number are close to those of the previous correlation. The ATU calculated using this correlation is compared with the experimental data in Fig. 6-20. Although the coefficient of determination (r^2) from regression analysis was only 0.61, the correlation predicts the ATU within +/-20 percent which is similar to what existing correlations can predict for conventional packed tower.

The proposed correlation has two advantages over existing correlations. First, it uses parameters which are easy to define for the centrifugal vapor-liquid contactor and no knowledge of interfacial

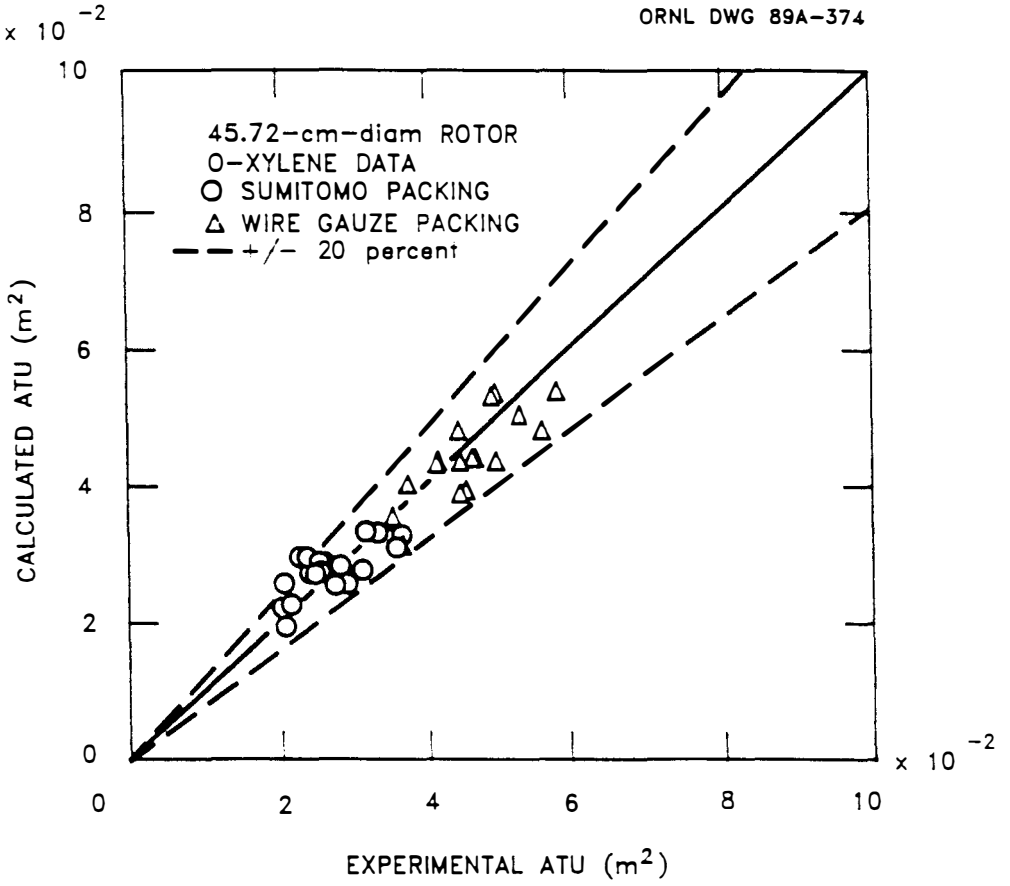

Fig. 6-20. Comparison of the experimental and calculated ATU using correlation based on the specific surface area of packing.

area is needed. Second, the dependence of ATU on specific surface is given more emphasis than other variables. It should be pointed out that the above correlation is based on the assumption the rate of mass transfer is liquid film controlled. For air stripping systems, this assumption may not be unreasonable since diffusivities in the gas phase are four orders of magnitude higher than in the liquid phase. The proposed correlation could be made more general by including the Schmidt number. Since the Schmidt number in the experimental data remained constant, it was not included.

6.3 Power Consumption

Knowledge of the power requirements of the centrifugal vapor-liquid contactor at various operating conditions is important in making economic comparisons. At first it would appear that power costs of an air stripping system employing a centrifugal vapor-liquid contactor must be much higher than a system employing a conventional packed tower. However, this may not necessarily be true because a centrifugal vapor-liquid contactor can be operated at low stripping factors while still obtaining high removal efficiencies that the blower costs for such a system may be much lower than for a conventional packed tower.

6.3.1 General Characteristics

The power consumed at various operating conditions was measured in order to determine the contribution from each variable. Since the power meter was located before the variable frequency drive, the

measured power consumption includes losses due to inefficiencies in the frequency drive and the motor. There was no attempt made to separate these losses out since they would have to be included in the design anyway.

The effect of gas flow rate on the power consumption is shown in Fig. 6-21. The power consumption decreases slightly with an increase in gas flow rate. This reduction results from the gas transferring the energy to the rotating packing as it flows from a region of high pressure (high energy) to a region of low pressure (low energy). The effects of outer rotor radius, rotor speed, and liquid flow rate on power consumption are shown in Figs. 6-22 through 6-24, respectively. The quantity of power used increases with square of the outer rotor radius and rotor speed, and linearly with the liquid flow rate. These relationships are not totally unexpected since similar behavior is observed in centrifugal pumps.

6.3.2 Development of an Empirical Correlation

Power consumption for a centrifugal vapor-liquid contactor can be modeled using two distinct terms. The first terms could be used to account for all the frictional losses and the second term used to account for the power required to accelerate the liquid entering the packing torus to the rotational speed at the outer radius. The frictional losses are highly dependent upon the design of the machine and cannot be predicted without advanced knowledge of the design (i.e. type of bearings, direct or pulley drive, etc.). The power required to accelerate the liquid on the other hand can be described by a

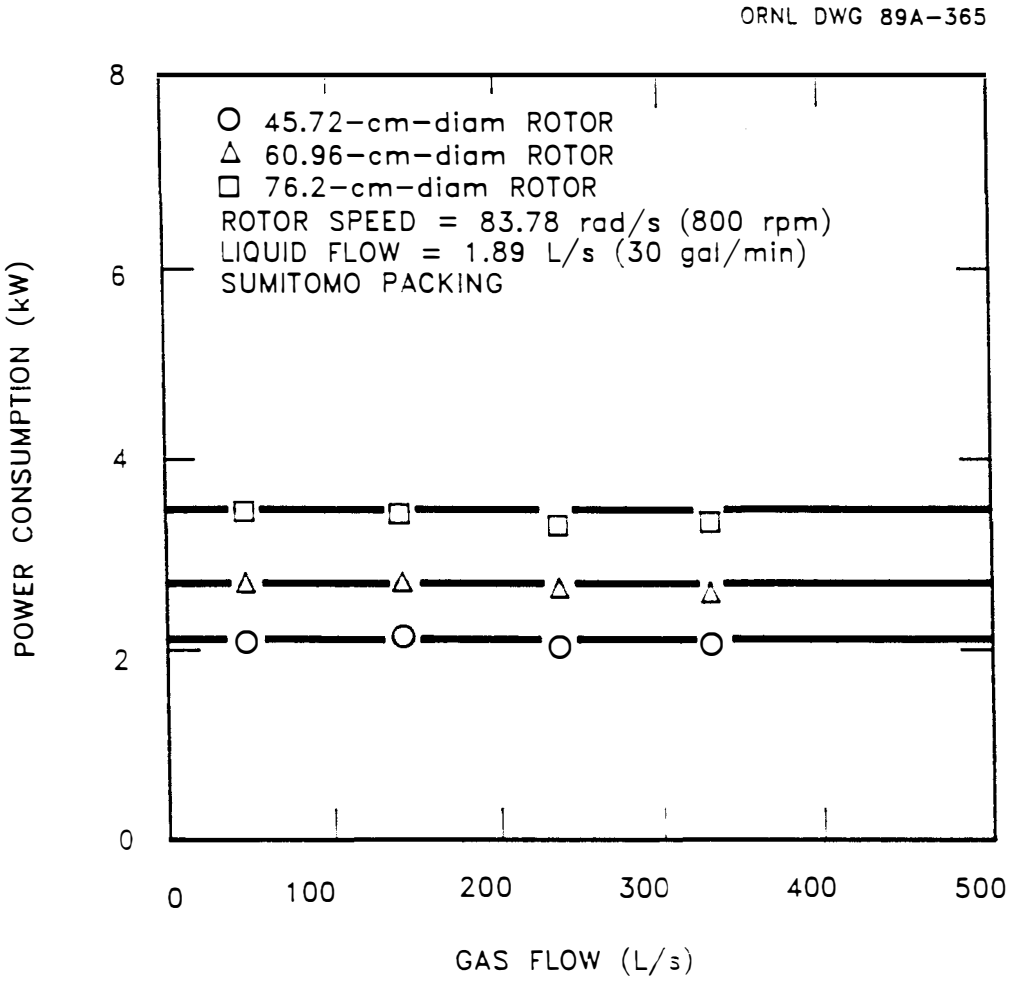

Fig. 6-21. Effect of gas flow rate on power consumption.

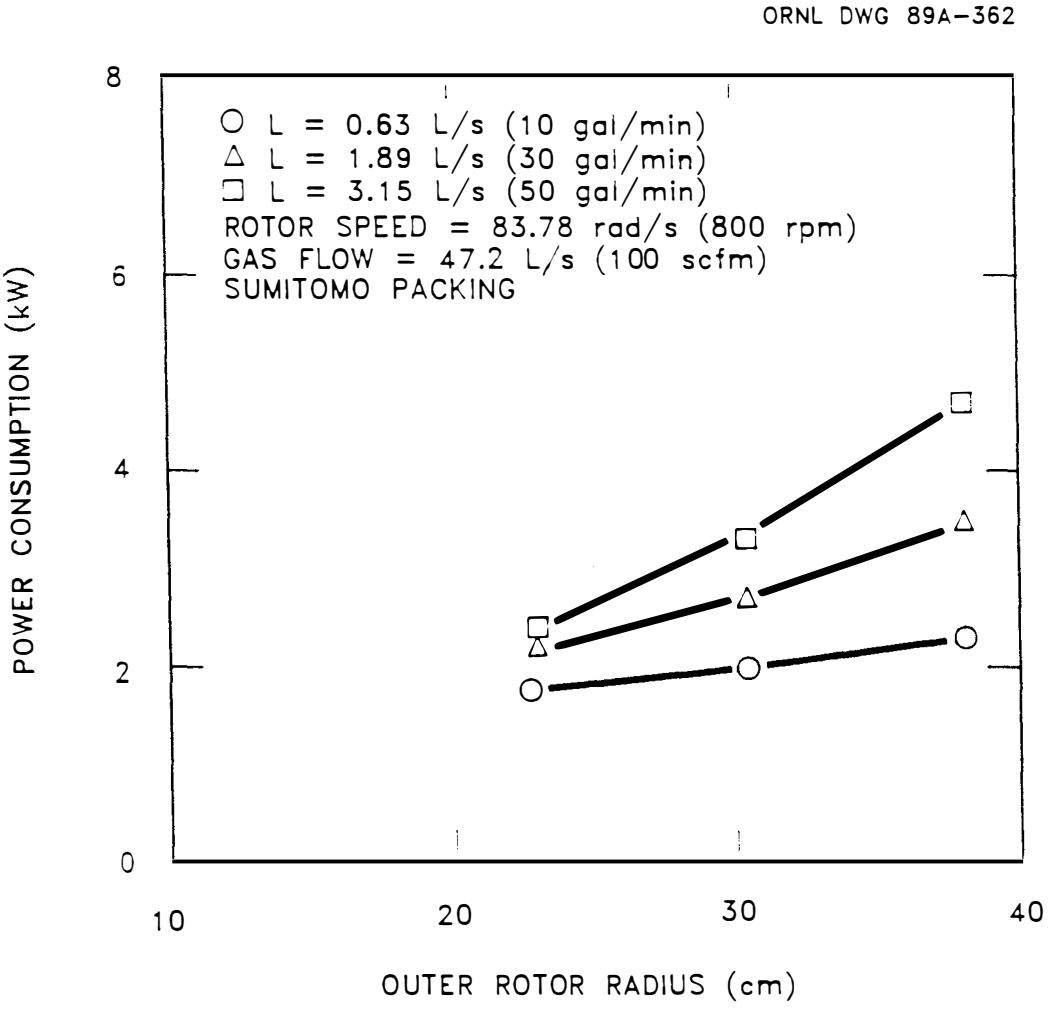

Fig. 6-22. Effect of outer rotor radius on power consumption.

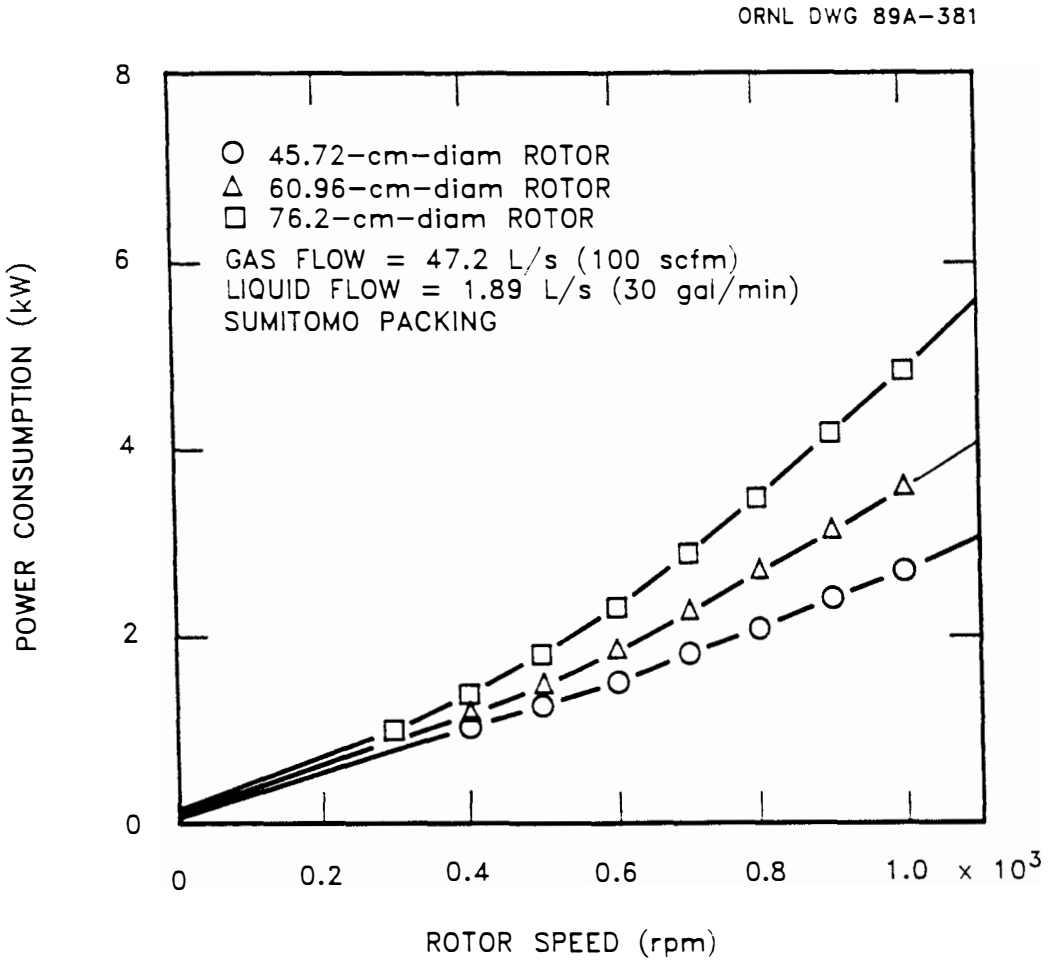

Fig. 6-23. Effect of rotor speed on power consumption.

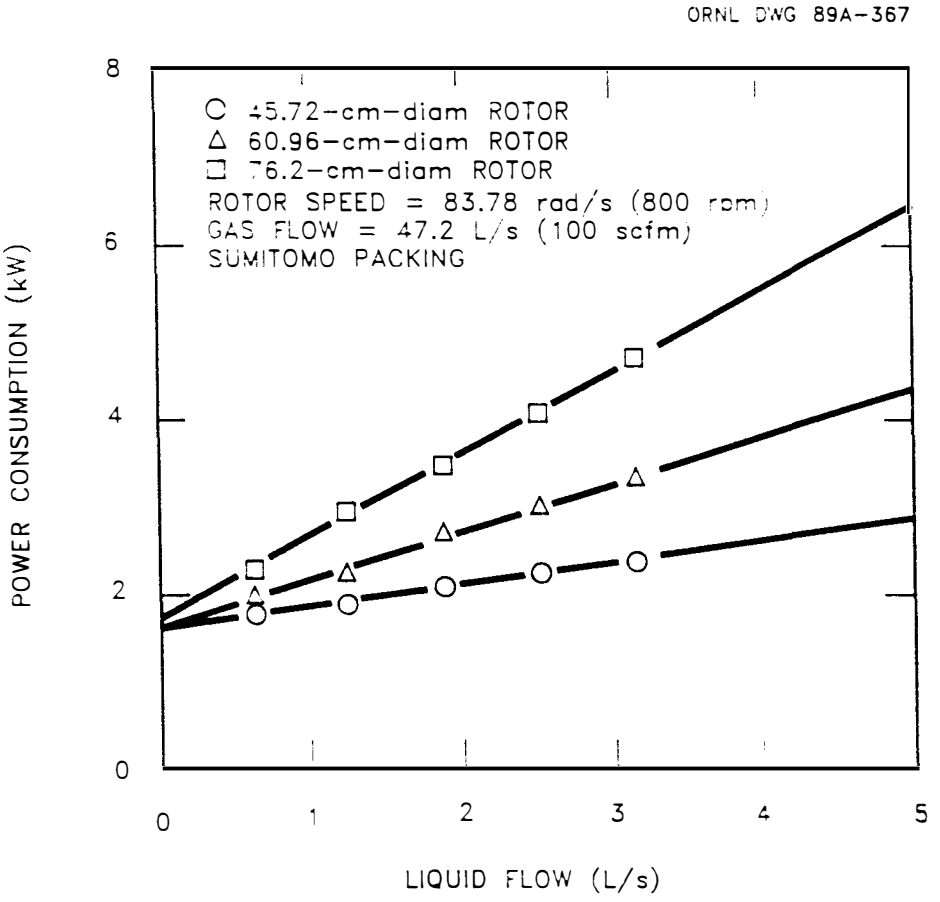

Fig. 6-24. Effect of liquid flow rate on power consumption.

theoretical model (Leonard, 1980). The overall power consumption can thus be written as:

$$P_c = Z_o + Z_1 \rho_L r_2^2 \omega^2 Q \qquad (6\text{-}18)$$

where P_c = power consumption (kW)

ρ_L = liquid density (kg/m^3)

r_2 = outer rotor radius (m)

ω = angular velocity (rad/s)

Q = volumetric flow rate of liquid (m^3/s)

Z_o, Z_1 = regression coefficients

In this model, the energy recovered from the gas phase is neglected since this is very small, and Z_1 accounts for the slippage between the packing and liquid phase that occurs as the liquid phase is being accelerated. The experimental data from all three rotors in a region where rotational speed was greater than the limit of operability speed gave the following equation:

$$P_c = 1.222 + 0.0011 \rho_L r_2^2 \omega^2 Q \qquad (6\text{-}19)$$

The coefficient of determination (r^2) for this equation was 0.92. The power consumption calculated using this equation is compared with the experimental data in Fig. 6-25. The correlation does a fairly good job in describing the power consumption over the operating conditions.

6.4 Fouling of the Packing

One of the advantages of a centrifugal vapor-liquid contactor over a conventional packed tower cited in literature is the ability to

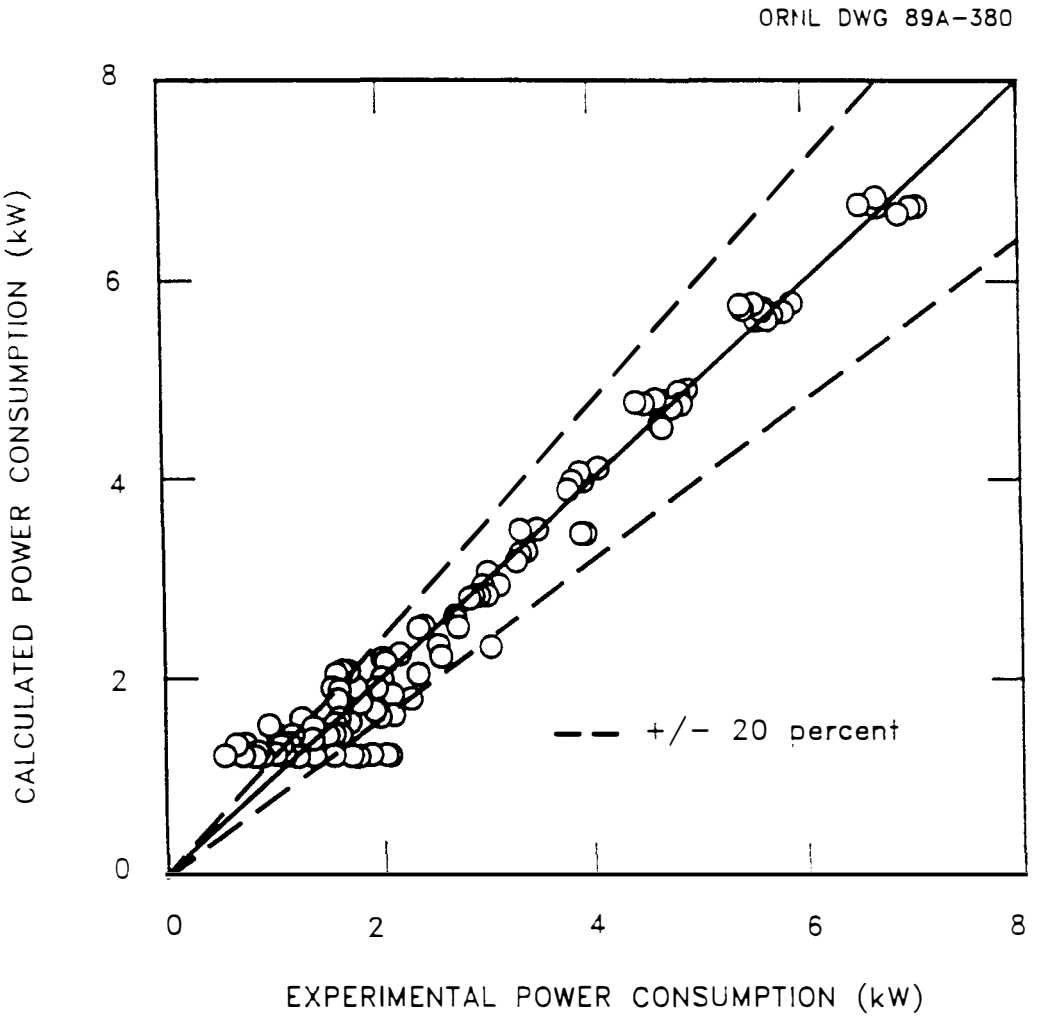

Fig. 6-25. Comparison of the experimental and calculated power consumption.

resist fouling of the packing. During the mass transfer tests, the center point run was used to monitor whether any change was taking place. These tests indicted that there was no change in pressure drop. During this time, hydraulic tests were also performed at 1.89 L/s (30 gal/min) of liquid flow and 141.6 L/s (300 scfm) of air at regular intervals. The results of these tests for the 45.72-cm-diam rotor are shown in Fig. 6-26. At these conditions, the packing appears to be fouling. Similar phenomenon was also observed for the 76.20-cm-diam rotor. The 60.96-cm-diam rotor which had unusual pressure drop behavior initially became plugged and unbalanced during continuous operation for four days at the end of the mass transfer tests.

When the Sumitomo packing was removed from the 45.72-cm-diam rotor, considerable coating of the outer layers of the packing was seen. In addition, the lower part of the rotor showed much more deposition than the upper part. There is no apparent explanation for this other than that the packing contains certain amount of water when the rotor is stopped and this water flows down the packing and out. This flow pattern would deposit more minerals on the lower part of the rotor as the water evaporates. Results of chemical analysis of the solids removed from the rotor are given in Table 6-3. The groundwater at Eglin AFB contains a significant amount of iron (9 ppm) and this appears to be the main culprit in plugging the rotor. The Al, Cr, and Ni in the precipitate came from the packing torus because the precipitate was removed from rotor by scraping. The quantity of these elements in the groundwater was small.

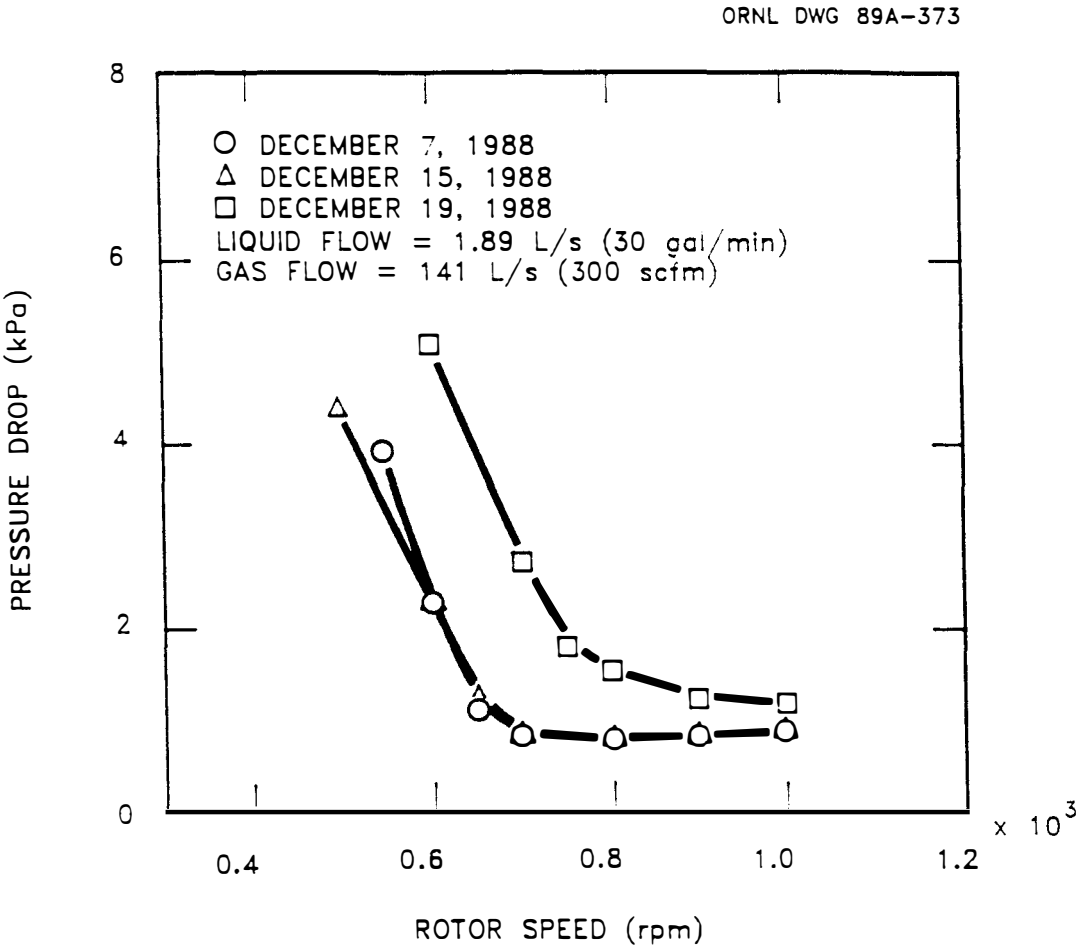

Fig. 6-26. Rise in pressure drop as a result of fouling for the 45.72-cm-diam rotor.

Table 6.3. Elemental analysis of the precipitate.

Element	Quantity (mg/kg)
Ag	< 8.7
Al	2.0E+5
As	8.7E+1
B	1.7E+2
Ba	9.5E+1
Be	< 7.0E-1
Ca	1.5E+3
Cd	< 3.5
Co	1.8E+1
Cr	5.9E+2
Cu	2.1E+2
Fe	1.9E+4
Ga	< 5.2E+2
Li	< 3.5E+2
Mg	1.3E+3
Mn	2.0E+2
Mo	< 7.0E+1
Na	< 8.7E+2
Ni	2.7E+4
P	9.0E+3
Pb	8.4E+1
Sb	8.5E+2
Se	< 1.4E+2
Si	1.9E+3
Sn	< 8.7E+1
Sr	< 8.7
Ti	3.6E+2
V	2.4E+1
Zn	1.6E+2
Zr	< 3.5E+1

From these observations, it appears that the shearing action is not able to scrub the packing as claimed previously and that centrifugal vapor-liquid contactor is susceptible to plugging when the mineral content of the groundwater is high. Thus, some pretreatment of the groundwater may be required. It should be pointed out that the packings used in the conventional packed tower for this project also showed considerable deposition of minerals and would eventually plug. Groundwater with iron content this high should be pretreated prior to any air stripping operations.

7. CONCLUSIONS AND RECOMMENDATIONS

The centrifugal vapor-liquid contactor used in this study appears to be a very efficient machine for air stripping of volatile organic compounds from groundwater. The techniques used in the design of conventional packed towers can be easily modified and expanded for the design of the centrifugal vapor-liquid contactor. Hydraulic test data indicate that the Sherwood flooding correlation shown in Fig. 7-1 underestimates the limit of operability rotational speed. The pressure drop in a region where the rotor speed is greater than limit of operability speed can be estimated from an empirical equation (Eq. 6-11):

$$P_{tot} = 0.923\ \rho_{air}\ \omega^2(r_2^2 - r_1^2) + 0.992\frac{a_p}{\epsilon}\ \rho_{air}(r_2 - r_1)V^2_{avg}$$

which contains terms to account for the pressure drop due to rotation and for the flow of a gas through a porous media.

Mass transfer concepts of number of transfer unit and height of transfer unit from conventional packed towers can be adopted to the centrifugal vapor-liquid contactor by deriving the equations in polar coordinates. The number of transfer units remains unchanged while an area of a transfer unit (ATU) concept seems more appropriate. The ATU appears to be more dependent upon the specific surface area of the packing than the rotor speed and liquid flow rate under the conditions used in this

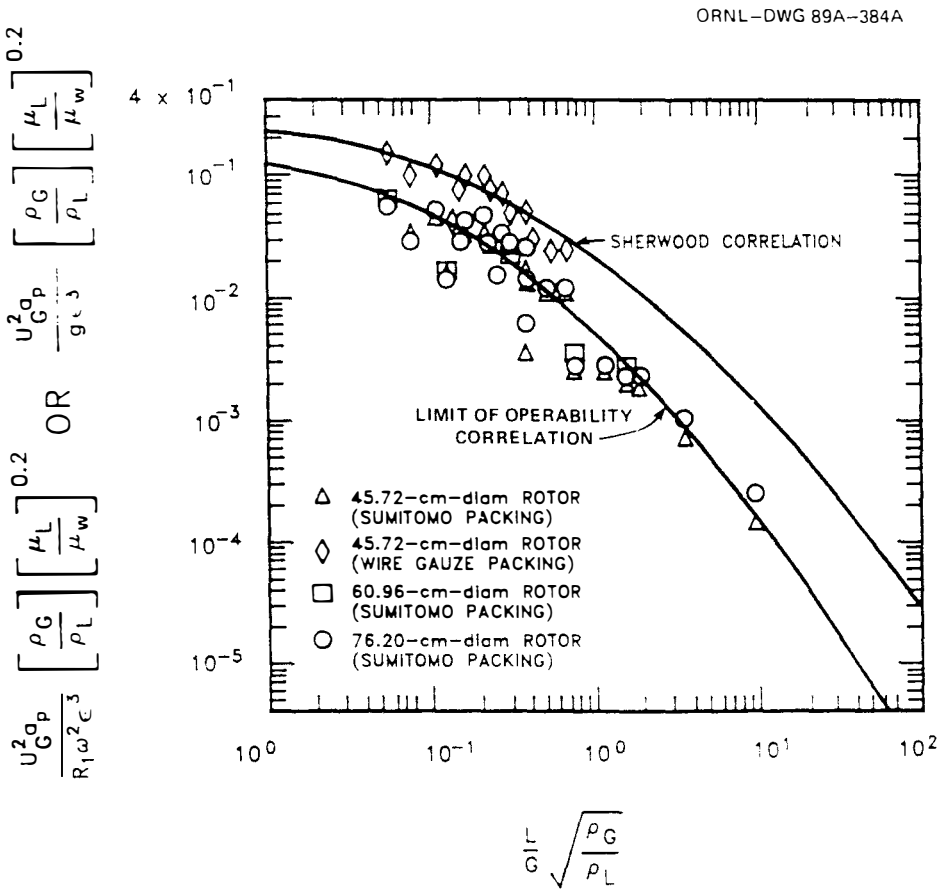

Fig. 7-1. Comparison of limit of operability data with that predicted by the Sherwood flooding correlation.

study. A new correlation for predicting ATU based on the specific surface area of the packing (Eq. 6-17):

$$ATU = \frac{337,143.86}{a_p^2} (L_f/\mu_L\ a_p)^{0.6} (\rho_L^2\ a_c/\mu_L^2\ a_p^3)^{-0.15}$$

describes the experimental data with reasonable degree of accuracy.

The power requirement of a centrifugal vapor-liquid contactor is mainly a function of the liquid flow rate, outer radius of the packing torus, and rotor speed. A correlation based on the power required to accelerate the liquid (Eq. 6-19):

$$P_c = 1.222 + 0.0011 \rho_L r_2^2\ \omega^2\ Q$$

was found to adequately predict the power consumption for the experimental conditions.

The previous claims in the literature that the centrifugal vapor-liquid contactor is not susceptible to fouling of the packing because of high shear forces were found not to be valid. Preliminary signs of plugging due to mineral deposition were observed in two of the rotors and the third rotor plugged completely after a very short operating time. It should be emphasized that the groundwater at Eglin Air Force Base has very high content (9 ppm) of iron and may not be a fair evaluation of the machine.

The use of a centrifugal vapor-liquid contactor for air stripping of volatile organic compounds will most likely be restricted to those sites where mineral content is low unless pretreatment of the water is done. However, the presence of a large number of transfer units makes the

machine a likely candidate for those operations where control of air emissions may be required because the centrifugal vapor-liquid contactor can be operated at very low stripping factors and still achieve high removals.

The following recommendations are proposed for possible work with the centrifugal vapor-liquid contactor in the future:

1. The performance of other packing materials should be investigated to extend the data base and to verify the pressure drop and mass transfer correlations proposed in this study.
2. The use of an inert gas such as nitrogen in a closed loop system using a centrifugal vapor-liquid contactor for air stripping and activated carbon for cleaning up the air stream should be tested. This could permit the use of the centrifugal vapor-liquid contactor for groundwater with high iron content.
3. The possible application of a centrifugal vapor-liquid contactor for air stripping of trihalomethanes from drinking water should be investigated. This application is particularly appealing because the water is fairly clean and the centrifugal vapor-liquid contactor can be built in modular units which can be turned on and off depending on the water demand.

REFERENCES

REFERENCES

Althoff, W. F., R. W. Cleary, and P. H. Roux, "Aquifer Decontamination for Volatile Organics: A Case History," Ground Water, 19(5), September-October 1981.

Anderson, V. L. and R. A. McLean, Design of Experiments: A Realistic Approach, Marcel Dekker, Inc., New York, pp. 353-60, 1974.

Andrews, C. C., "Photooxidative Treatment of TNT Contaminated Waste Water," Naval Sea Systems Command, Report No. WQEC/C 80-137, January 1980.

Ashworth, R. A., G. B. Howe, M. E. Mullins, and T. N. Rogers, "Air-Water Partitioning Coefficients of Organics in Dilute Aqueous Solutions," to be published in Journal of Hazardous Materials.

Baldauf, G., "Removal of Volatile Halogenated Hydrocarbons by Stripping and/or Activated Carbon Adsorption," Water Supply, 3(1), pp. 187-96, 1985.

Balzhiser, R. E., M. R. Samuels, and J. D. Eliassen, Chemical Engineering Thermodynamics: The Study of Energy, Entropy, and Equilibrium, Prentice-Hall, Inc., New Jersey, pp. 418-28, 1972.

Barbash, J. and P. V. Roberts, "Volatile Organic Chemical Contamination of Groundwater Resources in the U. S.," Journal WPCF, 58(5), pp. 343-348, May 1986.

Berger, L. M., A. P. Pajak, and A. E. Robb, Jr., "Contaminated Groundwater: Above-Ground Treatment Alternatives," J. Haz. Mat., 14, pp. 51-70, 1987.

Bird, R. B., W. E. Stewart, and E. N. Lightfoot, Transport Phenomena, John Wiley and Sons, Inc., pp. 196-200, 1960.

Bishop, M. M., D. A. Cornwell, and A. Dwarkanath, "Design and Operation of Air Stripping for Trihalomethane Removal," Proc. - AWWA Annu. Conf., pp. 1363-76, 1985.

Box, G. E. P. and K. B. Wilson, J. Royal Stat. Soc., B, 13:1, 1951.

Bucklin, R. W. and J. D. Johnston, "Field Tests of HIGEE to Confirm Its Potential," presented at Spring Annual Meeting of American Institute of Chemical Engineers in Houston, Texas, March 29-April 2, 1987.

Byers, W. D. and C. M. Morton, "Removing VOC from Groundwater; Pilot, Scale-up, and Operating Experience," Environmental Progress, 4(2), pp. 112-8, 1985.

Charpentier, J., "Mass-Transfer in Gas-Liquid Absorbers and Reactors" in Advances in Chemical Engineering, Volume II, edited by T. B. Drew et al., Academic Press, New York, 1981.

Cheremisinoff, P. N., "Solvent Recovery," Pollution Engineering, pp. 62-69, August 1987.

Colburn, A. P., "Simplified Calculation of Diffusional Process: Number of Transfer Units or Theoretical Plates," Industrial and Engineering Chemistry, 33(4), pp. 459-67, April 1941.

Crittenden, J. C., R. D. Cortright, B. Rick, S. Tang, D. Perram, and T. Rigg, "Removal of Volatile Organic Chemicals from Air Stripping Tower Off-Gas Using Granular Activated Carbon," Proceedings: Conference on Current Research in Drinking Water Treatment, EPA/600/9-88/004, pp. 54-89, March 1988.

Davidson, J. F., "The Hold-up and Liquid Film Coefficient of Packed Towers, Part II; Statistical Models of the Random Packings", Transaction of the Institution of Chemical Engineers, 37, 1959.

Davies, O. L. (Ed.), Design and Analysis of Industrial Experiments, 2nd ed., Oliver and Boyd, Edinburg, 1971.

Dietrich, C., D. Treichler, and J. Armstrong, An Evaluation of Rotary Air Stripping for Removal of Volatile Organics From Groundwater, Air Force Engineering & Services Center, ESL-TR-86-46, February 1987.

Dyksen, J. E., "Treatment Techniques for Removing Organic Compounds from Ground Water Supplies," Industrial Water Engineering, 19(3), pp. 16-21, 1982.

Downey, D. C., R. E. Hinchee and M. Westray, "Enhanced Bioreclamation of JP-4 Contaminated Aquifer," presented at the Society of Environmental Toxicology and Chemistry, 8th Annual Meeting, Environmental Risk: Recognition, Assessment and Management, Pensacola, Florida, November 9-12, 1987.

Foster, M. L., "Evaluation of Parameters Affecting Activated Carbon Adsorption of a Solvent-Laden Air Stream," presented at 78th Annual Meeting of the Air Pollution Control Association, Detroit, Michigan, June 1985.

Fowler, R., Glitsch, Inc., personal communication.

Fowler, R. and A. S. Khan, "VOC Removal with a Rotary Air Stripper," presented at the 1987 Annual Meeting of American Institute of Chemical Engineers in New York, New York, November 15-17, 1987.

Fredenslund, A., J. Gmehling, and P. Rasmussen, Vapor-Liquid Equilibria Using UNIFAC, A Group Contribution Method, Elsevier, Amsterdam, 1977.

Gossett, J. M., "Measurement of Henry's Law Constants for C_1 and C_2 Chlorinated Hydrocarbons", Environ. Sci. Technol., 21(2), pp. 202-8, 1987.

Gross, R. L., "Development of Packed-Tower Air Strippers for Trichloroethylene Removal at Wurthsmith Air Force Base, Michigan," Air Force Engineering & Services Center, ESL-TR-85-28, August 1985.

Gross, R. L. and S. G. TerMaath, "Packed Tower Aeration Strips Trichloroethylene from Groundwater," Environmental Progress, 4(2), pp. 119-124, May 1985.

Hall, D. W. and R. L. Mumford, "Interim Private Water Well Remediation Using Carbon Adsorption," Ground Water Monitoring Review, 7(1), pp. 77-83, Winter 1987.

Hebble, T. L., Oak Ridge National Laboratory, personal communication.

Howard, M. G., "New Solvent Recovery Process Using Activated Carbon," Filtr. Sep., 21(2), pp. 130-2, 1984.

Jennings, M. S., N. E. Krohn and R. S. Berry, Control of Industrial VOC Emissions by Catalytic Incineration: Volume 1, Assessment of Catalytic Incineration and Competing Controls, EPA-600/2-84-118a, July, 1984.

Kander, R. G. and M. E. Paulaitis, in Chemical Engineering at Supercritical Fluid Conditions: Paulaitis, M. E. et al., Eds.; Ann Arbor Science: Ann Arbor, Michigan, 1983; pp 463-75.

Kang, S. J. et al. "Removal of Total Toxic Organics at Ford Motor Company," Proceedings of the 40th Industrial Waste Conference, May 1985.

Keyvani, M. and N. C. Gardner, "Operating Characteristics of Rotating Bed," presented at AIChE Summer National Meeting, Denver, Colorado, August 21-24, 1988.

Kosusko, M., M. E. Mullins, T. N. Rogers and K. Ramanathan, "Catalytic Treatment of Air Stripping Effluents," presented at AIChE 1987 Annual Meeting, New York, November 1987.

Lee, M. D., J. T. Wilson, and C. H. Ward, "In Situ Restoration Techniques for Aquifers Contaminated with Hazardous Wastes," J. Haz. Mat., 14, pp. 71-82, 1987.

Leighton, D. T. and J. M. Calo, "Distribution Coefficients of Chlorinated Hydrocarbons in Dilute Air-Water Systems for Groundwater Contamination Applications", J. Chem. Eng. Data., 28(4), pp. 382-5, 1981.

Leonard, R. A., Prediction of Hydraulic Performance in Annular Centrifugal Contactors, Argonne National Laboratory, ANL-80-57, July 1980.

Love, O. T., Jr. and R. J. Miltner, "Removal of Volatile Organic Contaminants from Groundwater by Adsorption," Proc.-Atl. Workshop, 1st 1982, pp. 183-97, 1982.

Mackay, D. and W. Y. Shiu, "A Critical Review of Henry's Law Constants for Chemicals of Environmental Interest," J. Phys. Chem. Ref. Data, 10(4), 1981.

Malot, J. J. and P. R. Wood, "Low Cost, Site Specific Total Approach to Decontamination," presented at Environmental and Public Health Effects of Soils Contaminated with Petroleum Products, Amherst, Mass., October 30-31, 1985.

Mattia, M. M. "Process for Recovering Organic Vapors from Air Stream," U.S. Patent No. 3,534,529, October 20, 1970.

Mayo, F. T., C. A. Frank, and R. M. Clark, Removal of Organic Contaminants from Groundwater: Status of EPA Drinking Water Research Program, EPA/600/D-86/134, July 1986.

McCarty, P. L., "Removal of Organic Substances from Water by Air Stripping," Control of Organic Substances in Water and Wastewater, Edited by B. B. Berger, EPA-600/8-83-011, April 1983.

McCarthy, P. L. et al., "Evaluation of an Air Stripping-Ozone Contactor System," Proc. Ind. Waste Conf., pp. 310-24, 1977.

McIntyre, G. T., N. N. Hatch, Jr., S. R. Gelman, T. J. Peschman, "Design and Performance of a Groundwater Treatment System for Toxic Organics Removal," Journal WPCF, 58(1), pp. 41-46, January 1986.

McKinnon, R. J. and J. E. Dyksen, "Removing Organics Form Groundwater Through Aeration Plus GAC," Journal AWWA, pp. 42-47, May 1984.

McShea, L. J., M. D. Miller, and J. R. Smith, "Combining UV/Ozone to Oxidize Toxics," Pollution Engineering, pp. 58-9, March 1987.

Metcalfe, I. and C. S. H. Wilkins, "Solvent Recovery Using Activated Carbon," in Solvent Problems in Industry, Edited by George KaKabadge, 1984.

Mohr, R. J. and A. S. Khan, "HIGEE-A New Approach in Groundwater Clean-Up," presented at the 1987 AQTE Conference in Montreal, Canada.

Munjal, S., Fluid Flow and Mass Transfer in Rotating Packed Beds With Countercurrent Gas-Liquid Flow, PhD Thesis, Washington University, St. Louis, Missouri, 1986.

Munz, C. and P. V. Roberts, "Air-Water Phase Equilibria of Volatile Organic Solutes," Jour. AWWA, PP. 62-9, May 1987.

Myers, R., Response Surface Methodology, Allyn and Bacon, Boston, Massachusetts, 1971.

Nirmalakhandan, N. N. and R. E. Speece, "QSAR Model for Predicting Henry's Constant," Environ. Sci. Technol., 22(11), pp. 1349-57, 1988.

O'Brien, R. P., Air Stripping/Adsorption Process for Removing Organics from Water, U.S. Patent No. 4,544,488, October 1, 1985.

Ohneck, R. J. and G. L. Gardner, "Restoration of an Aquifer Contaminated by an Accidental Spill of Organic Chemicals," Ground Water Monitoring Review, 3(2), pp. 50-3, Fall 1982.

Onda, K., H. Tadeuchi, and Y. Okumoto, "Mass Transfer Coefficients Between Gas and Liquid Phases in Packed Columns," Jour. Chem. Eng. Japan, 1, 56, 1968.

Parmele, C. S., R. D. Allan, and M. Mehran, "Steam-Regenerated Activated Carbon: An Emission-Free, Cost-Effective Ground Water Treatment Process," Environmental Progress, 5(2), pp. 135-9, May 1986.

Perry, R. H. and C. H. Chilton, Chemical Engineers' Handbook, 5th Ed., McGraw-Hill, Inc., pp. 5-53 - 5-55, 1973.

Ramshaw, C., "'HIGEE' Distillation-An Example of Process Intensification," The Chemical Engineer, pp. 13-14, February 1983.

Ramshaw, C. and R. H. Mallinson, United States Patent 4,283,255, August 11, 1981.

Reijnen, G. K., J. van der Laan, and J. A. M. van Paassen, "Removal of Volatile Chlorinated Hydrocarbons by Air Stripping," Water Supply, 3, pp. 219-226, 1985.

Sherwood, T. K., R. L. Pigford, and C. R. Wilke, Mass Transfer, McGraw-Hill, Inc., New York, pp. 148-81, 1975.

Spivey, J. J., B. A. Tichener, and R. A. Ashworth, Catalytic Oxidation of VOCs: A Literature Review, Research Triangle Institute, North Carolina, January 1987.

Stenzel, M. H. and U. S. Gupta, "Treatment of Contaminated Groundwater with Granular Activated Carbon and Air Stripping," Journal of the Air Pollution Control Association, 35(12), pp. 1304-9, December 1985.

Tung, H. and R. S. H. Mah, "Modeling Liquid Mass Transfer in HIGEE Separation Process," Chem. Eng. Commun., Vol. 39, pp. 147-153, 1985.

U.S. Environmental Protection Agency, Air Stripping of Contaminated Water Sources - Air Emissions and Controls, EPA-450/3-87-017, August 1987.

U.S. Environmental Protection Agency, "Ground-Water Restoration," Handbook, Ground Water, EPA/625/6-87/016, pp. 35-50, March 1987.

Vivian, J. E. and C. J. King, "The Mechanism of Liquid-Phase Resistance to Gas Absorption in a Packed Column," AIChE J., 10(2), pp. 221-7, March 1964.

Vivian, J. E., P. L. T. Brian, and V. J. Krukonis, "The Influence of Gravitational Force on Gas Absorption in a Packed Column," AIChE Journal, pp. 1088-91, November 1965.

Weber, W. J., Physicochemical Processes for Water Quality Control, John Wiley & Sons, Inc., New York, 1972.

Weber, W. F. and W. Bowman, "Membranes Replacing Other Separation Technologies," Chemical Engineering Progress, 82(11), pp. 23-28, November 1986.

Wetzel, R. S., C. M. Durst, D. H. Davidson, and D. J. Sarno, In Situ Biological Treatment Test at Kelly Air Force Base, Volume II: Field Test Results and Cost Model, Air Force Engineering and Services Center, ESL-TR-85-52, Volume II, July 1987.

Wilke, C. R. and P. Chang, AIChE Journal, 1, 264-70, 1955.

Yaniga, P. M., "Alternatives in Decontamination for Hydrocarbon-Contaminated Aquifers," Proc. Natl. Symp. Aquifer Restor. Ground Water Monit., Edited by D. M. Nielsen, pp. 47-57, 1982.

Yaniga, P. M. and W. Smith, "Aquifer Restoration: In Situ Treatment and Removal of Organic and Inorganic Compounds," Groundwater Contam. Reclam., Proc. Symp., Edited by K. D. Schmidt, pp. 149-65, 1985.

Yurteri, C., D. F. Ryan, J. J. Callow, and M. D. Gurol, "The Effects of Chemical Composition of Water on Henry's Law Constant", Jour. WPCF, 59(11), pp. 950-6, November 1987.

APPENDIXES

APPENDIX A. HENRY'S LAW CONSTANT DETERMINATION

The EPICS method proposed by Gossett (1987) for determining Henry's Law constant uses concentration ratios at equilibrium from identical pair of sealed bottles that contain known but different amount of liquid. Although Gossett measured the concentration in the gas phase, the method is equally applicable to measuring concentration of the liquid phase. This method can be used to determine Henry's Law constants for volatile organic compounds (VOCs) in groundwater.

Suppose that known quantities of groundwater are added to two bottles of similar known volume. The total mass of a VOC added to bottle one is:

$$M_1 = C_w V_{L1} \tag{A-1}$$

where M_1 = mass of VOC added to bottle one

C_w = concentration of the VOC in the groundwater

V_{L1} = volume of groundwater added to bottle one

and to bottle two is:

$$M_2 = C_w V_{L2} \tag{A-2}$$

Dividing Eq. (A-2) by Eq. (A-1) gives:

$$M_2 = \frac{V_{L2}\, M_1}{V_{L1}} \tag{A-3}$$

If the two bottle are sealed immediately after addition of the groundwater and allowed to equilibrate at constant temperature, the sum of the VOC in each phase must equal the total mass of the VOC added to

the bottle. Thus at equilibrium, the following equations can be written:

$$M_1 = C_{L1}V_{L1} + C_{G1}V_{G1} \quad \text{(A-4)}$$

$$M_2 = C_{L2}V_{L2} + C_{G2}V_{G2} \quad \text{(A-5)}$$

where C_{L1}, C_{L2} = concentration of VOC in the liquid phase for bottles one and two

C_{G1}, C_{G2} = concentration of VOC in the gas phase for bottles one and two

V_{L1}, V_{L2} = volume of liquid phase in bottle one and two

V_{G1}, V_{G2} = volume of gas phase in bottle one and two

If the volume change of the liquid phase due to evaporation is small, the V_{L1} and V_{L2} are simply the quantity of groundwater added to each bottle. The volume of the gas phase can be calculated by subtracting the liquid volume from the volume of the bottle.

Substituting for M_2 in Eq. (A-5) with the expression from Eq. (A-3) and subsequent rearrangement gives:

$$M_1 = \frac{V_{L1}}{V_{L2}} (C_{L2}V_{L2} + C_{G2}V_{G2}) \quad \text{(A-6)}$$

Equating Eq. (A-4) with Eq. (A-6) results in the following expression:

$$C_{L1}V_{L1} + C_{G1}V_{G1} = \frac{V_{L1}}{V_{L2}} (C_{L2}V_{L2} + C_{G2}V_{G2}) \quad \text{(A-7)}$$

The gas phase concentration of the VOC in each bottle is related to the liquid phase concentration by:

$$C_G = H_c C_L \tag{A-8}$$

where H_c is the dimensionless Henry's Law constant. Substituting for gas phase concentrations in Eq. (A-7) with Eq. (A-8) and subsequent rearrangement gives:

$$H_c = \frac{V_{L1}V_{L2}\ (C_{L2} - C_{L1})}{V_{L2}C_{L1}V_{G1} - C_{L2}V_{G2}V_{L1}} \tag{A-9}$$

The Henry's Law constant can now be determined for the VOCs in the groundwater knowing the volume of liquid added to each bottle and the concentration in the liquid phase at equilibrium.

APPENDIX B. EXPERIMENTAL DATA

Hydraulic Test Data for the 45.92-cm-diam. Rotor, Sumitomo Packing

WATER FLOWRATE (GPM)	AIR FLOWRATE (SCFM)	ROTOR SPEED (RPM)	PRESSURE DROP (INCHES OF WATER)	POWER CONSUMPTION [KW]
0	0	100	0	
0	0	200	0	0.56
0	0	300	0.1	0.71
0	0	400	0.1	0.85
0	0	500	0.3	1.02
0	0	600	0.4	1.21
0	0	700	0.5	1.39
0	0	800	0.7	1.51
0	0	900	0.9	1.66
0	0	1000	1.1	1.8

WATER FLOWRATE (GPM)	AIR FLOWRATE (SCFM)	ROTOR SPEED (RPM)	PRESSURE DROP (INCHES OF WATER)	POWER CONSUMPTION [KW]
0	99	0	0.3 *	
0	99.1	100	0.3 *	0.42
0	99.2	200	0.3	0.57
0	99.4	300	0.3	0.73
0	99.2	400	0.4	0.88
0	99.1	500	0.5	1.04
0	99.6	600	0.6	1.19
0	99.6	700	0.8	1.35
0	99.2	800	1	1.5
0	99	900	1.2	1.63
0	98.9	1000	1.4	1.71

* WATER USED TO LUBRICATE THE SEAL STARTS TO LEAK INTO THE ROTOR

WATER FLOWRATE (GPM)	AIR FLOWRATE (SCFM)	ROTOR SPEED (RPM)	PRESSURE DROP (INCHES OF WATER)	POWER CONSUMPTION [KW]
0	298.1	0	1.3 *	
0	298.1	100	1.3 *	0.38
0	298.4	200	1.2	0.57
0	298.4	300	1.2	0.71
0	300.6	400	1.3	0.87
0	300.4	500	1.4	1.04
0	299.5	600	1.6	1.22
0	299.9	700	1.7	1.38
0	300.4	800	1.9	1.52
0	300.5	900	2.1	1.71
0	299.5	1000	2.4	1.84

Hydraulic Test Data for the 45.92-cm-diam. Rotor, Sumitomo Packing

WATER FLOWRATE (GPM)	AIR FLOWRATE (SCFM)	ROTOR SPEED (RPM)	PRESSURE DROP (INCHES OF WATER)	POWER CONSUMPTION [KW]
0	509.7	0	2.9 *	
0	507.4	100	3.1 *	0.4
0	507.5	200	2.6	0.57
0	509.9	300	2.6	0.72
0	507.4	400	2.8	0.86
0	505.2	500	2.9	1.01
0	507.4	600	3	1.19
0	506.4	700	3.2	1.36
0	500.8	800	3.3	1.55
0	500.5	900	3.6	1.73
0	506.8	1000	3.8	1.94

WATER FLOWRATE (GPM)	AIR FLOWRATE (SCFM)	ROTOR SPEED (RPM)	PRESSURE DROP (INCHES OF WATER)	POWER CONSUMPTION [KW]
0	689.5	100	5.1 *	0.4
0	698	200	4.1	0.56
0	695.6	300	4.1	0.7
0	696.1	400	4.2	0.82
0	695.4	500	4.4	0.98
0	692.4	600	4.6	1.14
0	695.7	700	4.8	1.29
0	693.3	800	4.9	1.42
0	690.6	900	5.1	1.55
0	691.8	1000	5.4	1.66

WATER FLOWRATE (GPM)	AIR FLOWRATE (SCFM)	ROTOR SPEED (RPM)	PRESSURE DROP (INCHES OF WATER)	POWER CONSUMPTION [KW]
10.1	100.8	300	8	0.76
10.1	99.5	400	0.9	0.91
10.2	99.4	500	0.8	1.11
10.3	99	600	0.8	1.32
10.3	98.8	700	1	1.54
10.3	100	800	1.2	1.75
10.3	99.6	900	1.4	1.94
10.2	99.4	1000	1.6	2.14

Hydraulic Test Data for the 45.92-cm-diam. Rotor, Sumitomo Packing

WATER FLOWRATE (GPM)	AIR FLOWRATE (SCFM)	ROTOR SPEED (RPM)	PRESSURE DROP (INCHES OF WATER)	POWER CONSUMPTION [KW]
10.1	302.7	500	12.8	1.16
10.1	304.9	525	10	
10.2	301.5	550	7.5	
10.1	301.5	575	3.3	
10.1	303.6	600	2.5	1.39
10.2	304.2	700	2.4	1.63
10.2	304.3	800	2.5	1.85
10.2	304.2	900	2.6	2.02
10.2	303	1000	2.6	2.11

WATER FLOWRATE (GPM)	AIR FLOWRATE (SCFM)	ROTOR SPEED (RPM)	PRESSURE DROP (INCHES OF WATER)	POWER CONSUMPTION [KW]
9.9	515.8	600	11.7	1.29
10	516.3	625	8.9	
9.9	509.5	650	5.1	1.37
9.9	500.6	700	4.5	1.48
9.9	501	800	4.3	1.65
9.9	503.5	900	4.4	1.85
9.9	508.4	1000	4.6	2.03

WATER FLOWRATE (GPM)	AIR FLOWRATE (SCFM)	ROTOR SPEED (RPM)	PRESSURE DROP (INCHES OF WATER)	POWER CONSUMPTION [KW]
10	704.2	600	22.8	1.3
10	707.4	650	14.7	1.38
10	689.2	675	9.9	
10	707.2	700	8.4	1.48
10	689.5	750	7	1.57
10	695.2	800	6.7	1.68
10	689.7	900	6.4	1.9
9.8	680.3	1000	6.4	2.07

Hydraulic Test Data for the 45.92-cm-diam. Rotor, Sumitomo Packing

WATER FLOWRATE (GPM)	AIR FLOWRATE (SCFM)	ROTOR SPEED (RPM)	PRESSURE DROP (INCHES OF WATER)	POWER CONSUMPTION [KW]
19.9	98.6	450	7.8	1.04
20.1	97.7	475	6.2	
20.1	100.2	500	1.1	1.15
20	100.4	600	1	1.37
20	100.5	700	1.1	1.63
20	100.5	800	1.3	1.89
20.1	100.4	900	1.5	2.14
20	100.2	1000	1.8	2.4

WATER FLOWRATE (GPM)	AIR FLOWRATE (SCFM)	ROTOR SPEED (RPM)	PRESSURE DROP (INCHES OF WATER)	POWER CONSUMPTION [KW]
20.1	301.3	550	11.6	1.32
20	299.2	575	8.9	
20.1	298.7	600	6.3	1.44
20.1	300.4	650	3.3	1.54
20.1	301.9	700	3	1.66
19.3	302.8	800	2.8	1.91
19.3	302.6	900	3	2.2
19.4	302.1	1000	3.2	2.43

WATER FLOWRATE (GPM)	AIR FLOWRATE (SCFM)	ROTOR SPEED (RPM)	PRESSURE DROP (INCHES OF WATER)	POWER CONSUMPTION [KW]
19.7	500.5	600	20.9	1.38
19.7	512.2	650	11.2	1.48
19.7	506.1	700	7.4	1.58
19.7	503.2	750	6.2	1.69
19.8	504.1	800	5.5	1.78
19.7	506.4	900	5.2	2.01
19.8	513.2	1000	5.2	2.3

Hydraulic Test Data for the 45.92-cm-diam. Rotor, Sumitomo Packing

WATER FLOWRATE (GPM)	AIR FLOWRATE (SCFM)	ROTOR SPEED (RPM)	PRESSURE DROP (INCHES OF WATER)	POWER CONSUMPTION [KW]
19.9	692.8	675	22.8	1.55
19.7	692.8	700	14.2	1.58
19.8	698.4	800	9.5	1.8
19.8	692.4	900	8	2.04
19.8	695.6	1000	7.6	2.31

WATER FLOWRATE (GPM)	AIR FLOWRATE (SCFM)	ROTOR SPEED (RPM)	PRESSURE DROP (INCHES OF WATER)	POWER CONSUMPTION [KW]
30.4	96.5	400	12.1	0.99
30.5	99.7	475	7.8	
30.5	100.1	500	1.3	1.23
30.5	99.6	600	1	1.5
30.5	100.4	700	1.2	1.8
30.5	100.2	800	1.4	2.08
30.5	99.9	900	1.6	2.4
30.5	99.5	1000	1.9	2.7

WATER FLOWRATE (GPM)	AIR FLOWRATE (SCFM)	ROTOR SPEED (RPM)	PRESSURE DROP (INCHES OF WATER)	POWER CONSUMPTION [KW]
29.6	295.5	550	15.7	1.41
29.6	300.7	600	9.1	1.54
29.6	299.6	625	6.6	
29.6	299.6	650	4.4	1.69
29.6	300.6	700	3.3	1.85
29.6	300.9	800	3.1	2.14
29.6	300.7	900	3.2	2.46
29.6	300.6	1000	3.4	2.79

Hydraulic Test Data for the 45.92-cm-diam. Rotor, Sumitomo Packing

WATER FLOWRATE (GPM)	AIR FLOWRATE (SCFM)	ROTOR SPEED (RPM)	PRESSURE DROP (INCHES OF WATER)	POWER CONSUMPTION [KW]
30.5	506.8	650	18.8	1.62
30.5	511.2	675	12.8	
30.5	509.2	700	10.6	1.77
30.5	507.5	750	7.8	1.9
30.5	499.6	800	6.7	2.01
30.4	504.9	900	5.9	2.36
30.4	507	1000	5.8	2.62

WATER FLOWRATE (GPM)	AIR FLOWRATE (SCFM)	ROTOR SPEED (RPM)	PRESSURE DROP (INCHES OF WATER)	POWER CONSUMPTION [KW]
30.1	690.2	700	26.7	1.83
30.2	697.2	750	15.5	1.92
30.3	692.8	800	12.8	2.05
30.3	689.5	900	9.5	2.31
31	695.8	1000	8.9	2.63

WATER FLOWRATE (GPM)	AIR FLOWRATE (SCFM)	ROTOR SPEED (RPM)	PRESSURE DROP (INCHES OF WATER)	POWER CONSUMPTION [KW]
40.5	99.8	500	7.5	1.28
41.1	99.5	525	5.9	
41.1	99.3	550	1.5	
40.5	100.5	600	1.2	1.58
40.5	100.6	700	1.3	1.9
40.5	100.2	800	1.5	2.25
40.5	99.7	900	1.7	2.63
41	99.6	1000	2	2.98

Hydraulic Test Data for the 45.92-cm-diam. Rotor, Sumitomo Packing

WATER FLOWRATE (GPM)	AIR FLOWRATE (SCFM)	ROTOR SPEED (RPM)	PRESSURE DROP (INCHES OF WATER)	POWER CONSUMPTION [KW]
40.3	284.3	550	18	1.48
40.3	299.2	600	11.4	1.61
40.3	298.6	625	9.3	
40.3	296.8	650	6.8	1.76
40.3	297.7	700	4.4	1.93
40.2	296.7	800	3.6	2.27
40.2	297	900	3.5	2.61
40.1	297.7	1000	3.6	3.07

WATER FLOWRATE (GPM)	AIR FLOWRATE (SCFM)	ROTOR SPEED (RPM)	PRESSURE DROP (INCHES OF WATER)	POWER CONSUMPTION [KW]
40.7	503.7	675	21.7	
40.6	505.4	700	14.3	1.89
40.7	498.5	750	10.3	2.04
40.8	502.4	800	8.7	2.17
40.6	513.2	900	7.2	2.55
40.6	500.5	1000	6.5	2.87

WATER FLOWRATE (GPM)	AIR FLOWRATE (SCFM)	ROTOR SPEED (RPM)	PRESSURE DROP (INCHES OF WATER)	POWER CONSUMPTION [KW]
40.6	693.2	750	27	2.09
40.6	700.6	800	17.2	2.19
40.4	681.5	800	15.9	
40.3	708	900	12.6	2.52
40.3	696.1	1000	10.5	2.92

Hydraulic Test Data for the 45.92-cm-diam. Rotor, Sumitomo Packing

WATER FLOWRATE (GPM)	AIR FLOWRATE (SCFM)	ROTOR SPEED (RPM)	PRESSURE DROP (INCHES OF WATER)	POWER CONSUMPTION [KW]
50.3	99.1	500	9.5	1.27
50.2	100.1	550	5.6	1.43
50.5	100.5	575	1.6	
50.5	100.7	600	1.4	1.6
50.6	100.6	700	1.4	1.97
50.7	100.4	800	1.6	2.37
50.8	100.5	900	1.8	2.75
50.9	99.9	1000	2.1	3.29

WATER FLOWRATE (GPM)	AIR FLOWRATE (SCFM)	ROTOR SPEED (RPM)	PRESSURE DROP (INCHES OF WATER)	POWER CONSUMPTION [KW]
49.6	289.6	600	16.5	1.62
49.7	298.1	650	9.4	1.82
49.6	298.2	700	6.2	2
49.6	299.6	750	4.9	2.18
49.8	295.6	800	4.2	2.37
49.8	296.3	900	3.9	2.83
50.1	297.2	1000	4	3.28

WATER FLOWRATE (GPM)	AIR FLOWRATE (SCFM)	ROTOR SPEED (RPM)	PRESSURE DROP (INCHES OF WATER)	POWER CONSUMPTION [KW]
50.1	496.8	700	23.4	1.96
49.9	501.1	800	11.2	2.29
50.6	491.9	900	8.5	2.72
49.2	496.5	1000	7.6	3.12

WATER FLOWRATE (GPM)	AIR FLOWRATE (SCFM)	ROTOR SPEED (RPM)	PRESSURE DROP (INCHES OF WATER)	POWER CONSUMPTION [KW]
49.9	701.3	850	21.8	2.3
50	689.5	900	15.7	2.71
50.3	699.6	1000	12.9	3.14

Hydraulic Test Data for the 45.92-cm-diam. Rotor, Sumitomo Packing

WATER FLOWRATE (GPM)	AIR FLOWRATE (SCFM)	ROTOR SPEED (RPM)	PRESSURE DROP (INCHES OF WATER)	POWER CONSUMPTION [KW]
49.5	56.2	450	9.3	1.14
49.5	57.8	475	6.9	
49.2	57.2	500	1.2	1.3
49.3	57.2	600	1	1.63
49.4	57.3	700	1.1	2
49.4	57	800	1.4	2.36
49.4	57	900	1.6	2.78
49.4	56.8	1000	1.9	3.2

WATER FLOWRATE (GPM)	AIR FLOWRATE (SCFM)	ROTOR SPEED (RPM)	PRESSURE DROP (INCHES OF WATER)	POWER CONSUMPTION [KW]
49	20.4	350	5.7	0.87
49	20.9	375	5.7	
49.1	20.6	400	0.6	1
49	20.7	500	0.6	1.29
49	20.7	600	0.7	1.62
49.3	20.5	700	1	1.99
49.1	20.5	800	1.2	2.38
49.5	20.4	900	1.5	2.78
49.3	20.4	1000	1.8	3.22

Hydraulic Test Data for the 45.92-cm-diam. Rotor, Wire Gauze Packing

WATER FLOWRATE (GPM)	AIR FLOWRATE (SCFM)	ROTOR SPEED (RPM)	PRESSURE DROP (INCHES OF WATER)	POWER CONSUMPTION [KW]
0	0	500	0	1.02
0	0	600	0.1	1.19
0	0	700	0.3	1.36
0	0	800	0.4	1.49
0	0	900	0.6	1.67
0	0	1000	0.8	1.86

WATER FLOWRATE (GPM)	AIR FLOWRATE (SCFM)	ROTOR SPEED (RPM)	PRESSURE DROP (INCHES OF WATER)	POWER CONSUMPTION [KW]
0	99.4	100	0.3	0.41
0	99.3	200	0.3	0.56
0	99.5	300	0.4	0.69
0	99.5	400	0.5	0.83
0	98.8	500	0.6	0.99
0	98.8	600	0.7	1.16
0	98.8	700	0.8	1.32
0	99.1	800	1	1.44
0	99.1	900	1.1	1.57
0	99.5	1000	1.2	1.64

WATER FLOWRATE (GPM)	AIR FLOWRATE (SCFM)	ROTOR SPEED (RPM)	PRESSURE DROP (INCHES OF WATER)	POWER CONSUMPTION [KW]
0	280	100	1.1	0.41
0	281.7	200	1.1	0.55
0	279	300	1.1	0.71
0	279	400	1.2	0.84
0	279	500	1.3	1.01
0	278.5	600	1.5	1.2
0	277.1	700	1.6	1.36
0	275.9	800	1.8	1.51
0	277	900	2	1.64
0	276.7	1000	2.3	1.73

Hydraulic Test Data for the 45.92-cm-diam. Rotor, Wire Gauze Packing

WATER FLOWRATE (GPM)	AIR FLOWRATE (SCFM)	ROTOR SPEED (RPM)	PRESSURE DROP (INCHES OF WATER)	POWER CONSUMPTION [KW]
0	506.4	200	2.3	0.57
0	504.3	300	2.3	0.73
0	504.6	400	2.4	0.87
0	502.4	500	2.5	1.04
0	502.4	600	2.7	1.23
0	502.5	700	2.9	1.4
0	500.6	800	3.1	1.56
0	500.8	900	3.3	1.68
0	503.2	1000	3.6	1.77

WATER FLOWRATE (GPM)	AIR FLOWRATE (SCFM)	ROTOR SPEED (RPM)	PRESSURE DROP (INCHES OF WATER)	POWER CONSUMPTION [KW]
0	703.4	100	4.2 *	0.42
0	706.2	200	3.6	0.57
0	703.2	300	3.7	0.72
0	705.9	400	3.8	0.86
0	708.5	500	3.9	1.03
0	714.6	600	4.2	1.22
0	711.7	700	4.4	1.41
0	714.8	800	4.6	1.56
0	708.4	900	4.8	1.7
0	709.4	1000	5	1.76

* WATER USED TO LUBRICATE THE SEAL STARTS TO LEAK INTO THE ROTOR

WATER FLOWRATE (GPM)	AIR FLOWRATE (SCFM)	ROTOR SPEED (RPM)	PRESSURE DROP (INCHES OF WATER)	POWER CONSUMPTION [KW]
9.9	99.1	100	2.3	0.4
10	99.2	200	0.8	0.55
9.9	99.2	300	0.5	0.7
9.9	99.2	400	0.6	0.86
9.9	99.2	500	0.7	1.04
10	99.2	600	0.8	1.23
9.9	99.3	700	1	1.45
10	99.2	800	1.2	1.62
10	99.3	900	1.4	1.82
9.9	99.3	1000	1.6	2

Hydraulic Test Data for the 45.92-cm-diam. Rotor, Wire Gauze Packing

WATER FLOWRATE (GPM)	AIR FLOWRATE (SCFM)	ROTOR SPEED (RPM)	PRESSURE DROP (INCHES OF WATER)	POWER CONSUMPTION [KW]
10.2	279.8	250	9.4	
10.2	280.6	300	1.7	0.76
10.2	280.9	350	1.7	0.84
10.2	280.2	400	1.7	0.92
10.3	279.4	500	1.7	1.14
10.3	278.9	600	1.9	1.36
10.4	276.8	700	2	1.59
10.2	279.9	800	2.2	1.76
10.2	276.2	900	2.4	1.94
10.5	276.8	1000	2.7	2.11

WATER FLOWRATE (GPM)	AIR FLOWRATE (SCFM)	ROTOR SPEED (RPM)	PRESSURE DROP (INCHES OF WATER)	POWER CONSUMPTION [KW]
10.4	498.1	300	12.9	
10.4	496.3	350	3.7	0.84
10.4	494.1	400	3.6	0.95
10.3	494.2	450	3.5	1.02
10.3	494.3	500	3.5	1.11
10.4	494.6	600	3.5	1.36
10.5	492.2	700	3.6	1.57
10.4	494.7	800	3.7	1.77
10.4	492.7	900	3.9	1.97
10	492.7	1000	4.2	2.11

WATER FLOWRATE (GPM)	AIR FLOWRATE (SCFM)	ROTOR SPEED (RPM)	PRESSURE DROP (INCHES OF WATER)	POWER CONSUMPTION [KW]
10.4	694.4	350	17.4	
10.4	720.8	400	6.5	0.92
10.4	703.2	500	5.8	1.11
10.3	700.7	600	5.7	1.33
10.5	703.8	700	5.7	1.55
10.4	703.8	800	5.7	1.73
10.4	703.4	900	5.8	2
10.4	700.2	1000	6	2.12

Hydraulic Test Data for the 45.92-cm-diam. Rotor, Wire Gauze Packing

WATER FLOWRATE (GPM)	AIR FLOWRATE (SCFM)	ROTOR SPEED (RPM)	PRESSURE DROP (INCHES OF WATER)	POWER CONSUMPTION [KW]
20.5	99	200	6.4	0.56
20.5	98.9	300	0.6	0.71
20.5	98.8	400	0.7	0.87
20.6	99.5	500	0.8	1.09
20.5	99.6	600	1	1.31
20.5	99	700	1.1	1.56
20.6	98.8	800	1.3	1.78
20.6	99	900	1.5	2.03
20.4	99	1000	1.8	2.31

WATER FLOWRATE (GPM)	AIR FLOWRATE (SCFM)	ROTOR SPEED (RPM)	PRESSURE DROP (INCHES OF WATER)	POWER CONSUMPTION [KW]
20.5	273.9	300	11.1	
20.5	275.3	350	2	
20.6	278.2	400	2	0.93
20.5	280.9	500	1.9	1.16
20.4	278.2	600	2.1	1.41
20.5	278.2	700	2.2	1.66
20.6	276.9	800	2.4	1.9
20.5	276.5	900	2.6	2.16
20.5	275.1	1000	2.9	2.35

WATER FLOWRATE (GPM)	AIR FLOWRATE (SCFM)	ROTOR SPEED (RPM)	PRESSURE DROP (INCHES OF WATER)	POWER CONSUMPTION [KW]
20.8	490.7	350	13.7	
20.7	501.8	400	4.5	0.94
20.6	501.8	500	4.2	1.15
20.6	501.8	600	4.1	1.4
20.7	501.7	700	4.1	1.65
20.6	506.1	800	4.2	1.87
20.7	501.9	900	4.3	2.12
20	500	1000	4.5	2.34

Hydraulic Test Data for the 45.92-cm-diam. Rotor, Wire Gauze Packing

WATER FLOWRATE (GPM)	AIR FLOWRATE (SCFM)	ROTOR SPEED (RPM)	PRESSURE DROP (INCHES OF WATER)	POWER CONSUMPTION [KW]
20.7	706	400	12.2	
20.9	703.2	450	7.3	1.05
20.8	709.4	500	7	1.16
20.9	709.6	600	6.7	1.4
20.9	709.7	700	6.5	1.65
20.9	712	800	6.4	1.89
20.4	706.2	900	6.5	2.16
20.7	715.3	1000	6.6	2.35

WATER FLOWRATE (GPM)	AIR FLOWRATE (SCFM)	ROTOR SPEED (RPM)	PRESSURE DROP (INCHES OF WATER)	POWER CONSUMPTION [KW]
30.3	99.2	200	6.8	0.55
30.3	99.2	250	0.7	0.64
30.3	99.1	300	0.6	0.74
30.4	99.8	400	0.7	0.91
30.4	99.2	500	0.8	1.17
30.4	99.8	600	1	1.44
30.4	99.1	700	1.2	1.7
30.4	99.1	800	1.4	2
30.5	99.2	900	1.6	2.31
30.2	98.4	1000	1.9	2.6

WATER FLOWRATE (GPM)	AIR FLOWRATE (SCFM)	ROTOR SPEED (RPM)	PRESSURE DROP (INCHES OF WATER)	POWER CONSUMPTION [KW]
30.7	274.5	300	12.5	
30.7	275.9	350	2.3	1.02
30.7	276	400	2.2	1.02
30.7	275.6	500	2.1	1.28
30.7	275.1	600	2.2	1.58
30.7	275.3	700	2.3	1.91
30.7	275.2	800	2.5	2.21
30.7	274.5	900	2.7	2.54
30.8	275	1000	3	2.89

Hydraulic Test Data for the 45.92-cm-diam. Rotor, Wire Gauze Packing

WATER FLOWRATE (GPM)	AIR FLOWRATE (SCFM)	ROTOR SPEED (RPM)	PRESSURE DROP (INCHES OF WATER)	POWER CONSUMPTION [KW]
31	468	350	16.6	
30	505	400	5.5	0.97
30.7	505	500	4.7	1.22
30.7	504.9	600	4.5	1.51
30.8	505	700	4.5	1.82
31	505	800	4.5	2.13
30.9	505	900	4.7	2.43
30.8	500	1000	4.9	2.74

WATER FLOWRATE (GPM)	AIR FLOWRATE (SCFM)	ROTOR SPEED (RPM)	PRESSURE DROP (INCHES OF WATER)	POWER CONSUMPTION [KW]
30.5	703.4	450	9.2	
30.5	712.3	500	8.5	1.3
30.5	700.2	600	7.6	1.64
30.6	706.5	700	7.3	2
30.6	710	800	7.1	2.29
30.6	710	900	7.1	2.65
30.4	717.7	1000	7.1	3.14

WATER FLOWRATE (GPM)	AIR FLOWRATE (SCFM)	ROTOR SPEED (RPM)	PRESSURE DROP (INCHES OF WATER)	POWER CONSUMPTION [KW]
39.8	98.1	250	9	0.64
39.8	99.3	300	0.8	0.74
39.8	99.3	400	0.8	0.94
39.9	99.5	500	0.9	1.2
39.8	100	600	1	1.51
40	99.6	700	1.2	1.82
40.2	99.6	800	1.4	2.16
39.5	99.7	900	1.7	2.52
39.5	99.7	1000	2	2.89

Hydraulic Test Data for the 45.92-cm-diam. Rotor, Wire Gauze Packing

WATER FLOWRATE (GPM)	AIR FLOWRATE (SCFM)	ROTOR SPEED (RPM)	PRESSURE DROP (INCHES OF WATER)	POWER CONSUMPTION [KW]
39.5	278.7	350	5.4	
39.9	277.9	400	2.7	1.02
39.6	277.5	500	2.5	1.29
39.5	278.4	600	2.5	1.63
39.4	277.9	700	2.5	1.97
39.4	277.4	800	2.7	2.22
39.5	277.5	900	2.9	2.69
39.6	274.6	1000	3.2	3.05

WATER FLOWRATE (GPM)	AIR FLOWRATE (SCFM)	ROTOR SPEED (RPM)	PRESSURE DROP (INCHES OF WATER)	POWER CONSUMPTION [KW]
39.4	500	400	7.7	1
39.5	500	500	5.4	1.25
39.5	502.1	600	5	1.57
39.6	502.1	700	4.8	1.89
39.7	502.1	800	4.8	2.26
39.7	500	900	4.9	2.6
39.8	502	1000	5.1	2.98

WATER FLOWRATE (GPM)	AIR FLOWRATE (SCFM)	ROTOR SPEED (RPM)	PRESSURE DROP (INCHES OF WATER)	POWER CONSUMPTION [KW]
39.4	688.2	450	11.6	
39.4	702.8	500	10	1.62
39.5	710	600	8.9	1.62
39.6	710.4	700	8.2	1.95
39.6	713.6	800	7.9	2.3
39.8	713.4	900	7.7	2.71
40	716.6	1000	7.7	3.1

Hydraulic Test Data for the 45.92-cm-diam. Rotor, Wire Gauze Packing

WATER FLOWRATE (GPM)	AIR FLOWRATE (SCFM)	ROTOR SPEED (RPM)	PRESSURE DROP (INCHES OF WATER)	POWER CONSUMPTION [KW]
49.5	97.7	250	9.6	
49.6	99.3	300	1.1	0.7
49.7	99.4	400	0.9	0.92
49.8	99.5	500	0.9	1.18
49.9	98.6	600	1.1	1.51
49.8	98.5	700	1.3	1.87
49.9	99	800	1.5	2.26
50.1	99.3	900	1.8	2.7
50.2	99.6	1000	2.1	3.13

WATER FLOWRATE (GPM)	AIR FLOWRATE (SCFM)	ROTOR SPEED (RPM)	PRESSURE DROP (INCHES OF WATER)	POWER CONSUMPTION [KW]
50.1	280	350	8.4	
50.1	276.4	400	3.4	0.97
49.7	275.9	500	2.9	1.27
49.7	278.3	600	2.7	1.62
50.5	277.7	700	2.7	2.01
50.1	278.2	800	2.8	2.4
50	278.2	900	3	2.82
49.9	278.7	1000	3.2	3.24

WATER FLOWRATE (GPM)	AIR FLOWRATE (SCFM)	ROTOR SPEED (RPM)	PRESSURE DROP (INCHES OF WATER)	POWER CONSUMPTION [KW]
50.2	500.2	400	12.7	
50.3	498.3	500	6.8	1.26
50.3	502.8	600	5.7	1.6
50.2	502.5	700	5.4	1.96
50.2	502.5	800	5.3	2.33
50.3	500.6	900	5.3	2.71
50.1	500.4	1000	5.4	3.15

WATER FLOWRATE (GPM)	AIR FLOWRATE (SCFM)	ROTOR SPEED (RPM)	PRESSURE DROP (INCHES OF WATER)	POWER CONSUMPTION [KW]
50.6	708.8	500	13.6	
50.6	715.7	600	10.8	1.64
50.6	697.3	700	9.1	2.01
50.7	706.3	800	8.5	2.36
50.7	708.7	900	8.3	2.8
50.1	709.4	1000	8.2	3.22

Hydraulic Test Data fro the 60.96-cm-diam. Rotor, Sumitomo Packing

WATER FLOWRATE (GPM)	AIR FLOWRATE (SCFM)	ROTOR SPEED (RPM)	PRESSURE DROP (INCHES OF WATER)	POWER CONSUMPTION (KILOWATTS)
0	0	100	0	
0	0	200	0.1	
0	0	300	0.2	0.81
0	0	400	0.4	0.99
0	0	500	0.6	1.19
0	0	600	0.8	1.42
0	0	700	1.1	1.54
0	0	800	1.5	1.72
0	0	900	1.9	1.94
0	0	1000	2.3	2.29

WATER FLOWRATE (GPM)	AIR FLOWRATE (SCFM)	ROTOR SPEED (RPM)	PRESSURE DROP (INCHES OF WATER)	POWER CONSUMPTION (KILOWATTS)
0	98.7	100	0.9 *	
0	98.7	200	0.9 *	
0	99	300	1	0.77
0	99.4	400	1.2	0.93
0	98.3	500	1.4	1.09
0	98.4	600	1.7	1.28
0	98.9	700	2	1.47
0	98.9	800	2.3	1.64
0	99.2	900	2.7	1.81
0	98.7	1000	3.1	2.03

* WATER USED TO LUBRICATE THE SEAL STARTS TO LEAK INTO THE ROTOR

WATER FLOWRATE (GPM)	AIR FLOWRATE (SCFM)	ROTOR SPEED (RPM)	PRESSURE DROP (INCHES OF WATER)	POWER CONSUMPTION (KILOWATTS)
0	297.4	100	5 *	
0	295.8	200	4.6 *	
0	297.4	300	3.9	0.73
0	298.8	400	4	0.88
0	295.7	500	4	1.04
0	298.4	600	4.3	1.2
0	298.2	700	4.6	1.37
0	301.1	800	5	1.51
0	296.9	900	5.4	1.66
0	300.7	1000	5.9	1.71

Hydraulic Test Data fro the 60.96-cm-diam. Rotor, Sumitomo Packing

WATER FLOWRATE (GPM)	AIR FLOWRATE (SCFM)	ROTOR SPEED (RPM)	PRESSURE DROP (INCHES OF WATER)	POWER CONSUMPTION (KILOWATTS)
0	494	300	10.8 *	0.73
0	501.2	400	9.7 *	0.89
0	498.7	500	8.9	1.04
0	501.5	600	8.7	1.23
0	501.5	700	8.8	1.4
0	503.8	800	9.2	1.56
0	501.6	900	9.7	1.72
0	499.4	1000	10.4	1.84

WATER FLOWRATE (GPM)	AIR FLOWRATE (SCFM)	ROTOR SPEED (RPM)	PRESSURE DROP (INCHES OF WATER)	POWER CONSUMPTION (KILOWATTS)
0	714.6	300	20.8 *	0.71
0	705.3	400	18 *	0.85
0	705.2	500	15.3	1.02
0	710.6	600	14.6	1.19
0	711	700	14.5	1.37
0	708.3	800	14.6	1.52
0	707.7	900	14.9	1.67
0	718.9	1000	16.2	1.75

WATER FLOWRATE (GPM)	AIR FLOWRATE (SCFM)	ROTOR SPEED (RPM)	PRESSURE DROP (INCHES OF WATER)	POWER CONSUMPTION (KILOWATTS)
9.8	98.3	250	6.3	
9.7	98.3	300	2	0.8
9.5	98.3	400	1.8	0.98
9.6	98.5	500	1.9	1.2
9.6	99.2	600	2	1.45
9.8	98.5	700	2.3	1.71
9.7	98.4	800	2.6	1.97
9.8	99.8	900	3	2.18
9.5	98.6	1000	3.5	2.44

Hydraulic Test Data fro the 60.96-cm-diam. Rotor, Sumitomo Packing

WATER FLOWRATE (GPM)	AIR FLOWRATE (SCFM)	ROTOR SPEED (RPM)	PRESSURE DROP (INCHES OF WATER)	POWER CONSUMPTION (KILOWATTS)
10	303.1	500	9.8	1.2
9.8	302.8	550	7.5	
10	302.9	600	6.8	1.45
10	302.9	700	6.6	1.68
9.6	303.1	800	6.7	1.92
9.7	303.1	900	7	2.16
10	304.8	1000	7.5	2.42

WATER FLOWRATE (GPM)	AIR FLOWRATE (SCFM)	ROTOR SPEED (RPM)	PRESSURE DROP (INCHES OF WATER)	POWER CONSUMPTION (KILOWATTS)
9.7	501.3	600	15.2	1.44
9.8	501.9	650	13	
9.7	498.1	700	12.2	1.69
9.8	500.4	800	11.8	1.93
9.8	502	900	12	2.18
9.7	493.4	1000	12	2.49

WATER FLOWRATE (GPM)	AIR FLOWRATE (SCFM)	ROTOR SPEED (RPM)	PRESSURE DROP (INCHES OF WATER)	POWER CONSUMPTION (KILOWATTS)
9.7	715.9	650	24	
9.7	707.6	700	20.5	1.63
9.7	714.8	800	19.5	1.88
9.7	713	900	20	2.25
9.9	716.3	1000	20.5	2.4

WATER FLOWRATE (GPM)	AIR FLOWRATE (SCFM)	ROTOR SPEED (RPM)	PRESSURE DROP (INCHES OF WATER)	POWER CONSUMPTION (KILOWATTS)
19.6	98.4	350	6	
19.7	98.2	400	3	1.01
19.8	98.3	450	2.5	1.01
19.6	98.2	500	2.3	1.28
19.6	98.1	600	2.3	1.58
19.7	98.1	700	2.5	1.91
19.6	98.6	800	2.9	2.23
19.7	98	900	3.3	2.6
20	98.1	1000	3.8	2.99

Hydraulic Test Data fro the 60.96-cm-diam. Rotor, Sumitomo Packing

WATER FLOWRATE (GPM)	AIR FLOWRATE (SCFM)	ROTOR SPEED (RPM)	PRESSURE DROP (INCHES OF WATER)	POWER CONSUMPTION (KILOWATTS)
19.8	303.4	500	13.4	1.33
19.8	301.9	600	8.9	1.6
19.8	303.6	650	8	
19.8	303.5	700	7.6	1.94
19.8	303.4	800	7.4	2.28
19.8	304	900	7.7	2.62
19.7	304	1000	8.2	3.01

WATER FLOWRATE (GPM)	AIR FLOWRATE (SCFM)	ROTOR SPEED (RPM)	PRESSURE DROP (INCHES OF WATER)	POWER CONSUMPTION (KILOWATTS)
20	499.4	600	19.7	1.58
20.1	498.9	700	15.1	1.94
20.1	500.6	750	14.7	
20	498.9	800	14	2.26
20	499.9	900	13.7	2.59
20	499.4	1000	13.9	2.94

WATER FLOWRATE (GPM)	AIR FLOWRATE (SCFM)	ROTOR SPEED (RPM)	PRESSURE DROP (INCHES OF WATER)	POWER CONSUMPTION (KILOWATTS)
19.6	712.1	700	25.5	1.89
19.7	709.4	800	22.5	2.2
19.5	710.6	900	22	2.52
19.5	718.4	1000	22.5	2.87

WATER FLOWRATE (GPM)	AIR FLOWRATE (SCFM)	ROTOR SPEED (RPM)	PRESSURE DROP (INCHES OF WATER)	POWER CONSUMPTION (KILOWATTS)
29.9	98.2	400	5.3	1.13
29.9	98.1	450	2.9	
30	98	500	2.6	1.45
29.9	98.1	600	2.6	1.82
30	99.5	700	2.8	2.23
30	99.3	800	3.1	2.68
29.9	99.3	900	3.5	3.1
29.9	98.5	1000	4	3.57

Hydraulic Test Data fro the 60.96-cm-diam. Rotor, Sumitomo Packing

WATER FLOWRATE (GPM)	AIR FLOWRATE (SCFM)	ROTOR SPEED (RPM)	PRESSURE DROP (INCHES OF WATER)	POWER CONSUMPTION (KILOWATTS)
30	299.5	500	18.2	1.49
30.1	305.7	600	10.8	1.87
30	308.4	650	9.5	
29.8	303	700	8.4	2.29
29.9	304.7	800	8	2.69
29.8	308.9	900	8.4	3.2
29.9	305.3	1000	8.7	3.88

WATER FLOWRATE (GPM)	AIR FLOWRATE (SCFM)	ROTOR SPEED (RPM)	PRESSURE DROP (INCHES OF WATER)	POWER CONSUMPTION (KILOWATTS)
29.8	495.2	600	25.6	1.79
29.7	502	700	18	2.18
29.8	500.4	750	16.6	
29.7	499.5	800	16	2.63
29.8	500.4	900	15.4	3.11
29.7	501.9	1000	15.6	3.48

WATER FLOWRATE (GPM)	AIR FLOWRATE (SCFM)	ROTOR SPEED (RPM)	PRESSURE DROP (INCHES OF WATER)	POWER CONSUMPTION (KILOWATTS)
29.6	710.2	800	25.5	2.58
29.7	712.5	900	24	3.05
29.6	713.8	1000	24	4.48

WATER FLOWRATE (GPM)	AIR FLOWRATE (SCFM)	ROTOR SPEED (RPM)	PRESSURE DROP (INCHES OF WATER)	POWER CONSUMPTION (KILOWATTS)
40.6	97.6	400	6.8	1.16
40.7	97.7	450	4.2	
40.6	97.6	500	3.2	1.55
40.5	97.7	600	2.9	2
40.6	97.7	700	3	2.47
40.6	97.6	800	3.3	2.99
40.7	98	900	3.7	3.53
40.5	98.1	1000	4.3	4.12

Hydraulic Test Data fro the 60.96-cm-diam. Rotor, Sumitomo Packing

WATER FLOWRATE (GPM)	AIR FLOWRATE (SCFM)	ROTOR SPEED (RPM)	PRESSURE DROP (INCHES OF WATER)	POWER CONSUMPTION (KILOWATTS)
39.8	295.7	500	24	1.55
39.8	301.7	600	12.6	1.96
39.8	297	650	10.4	
39.7	301.7	700	9.6	2.44
39.5	301.3	800	8.8	2.91
39.5	302	900	8.8	3.47
39.5	297.4	1000	8.9	4.09

WATER FLOWRATE (GPM)	AIR FLOWRATE (SCFM)	ROTOR SPEED (RPM)	PRESSURE DROP (INCHES OF WATER)	POWER CONSUMPTION (KILOWATTS)
40.3	499.4	700	21.4	2.43
40.3	499.4	800	18.4	2.92
40.4	500.8	900	17.5	3.51
40.4	502.8	1000	17.3	4.06

WATER FLOWRATE (GPM)	AIR FLOWRATE (SCFM)	ROTOR SPEED (RPM)	PRESSURE DROP (INCHES OF WATER)	POWER CONSUMPTION (KILOWATTS)
40.1	697.4	900	26	3.53
40	704.9	1000	25.5	3.95

WATER FLOWRATE (GPM)	AIR FLOWRATE (SCFM)	ROTOR SPEED (RPM)	PRESSURE DROP (INCHES OF WATER)	POWER CONSUMPTION (KILOWATTS)
49.9	97.8	400	8.1	1.19
49.7	97.8	450	6.1	
49.7	97.8	500	4.1	1.62
49.8	98	600	3.2	2.14
49.9	98	700	3.2	2.68
49.8	97.9	800	3.5	3.3
49.9	97.7	900	3.9	3.97
50	97.6	1000	4.4	4.52

Hydraulic Test Data fro the 60.96-cm-diam. Rotor, Sumitomo Packing

WATER FLOWRATE (GPM)	AIR FLOWRATE (SCFM)	ROTOR SPEED (RPM)	PRESSURE DROP (INCHES OF WATER)	POWER CONSUMPTION (KILOWATTS)
50.1	297.8	600	14.7	2.12
50.1	299.4	650	12.7	
50.2	296.3	700	10.8	2.67
50.3	298.2	800	9.7	3.24
50.3	299	900	9.3	3.89
50.5	297.4	1000	9.3	4.65

WATER FLOWRATE (GPM)	AIR FLOWRATE (SCFM)	ROTOR SPEED (RPM)	PRESSURE DROP (INCHES OF WATER)	POWER CONSUMPTION (KILOWATTS)
49.2	495.9	700	26.2	2.66
49.4	499	800	21.5	3.21
49.5	499.4	900	19.9	3.89
49.5	501.3	1000	19.3	4.65

WATER FLOWRATE (GPM)	AIR FLOWRATE (SCFM)	ROTOR SPEED (RPM)	PRESSURE DROP (INCHES OF WATER)	POWER CONSUMPTION (KILOWATTS)
50.8	55.1	300	4	0.89
50	55	350	3.3	
50.7	54.8	400	2.5	1.17
50.6	55.1	500	2	1.6
50.5	55.1	600	2.1	2.12
50.4	55.1	700	2.3	2.68
50.4	55.1	800	2.7	3.29
50.5	55.1	900	3.1	3.93
49.7	55.1	1000	3.6	4.61

WATER FLOWRATE (GPM)	AIR FLOWRATE (SCFM)	ROTOR SPEED (RPM)	PRESSURE DROP (INCHES OF WATER)	POWER CONSUMPTION (KILOWATTS)
49	20.4	200	2	
49	20.4	300	0.9	0.89
49.4	20.3	400	1	1.23
49.3	20.3	500	1.2	1.67
49.6	20.3	600	1.4	2.18
49.2	20.3	700	1.8	2.75
49.2	20.4	800	2.2	3.36
49.5	20.3	900	2.7	3.95
49.3	20.3	1000	3.3	4.77

Hydraulic Test Data for the 76.20-cm-diam. Rotor, Sumitomo Packing

WATER FLOWRATE (GPM)	AIR FLOWRATE (SCFM)	ROTOR SPEED (RPM)	PRESSURE DROP (INCHES OF WATER)	POWER CONSUMPTION (KILOWATTS)
0	0	100	0.08	
0	0	200	0.18	
0	0	300	0.37	0.82
0	0	400	0.63	1
0	0	500	0.98	1.19
0	0	600	1.4	1.46
0	0	700	1.9	1.59
0	0	800	2.48	1.9
0	0	900	3.17	
0	0	921		2.29
0	0	1000	3.9	2.65

WATER FLOWRATE (GPM)	AIR FLOWRATE (SCFM)	ROTOR SPEED (RPM)	PRESSURE DROP (INCHES OF WATER)	POWER CONSUMPTION (KILOWATTS)
0	103.3	0	0.73	
0	103.3	100	0.73	0.43
0	102.9	200	0.85	0.6
0	102.9	300	1	0.75
0	100.2	400	1.3	0.91
0	98.9	500	1.67	1.09
0	99	600	2.1	1.31
0	99.1	700	2.63	1.48
0	98.9	800	3.19	1.65
0	99	900	3.86	1.92
0	98.9	1000	4.37	2.14

WATER FLOWRATE (GPM)	AIR FLOWRATE (SCFM)	ROTOR SPEED (RPM)	PRESSURE DROP (INCHES OF WATER)	POWER CONSUMPTION (KILOWATTS)
0	312.3	0	2.91	
0	296.9	100	2.74	
0	300.8	200	2.87	
0	299.1	300	3.07	0.75
0	296.8	400	3.36	0.94
0	296.8	500	3.7	1.13
0	297.1	600	4.14	1.33
0	303	700	4.78	1.51
0	301.8	800	5.35	1.64
0	296.8	900	6.04	1.83
0	297	1000	6.76	2.06

Hydraulic Test Data for the 76.20-cm-diam. Rotor, Sumitomo Packing

WATER FLOWRATE (GPM)	AIR FLOWRATE (SCFM)	ROTOR SPEED (RPM)	PRESSURE DROP (INCHES OF WATER)	POWER CONSUMPTION (KILOWATTS)
0	529.8	0	5.6	
0	529.8	100	5.6	
0	523.3	200	5.7	
0	521.1	300	5.9	0.75
0	518.3	400	6.2	0.9
0	516.2	500	6.5	1.08
0	510.8	600	6.9	1.3
0	517.6	700	7.5	1.51
0	513.9	800	8	1.65
0	509.1	900	8.7	1.79
0	507.7	1000	9.4	1.96

WATER FLOWRATE (GPM)	AIR FLOWRATE (SCFM)	ROTOR SPEED (RPM)	PRESSURE DROP (INCHES OF WATER)	POWER CONSUMPTION (KILOWATTS)
0	712.6	0	8.9	
0	712.6	100	8.9	
0	711.6	200	9	
0	714.1	300	9.3	0.74
0	715.7	400	9.5	0.89
0	711.7	500	9.9	1.08
0	708.9	600	10.3	1.29
0	707.2	700	10.8	1.48
0	705.8	800	11.4	1.61
0	699.1	900	11.9	1.89
0	701.2	1000	12.6	2.24

WATER FLOWRATE (GPM)	AIR FLOWRATE (SCFM)	ROTOR SPEED (RPM)	PRESSURE DROP (INCHES OF WATER)	POWER CONSUMPTION (KILOWATTS)
10.1	96.8	0	9.9	
10.1	100.2	100	3	
10.1	99.4	200	3.7	
10.1	96.3	200	3.5	
10.1	98.6	250	4.2	
10.1	98.6	300	1.9	0.9
10.1	99.3	350	1.9	
10.1	99.3	400	1.8	1.07
10.1	100.4	400	1.7	
10.1	100.2	500	1.9	1.35
10.1	99.8	600	2.2	1.67
10.1	101.4	700	2.7	2.02
10.2	101	800	3.3	2.28
10.1	100.2	900	4	2.62
10.4	99.2	1000	4.7	2.95

Hydraulic Test Data for the 76.20-cm-diam. Rotor, Sumitomo Packing

WATER FLOWRATE (GPM)	AIR FLOWRATE (SCFM)	ROTOR SPEED (RPM)	PRESSURE DROP (INCHES OF WATER)	POWER CONSUMPTION (KILOWATTS)
10.1	309.4	200	11.2	
10.2	301.9	300	12.8	0.84
10.2	308.4	350	15.1	
10.2	291.2	400	16.5	1.04
10	296.4	450	14.4	
10.2	301	450	14.8	
10.1	296.1	475	12.9	
10	288.2	500	9.4	1.32
10	288.7	600	5.6	1.63
10.2	304	600	5.4	
10.2	303.6	700	5.7	1.93
10.2	302	800	6.2	2.26
10.1	304.8	900	6.8	2.52
10.1	307.4	1000	7.6	2.82

WATER FLOWRATE (GPM)	AIR FLOWRATE (SCFM)	ROTOR SPEED (RPM)	PRESSURE DROP (INCHES OF WATER)	POWER CONSUMPTION (KILOWATTS)
10.1	493.2	450	28.1	
10.1	517.8	500	24.3	
9.8	494.2	550	15.8 *	
10.1	490.9	550	15.9	
10.1	510.7	600	12.2	1.61
9.8	493.9	700	9.3	1.94
9.8	501.2	800	9.6	2.1
9.8	498.5	900	10.1	2.52
9.8	497.1	1000	10.6	2.83

*PERFORMED PRIOR TO MODIFYING THE LIQUID SEAL AT THE BOTTOM OF THE STRIPPER
AT THESE CONDITIONS THE LIQUID SEAL WAS LOST AND THUS THESE ARE NOT
TRUE PRESSURE DROP READINGS

Hydraulic Test Data for the 76.20-cm-diam. Rotor, Sumitomo Packing

WATER FLOWRATE (GPM)	AIR FLOWRATE (SCFM)	ROTOR SPEED (RPM)	PRESSURE DROP (INCHES OF WATER)	POWER CONSUMPTION (KILOWATTS)
10.1	610.4	500	30.9	1.29
10.1	665.9	550	28.4	1.39
10.1	727.9	600	23.6	1.54
9.8	689.5	650	15.4 +	1.78
9.8	698.1	700	14.7	1.95
9.9	700.6	750	14.5 *	2.1
9.8	700.8	800	14.7 *	2.23
9.9	703.6	850	14.7	2.41
9.8	700	900	14.9	2.59
9.9	702.2	950	15.2	2.75
9.9	701.3	1000	15.6	3.02

+ UNABLE TO MAINTAIN 700 SCFM AT THESE CONDITIONS BECAUSE OF HIGH PRESSURE DROP

WATER FLOWRATE (GPM)	AIR FLOWRATE (SCFM)	ROTOR SPEED (RPM)	PRESSURE DROP (INCHES OF WATER)	POWER CONSUMPTION (KILOWATTS)
20.2	98.2	200	5.5	
20.2	98.4	300	6.7	0.92
20.5	98.2	400	4.7	1.22
20.2	98.5	400	4.8	
20.5	98.6	450	2.3	
20.1	100.5	500	2.1	1.6
20.5	99.8	500	2.2	
20.5	99	550	2.3	
20.2	100	600	2.4	2.01
20.5	99.3	600	2.4	
20.2	99.4	700	2.9	2.45
20.2	99.9	800	3.4	2.93
20.1	100.3	900	4.1	3.39
20.1	101	1000	4.9	3.95

Hydraulic Test Data for the 76.20-cm-diam. Rotor, Sumitomo Packing

WATER FLOWRATE (GPM)	AIR FLOWRATE (SCFM)	ROTOR SPEED (RPM)	PRESSURE DROP (INCHES OF WATER)	POWER CONSUMPTION (KILOWATTS)
20.4	304.2	450	23.2	
20.3	290.7	500	14.9	1.47
20.4	297.2	500	15.6	
20.4	289.1	500	15.8	
20.4	303.1	550	9.8	
20	288.2	550	9.1	
20.5	291.8	575	6.8	
20.3	298.1	600	6.7	1.93
20.4	301.6	600	6.5	
20.5	292.2	600	6.2	
20.4	30.3	650	6.2	
20.2	300.7	700	6.4	2.37
20.5	300	700	6.2	
20.4	304.8	700	6.4	
20.4	302.2	800	6.6	2.83
20.3	299.8	800	6.8	
20.3	298.6	900	7.3	3.29
20.4	299.1	900	7.1	
20.2	297.5	1000	8	3.89

WATER FLOWRATE (GPM)	AIR FLOWRATE (SCFM)	ROTOR SPEED (RPM)	PRESSURE DROP (INCHES OF WATER)	POWER CONSUMPTION (KILOWATTS)
20.4	509.6	550	26.3	
20.3	483.3	600	15.7	1.89
20.4	514.1	650	13.8	
20.3	490.1	700	11.2	2.31
20.4	507.8	750	11.5	
20.3	488.1	800	10.9	2.76
20.3	487.7	900	11.2	3.22
20.3	488.4	1000	11.8	3.76

WATER FLOWRATE (GPM)	AIR FLOWRATE (SCFM)	ROTOR SPEED (RPM)	PRESSURE DROP (INCHES OF WATER)	POWER CONSUMPTION (KILOWATTS)
20.2	692	650	23.3	
20.1	691.8	650	21.9	
20.2	679.6	700	18.5	2.27
20.1	719.3	700	19.8	
20.2	699.7	725	17.8	
20	702.4	750	17.5	
20.2	702.3	775	17.3	
20.1	705	800	17.2	2.68
20.2	698.6	800	17.1	
20.2	701.2	900	17.1	3.17
20.3	683.3	1000	17.2	3.62

Hydraulic Test Data for the 76.20-cm-diam. Rotor, Sumitomo Packing

WATER FLOWRATE (GPM)	AIR FLOWRATE (SCFM)	ROTOR SPEED (RPM)	PRESSURE DROP (INCHES OF WATER)	POWER CONSUMPTION (KILOWATTS)
29.6	99.3	300	8.7	0.98
29.6	99.4	350	8.9	
29.7	99	400	6.3	1.35
29.7	97.8	450	3.1	
29.6	98.8	500	2.2	1.79
29.7	98.8	600	2.5	2.29
29.6	99.3	700	3	2.87
29.6	98.6	800	3.6	3.46
29.6	99.4	900	4.3	4.15
29.6	99.2	1000	5.1	4.82

WATER FLOWRATE (GPM)	AIR FLOWRATE (SCFM)	ROTOR SPEED (RPM)	PRESSURE DROP (INCHES OF WATER)	POWER CONSUMPTION (KILOWATTS)
29.5	298.3	500	21.4	1.74
29.4	302.4	550	12.7	
29.3	299.5	600	8.2	2.31
29.3	305.8	700	6.8	2.84
29.3	305.4	800	7.1	3.44
29.4	305.2	900	7.6	4.08
29.4	309.2	1000	8.2	4.74

WATER FLOWRATE (GPM)	AIR FLOWRATE (SCFM)	ROTOR SPEED (RPM)	PRESSURE DROP (INCHES OF WATER)	POWER CONSUMPTION (KILOWATTS)
29.5	509.3	600	23.5	2.2
29.5	493.8	650	15.4	
29.5	496	700	12.7	2.75
29.5	497.8	800	12.1	3.32
29.5	497.9	900	12.2	3.91
29.5	495.8	1000	12.6	4.68

WATER FLOWRATE (GPM)	AIR FLOWRATE (SCFM)	ROTOR SPEED (RPM)	PRESSURE DROP (INCHES OF WATER)	POWER CONSUMPTION (KILOWATTS)
29.6	691.5	650	26.9	2.52
29.7	692.4	700	21.2	2.77
29.6	695.7	800	18	3.35
29.6	696	900	17.8	3.95
29.7	681.1	1000	17.5	4.67

Hydraulic Test Data for the 76.20-cm-diam. Rotor, Sumitomo Packing

WATER FLOWRATE (GPM)	AIR FLOWRATE (SCFM)	ROTOR SPEED (RPM)	PRESSURE DROP (INCHES OF WATER)	POWER CONSUMPTION (KILOWATTS)
40.7	99.2	300	9.9	1.04
40.7	99	400	8.8	1.46
40.7	99.5	450	4.8	
40.8	99.4	500	2.7	2.01
40.7	99	600	2.7	2.65
40.7	98.8	700	3.1	3.29
40.7	100.3	800	3.7	4.05
40.8	99.2	900	4.4	4.92
40.9	98.3	1000	5.2	5.98

WATER FLOWRATE (GPM)	AIR FLOWRATE (SCFM)	ROTOR SPEED (RPM)	PRESSURE DROP (INCHES OF WATER)	POWER CONSUMPTION (KILOWATTS)
40	298	500	23.5	1.97
40.4	290.4	550	15.3	
40	301.7	550	14.9	
40.4	305.4	600	10.6	2.59
40.4	304.8	650	7.9	
40.3	301.8	700	7.3	3.26
40.4	306.8	800	7.5	3.98
40.3	304.8	900	8	4.88
40.4	302.5	1000	8.6	5.44

WATER FLOWRATE (GPM)	AIR FLOWRATE (SCFM)	ROTOR SPEED (RPM)	PRESSURE DROP (INCHES OF WATER)	POWER CONSUMPTION (KILOWATTS)
40.5	489.7	600	28	2.5
40.5	500.7	650	18.4	
40.5	507.7	700	15.7	3.19
40.4	497	800	13.3	3.89
40.4	498.7	900	13.1	4.63
40.4	498.5	1000	13.3	5.58

WATER FLOWRATE (GPM)	AIR FLOWRATE (SCFM)	ROTOR SPEED (RPM)	PRESSURE DROP (INCHES OF WATER)	POWER CONSUMPTION (KILOWATTS)
39.4	675	700	26.6	3.24
39.5	678.8	750	22.2	
39.6	685.1	800	20.8	3.99
39.5	697.9	900	20.1	4.88
39.5	664.5	1000	19.1	5.66

Hydraulic Test Data for the 76.20-cm-diam. Rotor, Sumitomo Packing

WATER FLOWRATE (GPM)	AIR FLOWRATE (SCFM)	ROTOR SPEED (RPM)	PRESSURE DROP (INCHES OF WATER)	POWER CONSUMPTION (KILOWATTS)
50	98.7	400	11.9	1.58
49.9	99.1	450	7.8	
50.2	100.6	500	3.3	2.26
50.1	101.1	600	2.9	2.95
50.1	100.7	700	3.3	3.73
50.2	100.3	800	3.8	4.68
50.2	99.5	900	4.2	5.63
50	98.5	1000	5.3	7.01

WATER FLOWRATE (GPM)	AIR FLOWRATE (SCFM)	ROTOR SPEED (RPM)	PRESSURE DROP (INCHES OF WATER)	POWER CONSUMPTION (KILOWATTS)
50.2	313.6	550	20.8	
50.8	299.1	600	12.1	2.83
49.5	302	650	9	
49.5	306	700	8.1	3.66
49.7	306.7	800	8	4.52
49.7	305.2	900	8.3	5.61
49.9	303.1	1000	8.9	6.67

WATER FLOWRATE (GPM)	AIR FLOWRATE (SCFM)	ROTOR SPEED (RPM)	PRESSURE DROP (INCHES OF WATER)	POWER CONSUMPTION (KILOWATTS)
50.3	493.2	650	23	
50.2	509	700	18.6	3.6
49.6	506.8	750	16.1	
50.2	500.2	800	14.9	4.42
50.3	507.4	900	14.3	5.43
50	509.5	1000	14.4	6.52

WATER FLOWRATE (GPM)	AIR FLOWRATE (SCFM)	ROTOR SPEED (RPM)	PRESSURE DROP (INCHES OF WATER)	POWER CONSUMPTION (KILOWATTS)
50.3	623.1	700	28.5	3.65
50.6	681.6	800	24.3	4.45
50.6	678.9	900	21.8	5.55
50.8	670.8	1000	20.7	6.67

Hydraulic Test Data for the 76.20-cm-diam. Rotor, Sumitomo Packing

WATER FLOWRATE (GPM)	AIR FLOWRATE (SCFM)	ROTOR SPEED (RPM)	PRESSURE DROP (INCHES OF WATER)	POWER CONSUMPTION (KILOWATTS)
50.1	55	100	3.8	
49.9	55.6	200	3.4	
50.1	55.3	300	3.5	1.11
50.3	54.2	400	2.2	1.61
50.2	54.5	500	1.8	2.21
50.2	55.8	600	2.1	3
50.9	55.6	700	2.6	3.84
49	55.2	800	3.2	4.7
49.1	55.1	900	4	5.55
49.4	55.2	1000	4.7	6.9

WATER FLOWRATE (GPM)	AIR FLOWRATE (SCFM)	ROTOR SPEED (RPM)	PRESSURE DROP (INCHES OF WATER)	POWER CONSUMPTION (KILOWATTS)
50.5	20.2	50	0.9	
50.3	20.1	100	0.7	
50.4	20.2	200	0.7	
50.3	20.2	300	0.8	1.13
50.4	20.1	400	1	1.6
50.4	20	500	1.3	2.22
49.1	19.9	600	1.7	2.98
49.3	19.9	700	2.2	3.81
49.3	19.9	800	2.9	4.7
49.4	19.9	900	3.6	5.72
49.9	20.1	1000	4.4	7.07

WATER FLOWRATE (GPM)	AIR FLOWRATE (SCFM)	ROTOR SPEED (RPM)	PRESSURE DROP (INCHES OF WATER)	POWER CONSUMPTION (KILOWATTS)
50	0	0	0	
50	0	100	0	
50	0	200	0.1	
50	0	300	0.3	1.1
50.1	0	400	0.6	1.6
50.1	0	500	1	2.24
50.2	0	600	1.5	3.07
50	0	700	2	3.89
50.1	0	800	2.6	4.78
50.1	0	900	3.3	5.8
50.2	0	1000	4.1	7.2

Mass Transfer Test Data for the 45.92-cm-diam. Rotor

SUMITOMO PACKING

SAMPLE NAME	RAS-18-1
WATER FLOW	35.4 GPM
GAS FLOW	46.7 SCFM
ROTOR SPEED	790 RPM
PRESSURE DROP	1.2 IN. WATER
G/L RATIO (vol)	9.9
WATER TEMPERATURE	
IN	
OUT	289.8 Kelvin
AIR TEMPERATURE	
IN	292.9 Kelvin
OUT	287 Kelvin

CONCENTRATION (ppb)	PENTANE	METHYLCYCLOHEXANE	NAPHTHALENE	BENZENE
IN	0	152.9	48.7	58.71
OUT	0	1.3	74.1	2.68
EXIT	0	1.02	70.3	1.88
STRIPPING FACTOR	524.2	16.4	0.2	1.8
NTU	ERR	5.0	-0.3	5.7
EXPERIMENTAL ATU (m^2)	ERR	2.26E-02	*********	2.00E-02
EXPERIMENTAL KLa (sec^-1)	ERR	7.79E-01	*********	8.80E-01
EXPERIMENTAL kl (m/sec)	ERR	3.11E-04	*********	3.52E-04

CONCENTRATION (ppb)	TOLUENE	O-XYLENE	M-XYLENE	1,2,4-TRIMETHYL BENZENE
IN	44.68	231.38	535.75	308.29
OUT	1.91	31.74	38.01	38.02
EXIT	1.42	22.75	27.39	27.86
STRIPPING FACTOR	2.1	1.6	2.2	2.1
NTU	5.1	3.6	4.1	3.2
EXPERIMENTAL ATU (m^2)	2.21E-02	3.11E-02	2.80E-02	3.59E-02
EXPERIMENTAL KLa (sec^-1)	7.96E-01	5.65E-01	6.28E-01	4.89E-01
EXPERIMENTAL kl (m/sec)	3.18E-04	2.26E-04	2.51E-04	1.96E-04

Note: Experimental kl calculated using a=2500m^2/m^3

Mass Transfer Test Data for the 45.92-cm-diam. Rotor

SUMITOMO PACKING		
SAMPLE NAME	RAS-18-2	
WATER FLOW	20.5	GPM
GAS FLOW	28.6	SCFM
ROTOR SPEED	790	RPM
PRESSURE DROP	1	IN. WATER
G/L RATIO (vol)	10.4	
WATER TEMPERATURE		
IN		
OUT	286.1	Kelvin
AIR TEMPERATURE		
IN	281.9	Kelvin
OUT	279	Kelvin

CONCENTRATION (ppb)	PENTANE	METHYLCYCLOHEXANE	NAPHTHALENE	BENZENE
IN	0	223.12	82.1	80.47
OUT	0	0.68	77.1	2
EXIT	0	0.68	66.2	1.41
STRIPPING FACTOR	561.6	17.5	0.2	1.7
NTU	ERR	6.1	ERR	7.6
EXPERIMENTAL ATU (m^2)	ERR	1.87E-02	ERR	1.50E-02
EXPERIMENTAL KLa (sec^-1)	ERR	5.46E-01	ERR	6.79E-01
EXPERIMENTAL kl (m/sec)	ERR	2.18E-04	ERR	2.72E-04

CONCENTRATION (ppb)	TOLUENE	O-XYLENE	M-XYLENE	1,2,4-TRIMETHYL BENZENE
IN	64.48	306.9	753.73	480.18
OUT	1.4	23.44	26.52	32.75
EXIT	0.8	16.48	18.78	22.83
STRIPPING FACTOR	1.9	1.5	2.0	1.9
NTU	7.0	5.5	5.6	4.5
EXPERIMENTAL ATU (m^2)	1.63E-02	2.05E-02	2.03E-02	2.51E-02
EXPERIMENTAL KLa (sec^-1)	6.25E-01	4.97E-01	5.02E-01	4.05E-01
EXPERIMENTAL kl (m/sec)	2.50E-04	1.99E-04	2.01E-04	1.62E-04

Note: Experimental kl calculated using a=2500m^2/m^3

Mass Transfer Test Data for the 45.92-cm-diam. Rotor

SUMITOMO PACKING

SAMPLE NAME	RAS-18-3
WATER FLOW	49 GPM
GAS FLOW	67.2 SCFM
ROTOR SPEED	790 RPM
PRESSURE DROP	1.4 IN. WATER
G/L RATIO (vol)	10.3
WATER TEMPERATURE	
IN	
OUT	286.6 Kelvin
AIR TEMPERATURE	
IN	285.7 Kelvin
OUT	283.1 Kelvin

CONCENTRATION (ppb)	PENTANE	METHYLCYCLOHEXANE	NAPHTHALENE	BENZENE
IN	0	214.63	77.3	78.57
OUT	0	2.47	77.7	5.43
EXIT	0	1.61	69.0	3.64
STRIPPING FACTOR	551.1	17.2	0.2	1.7
NTU	ERR	4.7	0.0	5.1
EXPERIMENTAL ATU (m^2)	ERR	2.42E-02	*********	2.20E-02
EXPERIMENTAL KLa (sec^-1)	ERR	1.01E+00	*********	1.10E+00
EXPERIMENTAL kl (m/sec)	ERR	4.03E-04	*********	4.42E-04

CONCENTRATION (ppb)	TOLUENE	O-XYLENE	M-XYLENE	1,2,4-TRIMETHYL BENZENE
IN	61.19	306.69	742.44	476.09
OUT	3.37	49.35	69.7	69.9
EXIT	2.63	34.2	47.72	48.53
STRIPPING FACTOR	1.9	1.5	2.0	1.9
NTU	4.8	3.6	3.8	3.0
EXPERIMENTAL ATU (m^2)	2.35E-02	3.20E-02	3.02E-02	3.74E-02
EXPERIMENTAL KLa (sec^-1)	1.04E+00	7.61E-01	8.07E-01	6.51E-01
EXPERIMENTAL kl (m/sec)	4.15E-04	3.05E-04	3.23E-04	2.60E-04

Note: Experimental kl calculated using a=2500m^2/m^3

Mass Transfer Test Data for the 45.92-cm-diam. Rotor

SUMITOMO PACKING
SAMPLE NAME RAS-18-4
WATER FLOW 34.8 GPM
GAS FLOW 47.3 SCFM
ROTOR SPEED 790 RPM
PRESSURE DROP 1.2 IN. WATER
G/L RATIO (vol) 10.2
WATER TEMPERATURE
IN
OUT 287.6 Kelvin
AIR TEMPERATURE
IN 285 Kelvin
OUT 282.6 Kelvin

CONCENTRATION (ppb)	PENTANE	METHYLCYCLOHEXANE	NAPHTHALENE	BENZENE
IN	0	210.14	76.1	78.08
OUT	0	1.35	77.7	2.82
EXIT	0	1.02	69.6	2.01
STRIPPING FACTOR	544.3	17.0	0.2	1.7
NTU	ERR	5.3	0.0	6.5
EXPERIMENTAL ATU (m^2)	ERR	2.14E-02	*********	1.76E-02
EXPERIMENTAL KLa (sec^-1)	ERR	8.09E-01	*********	9.84E-01
EXPERIMENTAL kl (m/sec)	ERR	3.24E-04	*********	3.94E-04

CONCENTRATION (ppb)	TOLUENE	O-XYLENE	M-XYLENE	1,2,4-TRIMETHYL BENZENE
IN	58.7	299.62	724.25	462.66
OUT	2.06	29.87	37.86	41.42
EXIT	1.4	21.45	27.54	30.5
STRIPPING FACTOR	2.0	1.5	2.1	2.0
NTU	5.7	4.6	4.7	3.9
EXPERIMENTAL ATU (m^2)	1.97E-02	2.46E-02	2.40E-02	2.95E-02
EXPERIMENTAL KLa (sec^-1)	8.75E-01	7.04E-01	7.20E-01	5.87E-01
EXPERIMENTAL kl (m/sec)	3.50E-04	2.82E-04	2.88E-04	2.35E-04

Note: Experimental kl calculated using a=2500m^2/m^3

Mass Transfer Test Data for the 45.92-cm-diam. Rotor

SUMITOMO PACKING
SAMPLE NAME RAS-18-5
WATER FLOW 34.7 GPM
GAS FLOW 47.4 SCFM
ROTOR SPEED 500 RPM
PRESSURE DROP 0.8 IN. WATER
G/L RATIO (vol) 10.2
WATER TEMPERATURE
IN
OUT 285.7 Kelvin
AIR TEMPERATURE
IN 284 Kelvin
OUT 282.6 Kelvin

CONCENTRATION (ppb)	PENTANE	METHYLCYCLOHEXANE	NAPHTHALENE	BENZENE
IN	0	212.52	73.3	78.57
OUT	0	7.66	8.5	8.54
EXIT	0	4.83	5.4	5.35
STRIPPING FACTOR	550.6	17.2	0.2	1.6
NTU	ERR	3.5	-0.8	4.3
EXPERIMENTAL ATU (m^2)	ERR	3.25E-02	*********	2.63E-02
EXPERIMENTAL KLa (sec^-1)	ERR	5.30E-01	*********	6.55E-01
EXPERIMENTAL kl (m/sec)	ERR	2.12E-04	*********	2.62E-04

CONCENTRATION (ppb)	TOLUENE	O-XYLENE	M-XYLENE	1,2,4-TRIMETHYL BENZENE
IN	64.36	298.24	724.16	464.18
OUT	5.07	59.05	96.98	86.21
EXIT	3.73	40.93	66	60.04
STRIPPING FACTOR	1.9	1.4	2.0	1.9
NTU	4.3	3.1	3.2	2.7
EXPERIMENTAL ATU (m^2)	2.65E-02	3.61E-02	3.56E-02	4.26E-02
EXPERIMENTAL KLa (sec^-1)	6.51E-01	4.78E-01	4.84E-01	4.04E-01
EXPERIMENTAL kl (m/sec)	2.60E-04	1.91E-04	1.94E-04	1.62E-04

Note: Experimental kl calculated using a=2500m^2/m^3

Mass Transfer Test Data for the 45.92-cm-diam. Rotor

SUMITOMO PACKING

SAMPLE NAME	RAS-18-6
WATER FLOW	43 GPM
GAS FLOW	77.2 SCFM
ROTOR SPEED	633 RPM
PRESSURE DROP	1.1 IN. WATER
G/L RATIO (vol)	13.4
WATER TEMPERATURE	
IN	
OUT	287.7 Kelvin
AIR TEMPERATURE	
IN	285.9 Kelvin
OUT	284 Kelvin

CONCENTRATION (ppb)	PENTANE	METHYLCYCLOHEXANE	NAPHTHALENE	BENZENE
IN	0	203.53	72.1	76.84
OUT	0	3.94	56.1	5
EXIT	0	2.64	49.1	2.93
STRIPPING FACTOR	718.7	22.5	0.2	2.2
NTU	ERR	4.1	ERR	4.3
EXPERIMENTAL ATU (m^2)	ERR	2.77E-02	ERR	2.65E-02
EXPERIMENTAL KLa (sec^-1)	ERR	7.71E-01	ERR	8.06E-01
EXPERIMENTAL kl (m/sec)	ERR	3.08E-04	ERR	3.22E-04

CONCENTRATION (ppb)	TOLUENE	O-XYLENE	M-XYLENE	1,2,4-TRIMETHYL BENZENE
IN	59.75	294.65	709.51	457.74
OUT	3.51	40.96	64.72	60.05
EXIT	2.33	27.83	43.29	41.28
STRIPPING FACTOR	2.6	2.0	2.8	2.6
NTU	4.1	3.1	3.3	2.8
EXPERIMENTAL ATU (m^2)	2.79E-02	3.67E-02	3.45E-02	4.07E-02
EXPERIMENTAL KLa (sec^-1)	7.65E-01	5.82E-01	6.19E-01	5.25E-01
EXPERIMENTAL kl (m/sec)	3.06E-04	2.33E-04	2.48E-04	2.10E-04

Note: Experimental kl calculated using a=2500m^2/m^3

Mass Transfer Test Data for the 45.92-cm-diam. Rotor

SUMITOMO PACKING

SAMPLE NAME	RAS-18-7
WATER FLOW	35 GPM
GAS FLOW	47.4 SCFM
ROTOR SPEED	790 RPM
PRESSURE DROP	1.2 IN. WATER
G/L RATIO (vol)	10.1
WATER TEMPERATURE	
IN	
OUT	287.7 Kelvin
AIR TEMPERATURE	
IN	284.5 Kelvin
OUT	282.4 Kelvin

CONCENTRATION (ppb)	PENTANE	METHYLCYCLOHEXANE	NAPHTHALENE	BENZENE
IN	0	212.32	78.2	77.02
OUT	0	1.29	73.2	2.84
EXIT	0	0.9	65.3	1.83
STRIPPING FACTOR	542.1	16.9	0.2	1.7
NTU	ERR	5.4	0.3	6.5
EXPERIMENTAL ATU (m^2)	ERR	2.11E-02	3.65E-01	1.74E-02
EXPERIMENTAL KLa (sec^-1)	ERR	8.24E-01	4.77E-02	9.99E-01
EXPERIMENTAL kl (m/sec)	ERR	3.30E-04	1.91E-05	4.00E-04

CONCENTRATION (ppb)	TOLUENE	O-XYLENE	M-XYLENE	1,2,4-TRIMETHYL BENZENE
IN	69.99	298.13	727.83	465.94
OUT	2.18	29.54	37.81	41.33
EXIT	1.21	19.91	25.42	28.57
STRIPPING FACTOR	2.0	1.5	2.1	2.0
NTU	6.1	4.7	4.8	3.9
EXPERIMENTAL ATU (m^2)	1.85E-02	2.40E-02	2.37E-02	2.90E-02
EXPERIMENTAL KLa (sec^-1)	9.40E-01	7.24E-01	7.34E-01	6.00E-01
EXPERIMENTAL kl (m/sec)	3.76E-04	2.89E-04	2.94E-04	2.40E-04

Note: Experimental kl calculated using a=2500m^2/m^3

Mass Transfer Test Data for the 45.92-cm-diam. Rotor

SUMITOMO PACKING		
SAMPLE NAME	RAS-18-8	
WATER FLOW	25.8	GPM
GAS FLOW	26.1	SCFM
ROTOR SPEED	921	RPM
PRESSURE DROP	1.4	IN. WATER
G/L RATIO (vol)	7.6	
WATER TEMPERATURE		
IN		
OUT	291.5	Kelvin
AIR TEMPERATURE		
IN	290.6	Kelvin
OUT	286	Kelvin

CONCENTRATION (ppb)	PENTANE	METHYLCYCLOHEXANE	NAPHTHALENE	BENZENE
IN	0	211.37	79.0	77.35
OUT	0	0.4	68.2	2.73
EXIT	0	0.4	68.2	2.27
STRIPPING FACTOR	399.7	12.5	0.1	1.4
NTU	ERR	6.7	ERR	7.6
EXPERIMENTAL ATU (m^2)	ERR	1.69E-02	ERR	1.48E-02
EXPERIMENTAL KLa (sec^-1)	ERR	7.59E-01	ERR	8.63E-01
EXPERIMENTAL kl (m/sec)	ERR	3.04E-04	ERR	3.45E-04

CONCENTRATION (ppb)	TOLUENE	O-XYLENE	M-XYLENE	1,2,4-TRIMETHYL BENZENE
IN	65.56	258.49	694.65	460.91
OUT	2.04	26.37	29.65	40.89
EXIT	2.04	21.77	24.45	33.92
STRIPPING FACTOR	1.7	1.3	1.8	1.7
NTU	6.5	5.3	5.6	4.2
EXPERIMENTAL ATU (m^2)	1.76E-02	2.13E-02	2.03E-02	2.73E-02
EXPERIMENTAL KLa (sec^-1)	7.30E-01	6.01E-01	6.32E-01	4.69E-01
EXPERIMENTAL kl (m/sec)	2.92E-04	2.40E-04	2.53E-04	1.88E-04

Note: Experimental kl calculated using a=2500m^2/m^3

Mass Transfer Test Data for the 45.92-cm-diam. Rotor

SUMITOMO PACKING

SAMPLE NAME	RAS-18-9
WATER FLOW	25.8 GPM
GAS FLOW	26.3 SCFM
ROTOR SPEED	633 RPM
PRESSURE DROP	0.7 IN. WATER
G/L RATIO (vol)	7.6
WATER TEMPERATURE	
IN	
OUT	291.3 Kelvin
AIR TEMPERATURE	
IN	291.8 Kelvin
OUT	286.2 Kelvin

CONCENTRATION (ppb)	PENTANE	METHYLCYCLOHEXANE	NAPHTHALENE	BENZENE
IN	0	204.85	72.0	77.45
OUT	0	1.59	69.8	4.45
EXIT	0	1.2	65.6	3.54
STRIPPING FACTOR	403.0	12.6	0.1	1.4
NTU	ERR	5.2	0.1	6.3
EXPERIMENTAL ATU (m^2)	ERR	2.18E-02	1.61E+00	1.81E-02
EXPERIMENTAL KLa (sec^-1)	ERR	5.88E-01	7.96E-03	7.07E-01
EXPERIMENTAL kl (m/sec)	ERR	2.35E-04	3.18E-06	2.83E-04

CONCENTRATION (ppb)	TOLUENE	O-XYLENE	M-XYLENE	1,2,4-TRIMETHYL BENZENE
IN	67.44	248.49	665.68	448.37
OUT	3.75	37.16	51.86	58.75
EXIT	2.81	30.02	41.58	48.18
STRIPPING FACTOR	1.7	1.3	1.8	1.7
NTU	5.5	4.1	4.3	3.3
EXPERIMENTAL ATU (m^2)	2.08E-02	2.77E-02	2.61E-02	3.39E-02
EXPERIMENTAL KLa (sec^-1)	6.16E-01	4.62E-01	4.90E-01	3.78E-01
EXPERIMENTAL kl (m/sec)	2.47E-04	1.85E-04	1.96E-04	1.51E-04

Note: Experimental kl calculated using a=2500m^2/m^3

Mass Transfer Test Data for the 45.92-cm-diam. Rotor

SUMITOMO PACKING

SAMPLE NAME	RAS-18-10
WATER FLOW	35.3 GPM
GAS FLOW	48.1 SCFM
ROTOR SPEED	790 RPM
PRESSURE DROP	1.2 IN. WATER
G/L RATIO (vol)	10.2
WATER TEMPERATURE	
IN	
OUT	291.3 Kelvin
AIR TEMPERATURE	
IN	293.6 Kelvin
OUT	287.5 Kelvin

CONCENTRATION (ppb)	PENTANE	METHYLCYCLOHEXANE	NAPHTHALENE	BENZENE
IN	0	203.91	81.5	73.85
OUT	0	1.09	71.5	2.19
EXIT	0	0.81	60.5	1.54
STRIPPING FACTOR	538.7	16.8	0.2	1.9
NTU	ERR	5.5	ERR	6.2
EXPERIMENTAL ATU (m^2)	ERR	2.06E-02	ERR	1.84E-02
EXPERIMENTAL KLa (sec^-1)	ERR	8.52E-01	ERR	9.53E-01
EXPERIMENTAL kl (m/sec)	ERR	3.41E-04	ERR	3.81E-04

CONCENTRATION (ppb)	TOLUENE	O-XYLENE	M-XYLENE	1,2,4-TRIMETHYL BENZENE
IN	67.9	253.5	673.37	451.41
OUT	1.92	20.94	29.28	33.98
EXIT	1.24	15.7	21.18	25.43
STRIPPING FACTOR	2.2	1.7	2.4	2.3
NTU	5.7	4.4	4.7	3.8
EXPERIMENTAL ATU (m^2)	1.99E-02	2.55E-02	2.42E-02	2.96E-02
EXPERIMENTAL KLa (sec^-1)	8.82E-01	6.87E-01	7.24E-01	5.92E-01
EXPERIMENTAL kl (m/sec)	3.53E-04	2.75E-04	2.90E-04	2.37E-04

Note: Experimental kl calculated using a=2500m^2/m^3

Mass Transfer Test Data for the 45.92-cm-diam. Rotor

SUMITOMO PACKING

SAMPLE NAME	RAS-18-11
WATER FLOW	35.2 GPM
GAS FLOW	27.9 SCFM
ROTOR SPEED	790 RPM
PRESSURE DROP	1.1 IN. WATER
G/L RATIO (vol)	5.9
WATER TEMPERATURE	
IN	
OUT	291 Kelvin
AIR TEMPERATURE	
IN	290.7 Kelvin
OUT	285.8 Kelvin

CONCENTRATION (ppb)	PENTANE	METHYLCYCLOHEXANE	NAPHTHALENE	BENZENE
IN	0	202.25	69.0	77.88
OUT	0	1.19	82.5	7.04
EXIT	0	0.84	69.1	5.14
STRIPPING FACTOR	313.7	9.8	0.1	1.1
NTU	ERR	5.6	ERR	8.4
EXPERIMENTAL ATU (m^2)	ERR	2.01E-02	ERR	1.35E-02
EXPERIMENTAL KLa (sec^-1)	ERR	8.68E-01	ERR	1.30E+00
EXPERIMENTAL kl (m/sec)	ERR	3.47E-04	ERR	5.18E-04

CONCENTRATION (ppb)	TOLUENE	O-XYLENE	M-XYLENE	1,2,4-TRIMETHYL BENZENE
IN	59.52	243.89	646.97	440.49
OUT	5.35	58.21	76.37	90.13
EXIT	4.16	43.5	55.98	67.78
STRIPPING FACTOR	1.3	1.0	1.4	1.3
NTU	5.9	4.4	4.6	3.1
EXPERIMENTAL ATU (m^2)	1.93E-02	2.60E-02	2.48E-02	3.61E-02
EXPERIMENTAL KLa (sec^-1)	9.04E-01	6.74E-01	7.04E-01	4.84E-01
EXPERIMENTAL kl (m/sec)	3.62E-04	2.70E-04	2.82E-04	1.94E-04

Note: Experimental kl calculated using a=2500m^2/m^3

Mass Transfer Test Data for the 45.92-cm-diam. Rotor

SUMITOMO PACKING

SAMPLE NAME	RAS-18-12
WATER FLOW	43.4 GPM
GAS FLOW	77.4 SCFM
ROTOR SPEED	921 RPM
PRESSURE DROP	1.8 IN. WATER
G/L RATIO (vol)	13.3
WATER TEMPERATURE	
IN	
OUT	286.5 Kelvin
AIR TEMPERATURE	
IN	285.5 Kelvin
OUT	282.6 Kelvin

CONCENTRATION (ppb)	PENTANE	METHYLCYCLOHEXANE	NAPHTHALENE	BENZENE
IN	0	213.43	67.5	95.81
OUT	0	0.94	60.0	1.14
EXIT	0	0.94	54.0	0.96
STRIPPING FACTOR	716.9	22.4	0.2	2.1
NTU	ERR	5.6	0.4	7.3
EXPERIMENTAL ATU (m^2)	ERR	2.02E-02	3.19E-01	1.56E-02
EXPERIMENTAL KLa (sec^-1)	ERR	1.07E+00	6.75E-02	1.39E+00
EXPERIMENTAL kl (m/sec)	ERR	4.28E-04	2.70E-05	5.54E-04

CONCENTRATION (ppb)	TOLUENE	O-XYLENE	M-XYLENE	1,2,4-TRIMETHYL BENZENE
IN	60.16	256.65	681.11	485.42
OUT	0.91	14.36	20.27	25.68
EXIT	0.91	12.14	17.36	21.73
STRIPPING FACTOR	2.5	1.9	2.6	2.5
NTU	6.1	4.8	5.0	4.2
EXPERIMENTAL ATU (m^2)	1.85E-02	2.37E-02	2.27E-02	2.70E-02
EXPERIMENTAL KLa (sec^-1)	1.17E+00	9.10E-01	9.50E-01	7.97E-01
EXPERIMENTAL kl (m/sec)	4.67E-04	3.64E-04	3.80E-04	3.19E-04

Note: Experimental kl calculated using a=2500m^2/m^3

Mass Transfer Test Data for the 45.92-cm-diam. Rotor

SUMITOMO PACKING
SAMPLE NAME RAS-18-13
WATER FLOW 34.6 GPM
GAS FLOW 49.2 SCFM
ROTOR SPEED 790 RPM
PRESSURE DROP 1.2 IN. WATER
G/L RATIO (vol) 10.6
WATER TEMPERATURE
IN
OUT 287.5 Kelvin
AIR TEMPERATURE
IN 288 Kelvin
OUT 283 Kelvin

CONCENTRATION (ppb)	PENTANE	METHYLCYCLOHEXANE	NAPHTHALENE	BENZENE
IN	0	197.86	72.1	80.8
OUT	0	1.39	68.6	2.2
EXIT	0	0.93	66.3	1.54
STRIPPING FACTOR	569.6	17.8	0.2	1.8
NTU	ERR	5.2	0.1	6.9
EXPERIMENTAL ATU (m^2)	ERR	2.18E-02	1.58E+00	1.66E-02
EXPERIMENTAL KLa (sec^-1)	ERR	7.89E-01	1.09E-02	1.04E+00
EXPERIMENTAL kl (m/sec)	ERR	3.16E-04	4.34E-06	4.15E-04

CONCENTRATION (ppb)	TOLUENE	O-XYLENE	M-XYLENE	1,2,4-TRIMETHYL BENZENE
IN	60.36	240.83	638.98	458.85
OUT	1.69	24.27	34.25	41.29
EXIT	1.08	16.63	23.17	28.25
STRIPPING FACTOR	2.1	1.6	2.2	2.1
NTU	6.1	4.5	4.6	3.8
EXPERIMENTAL ATU (m^2)	1.88E-02	2.55E-02	2.46E-02	2.99E-02
EXPERIMENTAL KLa (sec^-1)	9.16E-01	6.75E-01	6.98E-01	5.75E-01
EXPERIMENTAL kl (m/sec)	3.66E-04	2.70E-04	2.79E-04	2.30E-04

Note: Experimental kl calculated using a=2500m^2/m^3

Mass Transfer Test Data for the 45.92-cm-diam. Rotor

SUMITOMO PACKING

SAMPLE NAME	RAS-18-14
WATER FLOW	43.3 GPM
GAS FLOW	43.2 SCFM
ROTOR SPEED	633 RPM
PRESSURE DROP	0.9 IN. WATER
G/L RATIO (vol)	7.5
WATER TEMPERATURE	
IN	
OUT	287.2 Kelvin
AIR TEMPERATURE	
IN	288.3 Kelvin
OUT	282.8 Kelvin

CONCENTRATION (ppb)	PENTANE	METHYLCYCLOHEXANE	NAPHTHALENE	BENZENE
IN	0	210.36	71.2	91.61
OUT	0	4.66	72.9	8.05
EXIT	0	2.64	61.9	4.87
STRIPPING FACTOR	400.1	12.5	0.1	1.2
NTU	ERR	4.1	ERR	7.2
EXPERIMENTAL ATU (m^2)	ERR	2.78E-02	ERR	1.57E-02
EXPERIMENTAL KLa (sec^-1)	ERR	7.75E-01	ERR	1.37E+00
EXPERIMENTAL kl (m/sec)	ERR	3.10E-04	ERR	5.49E-04

CONCENTRATION (ppb)	TOLUENE	O-XYLENE	M-XYLENE	1,2,4-TRIMETHYL BENZENE
IN	62.35	251.8	666.45	482.83
OUT	6.98	67.98	114.96	119.41
EXIT	4.35	44.63	70.86	76.46
STRIPPING FACTOR	1.4	1.1	1.5	1.4
NTU	4.8	3.4	3.4	2.6
EXPERIMENTAL ATU (m^2)	2.38E-02	3.33E-02	3.34E-02	4.31E-02
EXPERIMENTAL KLa (sec^-1)	9.06E-01	6.46E-01	6.43E-01	4.99E-01
EXPERIMENTAL kl (m/sec)	3.62E-04	2.59E-04	2.57E-04	2.00E-04

Note: Experimental kl calculated using a=2500m^2/m^3

Mass Transfer Test Data for the 45.92-cm-diam. Rotor

SUMITOMO PACKING

SAMPLE NAME	RAS-18-15
WATER FLOW	42.9 GPM
GAS FLOW	43 SCFM
ROTOR SPEED	921 RPM
PRESSURE DROP	1.6 IN. WATER
G/L RATIO (vol)	7.5
WATER TEMPERATURE	
IN	
OUT	287.7 Kelvin
AIR TEMPERATURE	
IN	290 Kelvin
OUT	284.3 Kelvin

CONCENTRATION (ppb)	PENTANE	METHYLCYCLOHEXANE	NAPHTHALENE	BENZENE
IN	0	195	69.2	78.71
OUT	0	1.1	70.5	4.51
EXIT	0	0.68	58.7	2.59
STRIPPING FACTOR	401.2	12.5	0.1	1.3
NTU	ERR	5.6	0.1	8.9
EXPERIMENTAL ATU (m^2)	ERR	2.04E-02	1.08E+00	1.28E-02
EXPERIMENTAL KLa (sec^-1)	ERR	1.05E+00	1.97E-02	1.66E+00
EXPERIMENTAL kl (m/sec)	ERR	4.18E-04	7.87E-06	6.65E-04

CONCENTRATION (ppb)	TOLUENE	O-XYLENE	M-XYLENE	1,2,4-TRIMETHYL BENZENE
IN	57.07	238.21	634.1	455.03
OUT	3.64	44.53	58.96	73.48
EXIT	2.06	27.72	34.62	44.79
STRIPPING FACTOR	1.5	1.1	1.6	1.5
NTU	6.4	5.0	4.9	3.7
EXPERIMENTAL ATU (m^2)	1.78E-02	2.27E-02	2.32E-02	3.09E-02
EXPERIMENTAL KLa (sec^-1)	1.20E+00	9.41E-01	9.19E-01	6.89E-01
EXPERIMENTAL kl (m/sec)	4.80E-04	3.76E-04	3.68E-04	2.76E-04

Note: Experimental kl calculated using a=2500m^2/m^3

Mass Transfer Test Data for the 45.92-cm-diam. Rotor

SUMITOMO PACKING
SAMPLE NAME RAS-18-16
WATER FLOW 34.7 GPM
GAS FLOW 45.8 SCFM
ROTOR SPEED 790 RPM
PRESSURE DROP 1.2 IN. WATER
G/L RATIO (vol) 9.9
WATER TEMPERATURE
IN
OUT 288.5 Kelvin
AIR TEMPERATURE
IN 293.1 Kelvin
OUT 285.5 Kelvin

CONCENTRATION (ppb)	PENTANE	METHYLCYCLOHEXANE	NAPHTHALENE	BENZENE
IN	0	197.78	63.1	63.52
OUT	0	1.35	70.2	2.58
EXIT	0	0.81	65.5	1.47
STRIPPING FACTOR	526.9	16.5	0.2	1.7
NTU	ERR	5.3	-0.1	6.4
EXPERIMENTAL ATU (m^2)	ERR	2.15E-02	*********	1.77E-02
EXPERIMENTAL KLa (sec^-1)	ERR	8.00E-01	*********	9.74E-01
EXPERIMENTAL kl (m/sec)	ERR	3.20E-04	*********	3.89E-04

CONCENTRATION (ppb)	TOLUENE	O-XYLENE	M-XYLENE	1,2,4-TRIMETHYL BENZENE
IN	57.9	244.76	669.95	460.61
OUT	2.36	27.42	38.82	46.88
EXIT	1.38	16.2	24.39	28.34
STRIPPING FACTOR	2.0	1.5	2.1	2.0
NTU	5.6	4.6	4.6	3.7
EXPERIMENTAL ATU (m^2)	2.04E-02	2.49E-02	2.45E-02	3.04E-02
EXPERIMENTAL KLa (sec^-1)	8.45E-01	6.92E-01	7.02E-01	5.66E-01
EXPERIMENTAL kl (m/sec)	3.38E-04	2.77E-04	2.81E-04	2.27E-04

Note: Experimental kl calculated using a=2500m^2/m^3

Mass Transfer Test Data for the 45.92-cm-diam. Rotor

SUMITOMO PACKING

SAMPLE NAME	RAS-18-17
WATER FLOW	34.6 GPM
GAS FLOW	46.1 SCFM
ROTOR SPEED	1000 RPM
PRESSURE DROP	1.8 IN. WATER
G/L RATIO (vol)	10.0
WATER TEMPERATURE	
IN	
OUT	288.7 Kelvin
AIR TEMPERATURE	
IN	292.8 Kelvin
OUT	286 Kelvin

CONCENTRATION (ppb)	PENTANE	METHYLCYCLOHEXANE	NAPHTHALENE	BENZENE
IN	0	196.73	81.3	70.64
OUT	0	0.46	73.7	1.44
EXIT	0	0.46	65.1	0.86
STRIPPING FACTOR	531.5	16.6	0.2	1.7
NTU	ERR	6.4	ERR	7.9
EXPERIMENTAL ATU (m^2)	ERR	1.78E-02	ERR	1.44E-02
EXPERIMENTAL KLa (sec^-1)	ERR	9.66E-01	ERR	1.19E+00
EXPERIMENTAL kl (m/sec)	ERR	3.87E-04	ERR	4.76E-04

CONCENTRATION (ppb)	TOLUENE	O-XYLENE	M-XYLENE	1,2,4-TRIMETHYL BENZENE
IN	54.47	244.89	653.47	466.02
OUT	1.18	17.44	21.22	29.06
EXIT	0.69	10.93	13.56	18.48
STRIPPING FACTOR	2.0	1.5	2.1	2.0
NTU	6.7	5.6	5.6	4.6
EXPERIMENTAL ATU (m^2)	1.69E-02	2.03E-02	2.02E-02	2.48E-02
EXPERIMENTAL KLa (sec^-1)	1.02E+00	8.45E-01	8.52E-01	6.92E-01
EXPERIMENTAL kl (m/sec)	4.08E-04	3.38E-04	3.41E-04	2.77E-04

Note: Experimental kl calculated using a=2500m^2/m^3

Mass Transfer Test Data for the 45.92-cm-diam. Rotor

SUMITOMO PACKING

SAMPLE NAME	RAS-18-18
WATER FLOW	34.9 GPM
GAS FLOW	64.9 SCFM
ROTOR SPEED	790 RPM
PRESSURE DROP	1.5 IN. WATER
G/L RATIO (vol)	13.9
WATER TEMPERATURE	
IN	
OUT	289.4 Kelvin
AIR TEMPERATURE	
IN	291.3 Kelvin
OUT	285.2 Kelvin

CONCENTRATION (ppb)	PENTANE	METHYLCYCLOHEXANE	NAPHTHALENE	BENZENE
IN	0	196.54	71.9	76.5
OUT	0	1.91	66.3	1.6
EXIT	0	0.97	52.9	0.92
STRIPPING FACTOR	740.0	23.1	0.2	2.5
NTU	ERR	4.8	ERR	6.0
EXPERIMENTAL ATU (m^2)	ERR	2.35E-02	ERR	1.91E-02
EXPERIMENTAL KLa (sec^-1)	ERR	7.36E-01	ERR	9.10E-01
EXPERIMENTAL kl (m/sec)	ERR	2.94E-04	ERR	3.64E-04

CONCENTRATION (ppb)	TOLUENE	O-XYLENE	M-XYLENE	1,2,4-TRIMETHYL BENZENE
IN	56.61	215.94	633.07	474.84
OUT	1.46	16.39	27.21	32.77
EXIT	0.77	9.95	15.94	19.5
STRIPPING FACTOR	2.9	2.2	3.1	2.9
NTU	5.2	4.0	4.3	3.7
EXPERIMENTAL ATU (m^2)	2.17E-02	2.80E-02	2.63E-02	3.09E-02
EXPERIMENTAL KLa (sec^-1)	8.00E-01	6.18E-01	6.59E-01	5.62E-01
EXPERIMENTAL kl (m/sec)	3.20E-04	2.47E-04	2.64E-04	2.25E-04

Note: Experimental kl calculated using a=2500m^2/m^3

Mass Transfer Test Data for the 45.92-cm-diam. Rotor

SUMITOMO PACKING
SAMPLE NAME RAS-18-19
WATER FLOW 34.8 GPM
GAS FLOW 46.8 SCFM
ROTOR SPEED 790 RPM
PRESSURE DROP 1.5 IN. WATER
G/L RATIO (vol) 10.1
WATER TEMPERATURE
IN
OUT 289.9 Kelvin
AIR TEMPERATURE
IN 294.2 Kelvin
OUT 284.8 Kelvin

CONCENTRATION (ppb)	PENTANE	METHYLCYCLOHEXANE	NAPHTHALENE	BENZENE
IN	0	204.54	66.8	85.7
OUT	0	1.52	65.2	2.53
EXIT	0	0.89	58.0	1.52
STRIPPING FACTOR	534.2	16.7	0.2	1.8
NTU	ERR	5.2	0.1	6.7
EXPERIMENTAL ATU (m^2)	ERR	2.19E-02	1.50E+00	1.71E-02
EXPERIMENTAL KLa (sec^-1)	ERR	7.88E-01	1.15E-02	1.01E+00
EXPERIMENTAL kl (m/sec)	ERR	3.15E-04	4.59E-06	4.05E-04

CONCENTRATION (ppb)	TOLUENE	O-XYLENE	M-XYLENE	1,2,4-TRIMETHYL BENZENE
IN	60.19	222.22	645.16	483.96
OUT	2.02	24.21	36.73	46.73
EXIT	1.43	15.7	22.93	29.19
STRIPPING FACTOR	2.1	1.6	2.3	2.2
NTU	5.5	4.2	4.5	3.6
EXPERIMENTAL ATU (m^2)	2.05E-02	2.70E-02	2.54E-02	3.12E-02
EXPERIMENTAL KLa (sec^-1)	8.45E-01	6.41E-01	6.80E-01	5.54E-01
EXPERIMENTAL kl (m/sec)	3.38E-04	2.57E-04	2.72E-04	2.22E-04

Note: Experimental kl calculated using a=2500m^2/m^3

Mass Transfer Test Data for the 45.92-cm-diam. Rotor

SUMITOMO PACKING	
SAMPLE NAME	RAS-18-20
WATER FLOW	26 GPM
GAS FLOW	44.3 SCFM
ROTOR SPEED	921 RPM
PRESSURE DROP	1.5 IN. WATER
G/L RATIO (vol)	12.7
WATER TEMPERATURE	
IN	
OUT	288.9 Kelvin
AIR TEMPERATURE	
IN	295.8 Kelvin
OUT	285.4 Kelvin

CONCENTRATION (ppb)	PENTANE	METHYLCYCLOHEXANE	NAPHTHALENE	BENZENE
IN	0	203.47	70.3	82.67
OUT	0	0.77	59.4	0.71
EXIT	0	0.56	54.7	0.43
STRIPPING FACTOR	679.2	21.2	0.2	2.2
NTU	ERR	5.8	0.9	7.9
EXPERIMENTAL ATU (m^2)	ERR	1.95E-02	1.28E-01	1.43E-02
EXPERIMENTAL KLa (sec^-1)	ERR	6.62E-01	1.01E-01	9.01E-01
EXPERIMENTAL kl (m/sec)	ERR	2.65E-04	4.04E-05	3.60E-04

CONCENTRATION (ppb)	TOLUENE	O-XYLENE	M-XYLENE	1,2,4-TRIMETHYL BENZENE
IN	60.44	222.92	644.18	479.54
OUT	0.69	8.7	12.2	16.64
EXIT	0.36	5.5	8.01	10.58
STRIPPING FACTOR	2.6	2.0	2.8	2.6
NTU	6.8	5.6	5.7	4.9
EXPERIMENTAL ATU (m^2)	1.66E-02	2.03E-02	1.98E-02	2.31E-02
EXPERIMENTAL KLa (sec^-1)	7.77E-01	6.37E-01	6.52E-01	5.58E-01
EXPERIMENTAL kl (m/sec)	3.11E-04	2.55E-04	2.61E-04	2.23E-04

Note: Experimental kl calculated using a=2500m^2/m^3

Mass Transfer Test Data for the 45.92-cm-diam. Rotor

SUMITOMO PACKING
SAMPLE NAME RAS-18-21
WATER FLOW 25.9 GPM
GAS FLOW 44.6 SCFM
ROTOR SPEED 633 RPM
PRESSURE DROP 0.9 IN. WATER
G/L RATIO (vol) 12.9
WATER TEMPERATURE
IN
OUT 291.1 Kelvin
AIR TEMPERATURE
IN 291.3 Kelvin
OUT 285 Kelvin

CONCENTRATION (ppb)	PENTANE	METHYLCYCLOHEXANE	NAPHTHALENE	BENZENE
IN	0	165.41	53.1	72.98
OUT	0	1.56	52.3	1.54
EXIT	0	1.56	49.2	1.54
STRIPPING FACTOR	681.3	21.3	0.2	2.4
NTU	ERR	4.8	0.0	5.7
EXPERIMENTAL ATU (m^2)	ERR	2.34E-02	5.30E+00	2.00E-02
EXPERIMENTAL KLa (sec^-1)	ERR	5.49E-01	2.43E-03	6.44E-01
EXPERIMENTAL kl (m/sec)	ERR	2.20E-04	9.70E-07	2.58E-04

CONCENTRATION (ppb)	TOLUENE	O-XYLENE	M-XYLENE	1,2,4-TRIMETHYL BENZENE
IN	42.53	167.49	560.74	411.48
OUT	1.29	12.62	24.93	30.1
EXIT	1.29	10.67	21.34	25.18
STRIPPING FACTOR	2.8	2.2	3.0	2.9
NTU	4.8	3.9	4.2	3.5
EXPERIMENTAL ATU (m^2)	2.38E-02	2.91E-02	2.73E-02	3.26E-02
EXPERIMENTAL KLa (sec^-1)	5.40E-01	4.42E-01	4.71E-01	3.94E-01
EXPERIMENTAL kl (m/sec)	2.16E-04	1.77E-04	1.88E-04	1.58E-04

Note: Experimental kl calculated using a=2500m^2/m^3

Mass Transfer Test Data for the 45.92-cm-diam. Rotor

SUMITOMO PACKING

SAMPLE NAME	RAS-18-22
WATER FLOW	34.6 GPM
GAS FLOW	45.5 SCFM
ROTOR SPEED	790 RPM
PRESSURE DROP	1.2 IN. WATER
G/L RATIO (vol)	9.8
WATER TEMPERATURE	
IN	
OUT	291.3 Kelvin
AIR TEMPERATURE	
IN	292.7 Kelvin
OUT	285.9 Kelvin

CONCENTRATION (ppb)	PENTANE	METHYLCYCLOHEXANE	NAPHTHALENE	BENZENE
IN	0	178.65	53.8	67.19
OUT	0	0.89	56.7	1.76
EXIT	0	0.89	50.7	1.56
STRIPPING FACTOR	519.9	16.2	0.2	1.9
NTU	ERR	5.6	-0.1	6.4
EXPERIMENTAL ATU (m^2)	ERR	2.03E-02	*********	1.78E-02
EXPERIMENTAL KLa (sec^-1)	ERR	8.45E-01	*********	9.67E-01
EXPERIMENTAL kl (m/sec)	ERR	3.38E-04	*********	3.87E-04

CONCENTRATION (ppb)	TOLUENE	O-XYLENE	M-XYLENE	1,2,4-TRIMETHYL BENZENE
IN	47.05	183.55	609.68	439.36
OUT	1.23	15.08	25.92	33.86
EXIT	1.23	13.41	23.23	29.63
STRIPPING FACTOR	2.2	1.7	2.3	2.2
NTU	5.7	4.4	4.7	3.8
EXPERIMENTAL ATU (m^2)	2.00E-02	2.58E-02	2.42E-02	3.02E-02
EXPERIMENTAL KLa (sec^-1)	8.58E-01	6.67E-01	7.09E-01	5.70E-01
EXPERIMENTAL kl (m/sec)	3.43E-04	2.67E-04	2.84E-04	2.28E-04

Note: Experimental kl calculated using a=2500m^2/m^3

Mass Transfer Test Data for the 45.92-cm-diam. Rotor

WIRE GAUZE PACKING

SAMPLE NAME	Rs218-1
WATER FLOW	35.5 GPM
GAS FLOW	47.7 SCFM
ROTOR SPEED	790 RPM
PRESSURE DROP	1.1 IN. WATER
G/L RATIO (vol)	10.1
WATER TEMPERATURE	
IN	
OUT	291.9 Kelvin
AIR TEMPERATURE	
IN	300.6 Kelvin
OUT	291.2 Kelvin

CONCENTRATION (ppb)	PENTANE	METHYLCYCLOHEXANE	NAPHTHALENE	BENZENE
IN	67.08	194.66	60.1	96.92
OUT	0	4.12	60.7	12.71
EXIT	0	4.12	50.8	10.38
STRIPPING FACTOR	530.1	16.6	0.2	1.9
NTU	ERR	4.0	-0.1	3.1
EXPERIMENTAL ATU (m^2)	ERR	2.81E-02	*********	3.64E-02
EXPERIMENTAL KLa (sec^-1)	ERR	6.27E-01	*********	4.85E-01
EXPERIMENTAL kl (m/sec)	ERR	3.04E-04	*********	2.35E-04

CONCENTRATION (ppb)	TOLUENE	O-XYLENE	M-XYLENE	1,2,4-TRIMETHYL BENZENE
IN	57.44	77.67	679.19	312.78
OUT	7.73	17.75	92.27	60.48
EXIT	6.28	14.23	74.95	49.56
STRIPPING FACTOR	2.3	1.7	2.4	2.3
NTU	2.9	2.3	2.8	2.2
EXPERIMENTAL ATU (m^2)	3.97E-02	5.00E-02	4.12E-02	5.09E-02
EXPERIMENTAL KLa (sec^-1)	4.44E-01	3.53E-01	4.28E-01	3.47E-01
EXPERIMENTAL kl (m/sec)	2.15E-04	1.71E-04	2.07E-04	1.68E-04

Note: Experimental kl calculated using a=2067m^2/m^3

Mass Transfer Test Data for the 45.92-cm-diam. Rotor

WIRE GAUZE PACKING

SAMPLE NAME	Rs218-2
WATER FLOW	20.4 GPM
GAS FLOW	28 SCFM
ROTOR SPEED	790 RPM
PRESSURE DROP	1.1 IN. WATER
G/L RATIO (vol)	10.3
WATER TEMPERATURE	
IN	
OUT	291.8 Kelvin
AIR TEMPERATURE	
IN	300.5 Kelvin
OUT	292.4 Kelvin

CONCENTRATION (ppb)	PENTANE	METHYLCYCLOHEXANE	NAPHTHALENE	BENZENE
IN	58.01	171.38	62.0	103.42
OUT	0	2.42	63.5	8.84
EXIT	0	1.64	50.4	6.54
STRIPPING FACTOR	541.7	16.9	0.2	2.0
NTU	ERR	4.5	0.4	4.0
EXPERIMENTAL ATU (m^2)	ERR	2.53E-02	3.22E-01	2.87E-02
EXPERIMENTAL KLa (sec^-1)	ERR	4.00E-01	3.14E-02	3.53E-01
EXPERIMENTAL kl (m/sec)	ERR	1.94E-04	1.52E-05	1.71E-04

CONCENTRATION (ppb)	TOLUENE	O-XYLENE	M-XYLENE	1,2,4-TRIMETHYL BENZENE
IN	70.9	81.45	716.34	314.24
OUT	5.64	12.41	60.06	40.84
EXIT	4.05	9.13	45.67	33.18
STRIPPING FACTOR	2.3	1.8	2.5	2.4
NTU	3.8	3.1	3.5	2.8
EXPERIMENTAL ATU (m^2)	3.00E-02	3.66E-02	3.21E-02	3.99E-02
EXPERIMENTAL KLa (sec^-1)	3.38E-01	2.77E-01	3.16E-01	2.54E-01
EXPERIMENTAL kl (m/sec)	1.63E-04	1.34E-04	1.53E-04	1.23E-04

Note: Experimental kl calculated using a=2067m^2/m^3

Mass Transfer Test Data for the 45.92-cm-diam. Rotor

WIRE GAUGE PACKING
SAMPLE NAME Rs218-3
WATER FLOW 49.7 GPM
GAS FLOW 69 SCFM
ROTOR SPEED 790 RPM
PRESSURE DROP 1.3 IN. WATER
G/L RATIO (vol) 10.4
WATER TEMPERATURE
IN
OUT 292.4 Kelvin
AIR TEMPERATURE
IN 308 Kelvin
OUT 293.3 Kelvin

CONCENTRATION (ppb)	PENTANE	METHYLCYCLOHEXANE	NAPHTHALENE	BENZENE
IN	70.17	204.79	56.4	114.71
OUT	0	5.44	63.2	14.94
EXIT	0	4.71	54.3	13.7
STRIPPING FACTOR	546.8	17.1	0.2	2.0
NTU	ERR	3.8	-0.3	3.0
EXPERIMENTAL ATU (m^2)	ERR	2.99E-02	*********	3.82E-02
EXPERIMENTAL KLa (sec^-1)	ERR	8.27E-01	*********	6.46E-01
EXPERIMENTAL kl (m/sec)	ERR	4.00E-04	*********	3.12E-04

CONCENTRATION (ppb)	TOLUENE	O-XYLENE	M-XYLENE	1,2,4-TRIMETHYL BENZENE
IN	66.65	83.11	737.67	321.64
OUT	9.03	17.56	102.4	60.03
EXIT	8.28	15.7	95.53	56.32
STRIPPING FACTOR	2.4	1.8	2.6	2.5
NTU	2.7	2.3	2.6	2.2
EXPERIMENTAL ATU (m^2)	4.17E-02	4.99E-02	4.36E-02	5.21E-02
EXPERIMENTAL KLa (sec^-1)	5.92E-01	4.95E-01	5.66E-01	4.74E-01
EXPERIMENTAL kl (m/sec)	2.87E-04	2.39E-04	2.74E-04	2.29E-04

Note: Experimental kl calculated using a=2067m^2/m^3

Mass Transfer Test Data for the 45.92-cm-diam. Rotor

WIRE GAUZE PACKING

SAMPLE NAME	Rs218-4
WATER FLOW	35.5 GPM
GAS FLOW	46.3 SCFM
ROTOR SPEED	790 RPM
PRESSURE DROP	1.1 IN. WATER
G/L RATIO (vol)	9.8
WATER TEMPERATURE	
IN	
OUT	292.6 Kelvin
AIR TEMPERATURE	
IN	301.5 Kelvin
OUT	293.3 Kelvin

CONCENTRATION (ppb)	PENTANE	METHYLCYCLOHEXANE	NAPHTHALENE	BENZENE
IN	69.82	202.39	62.4	107.5
OUT	0	4.7	60.6	12.52
EXIT	0	3.62	53.3	10.15
STRIPPING FACTOR	513.3	16.0	0.2	1.9
NTU	ERR	4.0	0.1	3.4
EXPERIMENTAL ATU (m^2)	ERR	2.87E-02	8.51E-01	3.38E-02
EXPERIMENTAL KLa (sec^-1)	ERR	6.15E-01	2.07E-02	5.22E-01
EXPERIMENTAL kl (m/sec)	ERR	2.98E-04	1.00E-05	2.52E-04

CONCENTRATION (ppb)	TOLUENE	O-XYLENE	M-XYLENE	1,2,4-TRIMETHYL BENZENE
IN	63.51	81.22	731.75	316.91
OUT	7.45	14.87	84.51	52.49
EXIT	6.32	12.36	71.68	43.84
STRIPPING FACTOR	2.2	1.7	2.4	2.3
NTU	3.1	2.7	3.0	2.5
EXPERIMENTAL ATU (m^2)	3.70E-02	4.24E-02	3.79E-02	4.60E-02
EXPERIMENTAL KLa (sec^-1)	4.77E-01	4.16E-01	4.65E-01	3.83E-01
EXPERIMENTAL kl (m/sec)	2.31E-04	2.01E-04	2.25E-04	1.85E-04

Note: Experimental kl calculated using a=2067m^2/m^3

Mass Transfer Test Data for the 45.92-cm-diam. Rotor

WIRE GAUZE PACKING

SAMPLE NAME	Rs218-5
WATER FLOW	35.6 GPM
GAS FLOW	46.8 SCFM
ROTOR SPEED	500 RPM
PRESSURE DROP	0.7 IN. WATER
G/L RATIO (vol)	9.8
WATER TEMPERATURE	
IN	
OUT	292.7 Kelvin
AIR TEMPERATURE	
IN	301.3 Kelvin
OUT	293.7 Kelvin

CONCENTRATION (ppb)	PENTANE	METHYLCYCLOHEXANE	NAPHTHALENE	BENZENE
IN	78.97	217.92	58.4	111.04
OUT	3.2	12.38	56.3	18.81
EXIT	2.76	10.33	46.8	11.7
STRIPPING FACTOR	517.2	16.2	0.2	2.0
NTU	3.2	3.0	ERR	2.8
EXPERIMENTAL ATU (m^2)	3.54E-02	3.78E-02	ERR	4.02E-02
EXPERIMENTAL KLa (sec^-1)	5.00E-01	4.68E-01	ERR	4.40E-01
EXPERIMENTAL kl (m/sec)	2.42E-04	2.26E-04	ERR	2.13E-04

CONCENTRATION (ppb)	TOLUENE	O-XYLENE	M-XYLENE	1,2,4-TRIMETHYL BENZENE
IN	65.06	82.96	748.04	321.9
OUT	10.78	19.83	128.21	71.74
EXIT	9.3	16.97	112.24	62.44
STRIPPING FACTOR	2.3	1.7	2.4	2.4
NTU	2.5	2.1	2.4	2.0
EXPERIMENTAL ATU (m^2)	4.58E-02	5.33E-02	4.83E-02	5.74E-02
EXPERIMENTAL KLa (sec^-1)	3.86E-01	3.32E-01	3.66E-01	3.08E-01
EXPERIMENTAL kl (m/sec)	1.87E-04	1.61E-04	1.77E-04	1.49E-04

Note: Experimental kl calculated using a=2067m^2/m^3

Mass Transfer Test Data for the 45.92-cm-diam. Rotor

WIRE GAUZE PACKING

SAMPLE NAME	Rs218-6
WATER FLOW	43.8 GPM
GAS FLOW	77.7 SCFM
ROTOR SPEED	633 RPM
PRESSURE DROP	1 IN. WATER
G/L RATIO (vol)	13.3
WATER TEMPERATURE	
IN	
OUT	292.1 Kelvin
AIR TEMPERATURE	
IN	302.1 Kelvin
OUT	292.9 Kelvin

CONCENTRATION (ppb)	PENTANE	METHYLCYCLOHEXANE	NAPHTHALENE	BENZENE
IN	80.19	205.77	57.8	101.48
OUT	2.46	9.22	55.1	12.79
EXIT	2.17	6.57	50.3	11.35
STRIPPING FACTOR	699.4	21.9	0.2	2.6
NTU	3.5	3.2	0.1	2.8
EXPERIMENTAL ATU (m^2)	3.25E-02	3.52E-02	1.26E+00	4.11E-02
EXPERIMENTAL KLa (sec^-1)	6.69E-01	6.17E-01	1.72E-02	5.30E-01
EXPERIMENTAL kl (m/sec)	3.23E-04	2.99E-04	8.33E-06	2.56E-04

CONCENTRATION (ppb)	TOLUENE	O-XYLENE	M-XYLENE	1,2,4-TRIMETHYL BENZENE
IN	66.36	82.74	740.28	319.43
OUT	8.54	15.38	97.41	55.32
EXIT	7.4	13.08	80.54	46.42
STRIPPING FACTOR	3.0	2.3	3.2	3.1
NTU	2.6	2.3	2.5	2.2
EXPERIMENTAL ATU (m^2)	4.34E-02	4.96E-02	4.45E-02	5.19E-02
EXPERIMENTAL KLa (sec^-1)	5.02E-01	4.39E-01	4.89E-01	4.19E-01
EXPERIMENTAL kl (m/sec)	2.43E-04	2.12E-04	2.36E-04	2.03E-04

Note: Experimental kl calculated using a=2067m^2/m^3

Mass Transfer Test Data for the 45.92-cm-diam. Rotor

WIRE GAUZE PACKING

SAMPLE NAME	Rs218-7
WATER FLOW	35 GPM
GAS FLOW	46.5 SCFM
ROTOR SPEED	790 RPM
PRESSURE DROP	1.2 IN. WATER
G/L RATIO (vol)	9.9
WATER TEMPERATURE	
IN	
OUT	292.9 Kelvin
AIR TEMPERATURE	
IN	301.3 Kelvin
OUT	292.5 Kelvin

CONCENTRATION (ppb)	PENTANE	METHYLCYCLOHEXANE	NAPHTHALENE	BENZENE
IN	78.76	208.65	55.0	98.85
OUT	1.1	3.96	49.6	11.07
EXIT	1.1	3.47	41.3	8.61
STRIPPING FACTOR	522.4	16.3	0.2	2.0
NTU	4.3	4.2	ERR	3.4
EXPERIMENTAL ATU (m^2)	2.65E-02	2.73E-02	ERR	3.33E-02
EXPERIMENTAL KLa (sec^-1)	6.55E-01	6.38E-01	ERR	5.22E-01
EXPERIMENTAL kl (m/sec)	3.17E-04	3.09E-04	ERR	2.52E-04

CONCENTRATION (ppb)	TOLUENE	O-XYLENE	M-XYLENE	1,2,4-TRIMETHYL BENZENE
IN	64.88	82.39	720.03	310.87
OUT	7.23	15.06	78.6	48.04
EXIT	5.76	11.65	62.98	39.97
STRIPPING FACTOR	2.3	1.8	2.5	2.4
NTU	3.2	2.7	3.1	2.5
EXPERIMENTAL ATU (m^2)	3.60E-02	4.21E-02	3.69E-02	4.45E-02
EXPERIMENTAL KLa (sec^-1)	4.83E-01	4.13E-01	4.72E-01	3.90E-01
EXPERIMENTAL kl (m/sec)	2.34E-04	2.00E-04	2.28E-04	1.89E-04

Note: Experimental kl calculated using a=2067m^2/m^3

Mass Transfer Test Data for the 45.92-cm-diam. Rotor

WIRE GAUZE PACKING	
SAMPLE NAME	Rs218-8
WATER FLOW	25.9 GPM
GAS FLOW	29 SCFM
ROTOR SPEED	921 RPM
PRESSURE DROP	1.4 IN. WATER
G/L RATIO (vol)	8.4
WATER TEMPERATURE	
IN	
OUT	292.8 Kelvin
AIR TEMPERATURE	
IN	297.8 Kelvin
OUT	291.6 Kelvin

CONCENTRATION (ppb)	PENTANE	METHYLCYCLOHEXANE	NAPHTHALENE	BENZENE
IN	73.53	196.24	64.9	101.11
OUT	0	1.87	58.7	9.65
EXIT	0	1.27	52.0	8.7
STRIPPING FACTOR	440.4	13.8	0.1	1.7
NTU	ERR	5.0	ERR	4.0
EXPERIMENTAL ATU (m^2)	ERR	2.29E-02	ERR	2.82E-02
EXPERIMENTAL KLa (sec^-1)	ERR	5.63E-01	ERR	4.57E-01
EXPERIMENTAL kl (m/sec)	ERR	2.72E-04	ERR	2.21E-04

CONCENTRATION (ppb)	TOLUENE	O-XYLENE	M-XYLENE	1,2,4-TRIMETHYL BENZENE
IN	77.13	82.55	727.22	308.59
OUT	6.25	14.15	63.58	43.21
EXIT	5.08	11.1	52.42	36.74
STRIPPING FACTOR	1.9	1.5	2.1	2.0
NTU	4.0	3.2	3.7	2.9
EXPERIMENTAL ATU (m^2)	2.80E-02	3.55E-02	3.05E-02	3.90E-02
EXPERIMENTAL KLa (sec^-1)	4.59E-01	3.62E-01	4.21E-01	3.30E-01
EXPERIMENTAL kl (m/sec)	2.22E-04	1.75E-04	2.04E-04	1.60E-04

Note: Experimental kl calculated using a=2067m^2/m^3

Mass Transfer Test Data for the 45.92-cm-diam. Rotor

WIRE GAUZE PACKING

SAMPLE NAME	Rs218-9
WATER FLOW	26 GPM
GAS FLOW	28 SCFM
ROTOR SPEED	633 RPM
PRESSURE DROP	0.7 IN. WATER
G/L RATIO (vol)	8.1
WATER TEMPERATURE	
IN	
OUT	292.2 Kelvin
AIR TEMPERATURE	
IN	294.2 Kelvin
OUT	289.8 Kelvin

CONCENTRATION (ppb)	PENTANE	METHYLCYCLOHEXANE	NAPHTHALENE	BENZENE
IN	65.45	180.02	62.4	100.46
OUT	1.3	5.32	63.1	15.27
EXIT	1.3	3.81	56.8	11.62
STRIPPING FACTOR	424.4	13.3	0.1	1.6
NTU	3.9	3.7	0.0	3.4
EXPERIMENTAL ATU (m^2)	2.89E-02	3.03E-02	*********	3.39E-02
EXPERIMENTAL KLa (sec^-1)	4.47E-01	4.27E-01	*********	3.82E-01
EXPERIMENTAL kl (m/sec)	2.16E-04	2.06E-04	*********	1.85E-04

CONCENTRATION (ppb)	TOLUENE	O-XYLENE	M-XYLENE	1,2,4-TRIMETHYL BENZENE
IN	65.55	81.67	724.59	306.99
OUT	9.91	19.68	102.36	60.2
EXIT	7.85	15.36	84.21	51.52
STRIPPING FACTOR	1.8	1.4	2.0	1.9
NTU	3.0	2.5	3.0	2.4
EXPERIMENTAL ATU (m^2)	3.79E-02	4.47E-02	3.84E-02	4.75E-02
EXPERIMENTAL KLa (sec^-1)	3.40E-01	2.89E-01	3.37E-01	2.72E-01
EXPERIMENTAL kl (m/sec)	1.65E-04	1.40E-04	1.63E-04	1.32E-04

Note: Experimental kl calculated using a=2067m^2/m^3

Mass Transfer Test Data for the 45.92-cm-diam. Rotor

WIRE GAUZE PACKING

SAMPLE NAME	Rs218-10
WATER FLOW	35.5 GPM
GAS FLOW	46.5 SCFM
ROTOR SPEED	790 RPM
PRESSURE DROP	1.2 IN. WATER
G/L RATIO (vol)	9.8
WATER TEMPERATURE	
IN	
OUT	291.8 Kelvin
AIR TEMPERATURE	
IN	301.5 Kelvin
OUT	293 Kelvin

CONCENTRATION (ppb)	PENTANE	METHYLCYCLOHEXANE	NAPHTHALENE	BENZENE
IN	87.7	217.37	65.1	98.64
OUT	1.92	4.84	66.4	12.15
EXIT	1.7	4.77	59.7	11.83
STRIPPING FACTOR	517.0	16.2	0.2	1.9
NTU	3.8	4.0	0.0	3.1
EXPERIMENTAL ATU (m^2)	2.97E-02	2.84E-02	*********	3.61E-02
EXPERIMENTAL KLa (sec^-1)	5.95E-01	6.20E-01	*********	4.89E-01
EXPERIMENTAL kl (m/sec)	2.88E-04	3.00E-04	*********	2.36E-04

CONCENTRATION (ppb)	TOLUENE	O-XYLENE	M-XYLENE	1,2,4-TRIMETHYL BENZENE
IN	72.88	90.38	759.34	316.54
OUT	9.35	18.17	95.64	58.15
EXIT	9.35	17.61	92.87	55.75
STRIPPING FACTOR	2.2	1.7	2.4	2.3
NTU	2.8	2.4	2.8	2.3
EXPERIMENTAL ATU (m^2)	3.99E-02	4.74E-02	4.04E-02	5.04E-02
EXPERIMENTAL KLa (sec^-1)	4.42E-01	3.72E-01	4.37E-01	3.50E-01
EXPERIMENTAL kl (m/sec)	2.14E-04	1.80E-04	2.11E-04	1.69E-04

Note: Experimental kl calculated using a=2067m^2/m^3

Mass Transfer Test Data for the 45.92-cm-diam. Rotor

WIRE GAUZE PACKING

SAMPLE NAME	Rs218-11
WATER FLOW	35.5 GPM
GAS FLOW	28.1 SCFM
ROTOR SPEED	790 RPM
PRESSURE DROP	1.1 IN. WATER
G/L RATIO (vol)	5.9
WATER TEMPERATURE	
IN	
OUT	292.6 Kelvin
AIR TEMPERATURE	
IN	304.2 Kelvin
OUT	239.9 Kelvin

CONCENTRATION (ppb)	PENTANE	METHYLCYCLOHEXANE	NAPHTHALENE	BENZENE
IN	85.4	218.03	66.0	79.9
OUT	1.21	4.71	68.6	20.76
EXIT	0.89	3.5	59.9	16.25
STRIPPING FACTOR	311.5	9.7	0.1	1.2
NTU	4.3	4.2	ERR	2.8
EXPERIMENTAL ATU (m^2)	2.66E-02	2.71E-02	ERR	4.03E-02
EXPERIMENTAL KLa (sec^-1)	6.63E-01	6.50E-01	ERR	4.38E-01
EXPERIMENTAL kl (m/sec)	3.21E-04	3.15E-04	ERR	2.12E-04

CONCENTRATION (ppb)	TOLUENE	O-XYLENE	M-XYLENE	1,2,4-TRIMETHYL BENZENE
IN	86.77	91.62	761.68	317.48
OUT	15.37	30.16	156.11	93.96
EXIT	11.66	23.96	122.24	74.78
STRIPPING FACTOR	1.4	1.0	1.5	1.4
NTU	3.5	2.4	2.8	2.0
EXPERIMENTAL ATU (m^2)	3.28E-02	4.71E-02	4.03E-02	5.59E-02
EXPERIMENTAL KLa (sec^-1)	5.38E-01	3.74E-01	4.37E-01	3.15E-01
EXPERIMENTAL kl (m/sec)	2.60E-04	1.81E-04	2.12E-04	1.53E-04

Note: Experimental kl calculated using a=2067m^2/m^3

Mass Transfer Test Data for the 45.92-cm-diam. Rotor

WIRE GAUZE PACKING

SAMPLE NAME	Rs218-12
WATER FLOW	44.7 GPM
GAS FLOW	75.9 SCFM
ROTOR SPEED	921 RPM
PRESSURE DROP	1.7 IN. WATER
G/L RATIO (vol)	12.7
WATER TEMPERATURE	
IN	
OUT	292.6 Kelvin
AIR TEMPERATURE	
IN	302.6 Kelvin
OUT	292 Kelvin

CONCENTRATION (ppb)	PENTANE	METHYLCYCLOHEXANE	NAPHTHALENE	BENZENE
IN	78.08	206.39	65.0	98.74
OUT	0	3.55	63.2	9.17
EXIT	0	2.62	52.7	7.24
STRIPPING FACTOR	668.3	20.9	0.2	2.5
NTU	ERR	4.2	0.1	3.3
EXPERIMENTAL ATU (m^2)	ERR	2.68E-02	8.25E-01	3.41E-02
EXPERIMENTAL KLa (sec^-1)	ERR	8.27E-01	2.69E-02	6.51E-01
EXPERIMENTAL kl (m/sec)	ERR	4.00E-04	1.30E-05	3.15E-04

CONCENTRATION (ppb)	TOLUENE	O-XYLENE	M-XYLENE	1,2,4-TRIMETHYL BENZENE
IN	73.47	86.35	762.24	319.88
OUT	7.39	14.18	74.09	44.29
EXIT	5.92	11.05	59.46	35.95
STRIPPING FACTOR	2.9	2.2	3.1	3.0
NTU	3.0	2.6	3.0	2.5
EXPERIMENTAL ATU (m^2)	3.75E-02	4.44E-02	3.78E-02	4.49E-02
EXPERIMENTAL KLa (sec^-1)	5.92E-01	5.01E-01	5.88E-01	4.94E-01
EXPERIMENTAL kl (m/sec)	2.87E-04	2.42E-04	2.84E-04	2.39E-04

Note: Experimental kl calculated using a=2067m^2/m^3

Mass Transfer Test Data for the 45.92-cm-diam. Rotor

WIRE GAUZE PACKING	
SAMPLE NAME	Rs218-13
WATER FLOW	35.2 GPM
GAS FLOW	46.5 SCFM
ROTOR SPEED	790 RPM
PRESSURE DROP	1.2 IN. WATER
G/L RATIO (vol)	9.9
WATER TEMPERATURE	
IN	
OUT	292.7 Kelvin
AIR TEMPERATURE	
IN	301.5 Kelvin
OUT	292.5 Kelvin

CONCENTRATION (ppb)	PENTANE	METHYLCYCLOHEXANE	NAPHTHALENE	BENZENE
IN	80.43	208.26	63.9	97.69
OUT	1.06	4.19	58.5	11.1
EXIT	0.85	3.24	52.8	8.5
STRIPPING FACTOR	519.8	16.2	0.2	2.0
NTU	4.3	4.1	0.9	3.4
EXPERIMENTAL ATU (m^2)	2.62E-02	2.76E-02	1.23E-01	3.32E-02
EXPERIMENTAL KLa (sec^-1)	6.68E-01	6.33E-01	1.42E-01	5.26E-01
EXPERIMENTAL kl (m/sec)	3.23E-04	3.06E-04	6.88E-05	2.54E-04

CONCENTRATION (ppb)	TOLUENE	O-XYLENE	M-XYLENE	1,2,4-TRIMETHYL BENZENE
IN	71.58	90.59	755.62	316.8
OUT	8.27	16.51	85.28	51.45
EXIT	6.7	13.21	67.98	41.43
STRIPPING FACTOR	2.3	1.8	2.5	2.4
NTU	3.1	2.7	3.0	2.5
EXPERIMENTAL ATU (m^2)	3.66E-02	4.22E-02	3.73E-02	4.54E-02
EXPERIMENTAL KLa (sec^-1)	4.78E-01	4.15E-01	4.69E-01	3.85E-01
EXPERIMENTAL kl (m/sec)	2.31E-04	2.01E-04	2.27E-04	1.86E-04

Note: Experimental kl calculated using a=2067m^2/m^3

Mass Transfer Test Data for the 45.92-cm-diam. Rotor

WIRE GAUZE PACKING

SAMPLE NAME	Rs218-14
WATER FLOW	44.8 GPM
GAS FLOW	43.7 SCFM
ROTOR SPEED	633 RPM
PRESSURE DROP	0.8 IN. WATER
G/L RATIO (vol)	7.3
WATER TEMPERATURE	
IN	
OUT	291.9 Kelvin
AIR TEMPERATURE	
IN	299.6 Kelvin
OUT	291.1 Kelvin

CONCENTRATION (ppb)	PENTANE	METHYLCYCLOHEXANE	NAPHTHALENE	BENZENE
IN	75.95	193.23	62.9	93.25
OUT	2.51	9.06	61.5	20.96
EXIT	1.71	6.48	58.5	16.97
STRIPPING FACTOR	384.8	12.0	0.1	1.4
NTU	3.4	3.3	0.0	2.6
EXPERIMENTAL ATU (m^2)	3.32E-02	3.47E-02	2.70E+00	4.29E-02
EXPERIMENTAL KLa (sec^-1)	6.70E-01	6.42E-01	8.23E-03	5.18E-01
EXPERIMENTAL kl (m/sec)	3.24E-04	3.10E-04	3.98E-06	2.51E-04

CONCENTRATION (ppb)	TOLUENE	O-XYLENE	M-XYLENE	1,2,4-TRIMETHYL BENZENE
IN	80.08	92.92	731.64	310.94
OUT	15.32	30.44	165.22	92.59
EXIT	12.65	25.1	135.52	77.72
STRIPPING FACTOR	1.6	1.3	1.8	1.7
NTU	2.7	1.9	2.3	1.8
EXPERIMENTAL ATU (m^2)	4.23E-02	5.84E-02	5.04E-02	6.42E-02
EXPERIMENTAL KLa (sec^-1)	5.26E-01	3.81E-01	4.42E-01	3.47E-01
EXPERIMENTAL kl (m/sec)	2.55E-04	1.84E-04	2.14E-04	1.68E-04

Note: Experimental kl calculated using a=2067m^2/m^3

Mass Transfer Test Data for the 45.92-cm-diam. Rotor

WIRE GAUZE PACKING

SAMPLE NAME	Rs218-15
WATER FLOW	44.5 GPM
GAS FLOW	45 SCFM
ROTOR SPEED	921 RPM
PRESSURE DROP	1.6 IN. WATER
G/L RATIO (vol)	7.6
WATER TEMPERATURE	
IN	
OUT	291.7 Kelvin
AIR TEMPERATURE	
IN	301.6 Kelvin
OUT	292.1 Kelvin

CONCENTRATION (ppb)	PENTANE	METHYLCYCLOHEXANE	NAPHTHALENE	BENZENE
IN	89.79	589.35	96.7	99.41
OUT	5.11	117	88.0	20.75
EXIT	0	0	0.0	0
STRIPPING FACTOR	399.2	12.5	0.1	1.5
NTU	2.9	1.8	0.0	5.0
EXPERIMENTAL ATU (m^2)	3.95E-02	6.46E-02	*********	2.26E-02
EXPERIMENTAL KLa (sec^-1)	5.60E-01	3.42E-01	*********	9.77E-01
EXPERIMENTAL kl (m/sec)	2.71E-04	1.66E-04	*********	4.73E-04

CONCENTRATION (ppb)	TOLUENE	O-XYLENE	M-XYLENE	1,2,4-TRIMETHYL BENZENE
IN	82.67	176.54	1156.83	540.67
OUT	23.35	54.56	261.36	167.89
EXIT	0	0	0	0
STRIPPING FACTOR	1.7	1.3	1.8	1.7
NTU	3.1	5.2	3.3	2.7
EXPERIMENTAL ATU (m^2)	3.65E-02	2.20E-02	3.43E-02	4.16E-02
EXPERIMENTAL KLa (sec^-1)	6.05E-01	1.01E+00	6.45E-01	5.32E-01
EXPERIMENTAL kl (m/sec)	2.93E-04	4.86E-04	3.12E-04	2.57E-04

Note: Experimental kl calculated using a=2067m^2/m^3

Mass Transfer Test Data for the 45.92-cm-diam. Rotor

WIRE GAUZE PACKING

SAMPLE NAME	Rs218-16
WATER FLOW	35 GPM
GAS FLOW	46.9 SCFM
ROTOR SPEED	790 RPM
PRESSURE DROP	1.2 IN. WATER
G/L RATIO (vol)	10.0
WATER TEMPERATURE	
IN	
OUT	292.1 Kelvin
AIR TEMPERATURE	
IN	304.2 Kelvin
OUT	293.1 Kelvin

CONCENTRATION (ppb)	PENTANE	METHYLCYCLOHEXANE	NAPHTHALENE	BENZENE
IN	84.18	324.82	79.3	97.43
OUT	2.2	25.25	72.3	12.56
EXIT	1.85	23.46	68.8	10.3
STRIPPING FACTOR	528.3	16.5	0.2	2.0
NTU	3.6	2.7	0.2	3.1
EXPERIMENTAL ATU (m^2)	3.11E-02	4.26E-02	5.48E-01	3.61E-02
EXPERIMENTAL KLa (sec^-1)	5.59E-01	4.08E-01	3.17E-02	4.81E-01
EXPERIMENTAL kl (m/sec)	2.70E-04	1.97E-04	1.53E-05	2.33E-04

CONCENTRATION (ppb)	TOLUENE	O-XYLENE	M-XYLENE	1,2,4-TRIMETHYL BENZENE
IN	72.84	116.18	910.07	412.27
OUT	10.07	24	122.33	75.92
EXIT	8.81	20.21	103.37	64.5
STRIPPING FACTOR	2.3	1.7	2.4	2.4
NTU	2.8	2.4	2.7	2.3
EXPERIMENTAL ATU (m^2)	4.10E-02	4.69E-02	4.13E-02	4.97E-02
EXPERIMENTAL KLa (sec^-1)	4.24E-01	3.71E-01	4.21E-01	3.50E-01
EXPERIMENTAL kl (m/sec)	2.05E-04	1.79E-04	2.04E-04	1.69E-04

Note: Experimental kl calculated using a=2067m^2/m^3

Mass Transfer Test Data for the 45.92-cm-diam. Rotor

WIRE GAUZE PACKING

SAMPLE NAME	Rs218-17
WATER FLOW	35 GPM
GAS FLOW	46.5 SCFM
ROTOR SPEED	1000 RPM
PRESSURE DROP	1.7 IN. WATER
G/L RATIO (vol)	9.9
WATER TEMPERATURE	
IN	
OUT	292.1 Kelvin
AIR TEMPERATURE	
IN	301.8 Kelvin
OUT	293.2 Kelvin

CONCENTRATION (ppb)	PENTANE	METHYLCYCLOHEXANE	NAPHTHALENE	BENZENE
IN	85.18	292.68	73.1	96.74
OUT	0	9.26	66.5	8.52
EXIT	0	8.12	60.8	6.94
STRIPPING FACTOR	523.8	16.4	0.2	1.9
NTU	ERR	3.6	0.5	3.9
EXPERIMENTAL ATU (m^2)	ERR	3.13E-02	2.25E-01	2.92E-02
EXPERIMENTAL KLa (sec^-1)	ERR	5.55E-01	7.74E-02	5.95E-01
EXPERIMENTAL kl (m/sec)	ERR	2.68E-04	3.74E-05	2.88E-04

CONCENTRATION (ppb)	TOLUENE	O-XYLENE	M-XYLENE	1,2,4-TRIMETHYL BENZENE
IN	73.02	110.24	890.95	400.05
OUT	6.79	17.1	79.93	54.24
EXIT	5.64	13.95	66.99	45.65
STRIPPING FACTOR	2.2	1.7	2.4	2.3
NTU	3.5	3.0	3.4	2.8
EXPERIMENTAL ATU (m^2)	3.27E-02	3.75E-02	3.33E-02	4.08E-02
EXPERIMENTAL KLa (sec^-1)	5.32E-01	4.63E-01	5.22E-01	4.26E-01
EXPERIMENTAL kl (m/sec)	2.57E-04	2.24E-04	2.53E-04	2.06E-04

Note: Experimental kl calculated using a=2067m^2/m^3

Mass Transfer Test Data for the 45.92-cm-diam. Rotor

WIRE GAUZE PACKING

SAMPLE NAME	Rs218-18
WATER FLOW	35 GPM
GAS FLOW	69.8 SCFM
ROTOR SPEED	790 RPM
PRESSURE DROP	1.3 IN. WATER
G/L RATIO (vol)	14.9
WATER TEMPERATURE	
IN	
OUT	291.9 Kelvin
AIR TEMPERATURE	
IN	302.3 Kelvin
OUT	293.4 Kelvin

CONCENTRATION (ppb)	PENTANE	METHYLCYCLOHEXANE	NAPHTHALENE	BENZENE
IN	87.59	293.77	72.4	98.14
OUT	1.58	13.14	64.5	7.65
EXIT	1.28	11.95	59.7	6.56
STRIPPING FACTOR	786.8	24.6	0.3	2.9
NTU	4.0	3.2	0.2	3.4
EXPERIMENTAL ATU (m^2)	2.82E-02	3.55E-02	4.91E-01	3.35E-02
EXPERIMENTAL KLa (sec^-1)	6.16E-01	4.90E-01	3.54E-02	5.18E-01
EXPERIMENTAL kl (m/sec)	2.98E-04	2.37E-04	1.71E-05	2.51E-04

CONCENTRATION (ppb)	TOLUENE	O-XYLENE	M-XYLENE	1,2,4-TRIMETHYL BENZENE
IN	73.99	109.36	895.93	401.23
OUT	6.41	14.33	75.04	46.26
EXIT	5.64	12.38	66.75	41.7
STRIPPING FACTOR	3.3	2.6	3.6	3.5
NTU	3.1	2.7	3.1	2.7
EXPERIMENTAL ATU (m^2)	3.68E-02	4.17E-02	3.70E-02	4.28E-02
EXPERIMENTAL KLa (sec^-1)	4.72E-01	4.17E-01	4.69E-01	4.07E-01
EXPERIMENTAL kl (m/sec)	2.28E-04	2.02E-04	2.27E-04	1.97E-04

Note: Experimental kl calculated using a=2067m^2/m^3

Mass Transfer Test Data for the 45.92-cm-diam. Rotor

WIRE GAUZE PACKING

SAMPLE NAME	Rs218-19
WATER FLOW	35.7 GPM
GAS FLOW	48.3 SCFM
ROTOR SPEED	790 RPM
PRESSURE DROP	1.2 IN. WATER
G/L RATIO (vol)	10.1
WATER TEMPERATURE	
IN	
OUT	291 Kelvin
AIR TEMPERATURE	
IN	291 Kelvin
OUT	285.9 Kelvin

CONCENTRATION (ppb)	PENTANE	METHYLCYCLOHEXANE	NAPHTHALENE	BENZENE
IN	89.07	248.81	68.8	89.89
OUT	1.42	6.13	72.4	11.56
EXIT	1.11	4.83	59.7	9.21
STRIPPING FACTOR	535.4	16.7	0.2	1.9
NTU	4.1	3.9	-0.5	3.2
EXPERIMENTAL ATU (m^2)	2.74E-02	2.92E-02	*********	3.53E-02
EXPERIMENTAL KLa (sec^-1)	6.48E-01	6.08E-01	*********	5.03E-01
EXPERIMENTAL kl (m/sec)	3.13E-04	2.94E-04	*********	2.43E-04

CONCENTRATION (ppb)	TOLUENE	O-XYLENE	M-XYLENE	1,2,4-TRIMETHYL BENZENE
IN	65.67	97.41	814.53	377.06
OUT	8.55	20.7	108.35	71.4
EXIT	6.85	16.51	89.07	59.37
STRIPPING FACTOR	2.2	1.7	2.4	2.3
NTU	2.9	2.4	2.8	2.3
EXPERIMENTAL ATU (m^2)	3.85E-02	4.63E-02	4.04E-02	4.98E-02
EXPERIMENTAL KLa (sec^-1)	4.61E-01	3.83E-01	4.39E-01	3.56E-01
EXPERIMENTAL kl (m/sec)	2.23E-04	1.85E-04	2.12E-04	1.72E-04

Note: Experimental kl calculated using a=2067m^2/m^3

Mass Transfer Test Data for the 45.92-cm-diam. Rotor

WIRE GAUZE PACKING

SAMPLE NAME	Rs218-20
WATER FLOW	27.1 GPM
GAS FLOW	44.4 SCFM
ROTOR SPEED	921 RPM
PRESSURE DROP	1.5 IN. WATER
G/L RATIO (vol)	12.3
WATER TEMPERATURE	
IN	
OUT	291.1 Kelvin
AIR TEMPERATURE	
IN	291.9 Kelvin
OUT	286.2 Kelvin

CONCENTRATION (ppb)	PENTANE	METHYLCYCLOHEXANE	NAPHTHALENE	BENZENE
IN	89.3	169.9	70.0	89.38
OUT	0	4.24	66.6	5.42
EXIT	0	3.79	58.3	4.27
STRIPPING FACTOR	648.2	20.3	0.2	2.3
NTU	ERR	3.8	0.2	4.2
EXPERIMENTAL ATU (m^2)	ERR	2.96E-02	7.28E-01	2.72E-02
EXPERIMENTAL KLa (sec^-1)	ERR	4.55E-01	1.85E-02	4.95E-01
EXPERIMENTAL kl (m/sec)	ERR	2.20E-04	8.95E-06	2.40E-04

CONCENTRATION (ppb)	TOLUENE	O-XYLENE	M-XYLENE	1,2,4-TRIMETHYL BENZENE
IN	81.58	98.04	831.73	389.96
OUT	4.69	11.71	54.21	40.5
EXIT	3.91	9.3	44.02	32.9
STRIPPING FACTOR	2.7	2.1	2.9	2.8
NTU	4.0	3.2	3.7	3.0
EXPERIMENTAL ATU (m^2)	2.87E-02	3.53E-02	3.09E-02	3.75E-02
EXPERIMENTAL KLa (sec^-1)	4.70E-01	3.81E-01	4.36E-01	3.59E-01
EXPERIMENTAL kl (m/sec)	2.27E-04	1.84E-04	2.11E-04	1.74E-04

Note: Experimental kl calculated using a=2067m^2/m^3

Mass Transfer Test Data for the 45.92-cm-diam. Rotor

WIRE GAUZE PACKING

SAMPLE NAME	Rs218-21
WATER FLOW	26.6 GPM
GAS FLOW	44.7 SCFM
ROTOR SPEED	633 RPM
PRESSURE DROP	0.8 IN. WATER
G/L RATIO (vol)	12.6
WATER TEMPERATURE	
IN	
OUT	291.2 Kelvin
AIR TEMPERATURE	
IN	295.4 Kelvin
OUT	288.5 Kelvin

CONCENTRATION (ppb)	PENTANE	METHYLCYCLOHEXANE	NAPHTHALENE	BENZENE
IN	77.86	245.36	69.3	85.05
OUT	1.61	10.15	68.7	9.38
EXIT	1.24	8.43	60.8	7.2
STRIPPING FACTOR	664.6	20.8	0.2	2.4
NTU	3.9	3.3	0.0	3.1
EXPERIMENTAL ATU (m^2)	2.92E-02	3.43E-02	6.10E+00	3.61E-02
EXPERIMENTAL KLa (sec^-1)	4.52E-01	3.85E-01	2.17E-03	3.66E-01
EXPERIMENTAL kl (m/sec)	2.19E-04	1.86E-04	1.05E-06	1.77E-04

CONCENTRATION (ppb)	TOLUENE	O-XYLENE	M-XYLENE	1,2,4-TRIMETHYL BENZENE
IN	78.25	96.9	792.44	377.99
OUT	7.37	17.45	95.34	61.57
EXIT	5.95	13.69	76.53	50.18
STRIPPING FACTOR	2.8	2.1	3.0	2.9
NTU	3.2	2.5	2.8	2.3
EXPERIMENTAL ATU (m^2)	3.57E-02	4.60E-02	4.12E-02	4.85E-02
EXPERIMENTAL KLa (sec^-1)	3.70E-01	2.87E-01	3.20E-01	2.72E-01
EXPERIMENTAL kl (m/sec)	1.79E-04	1.39E-04	1.55E-04	1.32E-04

Note: Experimental kl calculated using a=2067m^2/m^3

Mass Transfer Test Data for the 45.92-cm-diam. Rotor

WIRE GAUZE PACKING

SAMPLE NAME	Rs218-22
WATER FLOW	35.5 GPM
GAS FLOW	46.7 SCFM
ROTOR SPEED	790 RPM
PRESSURE DROP	1.2 IN. WATER
G/L RATIO (vol)	9.8
WATER TEMPERATURE	
IN	
OUT	291.7 Kelvin
AIR TEMPERATURE	
IN	299.5 Kelvin
OUT	290.4 Kelvin

CONCENTRATION (ppb)	PENTANE	METHYLCYCLOHEXANE	NAPHTHALENE	BENZENE
IN	89.16	264.88	67.5	89.64
OUT	1.33	9.53	65.7	10.73
EXIT	1.18	8.53	59.3	8.6
STRIPPING FACTOR	519.4	16.2	0.2	1.9
NTU	4.2	3.5	0.1	3.4
EXPERIMENTAL ATU (m^2)	2.69E-02	3.26E-02	1.55E+00	3.38E-02
EXPERIMENTAL KLa (sec^-1)	6.54E-01	5.41E-01	1.14E-02	5.22E-01
EXPERIMENTAL kl (m/sec)	3.17E-04	2.62E-04	5.52E-06	2.53E-04

CONCENTRATION (ppb)	TOLUENE	O-XYLENE	M-XYLENE	1,2,4-TRIMETHYL BENZENE
IN	69.58	98.96	835.79	390.85
OUT	8.36	20.18	102.66	67.93
EXIT	6.64	16.07	85.27	57.3
STRIPPING FACTOR	2.2	1.7	2.4	2.3
NTU	3.1	2.5	2.9	2.4
EXPERIMENTAL ATU (m^2)	3.66E-02	4.47E-02	3.87E-02	4.71E-02
EXPERIMENTAL KLa (sec^-1)	4.82E-01	3.94E-01	4.56E-01	3.74E-01
EXPERIMENTAL kl (m/sec)	2.33E-04	1.91E-04	2.21E-04	1.81E-04

Note: Experimental kl calculated using a=2067m^2/m^3

Mass Transfer Test Data for the 60.96-cm-diam. Rotor

SUMITOMO PACKING

SAMPLE NAME	RAS-24-1
WATER FLOW	34.9 GPM
GAS FLOW	46.8 SCFM
ROTOR SPEED	790 RPM
PRESSURE DROP	2.5 IN. WATER
G/L RATIO (vol)	10.0
WATER TEMPERATURE	
IN	
OUT	291.4 Kelvin
AIR TEMPERATURE	
IN	299.9 Kelvin
OUT	289.8 Kelvin

CONCENTRATION (ppb)	PENTANE	METHYLCYCLOHEXANE	NAPHTHALENE	BENZENE
IN	0	168.4	72.9	64.91
OUT	0	0	57.4	0.34
EXIT	0	0	62.4	0.34
STRIPPING FACTOR	530.0	16.6	0.2	1.9
NTU	ERR	ERR	0.4	9.5
EXPERIMENTAL ATU (m^2)	ERR	ERR	6.14E-01	2.54E-02
EXPERIMENTAL KLa (sec^-1)	ERR	ERR	2.83E-02	6.82E-01
EXPERIMENTAL kl (m/sec)	ERR	ERR	1.13E-05	2.73E-04

CONCENTRATION (ppb)	TOLUENE	O-XYLENE	M-XYLENE	1,2,4-TRIMETHYL BENZENE
IN	49.58	160.8	632.42	467.02
OUT	0.8	3.5	4.93	8.48
EXIT	0.4	4.26	5.41	9.76
STRIPPING FACTOR	2.2	1.7	2.4	2.3
NTU	6.9	6.9	7.4	6.0
EXPERIMENTAL ATU (m^2)	3.49E-02	3.47E-02	3.27E-02	4.01E-02
EXPERIMENTAL KLa (sec^-1)	4.97E-01	4.99E-01	5.30E-01	4.32E-01
EXPERIMENTAL kl (m/sec)	1.99E-04	2.00E-04	2.12E-04	1.73E-04

Note: Experimental kl calculated using a=2500m^2/m^3

Mass Transfer Test Data for the 60.96-cm-diam. Rotor

SUMITOMO PACKING

SAMPLE NAME	RAS-24-2
WATER FLOW	43.9 GPM
GAS FLOW	77.4 SCFM
ROTOR SPEED	921 RPM
PRESSURE DROP	3.7 IN. WATER
G/L RATIO (vol)	13.2
WATER TEMPERATURE	
IN	
OUT	292 Kelvin
AIR TEMPERATURE	
IN	298.1 Kelvin
OUT	289.7 Kelvin

CONCENTRATION (ppb)	PENTANE	METHYLCYCLOHEXANE	NAPHTHALENE	BENZENE
IN	0	150.48	70.4	51.27
OUT	0	0	60.1	0
EXIT	0	0	52.8	0
STRIPPING FACTOR	695.4	21.7	0.2	2.6
NTU	ERR	ERR	ERR	ERR
EXPERIMENTAL ATU (m^2)	ERR	ERR	ERR	ERR
EXPERIMENTAL KLa (sec^-1)	ERR	ERR	ERR	ERR
EXPERIMENTAL kl (m/sec)	ERR	ERR	ERR	ERR

CONCENTRATION (ppb)	TOLUENE	O-XYLENE	M-XYLENE	1,2,4-TRIMETHYL BENZENE
IN	35.59	151.34	571.31	432.81
OUT	0.31	0.96	2.28	2.64
EXIT	0.31	0.96	2.28	2.64
STRIPPING FACTOR	3.0	2.3	3.2	3.1
NTU	6.5	8.0	7.5	7.0
EXPERIMENTAL ATU (m^2)	3.69E-02	3.02E-02	3.22E-02	3.46E-02
EXPERIMENTAL KLa (sec^-1)	5.91E-01	7.23E-01	6.78E-01	6.30E-01
EXPERIMENTAL kl (m/sec)	2.37E-04	2.89E-04	2.71E-04	2.52E-04

Note: Experimental kl calculated using a=2500m^2/m^3

Mass Transfer Test Data for the 60.96-cm-diam. Rotor

SUMITOMO PACKING

SAMPLE NAME	RAS-24-3
WATER FLOW	20.2 GPM
GAS FLOW	28 SCFM
ROTOR SPEED	790 RPM
PRESSURE DROP	2 IN. WATER
G/L RATIO (vol)	10.4
WATER TEMPERATURE	
IN	
OUT	291.6 Kelvin
AIR TEMPERATURE	
IN	294.3 Kelvin
OUT	288.9 Kelvin

CONCENTRATION (ppb)	PENTANE	METHYLCYCLOHEXANE	NAPHTHALENE	BENZENE
IN	0	134.43	70.8	43.96
OUT	0	0	59.8	0.16
EXIT	0	0	54.2	0
STRIPPING FACTOR	547.4	17.1	0.2	2.0
NTU	ERR	ERR	ERR	11.3
EXPERIMENTAL ATU (m^2)	ERR	ERR	ERR	2.13E-02
EXPERIMENTAL KLa (sec^-1)	ERR	ERR	ERR	4.70E-01
EXPERIMENTAL kl (m/sec)	ERR	ERR	ERR	1.88E-04

CONCENTRATION (ppb)	TOLUENE	O-XYLENE	M-XYLENE	1,2,4-TRIMETHYL BENZENE
IN	33.56	174.28	618.14	442.37
OUT	0.34	3.16	2.94	5.81
EXIT	0.34	2.4	2.94	4.23
STRIPPING FACTOR	2.3	1.8	2.5	2.4
NTU	7.1	7.7	8.1	6.7
EXPERIMENTAL ATU (m^2)	3.39E-02	3.14E-02	2.98E-02	3.58E-02
EXPERIMENTAL KLa (sec^-1)	2.96E-01	3.20E-01	3.37E-01	2.80E-01
EXPERIMENTAL kl (m/sec)	1.19E-04	1.28E-04	1.35E-04	1.12E-04

Note: Experimental kl calculated using a=2500m^2/m^3

Mass Transfer Test Data for the 60.96-cm-diam. Rotor

SUMITOMO PACKING	
SAMPLE NAME	RAS-24-4
WATER FLOW	35.2 GPM
GAS FLOW	47.2 SCFM
ROTOR SPEED	790 RPM
PRESSURE DROP	2.4 IN. WATER
G/L RATIO (vol)	10.0
WATER TEMPERATURE	
IN	
OUT	291.9 Kelvin
AIR TEMPERATURE	
IN	296.5 Kelvin
OUT	289.3 Kelvin

CONCENTRATION (ppb)	PENTANE	METHYLCYCLOHEXANE	NAPHTHALENE	BENZENE
IN	0	162.88	69.9	53.06
OUT	0	0	61.9	0.27
EXIT	0	0	56.8	0.27
STRIPPING FACTOR	529.0	16.5	0.2	1.9
NTU	ERR	ERR	ERR	9.4
EXPERIMENTAL ATU (m^2)	ERR	ERR	ERR	2.56E-02
EXPERIMENTAL KLa (sec^-1)	ERR	ERR	ERR	6.82E-01
EXPERIMENTAL kl (m/sec)	ERR	ERR	ERR	2.73E-04

CONCENTRATION (ppb)	TOLUENE	O-XYLENE	M-XYLENE	1,2,4-TRIMETHYL BENZENE
IN	39.89	185.63	644.88	460.21
OUT	0.38	4.69	4.62	8.82
EXIT	0.38	4.19	4.62	8.82
STRIPPING FACTOR	2.2	1.7	2.4	2.3
NTU	7.3	6.9	7.5	6.0
EXPERIMENTAL ATU (m^2)	3.29E-02	3.49E-02	3.21E-02	4.05E-02
EXPERIMENTAL KLa (sec^-1)	5.32E-01	5.00E-01	5.44E-01	4.32E-01
EXPERIMENTAL kl (m/sec)	2.13E-04	2.00E-04	2.18E-04	1.73E-04

Note: Experimental kl calculated using a=2500m^2/m^3

Mass Transfer Test Data for the 60.96-cm-diam. Rotor

SUMITOMO PACKING
SAMPLE NAME RAS-24-5
WATER FLOW 26.3 GPM
GAS FLOW 27.6 SCFM
ROTOR SPEED 921 RPM
PRESSURE DROP 2.6 IN. WATER
G/L RATIO (vol) 7.8
WATER TEMPERATURE
IN
OUT 291.8 Kelvin
AIR TEMPERATURE
IN 295.1 Kelvin
OUT 289.3 Kelvin

CONCENTRATION (ppb)	PENTANE	METHYLCYCLOHEXANE	NAPHTHALENE	BENZENE
IN	0	168.44	72.4	61.45
OUT	0	0	66.9	0.71
EXIT	0	0	55.3	0.71
STRIPPING FACTOR	414.2	12.9	0.1	1.5
NTU	ERR	ERR	-0.2	10.0
EXPERIMENTAL ATU (m^2)	ERR	ERR	*********	2.41E-02
EXPERIMENTAL KLa (sec^-1)	ERR	ERR	*********	5.43E-01
EXPERIMENTAL kl (m/sec)	ERR	ERR	*********	2.17E-04

CONCENTRATION (ppb)	TOLUENE	O-XYLENE	M-XYLENE	1,2,4-TRIMETHYL BENZENE
IN	45.72	194.66	669.14	470.69
OUT	0.34	14.02	7.75	21.57
EXIT	0.34	11.47	6.64	17.56
STRIPPING FACTOR	1.8	1.3	1.9	1.8
NTU	9.5	6.1	8.1	5.4
EXPERIMENTAL ATU (m^2)	2.55E-02	3.95E-02	2.99E-02	4.46E-02
EXPERIMENTAL KLa (sec^-1)	5.12E-01	3.31E-01	4.37E-01	2.93E-01
EXPERIMENTAL kl (m/sec)	2.05E-04	1.32E-04	1.75E-04	1.17E-04

Note: Experimental kl calculated using a=2500m^2/m^3

Mass Transfer Test Data for the 60.96-cm-diam. Rotor

SUMITOMO PACKING

SAMPLE NAME	RAS-24-6
WATER FLOW	34.7 GPM
GAS FLOW	28.4 SCFM
ROTOR SPEED	790 RPM
PRESSURE DROP	2.2 IN. WATER
G/L RATIO (vol)	6.1
WATER TEMPERATURE	
IN	
OUT	291 Kelvin
AIR TEMPERATURE	
IN	285.9 Kelvin
OUT	281.7 Kelvin

CONCENTRATION (ppb)	PENTANE	METHYLCYCLOHEXANE	NAPHTHALENE	BENZENE
IN	0	165.75	75.8	53.81
OUT	0	0	72.8	2.98
EXIT	0	0	68.4	2.41
STRIPPING FACTOR	323.9	10.1	0.1	1.1
NTU	ERR	ERR	0.2	10.0
EXPERIMENTAL ATU (m^2)	ERR	ERR	1.39E+00	2.42E-02
EXPERIMENTAL KLa (sec^-1)	ERR	ERR	1.24E-02	7.14E-01
EXPERIMENTAL kl (m/sec)	ERR	ERR	4.97E-06	2.85E-04

CONCENTRATION (ppb)	TOLUENE	O-XYLENE	M-XYLENE	1,2,4-TRIMETHYL BENZENE
IN	45.03	237.57	751.08	468.8
OUT	1.7	43	38.36	65.1
EXIT	1.7	35.27	31.38	52.86
STRIPPING FACTOR	1.3	1.0	1.4	1.4
NTU	8.0	5.2	6.6	4.0
EXPERIMENTAL ATU (m^2)	3.02E-02	4.66E-02	3.63E-02	6.08E-02
EXPERIMENTAL KLa (sec^-1)	5.71E-01	3.70E-01	4.75E-01	2.84E-01
EXPERIMENTAL kl (m/sec)	2.28E-04	1.48E-04	1.90E-04	1.13E-04

Note: Experimental kl calculated using a=2500m^2/m^3

Mass Transfer Test Data for the 60.96-cm-diam. Rotor

SUMITOMO PACKING

SAMPLE NAME	RAS-24-7
WATER FLOW	34.8 GPM
GAS FLOW	47.6 SCFM
ROTOR SPEED	790 RPM
PRESSURE DROP	2.5 IN. WATER
G/L RATIO (vol)	10.2
WATER TEMPERATURE	
IN	
OUT	291.5 Kelvin
AIR TEMPERATURE	
IN	287.7 Kelvin
OUT	283 Kelvin

CONCENTRATION (ppb)	PENTANE	METHYLCYCLOHEXANE	NAPHTHALENE	BENZENE
IN	0	172.68	77.6	46.39
OUT	0	0	66.0	0.36
EXIT	0	0	61.3	0.36
STRIPPING FACTOR	540.4	16.9	0.2	2.0
NTU	ERR	ERR	ERR	8.5
EXPERIMENTAL ATU (m^2)	ERR	ERR	ERR	2.84E-02
EXPERIMENTAL KLa (sec^-1)	ERR	ERR	ERR	6.09E-01
EXPERIMENTAL kl (m/sec)	ERR	ERR	ERR	2.44E-04

CONCENTRATION (ppb)	TOLUENE	O-XYLENE	M-XYLENE	1,2,4-TRIMETHYL BENZENE
IN	38.37	249.2	782.24	488.62
OUT	0	8.21	7.02	12.5
EXIT	0.51	7.85	7.02	12.5
STRIPPING FACTOR	2.3	1.7	2.4	2.3
NTU	8.2	6.2	7.1	5.5
EXPERIMENTAL ATU (m^2)	2.95E-02	3.91E-02	3.39E-02	4.42E-02
EXPERIMENTAL KLa (sec^-1)	5.86E-01	4.43E-01	5.09E-01	3.91E-01
EXPERIMENTAL kl (m/sec)	2.34E-04	1.77E-04	2.04E-04	1.56E-04

Note: Experimental kl calculated using a=2500m^2/m^3

Mass Transfer Test Data for the 60.96-cm-diam. Rotor

SUMITOMO PACKING

SAMPLE NAME	RAS-24-8
WATER FLOW	26.1 GPM
GAS FLOW	28 SCFM
ROTOR SPEED	633 RPM
PRESSURE DROP	1.6 IN. WATER
G/L RATIO (vol)	8.0
WATER TEMPERATURE	
IN	
OUT	292 Kelvin
AIR TEMPERATURE	
IN	289.2 Kelvin
OUT	284.2 Kelvin

CONCENTRATION (ppb)	PENTANE	METHYLCYCLOHEXANE	NAPHTHALENE	BENZENE
IN	0	167.16	74.8	54.97
OUT	0	0	72.7	1.39
EXIT	0	0	64.7	1.1
STRIPPING FACTOR	423.1	13.2	0.1	1.6
NTU	ERR	ERR	0.2	7.9
EXPERIMENTAL ATU (m^2)	ERR	ERR	9.85E-01	3.05E-02
EXPERIMENTAL KLa (sec^-1)	ERR	ERR	1.32E-02	4.25E-01
EXPERIMENTAL kl (m/sec)	ERR	ERR	5.27E-06	1.70E-04

CONCENTRATION (ppb)	TOLUENE	O-XYLENE	M-XYLENE	1,2,4-TRIMETHYL BENZENE
IN	42.68	243.24	751.3	474.85
OUT	1.11	22.67	22.66	33.74
EXIT	0.75	18.42	17.91	27.01
STRIPPING FACTOR	1.8	1.4	1.9	1.9
NTU	6.9	5.1	6.0	4.4
EXPERIMENTAL ATU (m^2)	3.51E-02	4.74E-02	4.02E-02	5.48E-02
EXPERIMENTAL KLa (sec^-1)	3.69E-01	2.74E-01	3.23E-01	2.37E-01
EXPERIMENTAL kl (m/sec)	1.48E-04	1.09E-04	1.29E-04	9.47E-05

Note: Experimental kl calculated using a=2500m^2/m^3

Mass Transfer Test Data for the 60.96-cm-diam. Rotor

SUMITOMO PACKING

SAMPLE NAME	RAS-24-9
WATER FLOW	43.7 GPM
GAS FLOW	78 SCFM
ROTOR SPEED	633 RPM
PRESSURE DROP	3.1 IN. WATER
G/L RATIO (vol)	13.4
WATER TEMPERATURE	
IN	
OUT	292.1 Kelvin
AIR TEMPERATURE	
IN	293.5 Kelvin
OUT	287.1 Kelvin

CONCENTRATION (ppb)	PENTANE	METHYLCYCLOHEXANE	NAPHTHALENE	BENZENE
IN	0	169.03	71.0	53.12
OUT	0	0.32	55.3	0.68
EXIT	0	0.32	51.7	0.68
STRIPPING FACTOR	703.7	22.0	0.2	2.6
NTU	ERR	6.5	ERR	6.3
EXPERIMENTAL ATU (m^2)	ERR	3.70E-02	ERR	3.83E-02
EXPERIMENTAL KLa (sec^-1)	ERR	5.87E-01	ERR	5.67E-01
EXPERIMENTAL kl (m/sec)	ERR	2.35E-04	ERR	2.27E-04

CONCENTRATION (ppb)	TOLUENE	O-XYLENE	M-XYLENE	1,2,4-TRIMETHYL BENZENE
IN	43.4	246.14	746.95	474.26
OUT	0.45	10.13	13.68	17
EXIT	0.45	9.35	12.6	15.79
STRIPPING FACTOR	3.0	2.3	3.2	3.1
NTU	6.2	4.7	5.3	4.4
EXPERIMENTAL ATU (m^2)	3.86E-02	5.10E-02	4.56E-02	5.51E-02
EXPERIMENTAL KLa (sec^-1)	5.62E-01	4.26E-01	4.76E-01	3.94E-01
EXPERIMENTAL kl (m/sec)	2.25E-04	1.70E-04	1.91E-04	1.58E-04

Note: Experimental kl calculated using a=2500m^2/m^3

Mass Transfer Test Data for the 60.96-cm-diam. Rotor

SUMITOMO PACKING

SAMPLE NAME	RAS-24-10
WATER FLOW	34.6 GPM
GAS FLOW	47.5 SCFM
ROTOR SPEED	790 RPM
PRESSURE DROP	2.6 IN. WATER
G/L RATIO (vol)	10.3
WATER TEMPERATURE	
IN	
OUT	292 Kelvin
AIR TEMPERATURE	
IN	292.8 Kelvin
OUT	285.6 Kelvin

CONCENTRATION (ppb)	PENTANE	METHYLCYCLOHEXANE	NAPHTHALENE	BENZENE
IN	0	166.63	71.4	53.27
OUT	0	0	65.4	0.36
EXIT	0	0	60.2	0.36
STRIPPING FACTOR	541.4	16.9	0.2	2.0
NTU	ERR	ERR	0.3	8.6
EXPERIMENTAL ATU (m^2)	ERR	ERR	8.21E-01	2.79E-02
EXPERIMENTAL KLa (sec^-1)	ERR	ERR	2.09E-02	6.16E-01
EXPERIMENTAL kl (m/sec)	ERR	ERR	8.37E-06	2.46E-04

CONCENTRATION (ppb)	TOLUENE	O-XYLENE	M-XYLENE	1,2,4-TRIMETHYL BENZENE
IN	43.44	243.28	749.84	474.36
OUT	0.39	7.96	7.01	11.47
EXIT	0.39	6.48	5.83	9.43
STRIPPING FACTOR	2.3	1.8	2.5	2.4
NTU	7.3	6.3	7.1	5.6
EXPERIMENTAL ATU (m^2)	3.29E-02	3.85E-02	3.41E-02	4.30E-02
EXPERIMENTAL KLa (sec^-1)	5.22E-01	4.46E-01	5.04E-01	4.00E-01
EXPERIMENTAL kl (m/sec)	2.09E-04	1.79E-04	2.02E-04	1.60E-04

Note: Experimental kl calculated using a=2500m^2/m^3

Mass Transfer Test Data for the 60.96-cm-diam. Rotor

SUMITOMO PACKING

SAMPLE NAME	RAS-24-11
WATER FLOW	34.2 GPM
GAS FLOW	67.8 SCFM
ROTOR SPEED	790 RPM
PRESSURE DROP	3 IN. WATER
G/L RATIO (vol)	14.8
WATER TEMPERATURE	
IN	
OUT	292 Kelvin
AIR TEMPERATURE	
IN	293.1 Kelvin
OUT	287.3 Kelvin

CONCENTRATION (ppb)	PENTANE	METHYLCYCLOHEXANE	NAPHTHALENE	BENZENE
IN	0	164.29	84.6	54.02
OUT	0	0	63.0	0
EXIT	0	0	54.5	0
STRIPPING FACTOR	781.9	24.4	0.3	2.9
NTU	ERR	ERR	ERR	ERR
EXPERIMENTAL ATU (m^2)	ERR	ERR	ERR	ERR
EXPERIMENTAL KLa (sec^-1)	ERR	ERR	ERR	ERR
EXPERIMENTAL kl (m/sec)	ERR	ERR	ERR	ERR

CONCENTRATION (ppb)	TOLUENE	O-XYLENE	M-XYLENE	1,2,4-TRIMETHYL BENZENE
IN	44.37	247.86	757.83	477.15
OUT	0	1.95	2.89	3.32
EXIT	0	1.65	2.89	3.32
STRIPPING FACTOR	3.3	2.6	3.6	3.5
NTU	ERR	7.2	7.3	6.5
EXPERIMENTAL ATU (m^2)	ERR	3.33E-02	3.32E-02	3.71E-02
EXPERIMENTAL KLa (sec^-1)	ERR	5.10E-01	5.12E-01	4.58E-01
EXPERIMENTAL kl (m/sec)	ERR	2.04E-04	2.05E-04	1.83E-04

Note: Experimental kl calculated using a=2500m^2/m^3

Mass Transfer Test Data for the 60.96-cm-diam. Rotor

SUMITOMO PACKING

SAMPLE NAME	RAS-24-12
WATER FLOW	34.9 GPM
GAS FLOW	47 SCFM
ROTOR SPEED	1000 RPM
PRESSURE DROP	3.4 IN. WATER
G/L RATIO (vol)	10.1
WATER TEMPERATURE	
IN	
OUT	291.3 Kelvin
AIR TEMPERATURE	
IN	294.6 Kelvin
OUT	286.5 Kelvin

CONCENTRATION (ppb)	PENTANE	METHYLCYCLOHEXANE	NAPHTHALENE	BENZENE
IN	0	190	93.5	60.9
OUT	0	0	82.6	0.86
EXIT	0	0	73.7	0.49
STRIPPING FACTOR	532.4	16.6	0.2	1.9
NTU	ERR	ERR	ERR	7.9
EXPERIMENTAL ATU (m^2)	ERR	ERR	ERR	3.04E-02
EXPERIMENTAL KLa (sec^-1)	ERR	ERR	ERR	5.71E-01
EXPERIMENTAL kl (m/sec)	ERR	ERR	ERR	2.28E-04

CONCENTRATION (ppb)	TOLUENE	O-XYLENE	M-XYLENE	1,2,4-TRIMETHYL BENZENE
IN	50.19	273.22	880.24	563.66
OUT	0	7.47	5.08	10.63
EXIT	0	5.35	3.85	7.8
STRIPPING FACTOR	2.2	1.7	2.4	2.3
NTU	ERR	7.1	8.1	6.3
EXPERIMENTAL ATU (m^2)	ERR	3.40E-02	2.96E-02	3.85E-02
EXPERIMENTAL KLa (sec^-1)	ERR	5.10E-01	5.85E-01	4.50E-01
EXPERIMENTAL kl (m/sec)	ERR	2.04E-04	2.34E-04	1.80E-04

Note: Experimental kl calculated using a=2500m^2/m^3

Mass Transfer Test Data for the 60.96-cm-diam. Rotor

SUMITOMO PACKING

SAMPLE NAME	RAS-24-13
WATER FLOW	35.1 GPM
GAS FLOW	47.2 SCFM
ROTOR SPEED	790 RPM
PRESSURE DROP	2.5 IN. WATER
G/L RATIO (vol)	10.1
WATER TEMPERATURE	
IN	
OUT	292 Kelvin
AIR TEMPERATURE	
IN	297.3 Kelvin
OUT	288.4 Kelvin

CONCENTRATION (ppb)	PENTANE	METHYLCYCLOHEXANE	NAPHTHALENE	BENZENE
IN	0	194.73	98.3	61.52
OUT	0	0	80.7	0.57
EXIT	0	0	72.1	0.76
STRIPPING FACTOR	530.4	16.6	0.2	2.0
NTU	ERR	ERR	ERR	7.8
EXPERIMENTAL ATU (m^2)	ERR	ERR	ERR	3.08E-02
EXPERIMENTAL KLa (sec^-1)	ERR	ERR	ERR	5.66E-01
EXPERIMENTAL kl (m/sec)	ERR	ERR	ERR	2.26E-04

CONCENTRATION (ppb)	TOLUENE	O-XYLENE	M-XYLENE	1,2,4-TRIMETHYL BENZENE
IN	53.54	273.75	876.8	566.07
OUT	0.25	9.59	8.46	14.65
EXIT	0.24	7.27	6.44	10.9
STRIPPING FACTOR	2.3	1.7	2.4	2.4
NTU	8.6	6.3	7.2	5.6
EXPERIMENTAL ATU (m^2)	2.80E-02	3.82E-02	3.37E-02	4.29E-02
EXPERIMENTAL KLa (sec^-1)	6.22E-01	4.56E-01	5.17E-01	4.06E-01
EXPERIMENTAL kl (m/sec)	2.49E-04	1.82E-04	2.07E-04	1.62E-04

Note: Experimental kl calculated using a=2500m^2/m^3

Mass Transfer Test Data for the 60.96-cm-diam. Rotor

SUMITOMO PACKING

SAMPLE NAME	RAS-24-14
WATER FLOW	49.9 GPM
GAS FLOW	66.6 SCFM
ROTOR SPEED	790 RPM
PRESSURE DROP	3.8 IN. WATER
G/L RATIO (vol)	10.0
WATER TEMPERATURE	
IN	
OUT	291.7 Kelvin
AIR TEMPERATURE	
IN	297.6 Kelvin
OUT	288.6 Kelvin

CONCENTRATION (ppb)	PENTANE	METHYLCYCLOHEXANE	NAPHTHALENE	BENZENE
IN	0	197.04	90.3	64.92
OUT	0	0	84.1	1.07
EXIT	0	0	77.0	0.75
STRIPPING FACTOR	526.9	16.5	0.2	1.9
NTU	ERR	ERR	0.2	7.4
EXPERIMENTAL ATU (m^2)	ERR	ERR	1.05E+00	3.25E-02
EXPERIMENTAL KLa (sec^-1)	ERR	ERR	2.35E-02	7.62E-01
EXPERIMENTAL kl (m/sec)	ERR	ERR	9.42E-06	3.05E-04

CONCENTRATION (ppb)	TOLUENE	O-XYLENE	M-XYLENE	1,2,4-TRIMETHYL BENZENE
IN	60.24	268.02	879.13	582.5
OUT	0.35	10.73	11.36	17.93
EXIT	0.35	8.95	9.69	14.98
STRIPPING FACTOR	2.2	1.7	2.4	2.3
NTU	8.3	6.0	6.7	5.3
EXPERIMENTAL ATU (m^2)	2.91E-02	4.02E-02	3.62E-02	4.55E-02
EXPERIMENTAL KLa (sec^-1)	8.51E-01	6.16E-01	6.85E-01	5.45E-01
EXPERIMENTAL kl (m/sec)	3.40E-04	2.46E-04	2.74E-04	2.18E-04

Note: Experimental kl calculated using a=2500m^2/m^3

Mass Transfer Test Data for the 60.96-cm-diam. Rotor

SUMITOMO PACKING

SAMPLE NAME	RAS-24-15
WATER FLOW	26.2 GPM
GAS FLOW	44.9 SCFM
ROTOR SPEED	633 RPM
PRESSURE DROP	1.9 IN. WATER
G/L RATIO (vol)	12.8
WATER TEMPERATURE	
IN	
OUT	291 Kelvin
AIR TEMPERATURE	
IN	287.5 Kelvin
OUT	284.4 Kelvin

CONCENTRATION (ppb)	PENTANE	METHYLCYCLOHEXANE	NAPHTHALENE	BENZENE
IN	0	198.79	88.5	77.59
OUT	0	0.23	70.4	1.54
EXIT	0	0.23	61.2	1.01
STRIPPING FACTOR	678.2	21.2	0.2	2.4
NTU	ERR	7.0	ERR	6.1
EXPERIMENTAL ATU (m^2)	ERR	3.42E-02	ERR	3.98E-02
EXPERIMENTAL KLa (sec^-1)	ERR	3.80E-01	ERR	3.27E-01
EXPERIMENTAL kl (m/sec)	ERR	1.52E-04	ERR	1.31E-04

CONCENTRATION (ppb)	TOLUENE	O-XYLENE	M-XYLENE	1,2,4-TRIMETHYL BENZENE
IN	67.71	236.74	837.93	578.04
OUT	0.41	7.79	10.28	15.46
EXIT	0.41	4.78	6.65	9.64
STRIPPING FACTOR	2.8	2.1	3.0	2.9
NTU	7.3	5.6	6.2	5.1
EXPERIMENTAL ATU (m^2)	3.32E-02	4.28E-02	3.90E-02	4.71E-02
EXPERIMENTAL KLa (sec^-1)	3.92E-01	3.04E-01	3.34E-01	2.76E-01
EXPERIMENTAL kl (m/sec)	1.57E-04	1.22E-04	1.34E-04	1.10E-04

Note: Experimental kl calculated using a=2500m^2/m^3

Mass Transfer Test Data for the 60.96-cm-diam. Rotor

SUMITOMO PACKING

SAMPLE NAME	RAS-24-16
WATER FLOW	35 GPM
GAS FLOW	47.6 SCFM
ROTOR SPEED	790 RPM
PRESSURE DROP	2.5 IN. WATER
G/L RATIO (vol)	10.2
WATER TEMPERATURE	
IN	
OUT	291.3 Kelvin
AIR TEMPERATURE	
IN	288.6 Kelvin
OUT	285.1 Kelvin

CONCENTRATION (ppb)	PENTANE	METHYLCYCLOHEXANE	NAPHTHALENE	BENZENE
IN	0	201.23	87.9	65.63
OUT	0	0	81.9	2.06
EXIT	0	0	74.7	2.06
STRIPPING FACTOR	537.7	16.8	0.2	1.9
NTU	ERR	ERR	0.2	5.7
EXPERIMENTAL ATU (m^2)	ERR	ERR	1.05E+00	4.20E-02
EXPERIMENTAL KLa (sec^-1)	ERR	ERR	1.66E-02	4.14E-01
EXPERIMENTAL kl (m/sec)	ERR	ERR	6.63E-06	1.65E-04

CONCENTRATION (ppb)	TOLUENE	O-XYLENE	M-XYLENE	1,2,4-TRIMETHYL BENZENE
IN	60.88	240.77	848.61	591.4
OUT	0.36	10.34	9.83	17.83
EXIT	0.36	7.85	7.61	13.56
STRIPPING FACTOR	2.2	1.7	2.4	2.3
NTU	8.2	5.9	6.9	5.4
EXPERIMENTAL ATU (m^2)	2.94E-02	4.08E-02	3.50E-02	4.48E-02
EXPERIMENTAL KLa (sec^-1)	5.92E-01	4.26E-01	4.97E-01	3.89E-01
EXPERIMENTAL kl (m/sec)	2.37E-04	1.71E-04	1.99E-04	1.55E-04

Note: Experimental kl calculated using a=2500m^2/m^3

Mass Transfer Test Data for the 60.96-cm-diam. Rotor

SUMITOMO PACKING

SAMPLE NAME	RAS-24-17
WATER FLOW	44 GPM
GAS FLOW	44.6 SCFM
ROTOR SPEED	921 RPM
PRESSURE DROP	2.9 IN. WATER
G/L RATIO (vol)	7.6
WATER TEMPERATURE	
IN	
OUT	291.4 Kelvin
AIR TEMPERATURE	
IN	288 Kelvin
OUT	285.2 Kelvin

CONCENTRATION (ppb)	PENTANE	METHYLCYCLOHEXANE	NAPHTHALENE	BENZENE
IN	0	203.73	91.4	67.73
OUT	0	0	93.2	2.5
EXIT	0	0	76.2	1.85
STRIPPING FACTOR	400.6	12.5	0.1	1.4
NTU	ERR	ERR	0.1	7.7
EXPERIMENTAL ATU (m^2)	ERR	ERR	3.61E+00	3.12E-02
EXPERIMENTAL KLa (sec^-1)	ERR	ERR	6.06E-03	7.02E-01
EXPERIMENTAL kl (m/sec)	ERR	ERR	2.42E-06	2.81E-04

CONCENTRATION (ppb)	TOLUENE	O-XYLENE	M-XYLENE	1,2,4-TRIMETHYL BENZENE
IN	65.95	238.52	831.81	591.7
OUT	1.25	28.23	22.7	46.02
EXIT	1.25	21.2	16.61	34
STRIPPING FACTOR	1.7	1.3	1.8	1.7
NTU	7.7	5.0	6.7	4.6
EXPERIMENTAL ATU (m^2)	3.15E-02	4.79E-02	3.60E-02	5.28E-02
EXPERIMENTAL KLa (sec^-1)	6.94E-01	4.56E-01	6.07E-01	4.14E-01
EXPERIMENTAL kl (m/sec)	2.78E-04	1.82E-04	2.43E-04	1.66E-04

Note: Experimental kl calculated using a=2500m^2/m^3

Mass Transfer Test Data for the 60.96-cm-diam. Rotor

SUMITOMO PACKING

SAMPLE NAME	RAS-24-18
WATER FLOW	43.6 GPM
GAS FLOW	44.7 SCFM
ROTOR SPEED	633 RPM
PRESSURE DROP	1.7 IN. WATER
G/L RATIO (vol)	7.7
WATER TEMPERATURE	
IN	
OUT	291.4 Kelvin
AIR TEMPERATURE	
IN	288.3 Kelvin
OUT	285 Kelvin

CONCENTRATION (ppb)	PENTANE	METHYLCYCLOHEXANE	NAPHTHALENE	BENZENE
IN	0	196.73	89.2	62.39
OUT	0	0.39	89.5	3.87
EXIT	0	0.39	74.5	3.13
STRIPPING FACTOR	405.2	12.7	0.1	1.5
NTU	ERR	6.7	0.0	5.9
EXPERIMENTAL ATU (m^2)	ERR	3.62E-02	1.59E+01	4.06E-02
EXPERIMENTAL KLa (sec^-1)	ERR	5.99E-01	1.37E-03	5.33E-01
EXPERIMENTAL kl (m/sec)	ERR	2.40E-04	5.46E-07	2.13E-04

CONCENTRATION (ppb)	TOLUENE	O-XYLENE	M-XYLENE	1,2,4-TRIMETHYL BENZENE
IN	49.92	233.31	819.93	584.25
OUT	2.59	34.98	49.81	67.05
EXIT	2.05	27.43	37.06	51.64
STRIPPING FACTOR	1.7	1.3	1.8	1.8
NTU	5.5	4.1	4.9	3.7
EXPERIMENTAL ATU (m^2)	4.38E-02	5.89E-02	4.92E-02	6.59E-02
EXPERIMENTAL KLa (sec^-1)	4.95E-01	3.68E-01	4.40E-01	3.28E-01
EXPERIMENTAL kl (m/sec)	1.98E-04	1.47E-04	1.76E-04	1.31E-04

Note: Experimental kl calculated using a=2500m^2/m^3

Mass Transfer Test Data for the 60.96-cm-diam. Rotor

SUMITOMO PACKING

SAMPLE NAME	RAS-24-19
WATER FLOW	35 GPM
GAS FLOW	47.9 SCFM
ROTOR SPEED	790 RPM
PRESSURE DROP	2.2 IN. WATER
G/L RATIO (vol)	10.2
WATER TEMPERATURE	
IN	
OUT	291.3 Kelvin
AIR TEMPERATURE	
IN	288.2 Kelvin
OUT	285.3 Kelvin

CONCENTRATION (ppb)	PENTANE	METHYLCYCLOHEXANE	NAPHTHALENE	BENZENE
IN	0	199.93	88.7	62.24
OUT	0	0	75.1	1.09
EXIT	0	0	68.1	1.09
STRIPPING FACTOR	541.1	16.9	0.2	1.9
NTU	ERR	ERR	ERR	6.9
EXPERIMENTAL ATU (m^2)	ERR	ERR	ERR	3.50E-02
EXPERIMENTAL KLa (sec^-1)	ERR	ERR	ERR	4.96E-01
EXPERIMENTAL kl (m/sec)	ERR	ERR	ERR	1.99E-04

CONCENTRATION (ppb)	TOLUENE	O-XYLENE	M-XYLENE	1,2,4-TRIMETHYL BENZENE
IN	50.61	231.59	815.77	582.3
OUT	0.31	9.78	9.4	16.4
EXIT	0.31	7.37	6.98	12.1
STRIPPING FACTOR	2.3	1.7	2.4	2.3
NTU	8.1	5.9	6.9	5.5
EXPERIMENTAL ATU (m^2)	2.97E-02	4.07E-02	3.50E-02	4.38E-02
EXPERIMENTAL KLa (sec^-1)	5.85E-01	4.27E-01	4.97E-01	3.97E-01
EXPERIMENTAL kl (m/sec)	2.34E-04	1.71E-04	1.99E-04	1.59E-04

Note: Experimental kl calculated using a=2500m^2/m^3

Mass Transfer Test Data for the 60.96-cm-diam. Rotor

SUMITOMO PACKING
SAMPLE NAME RAS-24-20
WATER FLOW 34.7 GPM
GAS FLOW 46.6 SCFM
ROTOR SPEED 500 RPM
PRESSURE DROP 2.1 IN. WATER
G/L RATIO (vol) 10.0
WATER TEMPERATURE
IN
OUT 291.7 Kelvin
AIR TEMPERATURE
IN 300.5 Kelvin
OUT 289.3 Kelvin

CONCENTRATION (ppb)	PENTANE	METHYLCYCLOHEXANE	NAPHTHALENE	BENZENE
IN	0	178.81	97.6	60.55
OUT	0	2.45	87.6	3.82
EXIT	0	1.65	77.9	3.14
STRIPPING FACTOR	530.2	16.6	0.2	1.9
NTU	ERR	4.5	ERR	4.5
EXPERIMENTAL ATU (m^2)	ERR	5.33E-02	ERR	5.32E-02
EXPERIMENTAL KLa (sec^-1)	ERR	3.23E-01	ERR	3.24E-01
EXPERIMENTAL kl (m/sec)	ERR	1.29E-04	ERR	1.30E-04

CONCENTRATION (ppb)	TOLUENE	O-XYLENE	M-XYLENE	1,2,4-TRIMETHYL BENZENE
IN	44.65	283.17	903.25	547.43
OUT	2.73	41.72	76.97	72.45
EXIT	2.15	34.97	62.88	60.53
STRIPPING FACTOR	2.2	1.7	2.4	2.3
NTU	4.2	3.1	3.5	2.8
EXPERIMENTAL ATU (m^2)	5.70E-02	7.76E-02	6.87E-02	8.52E-02
EXPERIMENTAL KLa (sec^-1)	3.02E-01	2.22E-01	2.51E-01	2.02E-01
EXPERIMENTAL kl (m/sec)	1.21E-04	8.89E-05	1.00E-04	8.10E-05

Note: Experimental kl calculated using a=2500m^2/m^3

Mass Transfer Test Data for the 60.96-cm-diam. Rotor

SUMITOMO PACKING

SAMPLE NAME	RAS-24-21
WATER FLOW	25.8 GPM
GAS FLOW	43.9 SCFM
ROTOR SPEED	921 RPM
PRESSURE DROP	3 IN. WATER
G/L RATIO (vol)	12.7
WATER TEMPERATURE	
IN	
OUT	291.8 Kelvin
AIR TEMPERATURE	
IN	301.6 Kelvin
OUT	289.7 Kelvin

CONCENTRATION (ppb)	PENTANE	METHYLCYCLOHEXANE	NAPHTHALENE	BENZENE
IN	0	194.88	89.9	68.61
OUT	0	0	65.5	0.37
EXIT	0	0	68.9	0.37
STRIPPING FACTOR	671.5	21.0	0.2	2.5
NTU	ERR	ERR	ERR	7.9
EXPERIMENTAL ATU (m^2)	ERR	ERR	ERR	3.04E-02
EXPERIMENTAL KLa (sec^-1)	ERR	ERR	ERR	4.22E-01
EXPERIMENTAL kl (m/sec)	ERR	ERR	ERR	1.69E-04

CONCENTRATION (ppb)	TOLUENE	O-XYLENE	M-XYLENE	1,2,4-TRIMETHYL BENZENE
IN	52.31	303.71	971.52	586.15
OUT	0.34	1.78	2.2	2.69
EXIT	0.34	1.78	2.2	2.69
STRIPPING FACTOR	2.8	2.2	3.1	3.0
NTU	7.1	8.4	8.5	7.5
EXPERIMENTAL ATU (m^2)	3.40E-02	2.89E-02	2.85E-02	3.21E-02
EXPERIMENTAL KLa (sec^-1)	3.77E-01	4.44E-01	4.49E-01	3.99E-01
EXPERIMENTAL kl (m/sec)	1.51E-04	1.78E-04	1.80E-04	1.60E-04

Note: Experimental kl calculated using a=2500m^2/m^3

Mass Transfer Test Data for the 60.96-cm-diam. Rotor

SUMITOMO PACKING

SAMPLE NAME	RAS-24-22
WATER FLOW	34.6 GPM
GAS FLOW	46.8 SCFM
ROTOR SPEED	790 RPM
PRESSURE DROP	2.6 IN. WATER
G/L RATIO (vol)	10.1
WATER TEMPERATURE	
IN	
OUT	292.2 Kelvin
AIR TEMPERATURE	
IN	301.6 Kelvin
OUT	290.8 Kelvin

CONCENTRATION (ppb)	PENTANE	METHYLCYCLOHEXANE	NAPHTHALENE	BENZENE
IN	0	191.4	94.9	61.3
OUT	0	0	84.1	0.82
EXIT	0	0	75.9	1.15
STRIPPING FACTOR	533.1	16.7	0.2	2.0
NTU	ERR	ERR	ERR	7.0
EXPERIMENTAL ATU (m^2)	ERR	ERR	ERR	3.46E-02
EXPERIMENTAL KLa (sec^-1)	ERR	ERR	ERR	4.96E-01
EXPERIMENTAL kl (m/sec)	ERR	ERR	ERR	1.99E-04

CONCENTRATION (ppb)	TOLUENE	O-XYLENE	M-XYLENE	1,2,4-TRIMETHYL BENZENE
IN	50.02	304.29	950.5	580.73
OUT	0.96	9.76	8.51	12.43
EXIT	0.96	8.82	6.37	11.14
STRIPPING FACTOR	2.3	1.8	2.5	2.4
NTU	6.0	6.2	7.2	5.8
EXPERIMENTAL ATU (m^2)	4.00E-02	3.87E-02	3.33E-02	4.17E-02
EXPERIMENTAL KLa (sec^-1)	4.29E-01	4.44E-01	5.16E-01	4.12E-01
EXPERIMENTAL kl (m/sec)	1.72E-04	1.78E-04	2.06E-04	1.65E-04

Note: Experimental kl calculated using a=2500m^2/m^3

Mass Transfer Test Data for the 60.96-cm-diam. Rotor

SUMITOMO PACKING

SAMPLE NAME	RAS-24-24
WATER FLOW	34.9 GPM
GAS FLOW	46.5 SCFM
ROTOR SPEED	790 RPM
PRESSURE DROP	2.5 IN. WATER
G/L RATIO (vol)	10.0
WATER TEMPERATURE	
IN	
OUT	292.2 Kelvin
AIR TEMPERATURE	
IN	298.8 Kelvin
OUT	290 Kelvin

CONCENTRATION (ppb)	PENTANE	METHYLCYCLOHEXANE	NAPHTHALENE	BENZENE
IN	0	184.85	88.9	60.05
OUT	0	0	78.1	1.1
EXIT	0	0	70.5	1.1
STRIPPING FACTOR	525.1	16.4	0.2	1.9
NTU	ERR	ERR	ERR	6.8
EXPERIMENTAL ATU (m^2)	ERR	ERR	ERR	3.56E-02
EXPERIMENTAL KLa (sec^-1)	ERR	ERR	ERR	4.87E-01
EXPERIMENTAL kl (m/sec)	ERR	ERR	ERR	1.95E-04

CONCENTRATION (ppb)	TOLUENE	O-XYLENE	M-XYLENE	1,2,4-TRIMETHYL BENZENE
IN	45.28	293.84	929.13	569.47
OUT	0.25	11.64	9.53	14.14
EXIT	0.25	9.01	7.52	10.77
STRIPPING FACTOR	2.3	1.7	2.4	2.4
NTU	8.3	6.0	7.0	5.7
EXPERIMENTAL ATU (m^2)	2.91E-02	4.01E-02	3.43E-02	4.25E-02
EXPERIMENTAL KLa (sec^-1)	5.96E-01	4.33E-01	5.06E-01	4.08E-01
EXPERIMENTAL kl (m/sec)	2.38E-04	1.73E-04	2.02E-04	1.63E-04

Note: Experimental kl calculated using a=2500m^2/m^3

Mass Transfer Test Data for the 76.20-cm-diam. Rotor

SUMITOMO PACKING

SAMPLE NAME	RAS-30-16
WATER FLOW	35 GPM
GAS FLOW	47.9 SCFM
ROTOR SPEED	790 RPM
PRESSURE DROP	3.2 IN. WATER
G/L RATIO (vol)	10.2
WATER TEMPERATURE	
IN	
OUT	293.9 Kelvin
AIR TEMPERATURE	
IN	302 Kelvin
OUT	293.9 Kelvin

CONCENTRATION (ppb)	PENTANE	METHYLCYCLOHEXANE	NAPHTHALENE	BENZENE
IN	58.01	366.15	83.2	78.31
OUT	0	0.68	48.1	0
EXIT	0	0.68	42.9	0
STRIPPING FACTOR	536.3	16.8	0.2	2.1
NTU	ERR	6.6	ERR	ERR
EXPERIMENTAL ATU (m^2)	ERR	6.12E-02	ERR	ERR
EXPERIMENTAL KLa (sec^-1)	ERR	2.84E-01	ERR	ERR
EXPERIMENTAL kl (m/sec)	ERR	1.14E-04	ERR	ERR

CONCENTRATION (ppb)	TOLUENE	O-XYLENE	M-XYLENE	1,2,4-TRIMETHYL BENZENE
IN	101.19	273.25	744.22	394.29
OUT	0	0.96	2.07	1.59
EXIT	0	0.96	2.07	1.59
STRIPPING FACTOR	2.4	1.9	2.7	2.6
NTU	ERR	10.4	8.7	8.2
EXPERIMENTAL ATU (m^2)	ERR	3.89E-02	4.67E-02	4.94E-02
EXPERIMENTAL KLa (sec^-1)	ERR	4.47E-01	3.72E-01	3.52E-01
EXPERIMENTAL kl (m/sec)	ERR	1.79E-04	1.49E-04	1.41E-04

Note: Experimental kl calculated using a=2500m^2/m^3

Mass Transfer Test Data for the 76.20-cm-diam. Rotor

SUMITOMO PACKING

SAMPLE NAME	RAS-30-17
WATER FLOW	43.5 GPM
GAS FLOW	77.8 SCFM
ROTOR SPEED	633 RPM
PRESSURE DROP	2.8 IN. WATER
G/L RATIO (vol)	13.4
WATER TEMPERATURE	
IN	
OUT	295.4 Kelvin
AIR TEMPERATURE	
IN	308.7 Kelvin
OUT	295.9 Kelvin

CONCENTRATION (ppb)	PENTANE	METHYLCYCLOHEXANE	NAPHTHALENE	BENZENE
IN	32.68	323.44	86.6	54.73
OUT	0	0.61	44.5	0.23
EXIT	0	0.61	38.9	0.23
STRIPPING FACTOR	697.3	21.8	0.2	2.9
NTU	ERR	6.5	ERR	7.7
EXPERIMENTAL ATU (m^2)	ERR	6.21E-02	ERR	5.27E-02
EXPERIMENTAL KLa (sec^-1)	ERR	3.48E-01	ERR	4.10E-01
EXPERIMENTAL kl (m/sec)	ERR	1.39E-04	ERR	1.64E-04

CONCENTRATION (ppb)	TOLUENE	O-XYLENE	M-XYLENE	1,2,4-TRIMETHYL BENZENE
IN	74.88	237.22	650.54	353.39
OUT	0.7	1.46	2.55	2.11
EXIT	0.7	1.17	2.55	2.11
STRIPPING FACTOR	3.4	2.6	3.7	3.6
NTU	6.2	7.6	7.2	6.7
EXPERIMENTAL ATU (m^2)	6.58E-02	5.32E-02	5.64E-02	6.09E-02
EXPERIMENTAL KLa (sec^-1)	3.28E-01	4.06E-01	3.83E-01	3.55E-01
EXPERIMENTAL kl (m/sec)	1.31E-04	1.63E-04	1.53E-04	1.42E-04

Note: Experimental kl calculated using a=2500m^2/m^3

Mass Transfer Test Data for the 76.20-cm-diam. Rotor

SUMITOMO PACKING

SAMPLE NAME	RAS-30-18
WATER FLOW	19.6 GPM
GAS FLOW	28.5 SCFM
ROTOR SPEED	790 RPM
PRESSURE DROP	3 IN. WATER
G/L RATIO (vol)	10.9
WATER TEMPERATURE	
IN	
OUT	292 Kelvin
AIR TEMPERATURE	
IN	296.8 Kelvin
OUT	291.1 Kelvin

CONCENTRATION (ppb)	PENTANE	METHYLCYCLOHEXANE	NAPHTHALENE	BENZENE
IN	41.79	330.87	82.4	51.07
OUT	0	0.38	35.4	0
EXIT	0	0.38	35.4	0
STRIPPING FACTOR	573.5	17.9	0.2	2.1
NTU	ERR	7.1	ERR	ERR
EXPERIMENTAL ATU (m^2)	ERR	5.70E-02	ERR	ERR
EXPERIMENTAL KLa (sec^-1)	ERR	1.71E-01	ERR	ERR
EXPERIMENTAL kl (m/sec)	ERR	6.83E-05	ERR	ERR

CONCENTRATION (ppb)	TOLUENE	O-XYLENE	M-XYLENE	1,2,4-TRIMETHYL BENZENE
IN	87.28	292.58	742.84	382.63
OUT	0	0.47	1.71	1.17
EXIT	0	0.47	1.71	1.17
STRIPPING FACTOR	2.4	1.9	2.6	2.5
NTU	ERR	12.1	9.0	8.7
EXPERIMENTAL ATU (m^2)	ERR	3.34E-02	4.50E-02	4.65E-02
EXPERIMENTAL KLa (sec^-1)	ERR	2.91E-01	2.17E-01	2.09E-01
EXPERIMENTAL kl (m/sec)	ERR	1.16E-04	8.66E-05	8.38E-05

Note: Experimental kl calculated using a=2500m^2/m^3

Mass Transfer Test Data for the 76.20-cm-diam. Rotor

SUMITOMO PACKING

SAMPLE NAME	RAS-30-19
WATER FLOW	35 GPM
GAS FLOW	45.7 SCFM
ROTOR SPEED	790 RPM
PRESSURE DROP	3.2 IN. WATER
G/L RATIO (vol)	9.8
WATER TEMPERATURE	
IN	
OUT	293.4 Kelvin
AIR TEMPERATURE	
IN	305 Kelvin
OUT	293.8 Kelvin

CONCENTRATION (ppb)	PENTANE	METHYLCYCLOHEXANE	NAPHTHALENE	BENZENE
IN	41.13	319.36	90.7	63.23
OUT	0	0.6	47.5	0
EXIT	0	0.6	47.5	0
STRIPPING FACTOR	512.5	16.0	0.2	2.0
NTU	ERR	6.6	ERR	ERR
EXPERIMENTAL ATU (m^2)	ERR	6.12E-02	ERR	ERR
EXPERIMENTAL KLa (sec^-1)	ERR	2.84E-01	ERR	ERR
EXPERIMENTAL kl (m/sec)	ERR	1.14E-04	ERR	ERR

CONCENTRATION (ppb)	TOLUENE	O-XYLENE	M-XYLENE	1,2,4-TRIMETHYL BENZENE
IN	80.57	332.55	843.3	430.52
OUT	0	1.11	1.89	1.26
EXIT	0	1.11	1.89	1.26
STRIPPING FACTOR	2.3	1.8	2.5	2.4
NTU	ERR	11.2	9.3	9.1
EXPERIMENTAL ATU (m^2)	ERR	3.62E-02	4.34E-02	4.48E-02
EXPERIMENTAL KLa (sec^-1)	ERR	4.80E-01	4.01E-01	3.88E-01
EXPERIMENTAL kl (m/sec)	ERR	1.92E-04	1.60E-04	1.55E-04

Note: Experimental kl calculated using a=2500m^2/m^3

Mass Transfer Test Data for tne 76.20-cm-diam. Rotor

SUMITOMO PACKING
SAMPLE NAME RAS-30-20
WATER FLOW 43.1 GPM
GAS FLOW 77.7 SCFM
ROTOR SPEED 921 RPM
PRESSURE DROP 4.8 IN. WATER
G/L RATIO (vol) 13.5
WATER TEMPERATURE
IN
OUT 294.9 Kelvin
AIR TEMPERATURE
IN 302.8 Kelvin
OUT 294.1 Kelvin

CONCENTRATION (ppb)	PENTANE	METHYLCYCLOHEXANE	NAPHTHALENE	BENZENE
IN	49.08	360.82	84.9	57.32
OUT	0	0.56	40.9	0.22
EXIT	0	0.56	36.4	0.22
STRIPPING FACTOR	704.0	22.0	0.2	2.9
NTU	ERR	6.7	ERR	7.9
EXPERIMENTAL ATU (m^2)	ERR	6.03E-02	ERR	5.16E-02
EXPERIMENTAL KLa (sec^-1)	ERR	3.55E-01	ERR	4.15E-01
EXPERIMENTAL kl (m/sec)	ERR	1.42E-04	ERR	1.66E-04

CONCENTRATION (ppb)	TOLUENE	O-XYLENE	M-XYLENE	1,2,4-TRIMETHYL BENZENE
IN	107.65	276.82	765.33	416.74
OUT	0.69	0.46	1.86	1.21
EXIT	0.69	0.46	1.86	1.21
STRIPPING FACTOR	3.3	2.6	3.6	3.5
NTU	6.7	9.7	7.9	7.7
EXPERIMENTAL ATU (m^2)	6.04E-02	4.19E-02	5.15E-02	5.27E-02
EXPERIMENTAL KLa (sec^-1)	3.55E-01	5.10E-01	4.16E-01	4.06E-01
EXPERIMENTAL kl (m/sec)	1.42E-04	2.04E-04	1.66E-04	1.62E-04

Note: Experimental kl calculated using a=2500m^2/m^3

Mass Transfer Test Data for the 76.20-cm-diam. Rotor

SUMITOMO PACKING
SAMPLE NAME RAS-30-21
WATER FLOW 34.9 GPM
GAS FLOW 28.9 SCFM
ROTOR SPEED 790 RPM
PRESSURE DROP 3.1 IN. WATER
G/L RATIO (vol) 6.2
WATER TEMPERATURE
IN
OUT 294.3 Kelvin
AIR TEMPERATURE
IN 299.2 Kelvin
OUT 292.5 Kelvin

CONCENTRATION (ppb)	PENTANE	METHYLCYCLOHEXANE	NAPHTHALENE	BENZENE
IN	56.8	375.01	75.5	56.44
OUT	0	0.44	43.9	0.57
EXIT	0	0.44	37.7	0.3
STRIPPING FACTOR	324.0	10.1	0.1	1.3
NTU	ERR	7.4	-0.4	15.6
EXPERIMENTAL ATU (m^2)	ERR	5.50E-02	*********	2.60E-02
EXPERIMENTAL KLa (sec^-1)	ERR	3.15E-01	*********	6.67E-01
EXPERIMENTAL kl (m/sec)	ERR	1.26E-04	*********	2.67E-04

CONCENTRATION (ppb)	TOLUENE	O-XYLENE	M-XYLENE	1,2,4-TRIMETHYL BENZENE
IN	84.29	273.69	765.57	415.99
OUT	0.56	9.99	3.03	4.29
EXIT	0.56	6.82	3.03	3.19
STRIPPING FACTOR	1.5	1.2	1.6	1.6
NTU	11.8	13.1	11.9	10.2
EXPERIMENTAL ATU (m^2)	3.44E-02	3.10E-02	3.41E-02	3.97E-02
EXPERIMENTAL KLa (sec^-1)	5.04E-01	5.59E-01	5.08E-01	4.37E-01
EXPERIMENTAL kl (m/sec)	2.02E-04	2.24E-04	2.03E-04	1.75E-04

Note: Experimental kl calculated using a=2500m^2/m^3

Mass Transfer Test Data for the 76.20-cm-diam. Rotor

SUMITOMO PACKING

SAMPLE NAME	RAS-30-22
WATER FLOW	34 GPM
GAS FLOW	45.3 SCFM
ROTOR SPEED	790 RPM
PRESSURE DROP	3.5 IN. WATER
G/L RATIO (vol)	10.0
WATER TEMPERATURE	
IN	
OUT	290.7 Kelvin
AIR TEMPERATURE	
IN	291.3 Kelvin
OUT	288.9 Kelvin

CONCENTRATION (ppb)	PENTANE	METHYLCYCLOHEXANE	NAPHTHALENE	BENZENE
IN	54.52	401.91	89.5	60.82
OUT	0	0.46	54.9	0
EXIT	0	0.46	54.9	0
STRIPPING FACTOR	527.8	16.5	0.2	1.9
NTU	ERR	7.1	ERR	ERR
EXPERIMENTAL ATU (m^2)	ERR	5.67E-02	ERR	ERR
EXPERIMENTAL KLa (sec^-1)	ERR	2.98E-01	ERR	ERR
EXPERIMENTAL kl (m/sec)	ERR	1.19E-04	ERR	ERR

CONCENTRATION (ppb)	TOLUENE	O-XYLENE	M-XYLENE	1,2,4-TRIMETHYL BENZENE
IN	101.95	413.85	979.18	461.92
OUT	0	0.92	1.58	1.1
EXIT	0	0.92	1.58	1.1
STRIPPING FACTOR	2.2	1.6	2.3	2.2
NTU	ERR	13.2	10.3	9.9
EXPERIMENTAL ATU (m^2)	ERR	3.08E-02	3.92E-02	4.09E-02
EXPERIMENTAL KLa (sec^-1)	ERR	5.49E-01	4.31E-01	4.13E-01
EXPERIMENTAL kl (m/sec)	ERR	2.20E-04	1.72E-04	1.65E-04

Note: Experimental kl calculated using a=2500m^2/m^3

Mass Transfer Test Data for the 76.20-cm-diam. Rotor

SUMITOMO PACKING

SAMPLE NAME	RAS-30-23
WATER FLOW	35 GPM
GAS FLOW	45.7 SCFM
ROTOR SPEED	500 RPM
PRESSURE DROP	2.6 IN. WATER
G/L RATIO (vol)	9.8
WATER TEMPERATURE	
IN	
OUT	291.4 Kelvin
AIR TEMPERATURE	
IN	293 Kelvin
OUT	289.3 Kelvin

CONCENTRATION (ppb)	PENTANE	METHYLCYCLOHEXANE	NAPHTHALENE	BENZENE
IN	47.81	357.17	85.5	54.08
OUT	0	0.53	61.0	0.52
EXIT	0	0.53	61.0	0.52
STRIPPING FACTOR	516.0	16.1	0.2	1.9
NTU	ERR	6.9	ERR	8.4
EXPERIMENTAL ATU (m^2)	ERR	5.90E-02	ERR	4.82E-02
EXPERIMENTAL KLa (sec^-1)	ERR	2.95E-01	ERR	3.61E-01
EXPERIMENTAL kl (m/sec)	ERR	1.18E-04	ERR	1.44E-04

CONCENTRATION (ppb)	TOLUENE	O-XYLENE	M-XYLENE	1,2,4-TRIMETHYL BENZENE
IN	78.53	371.42	865.91	413.64
OUT	1.02	11.81	9.63	8.04
EXIT	1.02	11.81	9.63	8.04
STRIPPING FACTOR	2.2	1.7	2.3	2.2
NTU	7.0	6.5	6.9	6.1
EXPERIMENTAL ATU (m^2)	5.82E-02	6.24E-02	5.85E-02	6.66E-02
EXPERIMENTAL KLa (sec^-1)	2.99E-01	2.79E-01	2.97E-01	2.61E-01
EXPERIMENTAL kl (m/sec)	1.19E-04	1.11E-04	1.19E-04	1.04E-04

Note: Experimental kl calculated using a=2500m^2/m^3

Mass Transfer Test Data for the 76.20-cm-diam. Rotor

SUMITOMO PACKING

SAMPLE NAME	RAS-30-24
WATER FLOW	26.5 GPM
GAS FLOW	45.9 SCFM
ROTOR SPEED	633 RPM
PRESSURE DROP	2.5 IN. WATER
G/L RATIO (vol)	13.0
WATER TEMPERATURE	
IN	
OUT	291.3 Kelvin
AIR TEMPERATURE	
IN	294.4 Kelvin
OUT	289.9 Kelvin

CONCENTRATION (ppb)	PENTANE	METHYLCYCLOHEXANE	NAPHTHALENE	BENZENE
IN	49.87	363.46	89.3	55.76
OUT	0	0.63	43.9	0
EXIT	0	0.63	43.9	0
STRIPPING FACTOR	684.8	21.4	0.2	2.5
NTU	ERR	6.6	ERR	ERR
EXPERIMENTAL ATU (m^2)	ERR	6.12E-02	ERR	ERR
EXPERIMENTAL KLa (sec^-1)	ERR	2.15E-01	ERR	ERR
EXPERIMENTAL kl (m/sec)	ERR	8.60E-05	ERR	ERR

CONCENTRATION (ppb)	TOLUENE	O-XYLENE	M-XYLENE	1,2,4-TRIMETHYL BENZENE
IN	93.59	374.84	884.76	415.25
OUT	0	0.47	1.66	0
EXIT	0	0.47	1.66	0
STRIPPING FACTOR	2.9	2.2	3.1	3.0
NTU	ERR	11.2	8.7	ERR
EXPERIMENTAL ATU (m^2)	ERR	3.62E-02	4.64E-02	ERR
EXPERIMENTAL KLa (sec^-1)	ERR	3.63E-01	2.84E-01	ERR
EXPERIMENTAL kl (m/sec)	ERR	1.45E-04	1.13E-04	ERR

Note: Experimental kl calculated using a=2500m^2/m^3

Mass Transfer Test Data for the 76.20-cm-diam. Rotor

SUMITOMO PACKING

SAMPLE NAME	RAS-30-25
WATER FLOW	35.4 GPM
GAS FLOW	45.8 SCFM
ROTOR SPEED	790 RPM
PRESSURE DROP	3.7 IN. WATER
G/L RATIO (vol)	9.7
WATER TEMPERATURE	
IN	
OUT	292.4 Kelvin
AIR TEMPERATURE	
IN	296.3 Kelvin
OUT	290.5 Kelvin

CONCENTRATION (ppb)	PENTANE	METHYLCYCLOHEXANE	NAPHTHALENE	BENZENE
IN	38.88	316.7	92.5	50.93
OUT	0	0.85	45.2	0
EXIT	0	0.85	45.2	0
STRIPPING FACTOR	509.6	15.9	0.2	1.9
NTU	ERR	6.2	ERR	ERR
EXPERIMENTAL ATU (m^2)	ERR	6.49E-02	ERR	ERR
EXPERIMENTAL KLa (sec^-1)	ERR	2.71E-01	ERR	ERR
EXPERIMENTAL kl (m/sec)	ERR	1.08E-04	ERR	ERR

CONCENTRATION (ppb)	TOLUENE	O-XYLENE	M-XYLENE	1,2,4-TRIMETHYL BENZENE
IN	71.32	362.63	836.72	370.65
OUT	0	1.2	1.49	0
EXIT	0	1.2	1.49	0
STRIPPING FACTOR	2.2	1.7	2.4	2.3
NTU	ERR	11.8	10.0	ERR
EXPERIMENTAL ATU (m^2)	ERR	3.45E-02	4.06E-02	ERR
EXPERIMENTAL KLa (sec^-1)	ERR	5.10E-01	4.33E-01	ERR
EXPERIMENTAL kl (m/sec)	ERR	2.04E-04	1.73E-04	ERR

Note: Experimental kl calculated using a=2500m^2/m^3

Mass Transfer Test Data for the 76.20-cm-diam. Rotor

SUMITOMO PACKING

SAMPLE NAME	RAS-30-26
WATER FLOW	43.1 GPM
GAS FLOW	45.6 SCFM
ROTOR SPEED	921 RPM
PRESSURE DROP	4.7 IN. WATER
G/L RATIO (vol)	7.9
WATER TEMPERATURE	
IN	
OUT	292 Kelvin
AIR TEMPERATURE	
IN	295.5 Kelvin
OUT	290.7 Kelvin

CONCENTRATION (ppb)	PENTANE	METHYLCYCLOHEXANE	NAPHTHALENE	BENZENE
IN	45.39	338.09	81.5	52.48
OUT	0	0.57	53.7	0
EXIT	0	0.57	53.7	0
STRIPPING FACTOR	417.3	13.0	0.1	1.5
NTU	ERR	6.8	ERR	ERR
EXPERIMENTAL ATU (m^2)	ERR	5.94E-02	ERR	ERR
EXPERIMENTAL KLa (sec^-1)	ERR	3.61E-01	ERR	ERR
EXPERIMENTAL kl (m/sec)	ERR	1.44E-04	ERR	ERR

CONCENTRATION (ppb)	TOLUENE	O-XYLENE	M-XYLENE	1,2,4-TRIMETHYL BENZENE
IN	73.77	369.14	853.96	399.02
OUT	0	2.64	2.02	1.49
EXIT	0	2.64	2.02	1.49
STRIPPING FACTOR	1.8	1.4	1.9	1.9
NTU	ERR	13.5	11.1	10.5
EXPERIMENTAL ATU (m^2)	ERR	2.99E-02	3.65E-02	3.87E-02
EXPERIMENTAL KLa (sec^-1)	ERR	7.16E-01	5.86E-01	5.53E-01
EXPERIMENTAL kl (m/sec)	ERR	2.86E-04	2.34E-04	2.21E-04

Note: Experimental kl calculated using a=2500m^2/m^3

Mass Transfer Test Data for the 76.20-cm-diam. Rotor

SUMITOMO PACKING
SAMPLE NAME RAS-30-27
WATER FLOW 43.3 GPM
GAS FLOW 46.6 SCFM
ROTOR SPEED 633 RPM
PRESSURE DROP 2.7 IN. WATER
G/L RATIO (vol) 8.1
WATER TEMPERATURE
IN
OUT 291.5 Kelvin
AIR TEMPERATURE
IN 294.3 Kelvin
OUT 288.2 Kelvin

CONCENTRATION (ppb)	PENTANE	METHYLCYCLOHEXANE	NAPHTHALENE	BENZENE
IN	50.42	370.62	83.0	55.72
OUT	0	0.8	48.5	0.35
EXIT	0	0.8	48.5	0.35
STRIPPING FACTOR	425.2	13.3	0.1	1.5
NTU	ERR	6.6	ERR	11.5
EXPERIMENTAL ATU (m^2)	ERR	6.19E-02	ERR	3.52E-02
EXPERIMENTAL KLa (sec^-1)	ERR	3.48E-01	ERR	6.12E-01
EXPERIMENTAL kl (m/sec)	ERR	1.39E-04	ERR	2.45E-04

CONCENTRATION (ppb)	TOLUENE	O-XYLENE	M-XYLENE	1,2,4-TRIMETHYL BENZENE
IN	130.91	386.9	916.47	423.45
OUT	0.52	7.93	4.33	3.74
EXIT	0.52	7.93	4.33	3.74
STRIPPING FACTOR	1.8	1.4	1.9	1.8
NTU	10.7	9.8	9.7	8.6
EXPERIMENTAL ATU (m^2)	3.78E-02	4.15E-02	4.20E-02	4.70E-02
EXPERIMENTAL KLa (sec^-1)	5.69E-01	5.18E-01	5.13E-01	4.58E-01
EXPERIMENTAL kl (m/sec)	2.28E-04	2.07E-04	2.05E-04	1.83E-04

Note: Experimental kl calculated using a=2500m^2/m^3

Mass Transfer Test Data for the 76.20-cm-diam. Rotor

SUMITOMO PACKING

SAMPLE NAME	RAS-30-28
WATER FLOW	35.2 GPM
GAS FLOW	44.6 SCFM
ROTOR SPEED	790 RPM
PRESSURE DROP	3.3 IN. WATER
G/L RATIO (vol)	9.5
WATER TEMPERATURE	
IN	
OUT	292.2 Kelvin
AIR TEMPERATURE	
IN	308 Kelvin
OUT	290.4 Kelvin

CONCENTRATION (ppb)	PENTANE	METHYLCYCLOHEXANE	NAPHTHALENE	BENZENE
IN	49.3	379.25	87.1	56.45
OUT	0	0.35	38.0	0
EXIT	0	0.35	38.0	0
STRIPPING FACTOR	499.4	15.6	0.2	1.9
NTU	ERR	7.4	ERR	ERR
EXPERIMENTAL ATU (m^2)	ERR	5.48E-02	ERR	ERR
EXPERIMENTAL KLa (sec^-1)	ERR	3.19E-01	ERR	ERR
EXPERIMENTAL KL (m/sec)	ERR	1.28E-04	ERR	ERR

CONCENTRATION (ppb)	TOLUENE	O-XYLENE	M-XYLENE	1,2,4-TRIMETHYL BENZENE
IN	103.97	396.94	933.97	437.43
OUT	0	1.29	1.83	1.01
EXIT	0	1.29	1.83	1.01
STRIPPING FACTOR	2.1	1.7	2.3	2.2
NTU	ERR	12.2	10.0	9.9
EXPERIMENTAL ATU (m^2)	ERR	3.33E-02	4.06E-02	4.09E-02
EXPERIMENTAL KLa (sec^-1)	ERR	5.26E-01	4.31E-01	4.28E-01
EXPERIMENTAL KL (m/sec)	ERR	2.10E-04	1.72E-04	1.71E-04

Note: Experimental KL calculated using a=2500m^2/m^3

Mass Transfer Test Data for the 76.20-cm-diam. Rotor

SUMITOMO PACKING

SAMPLE NAME	RAS-30-29
WATER FLOW	25.8 GPM
GAS FLOW	28 SCFM
ROTOR SPEED	633 RPM
PRESSURE DROP	2.1 IN. WATER
G/L RATIO (vol)	8.1
WATER TEMPERATURE	
IN	
OUT	291.8 Kelvin
AIR TEMPERATURE	
IN	288.8 Kelvin
OUT	286.8 Kelvin

CONCENTRATION (ppb)	PENTANE	METHYLCYCLOHEXANE	NAPHTHALENE	BENZENE
IN	49.8	380.13	84.2	57.24
OUT	0	0.38	39.8	0
EXIT	0	0.38	40.3	0
STRIPPING FACTOR	428.3	13.4	0.1	1.6
NTU	ERR	7.4	ERR	ERR
EXPERIMENTAL ATU (m^2)	ERR	5.49E-02	ERR	ERR
EXPERIMENTAL KLa (sec^-1)	ERR	2.33E-01	ERR	ERR
EXPERIMENTAL kl (m/sec)	ERR	9.34E-05	ERR	ERR

CONCENTRATION (ppb)	TOLUENE	O-XYLENE	M-XYLENE	1,2,4-TRIMETHYL BENZENE
IN	141.23	389.21	948.28	425.27
OUT	0	5.43	2.11	1.91
EXIT	0	4.17	2.11	1.91
STRIPPING FACTOR	1.8	1.4	2.0	1.9
NTU	ERR	11.4	11.0	9.9
EXPERIMENTAL ATU (m^2)	ERR	3.56E-02	3.67E-02	4.09E-02
EXPERIMENTAL KLa (sec^-1)	ERR	3.60E-01	3.49E-01	3.13E-01
EXPERIMENTAL kl (m/sec)	ERR	1.44E-04	1.40E-04	1.25E-04

Note: Experimental kl calculated using a=2500m^2/m^3

Mass Transfer Test Data for the 76.20-cm-diam. Rotor

SUMITOMO PACKING

SAMPLE NAME	RAS-30-30
WATER FLOW	25.9 GPM
GAS FLOW	27.2 SCFM
ROTOR SPEED	921 RPM
PRESSURE DROP	3.9 IN. WATER
G/L RATIO (vol)	7.9
WATER TEMPERATURE	
IN	
OUT	292.7 Kelvin
AIR TEMPERATURE	
IN	295.2 Kelvin
OUT	289.8 Kelvin

CONCENTRATION (ppb)	PENTANE	METHYLCYCLOHEXANE	NAPHTHALENE	BENZENE
IN	46.53	359.82	80.7	53.87
OUT	0	0.66	33.7	0
EXIT	0	0.66	32.3	0
STRIPPING FACTOR	413.2	12.9	0.1	1.6
NTU	ERR	6.7	ERR	ERR
EXPERIMENTAL ATU (m^2)	ERR	6.01E-02	ERR	ERR
EXPERIMENTAL KLa (sec^-1)	ERR	2.14E-01	ERR	ERR
EXPERIMENTAL kl (m/sec)	ERR	8.56E-05	ERR	ERR

CONCENTRATION (ppb)	TOLUENE	O-XYLENE	M-XYLENE	1,2,4-TRIMETHYL BENZENE
IN	111.44	381.88	894.76	405.69
OUT	0	1.39	1.35	0
EXIT	0	1.12	1.35	0
STRIPPING FACTOR	1.8	1.4	2.0	1.9
NTU	ERR	16.0	11.8	ERR
EXPERIMENTAL ATU (m^2)	ERR	2.53E-02	3.42E-02	ERR
EXPERIMENTAL KLa (sec^-1)	ERR	5.08E-01	3.76E-01	ERR
EXPERIMENTAL kl (m/sec)	ERR	2.03E-04	1.50E-04	ERR

Note: Experimental kl calculated using a=2500m^2/m^3

Mass Transfer Test Data for the 76.20-cm-diam. Rotor

SUMITOMO PACKING
SAMPLE NAME RAS-30-31
WATER FLOW 35 GPM
GAS FLOW 49.6 SCFM
ROTOR SPEED 790 RPM
PRESSURE DROP 3.4 IN. WATER
G/L RATIO (vol) 10.6
WATER TEMPERATURE
IN
OUT 293.7 Kelvin
AIR TEMPERATURE
IN 298.1 Kelvin
OUT 289.9 Kelvin

CONCENTRATION (ppb)	PENTANE	METHYLCYCLOHEXANE	NAPHTHALENE	BENZENE
IN	45.25	377.11	87.8	58.58
OUT	0	0.73	35.0	0
EXIT	0	0.73	35.0	0
STRIPPING FACTOR	555.7	17.4	0.2	2.2
NTU	ERR	6.6	ERR	ERR
EXPERIMENTAL ATU (m^2)	ERR	6.17E-02	ERR	ERR
EXPERIMENTAL KLa (sec^-1)	ERR	2.82E-01	ERR	ERR
EXPERIMENTAL kl (m/sec)	ERR	1.13E-04	ERR	ERR

CONCENTRATION (ppb)	TOLUENE	O-XYLENE	M-XYLENE	1,2,4-TRIMETHYL BENZENE
IN	114.3	405.86	465.34	437.13
OUT	0	0.6	1.32	1.01
EXIT	0	0.6	1.32	1.01
STRIPPING FACTOR	2.5	1.9	2.7	2.7
NTU	ERR	11.9	8.5	9.0
EXPERIMENTAL ATU (m^2)	ERR	3.39E-02	4.75E-02	4.51E-02
EXPERIMENTAL KLa (sec^-1)	ERR	5.12E-01	3.66E-01	3.86E-01
EXPERIMENTAL kl (m/sec)	ERR	2.05E-04	1.46E-04	1.54E-04

Note: Experimental kl calculated using a=2500m^2/m^3

Mass Transfer Test Data for the 76.20-cm-diam. Rotor

SUMITOMO PACKING

SAMPLE NAME	RAS-30-32
WATER FLOW	35.2 GPM
GAS FLOW	70.5 SCFM
ROTOR SPEED	790 RPM
PRESSURE DROP	3.8 IN. WATER
G/L RATIO (vol)	15.0
WATER TEMPERATURE	
IN	
OUT	293.1 Kelvin
AIR TEMPERATURE	
IN	298.1 Kelvin
OUT	292.6 Kelvin

CONCENTRATION (ppb)	PENTANE	METHYLCYCLOHEXANE	NAPHTHALENE	BENZENE
IN	44.75	357.28	80.9	54.61
OUT	0	0	24.3	0
EXIT	0	0	24.3	0
STRIPPING FACTOR	786.9	24.6	0.3	3.0
NTU	ERR	ERR	ERR	ERR
EXPERIMENTAL ATU (m^2)	ERR	ERR	ERR	ERR
EXPERIMENTAL KLa (sec^-1)	ERR	ERR	ERR	ERR
EXPERIMENTAL kl (m/sec)	ERR	ERR	ERR	ERR

CONCENTRATION (ppb)	TOLUENE	O-XYLENE	M-XYLENE	1,2,4-TRIMETHYL BENZENE
IN	80.91	380.92	887.28	412.58
OUT	0	0.23	0.96	0
EXIT	0	0.23	0.96	0
STRIPPING FACTOR	3.5	2.7	3.8	3.7
NTU	ERR	11.1	8.9	ERR
EXPERIMENTAL ATU (m^2)	ERR	3.67E-02	4.57E-02	ERR
EXPERIMENTAL KLa (sec^-1)	ERR	4.77E-01	3.83E-01	ERR
EXPERIMENTAL kl (m/sec)	ERR	1.91E-04	1.53E-04	ERR

Note: Experimental kl calculated using a=2500m^2/m^3

Mass Transfer Test Data for the 76.20-cm-diam. Rotor

SUMITOMO PACKING

SAMPLE NAME	RAS-30-33
WATER FLOW	25.6 GPM
GAS FLOW	46.8 SCFM
ROTOR SPEED	921 RPM
PRESSURE DROP	3.7 IN. WATER
G/L RATIO (vol)	13.7
WATER TEMPERATURE	
IN	
OUT	292.3 Kelvin
AIR TEMPERATURE	
IN	297.8 Kelvin
OUT	291.8 Kelvin

CONCENTRATION (ppb)	PENTANE	METHYLCYCLOHEXANE	NAPHTHALENE	BENZENE
IN	44.96	351.77	51.2	55.94
OUT	0	0.63	15.5	0
EXIT	0	0.63	15.5	0
STRIPPING FACTOR	720.3	22.5	0.2	2.7
NTU	ERR	6.6	ERR	ERR
EXPERIMENTAL ATU (m^2)	ERR	6.17E-02	ERR	ERR
EXPERIMENTAL KLa (sec^-1)	ERR	2.06E-01	ERR	ERR
EXPERIMENTAL kl (m/sec)	ERR	8.25E-05	ERR	ERR

CONCENTRATION (ppb)	TOLUENE	O-XYLENE	M-XYLENE	1,2,4-TRIMETHYL BENZENE
IN	98.3	390.63	900.67	411.37
OUT	0	0.47	1.85	1
EXIT	0	0.47	1.85	1
STRIPPING FACTOR	3.1	2.4	3.4	3.2
NTU	ERR	10.6	8.3	8.2
EXPERIMENTAL ATU (m^2)	ERR	3.81E-02	4.88E-02	4.96E-02
EXPERIMENTAL KLa (sec^-1)	ERR	3.34E-01	2.61E-01	2.57E-01
EXPERIMENTAL kl (m/sec)	ERR	1.33E-04	1.04E-04	1.03E-04

Note: Experimental kl calculated using a=2500m^2/m^3

Mass Transfer Test Data for the 76.20-cm-diam. Rotor

SUMITOMO PACKING

SAMPLE NAME	RAS-30-34
WATER FLOW	34.6 GPM
GAS FLOW	50.4 SCFM
ROTOR SPEED	790 RPM
PRESSURE DROP	3.5 IN. WATER
G/L RATIO (vol)	10.9
WATER TEMPERATURE	
IN	
OUT	289 Kelvin
AIR TEMPERATURE	
IN	290.4 Kelvin
OUT	287 Kelvin

CONCENTRATION (ppb)	PENTANE	METHYLCYCLOHEXANE	NAPHTHALENE	BENZENE
IN	49.57	346.63	62.6	53.09
OUT	0	0.79	50.1	0
EXIT	0	0.79	50.1	0
STRIPPING FACTOR	580.5	18.1	0.2	1.9
NTU	ERR	6.4	ERR	ERR
EXPERIMENTAL ATU (m^2)	ERR	6.35E-02	ERR	ERR
EXPERIMENTAL KLa (sec^-1)	ERR	2.70E-01	ERR	ERR
EXPERIMENTAL kl (m/sec)	ERR	1.08E-04	ERR	ERR

CONCENTRATION (ppb)	TOLUENE	O-XYLENE	M-XYLENE	1,2,4-TRIMETHYL BENZENE
IN	84.87	249.75	639.56	371.51
OUT	0	0.61	1.3	1.38
EXIT	0	0.61	1.3	1.38
STRIPPING FACTOR	2.2	1.7	2.4	2.3
NTU	ERR	12.5	9.8	9.0
EXPERIMENTAL ATU (m^2)	ERR	3.25E-02	4.15E-02	4.51E-02
EXPERIMENTAL KLa (sec^-1)	ERR	5.29E-01	4.14E-01	3.81E-01
EXPERIMENTAL kl (m/sec)	ERR	2.12E-04	1.66E-04	1.52E-04

Note: Experimental kl calculated using a=2500 m^2/m^3

Mass Transfer Test Data for the 76.20-cm-diam. Rotor

SUMITOMO PACKING

SAMPLE NAME	RAS-30-35
WATER FLOW	34.7 GPM
GAS FLOW	48.6 SCFM
ROTOR SPEED	1000 RPM
PRESSURE DROP	5.2 IN. WATER
G/L RATIO (vol)	10.5
WATER TEMPERATURE	
IN	
OUT	289.4 Kelvin
AIR TEMPERATURE	
IN	291.7 Kelvin
OUT	288.2 Kelvin

CONCENTRATION (ppb)	PENTANE	METHYLCYCLOHEXANE	NAPHTHALENE	BENZENE
IN	53.04	362.59	58.4	55.05
OUT	0	1.69	46.2	0
EXIT	0	1.69	46.2	0
STRIPPING FACTOR	557.3	17.4	0.2	1.9
NTU	ERR	5.6	ERR	ERR
EXPERIMENTAL ATU (m^2)	ERR	7.20E-02	ERR	ERR
EXPERIMENTAL KLa (sec^-1)	ERR	2.40E-01	ERR	ERR
EXPERIMENTAL kl (m/sec)	ERR	9.58E-05	ERR	ERR

CONCENTRATION (ppb)	TOLUENE	O-XYLENE	M-XYLENE	1,2,4-TRIMETHYL BENZENE
IN	60.26	255.16	685.3	381.45
OUT	0	0.7	2.44	2.23
EXIT	0	0.7	2.44	2.23
STRIPPING FACTOR	2.2	1.7	2.3	2.2
NTU	ERR	12.6	8.9	8.3
EXPERIMENTAL ATU (m^2)	ERR	3.23E-02	4.54E-02	4.89E-02
EXPERIMENTAL KLa (sec^-1)	ERR	5.35E-01	3.80E-01	3.53E-01
EXPERIMENTAL kl (m/sec)	ERR	2.14E-04	1.52E-04	1.41E-04

Note: Experimental k_l calculated using a=2500m^2/m^3

Mass Transfer Test Data for the 76.20-cm-diam. Rotor

SUMITOMO PACKING

SAMPLE NAME	RAS-30-36
WATER FLOW	48.8 GPM
GAS FLOW	69.2 SCFM
ROTOR SPEED	790 RPM
PRESSURE DROP	4.5 IN. WATER
G/L RATIO (vol)	10.6
WATER TEMPERATURE	
IN	
OUT	289.9 Kelvin
AIR TEMPERATURE	
IN	293.7 Kelvin
OUT	289.3 Kelvin

CONCENTRATION (ppb)	PENTANE	METHYLCYCLOHEXANE	NAPHTHALENE	BENZENE
IN	59.93	409.82	62.4	63.31
OUT	0	1.61	41.6	0
EXIT	0	1.61	41.6	0
STRIPPING FACTOR	563.3	17.6	0.2	1.9
NTU	ERR	5.8	ERR	ERR
EXPERIMENTAL ATU (m^2)	ERR	6.98E-02	ERR	ERR
EXPERIMENTAL KLa (sec^-1)	ERR	3.48E-01	ERR	ERR
EXPERIMENTAL kl (m/sec)	ERR	1.39E-04	ERR	ERR

CONCENTRATION (ppb)	TOLUENE	O-XYLENE	M-XYLENE	1,2,4-TRIMETHYL BENZENE
IN	66.71	285.99	766.32	426
OUT	0.51	2.27	1.99	2.43
EXIT	0.51	2.27	1.99	2.43
STRIPPING FACTOR	2.2	1.7	2.4	2.3
NTU	7.8	9.6	9.3	8.2
EXPERIMENTAL ATU (m^2)	5.22E-02	4.23E-02	4.35E-02	4.96E-02
EXPERIMENTAL KLa (sec^-1)	4.65E-01	5.73E-01	5.57E-01	4.89E-01
EXPERIMENTAL kl (m/sec)	1.86E-04	2.29E-04	2.23E-04	1.95E-04

Note: Experimental kl calculated using a=2500m^2/m^3

Mass Transfer Test Data for the 76.20-cm-diam. Rotor

SUMITOMO PACKING
SAMPLE NAME RAS-30-37
WATER FLOW 34.9 GPM
GAS FLOW 48.3 SCFM
ROTOR SPEED 790 RPM
PRESSURE DROP 3.5 IN. WATER
G/L RATIO (vol) 10.4
WATER TEMPERATURE
IN
OUT 290.3 Kelvin
AIR TEMPERATURE
IN 294.1 Kelvin
OUT 288.8 Kelvin

CONCENTRATION (ppb)	PENTANE	METHYLCYCLOHEXANE	NAPHTHALENE	BENZENE
IN	51.53	391.67	72.7	67.82
OUT	0	1.17	38.5	0
EXIT	0	1.17	38.5	0
STRIPPING FACTOR	549.0	17.2	0.2	1.9
NTU	ERR	6.1	ERR	ERR
EXPERIMENTAL ATU (m^2)	ERR	6.63E-02	ERR	ERR
EXPERIMENTAL KLa (sec^-1)	ERR	2.61E-01	ERR	ERR
EXPERIMENTAL kl (m/sec)	ERR	1.05E-04	ERR	ERR

CONCENTRATION (ppb)	TOLUENE	O-XYLENE	M-XYLENE	1,2,4-TRIMETHYL BENZENE
IN	94.62	273.72	739.01	412.22
OUT	0	0.95	1.35	1.39
EXIT	0	0.95	1.35	1.39
STRIPPING FACTOR	2.2	1.7	2.4	2.3
NTU	ERR	11.7	10.0	9.2
EXPERIMENTAL ATU (m^2)	ERR	3.46E-02	4.06E-02	4.43E-02
EXPERIMENTAL KLa (sec^-1)	ERR	5.01E-01	4.27E-01	3.91E-01
EXPERIMENTAL kl (m/sec)	ERR	2.00E-04	1.71E-04	1.57E-04

Note: Experimental kl calculated using a=2500m^2/m^3

Mass Transfer Test Data for the 76.20-cm-diam. Rotor

SUMITOMO PACKING
SAMPLE NAME RAS-30-38
WATER FLOW 34.6 GPM
GAS FLOW 48.1 SCFM
ROTOR SPEED 500 RPM
PRESSURE DROP 2.9 IN. WATER
G/L RATIO (vol) 10.4
WATER TEMPERATURE
IN
OUT 290.4 Kelvin
AIR TEMPERATURE
IN 296.5 Kelvin
OUT 289.7 Kelvin

CONCENTRATION (ppb)	PENTANE	METHYLCYCLOHEXANE	NAPHTHALENE	BENZENE
IN	47.48	325.36	73.8	81.54
OUT	0	0.55	38.6	0.41
EXIT	0	0.86	38.6	0.41
STRIPPING FACTOR	551.3	17.2	0.2	1.9
NTU	ERR	6.7	ERR	9.6
EXPERIMENTAL ATU (m^2)	ERR	6.07E-02	ERR	4.24E-02
EXPERIMENTAL KLa (sec^-1)	ERR	2.83E-01	ERR	4.05E-01
EXPERIMENTAL kl (m/sec)	ERR	1.13E-04	ERR	1.62E-04

CONCENTRATION (ppb)	TOLUENE	O-XYLENE	M-XYLENE	1,2,4-TRIMETHYL BENZENE
IN	120.05	270.12	741.02	411.35
OUT	0.64	6.53	5.46	6.2
EXIT	0.64	4.84	4.39	4.75
STRIPPING FACTOR	2.2	1.7	2.4	2.3
NTU	8.4	7.3	7.7	6.6
EXPERIMENTAL ATU (m^2)	4.80E-02	5.52E-02	5.28E-02	6.10E-02
EXPERIMENTAL KLa (sec^-1)	3.58E-01	3.11E-01	3.26E-01	2.82E-01
EXPERIMENTAL kl (m/sec)	1.43E-04	1.25E-04	1.30E-04	1.13E-04

Note: Experimental kl calculated using a=2500m^2/m^3

VITA

Surinder Paul Singh was born in Punjab, India, on January 4, 1959. He emigrated to the United States in November 1968. His parents are Dr. and Mrs. Dilbagh Singh of Carlinville, Illinois. He graduated from Carlinville High School in May 1977. He entered Blackburn College, Carlinville, the following September and received a Bachelor or Arts degree in May 1981. He entered the University of Illinois, Urbana, in September 1981 and received a Master of Science degree in Chemical Engineering in August 1983.

In September 1983, he joined the Fuel Recycle Division of Oak Ridge National Laboratory in Oak Ridge, Tennessee, as a research engineer. He entered the graduate school of University of Tennessee, Knoxville, in January 1985.

The author is a member of Alpha Chi, Phi Lambda Upsilon, and the American Institute of Chemical Engineers.